

**Study of full-counting statistics in heat  
transport in transient and steady state and  
quantum fluctuation theorems**

BIJAY KUMAR AGARWALLA

*(M.Sc., Physics, Indian Institute of Technology, Bombay)*

A THESIS SUBMITTED  
FOR THE DEGREE OF DOCTOR OF PHILOSOPHY

DEPARTMENT OF PHYSICS  
NATIONAL UNIVERSITY OF SINGAPORE

2013

## Declaration

I hereby declare that the thesis is my original work and it has been written by me in its entirety. I have duly acknowledged all the sources of information which have been used in the thesis.

This thesis has also not been submitted for any degree in any university previously.

*Bijay Kumar Agarwala*

---

Bijay Kumar Agarwala

May 17, 2013

©

Copyright by

Bijay Kumar Agarwalla

2013

All rights reserved

# Acknowledgements

First and foremost, I would like to express my deepest gratitude to my supervisors, Professor Wang Jian-Sheng and Professor Li Baowen for their continuous support, excellent guidance, patience and encouragement throughout my PhD study. Their instructions, countless discussions, insightful opinions are most valuable to me. Without their guidance and persistent help this dissertation would not have been possible.

I would like to take this opportunity to thank all my mentors who are responsible for what I am today. I am so fortunate to have their guidance and support. Particularly, I am very grateful to my master's supervisor Prof. Dibyendu Das, my summer project supervisor Prof. Jayanta Kumar Bhattacharjee, my undergraduate teachers specially Prof. Narayan Banerjee and Arindam Chakroborty and my school teachers Dr. Pintu Sinha, Dr. Piyush Kanti Dan, Dr. Rajib Narayan Mukherjee for their great efforts and patience to prepare me for the future.

I would also like to thank Prof. Abhishek Dhar and Prof. Sanjib Sabhapandit for organizing the schools on nonequilibrium statistical physics at Raman Research Institute every year starting from 2010 which helped me to develop the skills required in this field and also for giving the opportunity to interact with the leading physicists.

I am grateful to my collaborators Li Huanan, Zhang Lifa, Liu sha and our group members Juzar Thingna, Meng Lee, Eduardo Cuansing, Jinwu, Jose

Garcia, Ni Xiaoxi for all the valuable discussions and suggestions.

I would like to thank my friends and seniors Dr. Pradipto Shankar Maiti, Dr. Tanay Paramanik, Dr. Sabysachi Chakroborty, Dr. Sadananda Ranjit, Dr. Jayendra Nath Bandyopadhyay, Dr. Sarika Jalan, Dr. Jhinuk Gupta, Dr. Amrita Roy, Mr. Bablu Mukherjee, Mr. Shubhajit Paul, Mr. Shubham Dattagupta, Mr. Rajkumar Das, Dr. Animesh Samanta, Mr. Krishnakanta Ghosh, Mr. Bikram Keshari Agrawalla, Mr. Sk Sudipta Shaheen, Mr. Deepal Kanti Das, Ms. Madhurima Bagchi, Ms. Bani Suri, Ms. Shreya Shah for the help and contributions you all have made during these years. The life in Singapore wouldn't be so nice without the presence of two important people in my life Nimai Mishra and Tumpa Roy. You guys rock. I am also indebted for the support from my two childhood friends Saikat Sarkar and Pratik Chatterjee. Thank you friends for being so supportive. I also thank Rajasree Das for her constant encouragement and caring attitude during my undergraduate studies.

I would like to thank all my JU and IITB friends and all those unmentioned friends, relatives, teachers whose suggestions, love and support I deeply valued and I thank all of them from the bottom of my heart.

I also like to thank department of Physics and all administration assistants for their assistance on various issues.

The another important part in the journey of my PhD life here in NUS is to get myself involved in the spiritual path by listening to the lectures on Bhagavad Gita. My deepest gratitude to Devakinandan Das, Niketa Chotai, Sandeep Jangam and many others for enlighten me in the spiritual world.

Last but not least, I would like to thank my parents and my elder brother Ajay for their constant support, advice, encouragement and unconditional love.

# Table of Contents

<b>Acknowledgements</b>	<b>iii</b>
<b>Abstract</b>	<b>x</b>
<b>List of important Symbols and Abbreviations</b>	<b>xiv</b>
<b>List of Figures</b>	<b>xvi</b>
<b>1 Introduction</b>	<b>1</b>
1.1 Introduction to fluctuation theorems . . . . .	4
1.1.1 Jarzynski Equality . . . . .	5
1.1.2 Crooks relation . . . . .	7
1.1.3 Gallavotti-Cohen FT . . . . .	7
1.1.4 Experimental verification of Fluctuation theorems . .	8
1.1.5 Quantum Fluctuation theorems . . . . .	9
1.2 Two-time quantum Measurement Method . . . . .	11
1.3 Quantum Exchange Fluctuation theorem . . . . .	15
1.4 Full-Counting statistics (FCS) . . . . .	19
1.5 Problem addressed in this thesis . . . . .	23
1.6 Thesis structure . . . . .	25

<b>2</b>	<b>Introduction to Nonequilibrium Green's function (NEGF)</b>	
	<b>method</b>	<b>34</b>
2.1	Introduction . . . . .	35
2.2	Definitions of Green's functions . . . . .	37
2.3	Contour ordered Green's function . . . . .	42
2.3.1	Different pictures in quantum mechanics . . . . .	43
2.3.2	Closed time path formalism . . . . .	45
2.3.3	Important relations on the Keldysh Contour . . . . .	49
2.3.4	Dyson equation and Keldysh rotation . . . . .	51
2.4	Example: Derivation of Landauer formula for heat transport using NEGF approach . . . . .	56
<b>3</b>	<b>Full-counting statistics (FCS) in heat transport for ballistic lead-junction-lead setup</b>	<b>72</b>
3.1	The general lattice model . . . . .	74
3.2	Definition of current, heat and entropy-production . . . . .	76
3.3	Characteristic function (CF) . . . . .	77
3.4	Initial conditions for the density operator . . . . .	81
3.5	Derivation of the CF $\mathcal{Z}(\xi_L)$ for heat . . . . .	84
3.5.1	$\mathcal{Z}(\xi_L)$ for product initial state $\rho_{\text{prod}}(0)$ using Feyn- man diagrammatic technique . . . . .	84
3.5.2	Feynman path-integral formalism to derive $\mathcal{Z}(\xi_L)$ for initial conditions $\rho_{\text{NESS}}(0)$ and $\rho'(0)$ . . . . .	96

3.6	Long-time limit ( $t_M \rightarrow \infty$ ) and steady state fluctuation theorem (SSFT)	104
3.7	Numerical Results for the cumulants of heat	110
3.8	CF $\mathcal{Z}(\xi_L, \xi_R)$ corresponding to the joint probability distribution $P(Q_L, Q_R)$	117
3.9	Classical limit of the CF	122
3.10	Nazarov's definition of CF and long-time limit expression	123
3.11	Summary	128
<b>4</b>	<b>Full-counting statistics (FCS) and energy-current in the presence of driven force</b>	<b>133</b>
4.1	Long-time result for the driven part of the CGF $\ln \mathcal{Z}^d(\xi_L)$	135
4.2	Classical limit of $\ln \mathcal{Z}^d(\xi_L, \xi_R)$	139
4.3	The expression for transient current under driven force	141
4.3.1	Application to 1D chain	147
4.4	Behavior of energy-current	150
4.5	Summary	160
<b>5</b>	<b>Heat exchange between multi-terminal harmonic systems and exchange fluctuation theorem (XFT)</b>	<b>164</b>
5.1	Model Hamiltonian	166
5.2	Generalized characteristic function $\mathcal{Z}(\{\xi_\alpha\})$	167
5.3	Long-time result for the CGF for heat	170
5.4	Special Case: Two-terminal situation	173
5.4.1	Numerical Results and discussion	177
5.4.2	Exchange Fluctuation Theorem (XFT)	181

5.5	Effect of finite size of the system on the cumulants of heat . . . . .	183
5.6	Proof of transient fluctuation theorem . . . . .	186
5.7	Summary . . . . .	189
<b>6</b>	<b>Full-counting statistics in nonlinear junctions</b>	<b>192</b>
6.1	Hamiltonian Model . . . . .	194
6.2	Steady state limit . . . . .	202
6.3	Application and verification . . . . .	204
6.3.1	Numerical results . . . . .	207
6.4	Summary . . . . .	211
<b>7</b>	<b>Summary and future outlook</b>	<b>215</b>
<b>A</b>	<b>Derivation of cumulant generating function for product initial state</b>	<b>220</b>
<b>B</b>	<b>Vacuum diagrams</b>	<b>224</b>
<b>C</b>	<b>Details for the numerical calculation of cumulants of heat for projected and steady state initial state</b>	<b>227</b>
<b>D</b>	<b>Solving Dyson equation numerically for product initial state</b>	<b>231</b>
<b>E</b>	<b>Green's function <math>G_0[\omega]</math> for a harmonic center connected with heat baths</b>	<b>233</b>
<b>F</b>	<b>Example: Green's functions for isolated harmonic oscillator</b>	<b>244</b>

<b>G</b>	<b>Current at short time for product initial state <math>\rho_{\text{prod}}(0)</math></b>	<b>248</b>
<b>H</b>	<b>A quick derivation of the Levitov-Lesovik formula for electrons using NEGF</b>	<b>251</b>
	<b>List of Publications</b>	<b>257</b>

# Abstract

There are very few known universal relations that exist in the field of nonequilibrium statistical physics. Linear response theory is one such example which was developed by Kubo, Callen and Welton. However it is valid for systems close to equilibrium, *i.e.*, when external perturbations are weak. It is only in recent times that several other universal relations are discovered for systems driven arbitrarily far-from-equilibrium and they are collectively referred to as the fluctuation theorems. These theorems place conditions on the probability distribution for different nonequilibrium observables such as heat, injected work, particle number, generically referred to as entropy production. In the past 15 years or so different types of fluctuation theorems are discovered which are in general valid for deterministic as well as for stochastic systems both in classical and quantum regimes.

In this thesis, we study quantum fluctuations of energy flowing through a finite junction which is connected with multiple reservoirs. The reservoirs are maintained at different equilibrium temperatures. Due to the stochastic nature of the reservoirs the transferred energy during a finite time interval is not given by a single number, rather by a probability distribution. In

order to extract information about the probability distribution, the most convenient approach is to obtain the characteristic function (CF) or the cumulant generating function (CGF).

In the first part of the thesis, we study the so-called “full-counting statistics” (FCS) for heat and entropy-production for a phononic junction system modeled as harmonic chain and connected with two heat reservoirs. Based on the two-time projective measurement concept we derive the CF for transferred heat and obtain an explicit expression using the nonequilibrium Green’s function (NEGF) and Feynman path-integral technique. Considering different initial conditions for the density operator we found that in all cases the CGF can be expressed in terms of the Green’s functions for the junction and the self-energy with shifted time arguments. However the meaning of these Green’s functions are different and depends on the initial conditions. In the long-time limit we obtain an explicit expression for the CGF which obey the steady-state fluctuation theorem (SSFT), also known as Gallavotti-Cohen (GC) symmetry. We found the “counting” of energy is related to the shifting of time argument for the corresponding self-energy. The expression for the CGF is obtained under a very general scenario. It is valid both in transient and steady state regimes. Moreover, the coupling between the leads and the junction could have arbitrary time-dependence and also the leads could be finite in size. We also derive a generalized CGF to obtain the correlations between the heat-flux of the two reservoirs and also to calculate total entropy production in the reservoirs.

In the second part, we study the CGF for a forced driven harmonic junction.

For generalized CGF we obtain an explicit expression in the asymptotic limit and showed that force induced entropy-production in the reservoirs satisfy fluctuation symmetry. The long-time limit of the CGF is expressed in terms of a force-driven transmission function. For periodic driving we analyze the effect of different heat baths (Rubin, Ohmic) on the energy current for one-dimensional linear chain. We also consider the heat pumping behavior of this model.

Then we consider another important setup which is useful for the study of exchange fluctuation theorem (XFT) first put forward by Jarzynski and Wójcik. The system consists of  $N$ -terminals without any finite junction part and the systems are inter-connected via arbitrary time-dependent coupling. We derive the generalized CGF and discuss the transient fluctuation theorem (TFT). For two-terminal situation we address the effect of coupling strength on XFT. We also obtain a Caroli-like transmission function for this setup which is useful for the interface study.

In the last part of the thesis, we consider the generalization of the FCS problem by including nonlinear interaction such as phonon-phonon interaction. Based on the nonequilibrium version of Feynman-Hellmann theorem we derive a formal expression for the generalized current in the presence of arbitrary nonlinear interaction. As an example, we consider a single harmonic oscillator with quartic onsite potential and derive the long-time CGF by considering only the first order diagram for the nonlinear self-energy. We also discuss the SSFT for this model.

In conclusion, applying NEGF and two-time quantum measurement method

we investigate FCS for energy transport through a phononic lead-junction-lead setup in both transient and steady-state regimes. For harmonic junction we obtain the CGF considering many important aspects which are relevant for the experimental situations. We also analyze FCS for lead-lead setup *i.e.*, without the junction part and explored transient and steady state fluctuation theorems. For general nonlinear junction we develop a formalism based on nonequilibrium version of Feynman-Hellmann theorem. The power of this general method is shown by considering an oscillator model with quartic onsite potential. The methods that we develop here for energy transport can be easily extended for the charge transport as shown by an example in the appendix.

# List of important Symbols and Abbreviations

Symbol	Description
$\xi$	counting field
$\mathcal{Z}(\xi)$	CF
$\ln \mathcal{Z}(\xi)$	CGF
$\mathcal{T}[\omega]$	Transmission matrix
$\text{Tr}_{j,\tau}$	Trace over both space and contour time
$\text{Tr}_{j,t,\sigma}$	Trace over space, real time and branch index
$\text{Tr}_{j,\omega,\sigma}$	Trace over space, frequency and branch index
$\Sigma$	Self-energy
$g_\alpha$	Bare or isolated Green's functions for $\alpha$ -th system
$G_0$	Green's function for harmonic junction
$G$	Green's function for anharmonic junction
$\check{A}$	Matrix $A$ in the Keldysh representation
$\mathbf{G}$	Matrix in the discretize contour or real time
$\hat{A}$	Operator $A$ is in the interaction picture
$\langle Q^n \rangle$	$n$ -th moment of $Q$
$\langle\langle Q^n \rangle\rangle$	$n$ -th cumulant of $Q$
$T_C$	Contour-ordering operator
$T, \bar{T}$	Time and anti-time ordered operators
$f_\alpha$	Bose-Einstein distribution function for $\alpha$ -th system
$\Gamma_\alpha$	Spectral function for $\alpha$ -th system
$\omega_0$	applied driving frequency

Abbreviation	Description
FCS	Full-counting statistics
NEGF	Nonequilibrium Green's function
CF	Characteristic function
CGF	Cumulant generating function
NESS	Nonequilibrium steady state
FT	Fluctuation theorem
TFT	Transient fluctuation theorem
SSFT	Steady state fluctuation theorem
XFT	Exchange fluctuation theorem
KMS	Kubo-Martin-Schwinger
GC	Gallavotti-Cohen
JE	Jarzynski equality
1D	One dimension

# List of Figures

2.1	The complex-time contour in Keldysh formalism . . . . .	43
3.1	Lead-junction-lead setup for thermal transport . . . . .	74
3.2	The complex time contour for product initial state . . . . .	88
3.3	The complex time contour for projected initial state . . . . .	98
3.4	Cumulants of heat for projected initial state for 1D linear chain . . . . .	112
3.5	Cumulants of heat for product initial state for 1D linear chain	113
3.6	Cumulants of heat for steady state initial state for 1D linear chain . . . . .	114
3.7	The structure of a graphene junction . . . . .	115
3.8	Cumulants of heat for graphene junction . . . . .	116
3.9	Correlations between left and right lead heat flux . . . . .	119
3.10	The cumulants for entropy production . . . . .	121
4.1	The Feynman diagram for one-point Green's function of the center in the presence of time-dependent force . . . . .	143
4.2	Energy current as a function of applied frequency for even number of particles . . . . .	151

4.3	Energy current as a function of applied frequency for odd number of particles . . . . .	152
4.4	Energy current as a function of system size . . . . .	153
4.5	Energy current vs applied frequency for different friction coefficient . . . . .	155
4.6	Energy current vs applied frequency for Ohmic bath . . . . .	159
5.1	A schematic representation for exchange fluctuation theorem setup . . . . .	166
5.2	The cumulants of heat as a function of measurement time for different time dependent coupling between the leads . . .	178
5.3	Current as a function of measurement time for different time-dependent coupling . . . . .	179
5.4	Plot of $\langle e^{-\Delta\beta Q_L} \rangle$ as a function measurement time for different coupling strength . . . . .	182
5.5	Cumulants of heat for finite leads . . . . .	185
6.1	Steady state cumulants with non-linear coupling strength . .	209
6.2	Thermal conductance with temperature . . . . .	210

# Chapter 1

## Introduction

The field of statistical mechanics can be divided into equilibrium and nonequilibrium statistical mechanics. Equilibrium statistical mechanics has a very simple and elegant structure and is applicable for systems which are not subjected to any thermodynamic affinities or forces. Depending on the type of the system the equilibrium probability distribution for the microscopic degrees of freedom is well known. For example, microcanonical distribution for isolated systems, canonical distribution for a system which exchange energy with a weakly coupled environment or a grand canonical distribution for system which exchange both energy and particle with the environment. Knowing the Hamiltonian of the system the main task is then to obtain the partition function, the derivative of which is related to experimentally measurable quantities such as average energy, specific heat etc.

On the contrary very little is known for nonequilibrium systems which are most ubiquitous in nature. Typically a system can be driven out of equilibrium by applying thermal gradients or chemical potential gradients across the boundaries or may be triggered by time dependent or non-conservative forces. Unlike equilibrium case, no such general form for the probability distribution for microscopic degrees of freedom is known in nonequilibrium physics.

One of the primary interest in the study of nonequilibrium physics is to understand the heat or charge conduction through the system of interest. These conduction processes were first described by phenomenological laws namely Ohm's law for electrical transport and Fourier's law for thermal transport [1–3]. These laws are applicable in the linear-response regime meaning the system is near to equilibrium, *i.e.*, for weak electric field, temperature gradient, etc. A significant amount of research is devoted to understand the necessary and the sufficient conditions for the validity of these laws and also to derive these relations starting from a microscopic description, which is still an open problem. On the other hand, how to extend these laws in the far from equilibrium regime haunted physicists over the decades.

It is only in the past decade that a major breakthrough happened in this field with the discovery of *fluctuation relations* which are valid for systems driven *arbitrarily far from equilibrium*. Fluctuation relations make rigorous predictions for different types of nonequilibrium processes beyond linear-response theory. In particular, it puts severe restriction on the form of

the probability distribution for different nonequilibrium quantities such as work, heat flux, total entropy which are generally referred to as the entropy production.

In the year 1993, Evans, Cohen and Morriss [4–6] presented their first numerical evidence which predicts that the probability distribution of nonequilibrium entropy production is not arbitrary, rather obey a simple relation which was later formulated as entropy fluctuation theorem. Since then extensive research has been carried out to extend this relation for stochastic, deterministic and thermostated systems in both classical and quantum regime. All these relations are now collectively called as the fluctuation theorems (FT). These theorems are important for number of reasons [7]:

- They explain how macroscopic irreversibility emerges naturally in systems that obey time-reversible dynamics and therefore shed light on Loschmidt's paradox.
- They quantify probabilities of violating second law of thermodynamics which could be significant for small systems or during small time intervals.
- They are valid for systems that are driven arbitrarily far from equilibrium.
- In the linear-response regime, they reproduce the fluctuation-dissipation relations, Green-Kubo formula, Onsager's reciprocity relations.
- These relations can be verified by performing experiments.

Over the past 15 years or so this particular field has gathered a lot of attention and many different types of fluctuation relations have been discovered. Here we will discuss few of them. Since this thesis is based on quantum fluctuations we will mainly focus on the quantum aspect of this theorem. However the results are also valid for classical systems.

## 1.1 Introduction to fluctuation theorems

Fluctuation relation is a microscopic statement about the second law of thermodynamics which states that the probability of positive entropy production in nonequilibrium systems is exponentially larger than the corresponding negative value, typically expressed in the form [8]

$$\frac{P_F(x)}{P_R(-x)} = \exp[a(x - b)], \quad (1.1)$$

where  $x$  is the quantity of interest, for example, nonequilibrium work ( $W$ ) by an external force, heat, etc.  $P_F(x)$  ( $P_R(x)$ ) is the probability distribution for the the forward ( $F$ ) (reversed ( $R$ )) process, explained later.  $a$  and  $b$  are real constants with information about the system's initial equilibrium properties. The above relation can also be expressed as

$$\langle \exp[-ax] \rangle = \int e^{-ax} P_F(x) dx = e^{-ab} \int P_R(-x) dx = \exp[-ab]. \quad (1.2)$$

To derive different types of FT for classical and quantum systems two main

ingredients are required:

1. Initial condition for the system which is supposed to be in equilibrium and is described by the canonical distribution  $\rho(t = 0) = e^{-\beta\mathcal{H}(0)}/Z_0$  where  $\mathcal{H}$  is the Hamiltonian of the system,  $Z_0 = \text{Tr}(e^{-\beta\mathcal{H}(0)})$ ,  $\beta \equiv (k_B T)^{-1}$  and  $T$  is the temperature. For the classical case,  $\mathcal{H}$  becomes the function of phase space variables and the trace in  $Z_0$  is replaced by the integration over phase space.
2. The principle of microreversibility of the underlying dynamics [8].

In quantum case another crucial concept that is required to derive the FT is known as the two-time projective quantum measurement method [8–10] which we will elaborate in the later part of this chapter.

### 1.1.1 Jarzynski Equality

The first type of fluctuation relation deals with the fluctuation of work for an *isolated* Hamiltonian system  $\mathcal{H}(\lambda(t))$  that is driven by an external time dependent force protocol  $\lambda(t)$  with arbitrary driving speed. In the year 1977 Bochkov and Kuzovlev first provided a single compact classical expression for the work fluctuation [11]. Later in 1997 it was generalized by Jarzynski [12, 13] and thereby known as Jarzynski equality (JE). JE relates the nonequilibrium work with equilibrium free energy difference. In this prescription the force protocol  $\lambda(t)$  drives the system away from equilibrium

starting from the state  $A$  at time  $t = 0$  with Hamiltonian  $\mathcal{H}(\lambda(0))$  to the state  $B$  at  $t = \tau$  with Hamiltonian  $\mathcal{H}(\lambda(\tau))$ . During this process the work done by the external protocol defined as

$$W = \int_0^\tau \dot{\lambda} \frac{\partial \mathcal{H}(\lambda)}{\partial \lambda} dt, \quad (1.3)$$

satisfies the following equality

$$\left\langle \exp \left( -\beta W \right) \right\rangle = \exp(-\beta \Delta F), \quad (1.4)$$

where  $\beta$  is the initial equilibrium temperature (coming from the initial condition) and  $\Delta F$  is the free energy difference between final and initial equilibrium state corresponding to the Hamiltonian  $\mathcal{H}(\lambda(\tau))$  and  $\mathcal{H}(\lambda(0))$  respectively. The average here is taken over different realizations of work for the fixed protocol  $\lambda(t)$  and fixed initial condition. The remarkable fact about JE is that the free energy difference can be determined via a nonequilibrium, irreversible process which is of great practical importance. Applying Jensen inequality for real convex function, *i.e.*,  $\langle e^x \rangle \geq e^{\langle x \rangle}$ , to JE implies  $\langle W \rangle \geq \Delta F$  which is consistent with thermodynamic prediction. Note that JE is also valid when the system is in contact with the environment either via weak or strong coupling. For proof see [14, 15]. A simple proof for JE for the isolated quantum system starting with canonical initial condition is given later.

### 1.1.2 Crooks relation

Crooks [16] later provided a significant generalization to the JE by considering the probability distribution of work  $P(W)$  for the forward ( $F$ ) and the reverse ( $R$ ) process. Here forward process means that the external protocol  $\lambda(t)$  acts on the equilibrium state  $A$  at time  $t = 0$  and it ends at the nonequilibrium state  $B$  at time  $t = \tau$ . In the reverse process, the initial state  $B$  is first allowed to reach equilibrium and then the system evolves till  $t = \tau$  with the reversed protocol  $\tilde{\lambda}(t) = \lambda(\tau - t)$ . As a consequence of the time-reversal symmetry of the microscopic evolution Crooks showed that

$$\frac{P_F(W)}{P_R(-W)} = \exp\left(\beta(W - \Delta F)\right). \quad (1.5)$$

Jarzynski equality can be trivially obtained from Crooks relation by first multiplying both sides  $e^{-\beta W} P_R(-W)$  and then integrate over  $W$ .

### 1.1.3 Gallavotti-Cohen FT

Another class of FT is concerned with the entropy fluctuation in nonequilibrium steady state for closed systems described by deterministic thermostated equations of motions [4–6, 17, 18] as well as for open systems modeled via stochastic differential equations [19–21]. In this case a generic form is given as

$$\lim_{\tau \rightarrow \infty} \frac{1}{\tau} \ln \left[ \frac{P(S = \sigma\tau)}{P(S = -\sigma\tau)} \right] = \sigma, \quad (1.6)$$

where  $S$  is the net entropy-production during the nonequilibrium process and  $\sigma$  is the entropy production rate. For example, a system connected with two heat baths at different temperature  $T_L$  and  $T_R$ , the entropy production  $S$  is given as  $S = (T_R^{-1} - T_L^{-1})Q$  where  $Q$  is amount of heat transferred during the time  $\tau$ . Then the above relation says that in steady-state it is more likely to have heat flow from hotter to colder end ( $Q$  is positive) rather than in the opposite direction ( $Q$  is negative). This particular fluctuation symmetry is known as Gallavotti-Cohen (GC) relation and is valid in the asymptotic limit. Note that Crooks FT also resembles GC symmetry if one identifies  $\sigma\tau = (W - \Delta F)/T$ . However the main difference is that GC is valid in the long-time limit and therefore known as steady-state fluctuation theorem (SSFT) whereas Crooks theorem holds for any finite time  $\tau$  and often named as transient fluctuation theorem (TFT).

#### 1.1.4 Experimental verification of Fluctuation theorems

In recent times, rapid experimental progress has helped to verify some of these FT for micro and mesoscopic systems where fluctuations are large. In 2002, Evans's group verified the integrated version of FT [22] by performing an experiment with a microscopic bead which is captured in an optical trap and dragged through water. They observed the violation of second law *i.e.*, negative entropy production trajectories over time scales of the order of seconds. Later the same group verified the transient version of the FT

[23, 24].

The JE is also verified in macromolecule pulling experiments, such as RNA and single molecule [25, 26] and it is shown that how equilibrium free energies could be extracted from these experiments. Subsequently Collin et al. [27] confirms the Crooks relation by performing similar RNA pulling type experiment. Several other interesting experiments have also been carried out to verify FT, see for example [28–32]. For a review on FT experiments see [33].

### 1.1.5 Quantum Fluctuation theorems

Fluctuation theorems were first derived and formulated for classical systems. The derivations were mostly based on the notion of classical trajectory picture. The extension of these theorems to the quantum regime however was not at all straightforward for the following reasons:

- The absence of trajectory picture in the quantum domain.
- Difficulty in generalizing the definitions for work, heat because of the noncommutative nature of the operators at different time.

Originally Bochkov and Kuzovlev [11] tried to extend their classical results to the quantum regime by defining the work operator in analogy with classical expression but failed to provide any quantum analog. Many

other authors [34–36] subsequently tried in the same direction and arrived at the conclusion that quantum analog of JE is satisfied only when the time-dependent Hamiltonian  $\mathcal{H}(t)$  commute at different times *i.e.*,  $[\mathcal{H}(t), \mathcal{H}(t')] = 0$  for any  $t, t'$  which is obviously not valid in general.

### **Work is not an observable**

Kurchan, Tasaki, Mukamel and Talkner et al. [37–43] later pointed out that work is not a quantum observable and cannot be represented by a single Hermitian operator. Therefore its eigenvalue cannot be determined by performing single quantum measurement. Rather work characterizes a process from initial time to the final time just like work in the thermodynamical sense which is not a state function. Thus in order to obtain the statistics for work, the Hamiltonian of the system  $\mathcal{H}(t)$  must be measured twice, first at the initial time  $t = 0$  and then at the final time  $t = \tau$ . The value of the work, for a single realization, is then given as the difference of the two eigenvalues obtained from the two measurements. By repeating this measurement procedure with the same initial condition and the force protocol the distribution  $P(W)$  is constructed. This particular approach of getting the distribution is known as the two-time measurement method and is the starting point to derive different quantum fluctuation relations.

In the following, we first review the two-time measurement method following the references [8–10] and then present a simple derivation for one particular type of FT, known as exchange fluctuation theorem (XFT), to illustrate the main concepts.

## 1.2 Two-time quantum Measurement Method

In this section, we elaborate the concept of two-time measurement method which will be used in the subsequent chapters. Let us suppose that we are interested in the statistics of a quantity which can be written as the difference of an operator at two different time. For example, the work operator for an isolated driven system, described by a time-dependent Hamiltonian  $\mathcal{H}(t)$ , can be defined as the change of energy of the system *i.e.*,

$$\mathcal{W}(t) = \mathcal{H}^H(t) - \mathcal{H}(0), \quad (1.7)$$

(calligraphic fonts are used to represent quantum operators) with  $\mathcal{H}^H(t) = \mathcal{U}^\dagger(t, 0)\mathcal{H}(t)\mathcal{U}(t, 0)$  is the Hamiltonian in the Heisenberg picture.  $\mathcal{U}(t, 0) = T \exp \left[ -\frac{i}{\hbar} \int_0^t \mathcal{H}(t') dt' \right]$  for  $t > t'$ . Therefore let us consider a general operator  $\mathcal{A}(t)$  in the Schrödinger picture which may have explicit time dependence. The operator in its eigenbasis can be written as

$$\mathcal{A}(t) = \sum_{a_t} a_t |a_t\rangle \langle a_t| = \sum_{a_t} a_t \Pi_{a_t}, \quad (1.8)$$

where  $a_t$  is the instantaneous eigenvalue (discrete) and  $\Pi_{a_t}$  is the corresponding projection operator satisfying  $\Pi_{a_t}^2 = \Pi_{a_t}$  and  $\sum_{a_t} \Pi_{a_t} = 1$ . Let us also assume that the full system is in a pure state  $|\Psi_0\rangle$  at  $t = 0$ . The generalization for the mixed states can be done easily. The concept of two-time measurement is the following:

1. First we measure the operator  $\mathcal{A}(t)$  at  $t = 0$ . Then according to

quantum mechanics, the outcome of the measurement can only be an eigenvalue of the (Schrödinger) operator  $\mathcal{A} = \mathcal{A}(t = 0)$  and the wave function collapses to an eigenstate of  $\mathcal{A}$ . Let the eigenvalue is  $a_0$  and the corresponding eigenstate is  $|a_0\rangle$ . Then we can write

$$\mathcal{A}|a_0\rangle = a_0|a_0\rangle, \quad \Pi_{a_0} = |a_0\rangle\langle a_0|. \quad (1.9)$$

We assume that the eigenvalues are discrete and nondegenerate. The probability of obtaining the eigenvalue  $a_0$  is given by

$$P(a_0) = |\langle a_0|\Psi_0\rangle|^2 = \text{Tr}[\rho_0\Pi_{a_0}], \quad (1.10)$$

where  $\rho(0) = |\Psi_0\rangle\langle\Psi_0|$ . Immediately after the first measurement at  $t = 0$ , the wave function collapses to

$$|\Psi'_0\rangle = \frac{\Pi_{a_0}|\Psi_0\rangle}{\sqrt{\text{Tr}[\Pi_{a_0}\rho_0]}}. \quad (1.11)$$

2. Then propagate the state  $|\Psi'_0\rangle$  up to the time of interest  $t$  with the full Hamiltonian  $\mathcal{H}(t)$  and then perform a second measurement of the operator  $\mathcal{A}(t)$ . The outcome now is another eigenvalue say  $a_t$ . Then the conditional probability to obtain  $a_t$  given  $a_0$  is given as

$$P(a_t|a_0) = |\langle a_t|\mathcal{U}(t, 0)|\Psi'_0\rangle|^2 = \frac{1}{\text{Tr}[\rho_0\Pi_{a_0}]} \text{Tr}[\Pi_{a_0}\rho(0)\Pi_{a_0}\mathcal{U}^\dagger(t, 0)\Pi_{a_t}\mathcal{U}(t, 0)], \quad (1.12)$$

where  $\mathcal{U}(t, 0)$  is the unitary operator satisfies the Schrödinger equation

$$i\hbar \frac{\partial \mathcal{U}(t, 0)}{\partial t} = \mathcal{H}(t) \mathcal{U}(t, 0). \quad (1.13)$$

Therefore the joint probability of getting  $a_0$  at time 0 and  $a_t$  at time  $t$  is given as

$$P(a_t, a_0) = P(a_t|a_0)P(a_0) = \text{Tr} \left[ \Pi_{a_0} \rho(0) \Pi_{a_0} \mathcal{U}^\dagger(t, 0) \Pi_{a_t} \mathcal{U}(t, 0) \right]. \quad (1.14)$$

If the initial state is in a mixed state, we add up the initial probability classically, *i.e.*, the density matrix will be given as

$$\rho(0) = \sum_k w_k |\Psi_0^k\rangle \langle \Psi_0^k|, \quad w_k > 0, \quad \sum_k w_k = 1. \quad (1.15)$$

Now, we are interested in the probability distribution for  $Q$  given as difference of the eigenvalues  $a_t$  and  $a_0$  respectively *i.e.*,  $Q = a_t - a_0$ . ( $Q$  of non-calligraphic font is a classical variable) Then the probability distribution  $P(Q)$  can be constructed as

$$P(Q) = \sum_{a_t, a_0} \delta(Q - (a_t - a_0)) P(a_t, a_0), \quad (1.16)$$

where  $\delta(x)$  is the Dirac-delta distribution. The characteristic function (CF) associated with this probability distribution  $P(Q)$  is defined as

$$\mathcal{Z}(\xi) = \int_{-\infty}^{\infty} dQ e^{i\xi Q} P(Q) = \sum_{a_t, a_0} e^{i\xi(a_t - a_0)} P(a_t, a_0). \quad (1.17)$$

Substituting the expression for  $P(a_t, a_0)$ , using the cyclic property of the trace and the properties of the projection operator we obtain

$$\begin{aligned}
 \mathcal{Z}(\xi) &= \sum_{a_t, a_0} e^{i\xi(a_t - a_0)} \text{Tr} \left[ \Pi_{a_0} \rho(0) \Pi_{a_0} \mathcal{U}^\dagger(t, 0) \Pi_{a_t} \mathcal{U}(t, 0) \right] \\
 &= \sum_{a_t, a_0} \text{Tr} \left[ \Pi_{a_0} \rho(0) \Pi_{a_0} e^{-i\xi \mathcal{A}(0)} \mathcal{U}^\dagger(t, 0) \Pi_{a_t} e^{i\xi \mathcal{A}(t)} \mathcal{U}(t, 0) \right] \\
 &= \text{Tr} \left[ \rho'(0) e^{-i\xi \mathcal{A}(0)} e^{i\xi \mathcal{A}^H(t)} \right] \\
 &= \langle e^{-i\xi \mathcal{A}(0)} e^{i\xi \mathcal{A}^H(t)} \rangle_{\rho'(0)} = \langle e^{i\xi \mathcal{A}^H(t)} e^{-i\xi \mathcal{A}(0)} \rangle_{\rho'(0)}, \quad (1.18)
 \end{aligned}$$

where now the average is with respect to the modified density operator  $\rho'(0) = \sum_{a_0} \Pi_{a_0} \rho(0) \Pi_{a_0}$ , containing information about the initial measurement. We call  $\rho'(0)$  as the *projected* density matrix. Note that the projected density matrix coincides with the initial density matrix if  $\rho(0)$  commutes with  $\Pi_{a_0}$  and therefore commutes with the operator  $\mathcal{A}(0)$  *i.e.*,

$$\rho'(0) = \rho(0) \Leftrightarrow [\rho(0), \mathcal{A}(0)] = 0. \quad (1.19)$$

This particular derivation can be easily generalized for systems in contact with environment as shown in chapter 3.

### **Example: Work operator and JE**

For the work operator defined in Eq. (1.7) we can identify  $\mathcal{A}(t)$  as  $\mathcal{H}(t)$ . Therefore the CF corresponding to the work distribution  $P(W)$  can be immediately written down as

$$\mathcal{Z}(\xi) \equiv \langle e^{i\xi W} \rangle = \langle e^{-i\xi \mathcal{H}(0)} e^{i\xi \mathcal{H}^H(t)} \rangle_{\rho'(0)}. \quad (1.20)$$

We now choose the initial condition for the isolated system as  $\rho(0) = e^{-\beta\mathcal{H}(0)}/Z_0$  by imagining that at  $t < 0$  the system was in weak contact with a heat bath at temperature  $T = 1/k_B\beta$ . Therefore we can write

$$\mathcal{Z}(\xi) = \frac{1}{Z_0} \text{Tr} \left[ e^{-\beta\mathcal{H}(0)} e^{-i\xi\mathcal{H}(0)} e^{i\xi\mathcal{H}^H(t)} \right]. \quad (1.21)$$

Now substituting  $\xi = i\beta$  and defining  $Z_t = \text{Tr}[\exp[-\beta\mathcal{H}(t)]]$  we obtain

$$\mathcal{Z}(i\beta) = \langle \exp[-\beta W] \rangle = \frac{Z_t}{Z_0} = \exp[-\beta\Delta F], \quad (1.22)$$

with  $F(t) = -\frac{1}{\beta} \ln Z_t$  and  $\Delta F = F(t) - F(0)$  is the free energy change between the final and initial equilibrium state.

### 1.3 Quantum Exchange Fluctuation theorem

In this section we derive one particular form of the fluctuation theorem known as Exchange Fluctuation theorem (XFT) to illustrate how fluctuation symmetry emerges out from very few basic fundamental principles. For the derivation we mostly follow reference [8]. We will also discuss the FT in chapter 5.

Using the principle of microreversibility XFT was first written down by Jarzynski and Wójcik [44] for both classical and quantum systems and it was generalized later by Saito and Utsumi [45] and Andrieux et al. [46].

This FT is valid for several interacting systems, initially at different temperatures and chemical potentials, which are allowed to interact within the time interval  $[0, \tau]$ . The interaction between the systems could be time-dependent. The total Hamiltonian is then written as

$$\mathcal{H}(\mathcal{V}_t) = \sum_{i=1}^r \mathcal{H}_i + \mathcal{V}_t \quad (1.23)$$

$\mathcal{H}_i$  is the Hamiltonian of the  $i$ -th system and  $\mathcal{V}_t$  is the time-dependent interaction between the systems which is switched on at time  $t = 0$  and switched off at  $t = \tau$  and nonzero within the interval  $[0, \tau]$ .

We assume that the systems are initially decoupled and present at their respective equilibrium temperature and chemical potential. Then the initial condition for the density operator is given as

$$\rho_0 = \prod_i \rho_i = \prod_{i=1}^r \frac{e^{-\beta_i[\mathcal{H}_i - \mu_i \mathcal{N}_i]}}{\mathcal{E}_i}, \quad (1.24)$$

where  $\beta_i, \mu_i$  and  $\mathcal{E}_i = \text{Tr} e^{-\beta_i[\mathcal{H}_i - \mu_i \mathcal{N}_i]}$  the inverse temperature, chemical potential and grand partition function respectively of  $i$ -th system.  $\mathcal{N}_i$  here is the particle number operator. It is also assumed that the particle numbers in each subsystems are conserved in the absence of interaction *i.e.*,  $[\mathcal{H}_i, \mathcal{N}_i] = 0$ . So in this case we can simultaneously measure both  $\mathcal{H}_i$  and  $\mathcal{N}_i$  for each system  $i$  as they all commute with each other. We perform two-time measurement one at  $t = 0$  and another at  $t = \tau$  for all  $\mathcal{H}_i$  and  $\mathcal{N}_i$ .

Let us assume that after the first measurement of all  $\mathcal{H}_i$ 's and all  $\mathcal{N}_i$ 's at  $t = 0$  the wave function collapses onto a common eigenstate  $|\psi_n\rangle$  with eigenvalues  $E_n^i$  and  $N_n^i$ . Then the wavefunction evolves under the full Hamiltonian  $\mathcal{H}(\mathcal{V}_t)$  up to time  $\tau$  when the second measurement of all  $\mathcal{H}_i$  and all  $\mathcal{N}_i$ 's is performed and the wave function collapse to another common eigenstate  $|\psi_m\rangle$  with eigenvalues  $E_m^i$  and  $N_m^i$ .

Using Eq. (1.14) the joint probability distribution  $p(m, n; \mathcal{V})$  for obtaining the eigenvalues  $E_n^i, N_n^i$  at  $t = 0$  and  $E_m^i, N_m^i$  at  $t = \tau$  is given as

$$p(m, n; \mathcal{V}) = p_{n \rightarrow m}[\mathcal{V}] p_n^0, \quad (1.25)$$

where  $p_{n \rightarrow m}[\mathcal{V}]$  is the transition probability from state  $|\psi_n\rangle$  to  $|\psi_m\rangle$  given as

$$p_{n \rightarrow m}[\mathcal{V}] = |\langle \psi_m | \mathcal{U}(\tau, 0) | \psi_n \rangle|^2 \quad (1.26)$$

with  $\mathcal{U}(t, 0) = T \exp \left[ -\frac{i}{\hbar} \int_0^t \mathcal{H}(\mathcal{V}_{t'}) dt' \right]$  and  $p_n^0 = \prod_i e^{-\beta_i [E_n^i - \mu_i N_n^i]} / \mathcal{E}_i$  is the initial probability for the  $n$ -th state.

Now let us construct the joint probability distribution for energy and particle exchanges  $p[\Delta \mathbf{E}, \Delta \mathbf{N}; \mathcal{V}]$  where the notation  $\Delta \mathbf{E}$  and  $\Delta \mathbf{N}$  is for the individual energy and particle number changes of all the systems *i.e.*,  $\Delta E_1, \Delta E_2, \dots, \Delta E_r$  and  $\Delta N_1, \Delta N_2, \dots, \Delta N_r$  respectively. The joint probability distribution  $p[\Delta \mathbf{E}, \Delta \mathbf{N}; \mathcal{V}]$  is then given as

$$p[\Delta \mathbf{E}, \Delta \mathbf{N}; \mathcal{V}] = \sum_{m,n} \left( \prod_{i=1}^r \delta(\Delta E_i - (E_m^i - E_n^i)) \delta(\Delta N_i - (N_m^i - N_n^i)) \right) p(m, n; \mathcal{V}), \quad (1.27)$$

Now if the total Hamiltonian commutes with the time-reversal operator  $\Theta$  at any instant of time *i.e.*,  $\Theta\mathcal{H}(\mathcal{V}_t) = \mathcal{H}(\mathcal{V}_t)\Theta$  then the microreversibility of non-autonomous system implies that  $p_{n \rightarrow m}[\mathcal{V}] = p_{m \rightarrow n}[\tilde{\mathcal{V}}]$  where  $\tilde{\mathcal{V}}_t = \mathcal{V}_{\tau-t}$  is the time-reversed protocol. Therefore we simply have

$$\frac{p(m, n, \mathcal{V})}{p(n, m, \tilde{\mathcal{V}})} = \frac{p_n^0}{p_m^0} = \prod_{i=1}^r e^{\beta_i \left[ (E_m^i - E_n^i) - \mu_i (N_m^i - N_n^i) \right]} \quad (1.28)$$

Then using Eq. (1.27) we write

$$\begin{aligned} p[\Delta\mathbf{E}, \Delta\mathbf{N}; \mathcal{V}] &= \sum_{m,n} \prod_i \delta(\Delta E_i - (E_m^i - E_n^i)) \delta(\Delta N_i - (N_m^i - N_n^i)) p(n, m; \tilde{\mathcal{V}}) \frac{p_n^0}{p_m^0} \\ &= \left( \prod_{i=1}^r e^{\beta_i (\Delta E_i - \mu_i \Delta N_i)} \right) \sum_{m,n} \prod_i \delta(\Delta E_i - (E_m^i - E_n^i)) \delta(\Delta N_i - (N_m^i - N_n^i)) p(n, m; \tilde{\mathcal{V}}) \\ &= \left( \prod_{i=1}^r e^{\beta_i (\Delta E_i - \mu_i \Delta N_i)} \right) \sum_{m,n} \prod_i \delta(\Delta E_i - (E_n^i - E_m^i)) \delta(\Delta N_i - (N_n^i - N_m^i)) p(m, n; \tilde{\mathcal{V}}) \\ &= \left( \prod_{i=1}^r e^{\beta_i (\Delta E_i - \mu_i \Delta N_i)} \right) p[-\Delta\mathbf{E}, -\Delta\mathbf{N}; \tilde{\mathcal{V}}] \end{aligned} \quad (1.29)$$

Therefore we have

$$\frac{p[\Delta\mathbf{E}, \Delta\mathbf{N}; \mathcal{V}]}{p[-\Delta\mathbf{E}, -\Delta\mathbf{N}; \tilde{\mathcal{V}}]} = \prod_{i=1}^r e^{\beta_i [\Delta E_i - \mu_i \Delta N_i]}. \quad (1.30)$$

The above relation can also be derived starting from the definition of the CF

$$\mathcal{Z}(\{\xi_\alpha^e\}, \{\xi_\alpha^p\}, \mathcal{V}) = \langle e^{\sum_\alpha i\xi_\alpha^e \mathcal{H}_\alpha^H(t) + i\xi_\alpha^p \mathcal{N}_\alpha^H(t)} e^{\sum_\alpha -i\xi_\alpha^e \mathcal{H}_\alpha(0) - i\xi_\alpha^p \mathcal{N}_\alpha(0)} \rangle. \quad (1.31)$$

In this case the fluctuation symmetry reads as

$$\mathcal{Z}(\{\xi_\alpha^e\}, \{\xi_\alpha^p\}, \mathcal{V}) = \mathcal{Z}(\{-\xi_\alpha^e + i\beta_\alpha\}, -\{\xi_\alpha^p - i\mu_\alpha\beta_\alpha\}, \tilde{\mathcal{V}}), \quad (1.32)$$

where  $\{\xi_\alpha^e\}$  and  $\{\xi_\alpha^p\}$  is the set of counting fields for the energy and particle number respectively. Inverse Fourier transform of this CF will produce the symmetry given in Eq. (1.30).

## 1.4 Full-Counting statistics (FCS)

As mentioned before that with the advent of micro-manipulation techniques and nanotechnologies in recent years, it is now possible to measure probabilities of nonequilibrium quantities such as  $P(W)$  by manipulating single atoms or electrons. This generate an immense interest to both experimentalists and theorists to study nonequilibrium problems in small or low-dimensional systems such as molecular junction which has already shown many practical advancement [47–51]. Since these small systems are always in contact with the environment they show random thermal and quantum fluctuations, also called noise, which are typically of the same order (few times  $k_B T$ ) with the system energy scale. This fluctuations shows large deviations from systems average behavior and thus make it an experimentally measurable quantity. This random fluctuations may even lead to instantaneous transfer of heat or charge against the gradients and could play an important role in controlling the transport. Therefore for small

systems understanding the properties of higher order fluctuations seems necessary, in the context of transport theory, which cannot be obtained just by calculating the mean value. With increasing system size however these relative fluctuations are suppressed with  $1/\sqrt{N}$ , where  $N$  is the system size, making the average as the dominant behavior and the fluctuations hard to measure.

Generically speaking, to extract information about these fluctuations it is necessary to talk about the statistical distribution  $P(Q)$ , where  $Q$  is the quantity of interest such as heat, charge, transferred through the system during a time interval  $\tau$ . From this distribution, we can go on to calculate not only the mean and the variance of  $Q$  but in principle all higher order fluctuations such as skewness, Kurtosis etc. Therefore  $P(Q)$  constitutes a complete knowledge (zero frequency) about the properties of  $Q$  and thus known as the *full-counting statistics* (FCS). Finding out this distribution function for different nonequilibrium system is one of the key interest in the field of nonequilibrium physics.

Parallel to this distribution function a quantity which is often useful for the actual calculation is the Fourier transformation of this distribution, known as the characteristic function (CF). It contains the same information as the distribution function. The CF is defined as,

$$\mathcal{Z}(\xi) \equiv \langle e^{i\xi Q} \rangle \equiv \int dQ e^{i\xi Q} P(Q), \quad (1.33)$$

(If  $Q$  is a discrete variable, the integration should be replaced by a summation) where  $\xi$  is known as the counting field or the counting parameter. Once  $\mathcal{Z}(\xi)$  is known  $P(Q)$  can be obtained by an inverse Fourier transform. The CF is similar in notion with the partition function in equilibrium statistical physics. The moments of  $Q$  (denoted by single angular bracket) are obtained from the CF by taking derivatives with respect to the counting field  $\xi$  and evaluated at  $\xi = 0$ . *i.e.*,

$$\langle Q^n \rangle = \left. \frac{\partial^n \mathcal{Z}(\xi)}{\partial (i\xi)^n} \right|_{\xi=0}. \quad (1.34)$$

In analogy with the equilibrium free-energy, the logarithm of the CF is also defined and is known as the cumulant generating function (CGF). It generates the irreducible moments or the cumulants (denoted by double angular bracket) of  $Q$  given as

$$\langle\langle Q^n \rangle\rangle = \left. \frac{\partial^n \ln \mathcal{Z}(\xi)}{\partial (i\xi)^n} \right|_{\xi=0}. \quad (1.35)$$

The cumulants can be expressed in terms of the moments for example

$$\begin{aligned} \langle\langle Q \rangle\rangle &= \langle Q \rangle, \\ \langle\langle Q^2 \rangle\rangle &= \langle Q^2 \rangle - \langle Q \rangle^2 = \langle (Q - \langle Q \rangle)^2 \rangle, \\ \langle\langle Q^3 \rangle\rangle &= \langle Q^3 \rangle - 3\langle Q \rangle^2 \langle Q \rangle + 2\langle Q \rangle^3 = \langle (Q - \langle Q \rangle)^3 \rangle, \\ \langle\langle Q^4 \rangle\rangle &= \langle Q^4 \rangle - 3\langle Q^2 \rangle^2 - 4\langle Q^3 \rangle \langle Q \rangle + 12\langle Q^2 \rangle \langle Q \rangle^2 - 6\langle Q \rangle^4, \end{aligned} \quad (1.36)$$

and similarly for higher orders. The first cumulant, same as the moment, is the average value of  $Q$  and represents the peak of the distribution  $P(Q)$ . The second cumulant  $\langle\langle Q^2 \rangle\rangle = \langle Q^2 \rangle - \langle Q \rangle^2$  is the fluctuation about the mean value and represents the width of the distribution. The third cumulant, known as skewness, describes the asymmetry of the distribution. In the same way all the higher order cumulants give specific information and thus construct the distribution function.

The theory of FCS has recently become a subject of significant interest in the study of quantum transport. But it has its origin dates back in quantum optics where the statistics of the number of photons, emitted from a source, is studied by counting them using a photo-detector [52–54]. Thereafter Levitov and Lesovik apply this concept for electrons in mesoscopic systems where the transmission of single electrons through a conductor is counted using a spin detector by coupling it with the current operator [55, 56]. This coupling parameter turns out to be the counting field for the problem. Based on the scattering matrix approach these authors for the first time give a definite answer for charge transport of non-interacting electrons in a two-terminal setup by obtaining the CF. Their pioneering work is now celebrated as Levitov-Lesovik formula. Over the years numerous other techniques are developed to study FCS for charge transport in different nonequilibrium systems. For example, a semi-classical theory is put forward by Pilgram et al. [57] based on stochastic path integral. Later on Keldysh Green’s function approach to FCS is proposed by Nazarov et al. [58]. Using these approaches many works followed [9, 59–61]. With

the physics of noninteracting electrons well understood, the full counting statistics of strongly interacting systems is now actively pursued [62–65]. Recently, experimentalists have been able to determine the FCS for electrons in quantum dot systems [66–68].

## 1.5 Problem addressed in this thesis

Study of FCS for electrons have achieved a lot of progress since the pioneering work by Levitov and Lesovik. But in contrast to the FCS for electron transport, much less attention has been paid for FCS study of heat transport via phonons. Although calculating steady state heat current through nonequilibrium lattice systems is one of the most well studied aspects of nonequilibrium physics [1, 2, 69, 70], the extension to FCS study for these systems is proposed recently by Saito and Dhar [71]. They obtain the long-time limit for the CGF of heat for one-dimensional linear chain connected with two thermal baths and derived an equivalent form of Levitov-Lesovik formula for phonons. Later on Ren et al. study FCS problem for two-level systems [72, 73] using quantum master equation approach. FCS of energy fluctuations in a driven quantum resonator is recently carried out by Clerk [74]. Most of these current theories however mainly focus on the asymptotic limit of the CF where the initial distribution as well as the quantum effect of measurement generally speaking do not play any role. Therefore one of the main aim of this thesis is to study the FCS for heat transport in general lattice systems, both harmonic and anharmonic, treating transient

and asymptotic limit on equal footing. We study the transport problems from a very general perspective such as, analyzing the effects due to different initial conditions of the density operator, investigating the effects of quantum measurement etc . Moreover we enquire the conditions that leads to different types of FT's by obtaining the CF. The main objectives of this thesis are

- To develop a rigorous formalism based on nonequilibrium Green's functions (NEGF) and two-time quantum measurement method to study the FCS problem for a ballistic lead-junction-lead system considering many relevant aspects such as incorporating both transient and steady state behavior, time-dependent coupling between the leads and the center, finite size of the leads, time-dependent driving force etc.
- To examine conditions which leads to the steady state fluctuation theorems for these models.
- To generalize the theory for  $N$ -terminals with and without the center. For without the junction setup a recent experiment validates exchange fluctuation theorem [75].
- To extend the ballistic FCS theory for general anharmonic lattice systems employing nonequilibrium version of Feynman-Hellmann theorem.

The result of the present research may have significance on the understanding of the FCS as well as the fluctuation theorems for phonons transport both in transient and steady state for general lattice systems. It provide insight on the two-time measurement aspect which is the central ingredient to obtain correct probability distribution in the sense of fluctuation symmetry. Some of these results are worthy of experimental verifications. A recent experiment by Clerk et al [76] has measured phonon shot noise of mechanical resonator which also seems to be a potential candidate for FCS experiments.

It is worth mentioning that a significant progress has been achieved in the FCS for heat transport in the classical regime. Using Langevin dynamics Kundu et al. [77] presented analytical results for harmonic junction which later generalized for arbitrary harmonic network by Saito and Dhar [78]. Few numerical studies has also addressed FCS problems for nonlinear systems [79]. Very recently an exact result in classical nonlinear molecular junction is obtained by Liu et al. [80].

## 1.6 Thesis structure

In the following of this thesis, we will introduce the Nonequilibrium Green's function (NEGF) method in chapter 2 which will be used extensively in the later chapters; followed by the study of FCS for lead-junction-lead ballistic system in chapter 3. In chapter 4 we study the the FCS and heat generation

due to driven force in the junction part. In chapter 5 we extend this FCS study for  $N$ -terminal setup without the junction. In chapter 6 we develop a method to generalize the FCS approach for arbitrary nonlinear junction. Finally a conclusion of this study and future prospects is given in chapter 7.

# Bibliography

- [1] A. Dhar, *Adv. in Phys.*, **57**, 457-537 (2008).
- [2] S. Lepri, R. Livi, and A. Politi, *Phys. Rep.* **377**, 1 (2003).
- [3] F. Bonetto, J. L. Lebowitz, and L. Rey-Bellet, “Fourier’s Law: A Challenge to Theorists,” *Mathematical Physics 2000* (Imp. Coll. Press, London, 2000).
- [4] D. J. Evans, E. G. D. Cohen, and G. P. Morriss, *Phys. Rev. Lett.* **71**, 2401 (1993).
- [5] G. Gallavotti and E. G. D. Cohen. *Phys. Rev. Lett.* **74**, 2694 (1995).
- [6] G. Gallavotti and E. G. D. Cohen. *J. Stat. Phys.* **80**, 931 (1995).
- [7] D. J. Evans and D. J. Searles, *Adv. Phys.* **51**, 1529 (2002).
- [8] M. Campisi, P. Hänggi, and P. Talkner, *Rev. Mod. Phys.* **83**, 771 (2011).
- [9] M. Esposito, U. Harbola, and S. Mukamel, *Rev. Mod. Phys.* **81**, 1665 (2009).

## BIBLIOGRAPHY

---

- [10] J. von Neumann, *Mathematical Foundations of Quantum Mechanics*, Princeton Univ. Press, Princeton, (1955).
- [11] G. N. Bochkov, and Y. E. Kuzovlev, *Sov. Phys. JETP* **45**, 125 (1977).
- [12] C. Jarzynski, *Phys. Rev. Lett.* **78**, 2690 (1997).
- [13] C. Jarzynski, *Annu. Rev. Cond. Matter Phys.* **2**, 329-351, (2011).
- [14] P. Talkner, M. Campisi, and P. Hänggi, *J. Stat. Mech.* P02025 (2009).
- [15] M. Campisi, P. Talkner, and P. Hänggi, *Phys. Rev. Lett.* **102**, 210401 (2009).
- [16] G. E. Crooks, *Phys. Rev. E* **60**, 2721 (1999).
- [17] D. J. Evans and D. J. Searles, *Phys. Rev. E* **50**, 1645 (1994).
- [18] D. J. Evans and D. J. Searles, *Phys. Rev. E* **52**, 5839 (1995).
- [19] J. L. Levowitz, and H. Spohn, *J. Stat. Phys.* **95**, 333 (1999).
- [20] T. Hatano, and S. I. Sasa, *Phys. Rev. Lett.* **86**, 3463 (2001).
- [21] U. Seifert, 2005, *Phys. Rev. Lett.* **95**, 040602 (2005).
- [22] G. M. Wang, E. M. Sevick, E. Mittag, D. J. Searles, D. J. Evans, *Phys. Rev. Lett* **89**, 050601 (2002).
- [23] D. M. Carberry, J. C. Reid, G. M. Wang, E. M. Sevick, Debra J. Searles, and Denis J. Evans, *Phys. Rev. Lett* **92**, 140601 (2004).
- [24] D. M. Carberry, M. A. B. Baker, G. M. Wang, E. M. Sevick and Denis. J. Evans, *J. Opt. A: Pure Appl. Opt.* **9** S204 (2007).

## BIBLIOGRAPHY

---

- [25] G. Hummer, A. Szabo, *Proc. Natl. Acad. Sci. USA* **98**, 3658 (2001).
- [26] J. Liphardt, S. Dumont, S.B. Smith, I. Tinoco Jr., C. Bustamante, *Science* **296**, 1832 (2002).
- [27] D. Collin, F. Ritort, C. Jarzynski, S.B. Smith, I. Tinoco Jr., C. Bustamante, *Nature* **437**, 231 (2005).
- [28] N. Garnier and S. Ciliberto, *Phys. Rev. E*, **71**, 060101 (2005).
- [29] S. Majumdar and A. K.Sood, *Phys. Rev. Lett.*, **101**, 078301 (2008).
- [30] N. Kumar, S. Ramaswamy, and A. K. Sood , *Phys. Rev.Lett.*, **106** 118001 (2011).
- [31] É. Falcon, Sébastien Aumaître, Claudio Falcón, Claude Laroche, and Stéphan Fauve *Phys. Rev. Lett*, **100**, 064503 (2008).
- [32] M. Bonaldi et al; *Phys. Rev. Lett.*, 103 010601 (2009).
- [33] S. Ciliberto, S. Joubaud and A. Petrosyan, *J. Stat. Mech.* P12003 (2010).
- [34] S. Yukawa, *J. Phys. Soc. Jpn.* **69**, 2367 (2000).
- [35] A. E. Allahverdyan and T. M. Nieuwenhuizen, *Phys. Rev. E* **71**, 066102, (2005).
- [36] T. Monnai, and S. Tasaki, arXiv:cond-mat/0308337 (2003).
- [37] J. Kurchan, arXiv:cond-mat/0007360 (2000).
- [38] H. Tasaki, arXiv:cond-mat/0009244 (2000).

## BIBLIOGRAPHY

---

- [39] S. Mukamel, Phys. Rev. Lett. **90**, 170604, (2003).
- [40] T. Monnai, Phys. Rev. E **72**, 027102 (2005).
- [41] P. Talkner, and P. Hänggi, J.Phys.A: Math. Theor. **40**, F569, (2007).
- [42] P. Talkner, P. Hänggi, and M. Morillo, Phys. Rev. E **77**, 051131 (2008).
- [43] P. Talkner, E. Lutz, and P. Hänggi, Phys. Rev. E **75**, 050102(R) (2007).
- [44] C. Jarzynski, D. K. Wójcik, Phys. Rev. Lett. **92** 230602 (2004).
- [45] K. Saito and Y. Utsumi, Phys. Rev. B **78**, 115429 (2008).
- [46] D. Andrieux, P. Gaspard, T. Monnai, and S. Tasaki, New. J. Phys. **11**, 043014 (2009).
- [47] M. Terraneo, M. Peyrard, and G. Casati, Phys. Rev. Lett. **88**, 094302 (2002).
- [48] B. Li, L. Wang, and G. Casati, Phys. Rev. Lett. **93**, 184301 (2004).
- [49] B. Li, L. Wang, and G. Casati, Appl. Phys. Lett. **88**, 143501 (2006).
- [50] C. W. Chang, D. Okawa, H. Garcia, A. Majumdar, and A. Zettl, Phys. Rev. Lett. **99**, 045901 (2007).
- [51] R.-G. Xie, C.-T. Bui, B. Varghese, M.-G. Xia, Q.-X. Zhang, C.-H. Sow, B. Li, and J. T. L. Thong, Adv. Funct. Mat **21**, 1602 (2011).
- [52] L. Mandel, Optics Lett. **4**, 205 (1979).
- [53] R. J. Cook, Phys. Rev. A, **23**, 1243 (1981).

## BIBLIOGRAPHY

---

- [54] L. Mandel and E. Wolf, *Optical Coherence and Quantum Optics*, Cambridge University Press, 1995.
- [55] L. S. Levitov and G. B. Lesovik, JETP Lett. **58**, 230 (1993).
- [56] L. S. Levitov, H.-W. Lee, and G. B. Lesovik, J. Math. Phys. **37**, 4845 (1996).
- [57] S. Pilgram, A. N. Jordan, and E. V. Sukhorukov, and M. Büttiker, Phys. Rev. Lett. **90**, 206801 (2003).
- [58] Yu. V. Nazarov, Ann. Phys. (Leipzig) 8 SI-193, 507 (1999).
- [59] I. Klich, in *Quantum Noise in Mesoscopic Physics*, NATO Science Series II, Vol. 97, edited by Yu. V. Nazarov (Kluwer, Dordrecht, 2003).
- [60] W. Belzig and Y. V. Nazarov, Phys. Rev. Lett. **87**, 197006 (2001); Y. V. Nazarov and M. Kindermann, Eur. Phys. J. B **35**, 413 (2003).
- [61] K. Schönhammer, Phys. Rev. B **75**, 205329 (2007); J. Phys.:Condens. Matter **21**, 495306 (2009).
- [62] D. A. Bagrets and Y. V. Nazarov, Phys. Rev. B **67**, 085316 (2003).
- [63] A. O. Gogolin and A. Komnik, Phys. Rev. B **73**, 195301 (2006).
- [64] D. F. Urban, R. Avriller and A. Levy Yeyati, Phys. Rev. B **82**, 121414(R) (2010).
- [65] D. B. Gutman, Y. Gefen, and A. D. Mirlin, Phys. Rev. Lett. **105**, 256802 (2010).

## BIBLIOGRAPHY

---

- [66] S. Gustavsson, R. Leturcq, B. Simovič, R. Schleser, T. Ihn, P. Studerus, K. Ensslin, D. C. Driscoll, and A. C. Gossard, *Phys. Rev. Lett.* **96**, 076605 (2006).
- [67] C. Flindt, C. Fricke, F. Hohls, T. Novotný, K. Netočný, T. Brandes, and R. J. Haug, *PNAS*, **106**, 10116 (2009).
- [68] C. Fricke, F. Hohls, W. Wegscheider, and R. J. Haug, *Phys. Rev. B* **76**, 155307 (2007).
- [69] Z. Rieder, J.L. Lebowitz, and E. Lieb, *J. Math. Phys.* **8** (1967), p. 1073.
- [70] J.-S. Wang, J. Wang, N. Zeng, *Phys. Rev. B* **74**, 033408 (2006).
- [71] K. Saito and A. Dhar, *Phys. Rev. Lett.* **99**, 180601 (2007).
- [72] J. Ren, P. Hänggi, and B. Li, *Phys. Rev. Lett.* **104**, 170601 (2010).
- [73] L. Nicolin and D. Segal, *J. Chem. Phys.* **135**, 164106 (2011).
- [74] A. A. Clerk, *Phys. Rev. A* **84**, 043824 (2011).
- [75] Y. Utsumi, D. S. Golubev, M. Marthaler, K. Saito, T. Fujisawa, and Gerd Schön, *Phys. Rev. B* **81**, 125331 (2010).
- [76] A. A. Clerk, Florian Marquardt, and J. G. E. Harris, *Phys. Rev. Lett.* **104**, 213603 (2010).
- [77] A. Kundu, S. Sabhapandit, and A. Dhar, *J. Stat. Mech* P03007 (2011).
- [78] K. Saito and A. Dhar, *Phys. Rev. E* **83**, 041121 (2011).

## BIBLIOGRAPHY

---

- [79] H. C. Fogedby and A. Imparato, *J. Stat. Mech.* 2011, P05015 (2011).
- [80] S. Liu, B. K. Agarwalla, B. Li, and J.-S. Wang, arXiv:1211.5876.

## Chapter 2

# Introduction to Nonequilibrium Green's function (NEGF) method

In this thesis, to study the full-counting statistics (FCS) for nonequilibrium systems we employ nonequilibrium Green's functions (NEGF) method, also referred to as Keldysh formalism. In the following we give a brief introduction of this method.

## 2.1 Introduction

NEGF is an elegant and powerful method which is used for evaluating properties of many-body systems in both equilibrium and nonequilibrium. The method has its root from quantum field theory. NEGF method was first developed by Schwinger [1], Kadanoff and Baym [2] and later on by Keldysh [3]. By generalizing time ordered operators to contour-ordered operators Keldysh developed Feynman diagrammatic expansion method using Wick's theorem for nonequilibrium systems [4, 5]. Kadanoff and Baym developed the equation of motion approach for the Green's functions. Both approaches are equally applicable for studying a dynamic system in nonequilibrium state. NEGF has found many applications for example, in electronic transport for mesoscopic systems, in solid state physics, nuclear physics, plasma physics and also in the study of superconductivity and superfluidity. For quantum transport, NEGF addresses the problem based on microscopic theory in a complete and consistent way, including nonlinear interactions. One of the main application of NEGF in quantum transport is to calculate the steady state properties of a finite system connected with two heat baths at different fixed temperatures and/or chemical potentials. NEGF is one of the most commonly used methods in electronic transport study. However its application in thermal transport has gained significant interest only in recent times for both linear [6–8] and nonlinear systems [9–13]. For extensive study on NEGF we recommend the books by Datta, Haug and Jauho, Rammer, Di Ventra [4, 5, 14–16] and a review article by Wang et al [17]. Let us very briefly list few important features of NEGF

[18]:

- The main ingredient in NEGF is the Green's function, which is in general a function of two space-time coordinates. Based on the knowledge of these functions one can compute time-dependent expectation values such as current, densities etc.
- In the absence of external driving, thermodynamic affinities, NEGF reduces to the equilibrium Green's function method which has important applications in many branches of physics and also in quantum chemistry.
- Generalizing time-ordered operators to contour-ordered operators NEGF can be mapped to a formally equivalent equilibrium theory.
- NEGF method can handle both finite and extended systems and in transport theory the formalism can be well applied to study both transient and steady state properties.

In the following, we introduce different types of Green's functions, their importance and also the relations between them. After that we will discuss a generalized version of the Green's function known as contour-ordered Green's function, which opens up the possibility to perform perturbative expansion with respect to interacting Hamiltonian, similar to what is done in quantum field theory. At the end of this chapter we will apply all these techniques to derive the Landauer formula for current.

## 2.2 Definitions of Green's functions

In NEGF approach it is advantageous to define various (six) Green's functions (retarded ( $r$ ), advanced ( $a$ ), lesser ( $<$ ), greater ( $>$ ), time-ordered ( $t$ ), anti-time-ordered ( $\bar{t}$ )) which describes the expectation value of a product of operators evaluated at different instant of times. Keeping in mind the lattice models to discuss thermal transport in subsequent chapters we choose these operators as position operators in the first quantized representation. However these definitions can be easily generalized for any two arbitrary operators which need not to be even Hermitian. The reasoning for defining such objects is that experimentally relevant quantities can be immediately expressed in terms of these Green's functions. We start by defining the retarded Green's function [19, 20]

$$G^r(t, t') = -\frac{i}{\hbar}\theta(t - t')\langle[u(t), u(t')^T]\rangle, \quad (2.1)$$

where  $u(t)$  is a column vector of the particle displacements in the Heisenberg picture *i.e.*, it's dynamics is governed by some Hamiltonian  $\mathcal{H}(t)$  which can depend on time explicitly. For brevity, we have set all the atomic masses to 1, but the formulas are equally applicable to variable masses with a transformation  $u_j \rightarrow \sqrt{m_j}x_j$ . The square brackets are the commutators. Here  $\theta(t)$  is the Heaviside step function. The notation  $\langle \dots \rangle$  means the average is with respect to an initial density matrix  $\rho(t_0)$  *i.e.*,  $\langle \dots \rangle = \text{Tr}[\rho(t_0) \dots]$ , typically taken in the form of canonical distribution. Here  $t_0$  is the reference time. Also  $\langle [A, B^T] \rangle$  represents a matrix and should

be interpreted as  $\langle AB^T \rangle - \langle BA^T \rangle^T$ . The physical dimension of  $G^r(t, t')$  is time. Retarded Green's function often termed as the response function in the linear-response theory because it differs from zero only for times  $t > t'$  and hence can be used to calculate response at time  $t$  due to some external perturbation at time  $t'$ . In addition, information about the density of states, spectral properties are also contained in this Green's function.

In a similar notion the advanced Green's functions is defined as

$$G^a(t, t') = \frac{i}{\hbar} \theta(t' - t) \langle [u(t), u(t')^T] \rangle. \quad (2.2)$$

We also define the lesser and greater Green's functions as

$$\begin{aligned} G^<(t, t') &= -\frac{i}{\hbar} \langle u(t') u(t)^T \rangle^T, \\ G^>(t, t') &= -\frac{i}{\hbar} \langle u(t) u(t')^T \rangle. \end{aligned} \quad (2.3)$$

These two Green's functions are directly linked to many physical observables such as average kinetic energy, current, particle density, etc. As a simple example the expectation value for the kinetic energy (K.E) can be written as

$$\begin{aligned} \langle K.E \rangle &= \frac{1}{2} \langle \dot{u}^T(t) \dot{u}(t) \rangle \\ &= \frac{1}{2} \lim_{t \rightarrow t'} \frac{\partial^2}{\partial t \partial t'} \langle u^T(t) u(t') \rangle \\ &= \frac{i\hbar}{2} \lim_{t \rightarrow t'} \frac{\partial^2}{\partial t \partial t'} \text{Tr} [G^>(t, t')] \\ &= \frac{i\hbar}{2} \lim_{t \rightarrow t'} \frac{\partial^2}{\partial t \partial t'} \text{Tr} [G^<(t', t)]. \end{aligned} \quad (2.4)$$

Finally we define time and anti-time ordered Green's functions as

$$\begin{aligned} G^t(t, t') &= -\frac{i}{\hbar} \langle T u(t) u(t')^T \rangle, \\ G^{\bar{t}}(t, t') &= -\frac{i}{\hbar} \langle \bar{T} u(t) u(t')^T \rangle. \end{aligned} \quad (2.5)$$

where  $T$  ( $\bar{T}$ ) is the time (anti-time) ordering operator which moves the operator with the earlier time argument to the right (left). These two Green's functions allow the construction of a systematic perturbation theory in thermal equilibrium.

### Relations among the Green's functions:

From the definitions of the Green's functions it is clear that these functions are not all independent. In fact they obey the following relations which are true in both time and frequency space,

$$\begin{aligned} G^r - G^a &= G^> - G^<, \\ G^t + G^{\bar{t}} &= G^> + G^<, \\ G^t - G^{\bar{t}} &= G^r + G^a. \end{aligned} \quad (2.6)$$

Here we have simplified the notation as we don't specify the arguments for the Green's functions, which means it could be either in time or in frequency domain. In equilibrium or nonequilibrium steady state (NESS) Green's functions depend only on the time difference, say  $G^r(t, t') = G^r(t - t')$ . In that case it is often useful to work in the Fourier space. We define the Fourier transformation as (we will follow this convention throughout this

thesis)

$$G^r[\omega] = \int_{-\infty}^{+\infty} dt G^r(t) e^{i\omega t}. \quad (2.7)$$

Then the inverse Fourier transform is given by

$$G^r(t) = \int_{-\infty}^{+\infty} \frac{d\omega}{2\pi} G^r[\omega] e^{-i\omega t}. \quad (2.8)$$

Based on the above relations, out of six Green's functions, only three of them are linearly independent. Moreover, in stationary state  $G^r[\omega]$  and  $G^a[\omega]$  are Hermitian conjugate of one another *i.e.*,  $G^a[\omega] = (G^r[\omega])^\dagger$ . Therefore in nonequilibrium steady-state only two Green's functions are independent which we can choose as  $G^r[\omega]$  and  $G^<[\omega]$ .

### Fluctuation-dissipation relation

In thermal equilibrium, there is an additional relation between  $G^r[\omega]$  and  $G^<[\omega]$  in the frequency space, given as:

$$G^<[\omega] = f(\omega) \left( G^r[\omega] - G^a[\omega] \right), \quad (2.9)$$

where  $f(\omega) = 1/(e^{\beta\hbar\omega} - 1)$  is the Bose-Einstein distribution function at temperature  $T = 1/k_B\beta$ . The above equation is one particular form of fluctuation-dissipation theorem as the correlation function  $G^<[\omega]$  carries information about the fluctuations and is related to the imaginary part of the response function which is responsible for the dissipation. The above relation can be proved with the help of an important identity in the time-domain, known as Kubo-Martin-Schwinger (KMS) boundary condition [21]

and is given as

$$G^<(t) = G^>(t - i\beta\hbar), \quad (2.10)$$

where we assume that  $G^<(t)$  can be analytically continued in the complex  $t$  plane.

---

**Proof:**

The  $ij$  component of  $G^<$  matrix is given as

$$\begin{aligned} G_{ij}^<(t) &= -\frac{i}{\hbar} \text{Tr} \left[ \rho(0) u_j(0) u_i(t) \right] \\ &= -\frac{i}{\hbar} \text{Tr} \left[ \rho(0) u_j(-t) u_i(0) \right] = G_{ji}^>(-t) \\ &= -\frac{i}{\hbar} \text{Tr} \left[ \frac{e^{-\beta\mathcal{H}}}{Z} e^{-\frac{i}{\hbar}\mathcal{H}t} u_j e^{\frac{i}{\hbar}\mathcal{H}t} u_i(0) \right] \\ &= -\frac{i}{\hbar} \text{Tr} \left[ \frac{1}{Z} e^{\frac{i\mathcal{H}}{\hbar}(-t+i\beta\hbar)} u_j e^{-\frac{i\mathcal{H}}{\hbar}(-t+i\beta\hbar)} e^{-\beta\mathcal{H}} u_i(0) \right] \\ &= -\frac{i}{\hbar} \text{Tr} \left[ \rho(0) u_i(0) u_j(-t + i\beta\hbar) \right] \\ &= G_{ji}^<(-t + i\beta\hbar) = G_{ij}^>(t - i\beta\hbar). \end{aligned} \quad (2.11)$$


---

where the equilibrium density matrix  $\rho(0) = e^{-\beta\mathcal{H}}/Z$  and  $Z = \text{Tr}(e^{-\beta\mathcal{H}})$  is the canonical partition function. (Here we choose  $t_0 = 0$ ). Now performing Fourier transformation of the above relation we get the detailed balance condition.

$$G^>[\omega] = e^{\beta\hbar\omega} G^<[\omega]. \quad (2.12)$$

Using this relation and  $G^r - G^a = G^> - G^<$  proves Eq. (2.9). It is important

to mention that this detailed balance condition is one of the fundamental basis behind the fluctuation theorems (FT's) as it is valid for heat baths which are always maintained in thermal equilibrium. Therefore one of the important properties of equilibrium theory is that all Green's functions are linked via fluctuation-dissipation theorem and hence there is only one independent Green's function; which can be taken as the retarded one *i.e.*,  $G^r$ . However we will later see that in NEGF-FCS case relations between different Green's functions like in Eq. (2.6) do not exist and we need to compute all Green's functions independently which makes the problem non-trivial in general.

## 2.3 Contour ordered Green's function

NEGF theory is formally equivalent to the equilibrium one, with the only difference that in nonequilibrium case the Green's functions are defined on a contour, referred to as Keldysh contour (see Fig. 2.1). This contour runs from the remote past where the system was in equilibrium to the highest relevant time and back to the remote past again. It plays an analogous role as the time-ordered Green's function plays in equilibrium. The Contour ordered Green's function is the central quantity in NEGF for constructing the perturbation theory based on Wick's theorem and Feynman diagrams. Before getting into the details about this function, we first very briefly review three different representation pictures in quantum mechanics.

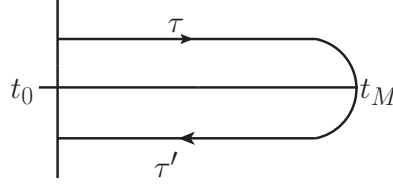


Figure 2.1: The complex-time contour  $C$  in the Keldysh formalism. The path of the contour begins at time  $t_0$ , goes to time  $t_M$ , and then goes back to time  $t = t_0$ .  $\tau$  and  $\tau'$  are complex-time variables along the contour.

### 2.3.1 Different pictures in quantum mechanics

Let us consider a system with Hamiltonian  $\mathcal{H}(t)$  and assume that it can be written as a sum of a noninteracting or free part  $\mathcal{H}_0$  and a complicated interaction part  $\mathcal{V}(t)$ , which could depend on time explicitly. Therefore the total Hamiltonian is given as  $\mathcal{H}(t) = \mathcal{H}_0 + \mathcal{V}(t)$ .

#### Schrödinger Picture:

In this picture the wavefunction  $|\psi(t)\rangle$  is time-dependent and its dynamics is governed by the Schrödinger equation:

$$i\hbar \frac{\partial}{\partial t} |\psi(t)\rangle = \mathcal{H}(t) |\psi(t)\rangle. \quad (2.13)$$

The formal solution of this equation is written as

$$|\psi(t)\rangle = \mathcal{U}(t, t_0) |\psi(t_0)\rangle, \quad \mathcal{U}(t, t_0) \mathcal{U}^\dagger(t, t_0) = \mathcal{U}^\dagger(t, t_0) \mathcal{U}(t, t_0) = 1, \quad (2.14)$$

$$\mathcal{U}(t, t_0) = T \exp \left[ -\frac{i}{\hbar} \int_{t_0}^t dt' \mathcal{H}(t') \right]. \quad (2.15)$$

We choose  $t_0$  as the synchronization time. The operators in this picture

are constant.

### Heisenberg Picture:

In this picture the wavefunctions are constant *i.e.*,  $|\psi_H(t)\rangle = |\psi(t_0)\rangle$  and the operators are time-dependent with the evolution

$$\mathcal{O}_H(t) = \mathcal{U}^\dagger(t, t_0)\mathcal{O}(t)\mathcal{U}(t, t_0), \quad (2.16)$$

where  $\mathcal{O}(t)$  is in the Schrödinger picture with explicit time-dependence.

### Interaction Picture:

The state vector in this picture is defined as

$$|\psi_I(t)\rangle = e^{\frac{i}{\hbar}\mathcal{H}_0(t-t_0)}|\psi(t)\rangle. \quad (2.17)$$

Therefore the wavefunctions propagate with respect to the interacting Hamiltonian  $\mathcal{V}(t)$  only and satisfy the following equation

$$i\hbar\frac{\partial}{\partial t}|\psi_I(t)\rangle = \mathcal{V}_I(t)|\psi_I(t)\rangle. \quad (2.18)$$

with formal solution

$$|\psi_I(t)\rangle = \mathcal{U}_I(t, t')|\psi_I(t')\rangle. \quad (2.19)$$

$\mathcal{U}_I(t, t')$  is often called the scattering or  $\mathcal{S}$ -matrix and is defined as

$$\mathcal{S}(t, t') = \mathcal{U}_I(t, t_0)\mathcal{U}_I^\dagger(t', t_0) = T \exp \left[ -\frac{i}{\hbar} \int_{t'}^t dt' \mathcal{V}_I(t') \right], \quad (2.20)$$

which appears in the perturbative expansions. The operators in this picture evolve under the influence of the free Hamiltonian  $\mathcal{H}_0$  *i.e.*,

$$\mathcal{O}_I(t) = \mathcal{U}_0^\dagger(t, t_0) \mathcal{O}(t) \mathcal{U}_0(t, t_0), \quad (2.21)$$

and similarly for  $\mathcal{V}_I(t)$  in Eq. (2.18). Here

$$\begin{aligned} \mathcal{U}_0(t, t_0) &= \exp \left[ -\frac{i}{\hbar} \mathcal{H}_0(t - t_0) \right], \\ \mathcal{U}_I(t, t_0) &= T \exp \left[ -\frac{i}{\hbar} \int_{t_0}^t dt' \mathcal{V}_I(t') \right]. \end{aligned} \quad (2.22)$$

Then it can be easily shown that the full unitary operator  $\mathcal{U}(t, t_0)$  can be decomposed as a product of free evolution part  $\mathcal{U}_0(t, t_0)$  and the interacting evolution part  $\mathcal{U}_I(t, t_0)$  *i.e.*,

$$\mathcal{U}(t, t_0) = \mathcal{U}_0(t, t_0) \mathcal{U}_I(t, t_0). \quad (2.23)$$

More importantly using Eq. (2.16) and Eq. (2.21) the relation between the operators in Heisenberg and interaction picture is given as

$$\mathcal{O}_H(t) = \mathcal{U}_I^\dagger(t, t_0) \mathcal{O}_I(t) \mathcal{U}_I(t, t_0). \quad (2.24)$$

### 2.3.2 Closed time path formalism

We now introduce the contour, the closed time path, which starts at initial time  $t_0$  and go upto maximum relevant time  $t = t_M$  and then back again

to  $t_0$  (see Fig. (2.1)). The key observation is that the transformation of the operator between Heisenberg picture and interaction picture given in Eq. (2.24) can be expressed on closed contour form as

$$\mathcal{O}_H(t_M) = \left( T_C e^{-\frac{i}{\hbar} \int_C \mathcal{V}_I(\tau) d\tau} \mathcal{O}_I(t_M) \right). \quad (2.25)$$

Here  $\tau$  is the contour-time variable which runs over the contour from time  $t_0$  to  $t_M$  on the upper branch and from  $t_M$  to  $t_0$  on the lower branch.  $T_C$  is the contour-ordered operator which orders operator according to their contour time argument, earlier contour time places an operator to the right. This crucial equivalence of Eq. (2.24) and Eq. (2.25) is the basis for formulating the perturbation theory on contour. Note that under the contour ordering operator the algebra of operators become equivalent to the algebra of numbers.

Now expanding the exponential and splitting the contour into upper and lower branch it can be shown that [4]

$$\left( T_C e^{-\frac{i}{\hbar} \int_C \mathcal{V}_I(\tau) d\tau} \mathcal{O}_I(t_M) \right) = \left( T_{\overleftarrow{C}} e^{-\frac{i}{\hbar} \int_{\overleftarrow{C}} \mathcal{V}_I(\tau) d\tau} \right) \mathcal{O}_I(t_M) \left( T_{\overrightarrow{C}} e^{-\frac{i}{\hbar} \int_{\overrightarrow{C}} \mathcal{V}_I(\tau) d\tau} \right), \quad (2.26)$$

where  $T_{\overrightarrow{C}}$  and  $T_{\overleftarrow{C}}$  denotes contour ordering on the upper and lower branch respectively. Now parameterizing the contour according to  $\tau(t') = t'$ ,  $t' \in [t_0, t_M]$  we see that

$$\begin{aligned} T_{\overrightarrow{C}} \left( e^{-\frac{i}{\hbar} \int_{\overrightarrow{C}} \mathcal{V}_I(\tau) d\tau} \right) &= T e^{-\frac{i}{\hbar} \int_{t_0}^{t_M} \mathcal{V}_I(t') dt'} = \mathcal{U}_I(t_M, t_0), \\ T_{\overleftarrow{C}} \left( e^{-\frac{i}{\hbar} \int_{\overleftarrow{C}} \mathcal{V}_I(\tau) d\tau} \right) &= \bar{T} e^{\frac{i}{\hbar} \int_{t_0}^{t_M} \mathcal{V}_I(t') dt'} = \mathcal{U}_I^\dagger(t_M, t_0), \end{aligned} \quad (2.27)$$

*i.e.*, contour ordering on the upper (lower) branch is identical to the time ordering (anti-time ordering)  $T_{\vec{C}} = T (T_{\bar{C}} = \bar{T})$ . This idea for one point operator can be easily generalized for product of two operators and hence for the Green's functions. The main idea for the general case is as follows

- Transform each Heisenberg operator appearing in the Green's function to the interaction picture.
- Read the time-evolution from the right to represent the evolution on the contour.

For example let us consider the time-ordered Green's function

$$G^t(t, t') = -\frac{i}{\hbar} \langle T u(t) u^T(t') \rangle, \quad (2.28)$$

if  $t > t'$  then the above Green's function can be written as (in the interaction picture)

$$G^>(t, t') = -\frac{i}{\hbar} \text{Tr} \left[ \rho(t_0) \mathcal{S}(t_0, t) u_I(t) \mathcal{S}(t, t') u_I^T(t') \mathcal{S}(t', t_0) \right], \quad (2.29)$$

where we have used the fact that  $\mathcal{S}(t, t_0) = \mathcal{U}_I(t, t_0)$ . Now let us read the time evolution from the right side. Given a state at initial time  $t_0$  it evolves from  $t_0$  till the time  $t'$  at which point operator  $u_I(t')$  acts. Then it evolves from  $t'$  to  $t$  where the operator  $u_I(t)$  acts. Finally it evolves from  $t$  back to  $t_0$  *i.e.*,

$$\mathcal{S}(t', t_0) \rightarrow u_I^T(t') \rightarrow \mathcal{S}(t, t') \rightarrow u_I(t) \rightarrow \mathcal{S}(t_0, t). \quad (2.30)$$

Similarly for  $t' > t$  we can write,

$$G^<(t, t') = -\frac{i}{\hbar} \text{Tr} \left[ \rho(t_0) \mathcal{S}(t_0, t') u_I^T(t') \mathcal{S}(t', t) u_I(t) \mathcal{S}(t, t_0) \right]. \quad (2.31)$$

Therefore the contour-ordered version of the Green's function can be written as

$$G(\tau, \tau') = -\frac{i}{\hbar} \langle T_C u_I(\tau) u_I^T(\tau') e^{-\frac{i}{\hbar} \int_C \mathcal{V}_I(\tau'') d\tau''} \rangle \quad (2.32)$$

$$\equiv -\frac{i}{\hbar} \langle T_C u(\tau) u^T(\tau') \rangle. \quad (2.33)$$

where  $\tau, \tau'$  are the contour time variables and depending on the positions of these variables on the two branches of the contour, different real time Green's functions can be obtained. Therefore writing contour-ordered Green's function in the interaction picture gives us the opportunity to perform perturbative expansion (see Eq. (2.32)) and the topological structure immediately becomes identical to the equilibrium theory. We will also show this by an example at the end of this chapter.

### Contour time $\tau, \tau'$ to real time $t, t'$

Since the two contour variables  $\tau, \tau'$  can lie either on the upper or lower branch there are four different real time Green's functions that can be obtained. They are given as,

$$G^{\sigma\sigma'}(t, t') = \lim_{\epsilon \rightarrow 0^+} G(t + i\epsilon\sigma, t' + i\epsilon\sigma'), \quad \sigma, \sigma' = \pm 1. \quad (2.34)$$

where we have introduced a branch index  $\sigma$ , such that  $\tau = t + i\epsilon\sigma$ . Here

$\sigma$  can take two possible values  $\pm 1$  with  $\sigma = +1(-1)$  means  $\tau$  is on the upper (lower) branch. Following this notation, we can identify that in real time  $G^{++}(t, t') = G^t(t, t')$ ,  $G^{--}(t, t') = G^{\bar{t}}(t, t')$ ,  $G^{+-}(t, t') = G^<(t, t')$ , and  $G^{-+}(t, t') = G^>(t, t')$ , or in the matrix form

$$G(\tau, \tau') \rightarrow \begin{bmatrix} G^{++}(t, t') & G^{+-}(t, t') \\ G^{-+}(t, t') & G^{--}(t, t') \end{bmatrix} = \begin{bmatrix} G^t(t, t') & G^<(t, t') \\ G^>(t, t') & G^{\bar{t}}(t, t') \end{bmatrix} = G(t, t'). \quad (2.35)$$

For later convenience we also define a new matrix  $\bar{G}(t, t')$  given by  $\bar{G}(t, t') = \sigma_z G(t, t')$  where  $\sigma_z$  is the third Pauli matrix *i.e.*,

$$\sigma_z = \begin{bmatrix} 1 & 0 \\ 0 & -1 \end{bmatrix}. \quad (2.36)$$

Here we identify  $\sigma_z$  as the matrix related to the branch index.

### 2.3.3 Important relations on the Keldysh Contour

In order to work on the contour we need to generalize few definitions that are known in real time to the contour time. For example, we define the contour version of the Dirac-delta function as

$$\int d\tau' \delta(\tau, \tau') f(\tau') = f(\tau). \quad (2.37)$$

Note that, here we can not write  $\delta(\tau, \tau')$  as  $\delta(\tau - \tau')$  since  $\tau$  and  $\tau'$  may lie on two different branches and then the meaning of  $\tau - \tau'$  is ambiguous.

We generalize the Heaviside theta function on the contour as  $\theta(\tau, \tau')$ , defined to be 1 if  $\tau$  is later than  $\tau'$  on the contour and 0 otherwise. The delta function then can be obtained from the theta function by taking contour time derivative, given as  $\delta(\tau, \tau') = d\theta(\tau, \tau')/d\tau$ . This fact is required to derive the equations of motion for the contour-ordered Green's functions.

Note that the derivative on the contour is defined as

$$\frac{df(\tau)}{d\tau} = \lim_{\tau' \rightarrow \tau} \frac{f(\tau') - f(\tau)}{\tau' - \tau}, \quad (2.38)$$

The limit  $\tau' \rightarrow \tau$  suggests that  $\tau, \tau'$  should lie on the same branch.

The Heisenberg equation of motion on the contour is written in a similar form as given in the real time,

$$\frac{d\mathcal{A}^H(\tau)}{d\tau} = \frac{1}{i\hbar} [\mathcal{A}^H(\tau), \mathcal{H}^H(\tau)], \quad (2.39)$$

and since the transformation from Schrödinger operator to Heisenberg operator is a unitary transformation, the canonical commutation relation holds for equal contour time *i.e.*,

$$[u_i(\tau), p_j(\tau)] = i\hbar\delta_{ij}. \quad (2.40)$$

The transformation for contour time integral to the real time is done as

follows

$$\int d\tau f(\tau) \cdots \rightarrow \int_{t_0}^{t_M} f^+(t) dt + \int_{t_M}^{t_0} f^-(t) dt = \sum_{\sigma=\pm 1} \sigma \int_{t_0}^{t_M} f^\sigma(t) dt. \quad (2.41)$$

As an example the contour-ordered delta function, defined in Eq. (2.37), transforms as

$$\delta(\tau, \tau') \rightarrow \sigma \delta_{\sigma\sigma'} \delta(t - t'), \quad (2.42)$$

with  $\delta_{\sigma,\sigma'}$  is the Kronecker delta. More explicitly, we can write,

$$\delta(\tau, \tau') = \begin{cases} \delta(t - t') & \text{for } \tau, \tau' \text{ on upper branch} \\ -\delta(t - t') & \text{for } \tau, \tau' \text{ on lower branch} \\ 0 & \text{for } \tau, \tau' \text{ on different branches} \end{cases}$$

### 2.3.4 Dyson equation and Keldysh rotation

We see from Eq. (2.32) that contour ordered Green's functions are useful for performing perturbative expansion with respect to scattering matrix  $\mathcal{V}_I(\tau)$  in the interaction picture. Expanding the exponential or the  $S$ -matrix in Eq. (2.32) we get an infinite series corresponding to different orders of  $\mathcal{V}_I$  with each term is averaged with respect to the initial density operator  $\rho(t_0)$ . In perturbation theory the main task is to evaluate such terms or rather first break down the terms into Gaussian products as accomplished by Wick's theorem, which is valid when  $\rho(t_0)$  is Gaussian or quadratic. Therefore each term in the expansion consists of product of free thermal equilibrium

contour-ordered Green's functions. In some situations, this infinite series can be summed exactly with the help of Feynman diagrams [22, 23] which then gives rise to Dyson's equation. A general form of it in contour time can be written as (see for example the derivation of Eq. 2.85)

$$G(\tau, \tau') = g(\tau, \tau') + \int_C \int_C d\tau_1 d\tau_2 g(\tau, \tau_1) \Sigma(\tau_1, \tau_2) G(\tau_2, \tau'), \quad (2.43)$$

where  $g$  is the bare or free Green's function.  $\Sigma$  is called the self-energy, includes the effects of interaction coming from  $\mathcal{V}_I$ . We realize that  $G$  here is the sum of infinite number of terms *i.e.*,  $G = g + \int \int g \Sigma g + \int \int \int g \Sigma g \Sigma g + \dots$

Now using the transformation rule for integration going from contour to real time, we write the components of the Dyson equation as

$$G^{\sigma\sigma'}(t, t') = g^{\sigma\sigma'}(t, t') + \int_{t_0}^{t_M} \int_{t_0}^{t_M} dt_1 dt_2 \sum_{\sigma_1, \sigma_2 = \pm 1} \sigma_1 \sigma_2 g^{\sigma\sigma_1}(t, t_1) \Sigma^{\sigma_1\sigma_2}(t_1, t_2) G^{\sigma_2\sigma'}(t_2, t'). \quad (2.44)$$

Multiplying  $\sigma$  on both sides, we obtain

$$\sigma G^{\sigma\sigma'}(t, t') = \sigma g^{\sigma\sigma'}(t, t') + \int_{t_0}^{t_M} \int_{t_0}^{t_M} dt_1 dt_2 \sum_{\sigma_1, \sigma_2 = \pm 1} \sigma g^{\sigma\sigma_1}(t, t_1) \sigma_1 \Sigma^{\sigma_1\sigma_2}(t_1, t_2) \sigma_2 G^{\sigma_2\sigma'}(t_2, t'), \quad (2.45)$$

which in simplified notation reads

$$\bar{G}(t, t') = \bar{g}(t, t') + \int_{t_0}^{t_M} \int_{t_0}^{t_M} dt_1 dt_2 \bar{g}(t, t_1) \bar{\Sigma}(t_1, t_2) \bar{G}(t_2, t'), \quad (2.46)$$

where  $\bar{G}(t, t') = \sigma_z G(t, t')$  as introduced before. Similarly we define  $\bar{g}$  and  $\bar{\Sigma}$ . Such a form of the matrix however is not very useful for actual calculation and one performs a Keldysh rotation which for any arbitrary matrix  $M$  is given as

$$\check{M} = O^T \bar{M} O = O^T \sigma_z M O. \quad (2.47)$$

where the rotation matrix  $O$  (rotation by an angle  $45^\circ$  in the space of branches) is given by

$$O = \frac{1}{\sqrt{2}} \begin{bmatrix} 1 & 1 \\ -1 & 1 \end{bmatrix}, \quad O O^T = O^T O = I. \quad (2.48)$$

The effect of the Keldysh rotation is to change any given matrix  $\bar{M}$  to  $\check{M}$  as,

$$\check{M} = \begin{bmatrix} M^r & M^K \\ M^{\bar{K}} & M^a \end{bmatrix} \quad (2.49)$$

$$= \frac{1}{2} \begin{bmatrix} M^t - M^< + M^> - M^{\bar{t}}, & M^t + M^{\bar{t}} + M^< + M^> \\ M^t + M^{\bar{t}} - M^< - M^>, & M^< - M^{\bar{t}} + M^t - M^> \end{bmatrix} \quad (2.50)$$

In this case we define the quantities  $M^r$ ,  $M^a$ ,  $M^K$ , and  $M^{\bar{K}}$  following Eq. (2.50). The Keldysh rotation transforms the matrix  $\bar{G}$  as

$$\check{G} = \begin{bmatrix} G^r & G^K \\ 0 & G^a \end{bmatrix}, \quad (2.51)$$

where the  $G^{\bar{K}}$  component is 0 due to the standard relation among Green's functions  $G^> + G^< = G^t + G^{\bar{t}}$ . We define  $G^K = G^< + G^>$ , known as the Keldysh Green's function. These three Green's functions (retarded, advanced and Keldysh) appears in  $\check{G}$  are the fundamental objects of the Keldysh technique. We will later see that for FCS problems, because of the presence of the counting field, the  $\bar{K}$  component will be nonzero in general.

Finally after Keldysh rotation, we write the Dyson equation in Eq. (2.46) as (by multiplying  $O^T$  from left and  $O$  from right and using the fact that  $O$  is an orthogonal matrix)

$$\check{G}(t, t') = \check{g}(t, t') + \int_{t_0}^{t_M} \int_{t_0}^{t_M} dt_1 dt_2 \check{g}(t, t_1) \check{\Sigma}(t_1, t_2) \check{G}(t_2, t'). \quad (2.52)$$

Since all this matrices are now upper-triangular and as product of any number of triangular matrices is again a triangular matrix, we can immediately conclude that, the convolution of any number of retarded (advanced) Green's functions is also a retarded (advanced) Green's function.

If the Green's functions are now time translationally invariant then the above convolutions in the  $\omega$  domain becomes multiplication in the limit  $t_0 \rightarrow -\infty$  and  $t \rightarrow \infty$  and we obtain

$$\check{G}[\omega] = \check{g}[\omega] + \check{g}[\omega] \check{\Sigma}[\omega] \check{G}[\omega], \quad (2.53)$$

with different components written down explicitly as

$$\begin{aligned}
 G^r[\omega] &= g^r[\omega] + g^r[\omega]\Sigma^r[\omega]G^r[\omega], \\
 G^a[\omega] &= g^a[\omega] + g^a[\omega]\Sigma^a[\omega]G^a[\omega], \\
 G^K[\omega] &= g^K[\omega] + g^r[\omega]\Sigma^r[\omega]G^K[\omega] + g^r[\omega]\Sigma^K[\omega]G^a[\omega] + g^K[\omega]\Sigma^a[\omega]G^a[\omega].
 \end{aligned}
 \tag{2.54}$$

### Generalization

Often in NEGF we encounter convolutions involving many Green's functions in contour time such as

$$B(\tau, \tau') = \int d\tau_1 \int d\tau_2 \cdots A_1(\tau, \tau_1) A_2(\tau_1, \tau_2) \cdots A_n(\tau_{n-1}, \tau'). \tag{2.55}$$

Based on the above technique we can immediately write down the relations in frequency space as [4, 15]

$$\begin{aligned}
 \check{B}[\omega] &= \check{A}_1[\omega] \check{A}_2[\omega] \cdots \check{A}_n[\omega], \quad n = 2, 3, \cdots \\
 B^r[\omega] &= A_1^r[\omega] A_2^r[\omega] \cdots A_n^r[\omega], \quad n = 2, 3, \cdots
 \end{aligned}
 \tag{2.56}$$

$$B^a[\omega] = A_1^a[\omega] A_2^a[\omega] \cdots A_n^a[\omega], \quad n = 2, 3, \cdots \tag{2.57}$$

$$\begin{aligned}
 B^K[\omega] &= A_1^r[\omega] \cdots A_{n-1}^r[\omega] A_n^K[\omega] + A_1^r[\omega] \cdots A_{n-2}^r[\omega] A_{n-1}^K[\omega] A_n^a[\omega] + \\
 &\quad \cdots + A_1^K[\omega] A_2^a[\omega] \cdots A_{n-1}^a[\omega] A_n^a[\omega].
 \end{aligned}
 \tag{2.58}$$

This particular transformation of going from contour time to the real time is known as Langreth's rule [4, 20].

## 2.4 Example: Derivation of Landauer formula for heat transport using NEGF approach

One of the primary interest in quantum transport is to calculate steady state current. We therefore in this section introduce a harmonic lattice model to study heat transport using NEGF method and illustrate the main concepts developed in this chapter. We derive the steady state expression for the heat current for this model, known as Landauer like formula. This formula was first derived for the electron transport [24–27] and later extended for heat transport [7, 28]. For alternate derivation of this formula such as using Generalized Langevin equation, see [29, 30].

### Harmonic lattice model

A typical setup to study transport consists of three parts called as the Left lead (denoted by  $L$ ), the center (denoted by  $C$ ) and the right lead (denoted by  $R$ ). The center part is the system of interest which can be an insulator or a metal or a semi-conductor and is finite in size. The left and right leads (also known as reservoir, bath) are maintained at different temperatures and/or chemical potential difference. To satisfy the criterion of a bath they are modeled by non-interacting Hamiltonians with infinite degrees of freedom. The system and the leads are connected via some coupling Hamiltonian.

For harmonic lattice model the center part is modelled as finite number of coupled harmonic oscillators and the coupling Hamiltonians between the leads and the center are taken in bilinear form in position variables. The leads are collections of infinite coupled harmonic oscillators with zero chemical potential. The Hamiltonian for the entire system is then written as

$$\mathcal{H} = \mathcal{H}_L + \mathcal{H}_C + \mathcal{H}_R + \mathcal{H}_{LC} + \mathcal{H}_{RC}, \quad (2.59)$$

where  $\mathcal{H}_\alpha = \frac{1}{2}p_\alpha^T p_\alpha + \frac{1}{2}u_\alpha^T K^\alpha u_\alpha$ ,  $\alpha = L, C, R$ , for the left, right, and the finite central region. Masses are redefined as  $u = \sqrt{m}x$ .  $u_\alpha$  and  $p_\alpha$  are column vectors of coordinates and momenta.  $K^\alpha$  is the spring constant matrix of region  $\alpha$ . The coupling  $\mathcal{H}_{\alpha C}$  is given as

$$\mathcal{H}_{\alpha C} = u_\alpha^T V^{\alpha C} u_C, \quad \alpha = L, R. \quad (2.60)$$

and  $V^{\alpha C} = [V^{C\alpha}]^T$ .

### Initial condition for the density operator

At initial time  $t = t_0 \rightarrow -\infty$ , we consider three systems  $\mathcal{H}_\alpha$ ,  $\alpha = L, C, R$  to be decoupled from each other and are at separate temperatures,  $T_L$ ,  $T_C$ , and  $T_R$  with respective equilibrium distributions. Then the density operator for the full system is in the the direct product state of  $L, C$  and  $R$  *i.e.*,

$$\rho_{\text{prod}}(t_0) = \rho_L \otimes \rho_C \otimes \rho_R, \quad \rho_\alpha = \frac{e^{-\beta_\alpha \mathcal{H}_\alpha}}{\text{Tr}[e^{-\beta_\alpha \mathcal{H}_\alpha}]} \text{ for } \alpha = L, C, R. \quad (2.61)$$

For  $t > t_0 \rightarrow -\infty$ , the coupling elements  $V^{LC}$  and  $V^{CR}$  are turned on

slowly so that a steady state for the entire system can be established at time  $t = 0$ . The full density operator at  $t = 0$  (denoted by  $\rho_{\text{NESS}}(0)$ ) is then given as

$$\rho_{\text{NESS}}(0) = \mathcal{U}(0, t_0)\rho_{\text{prod}}(t_0)\mathcal{U}^\dagger(0, t_0), \quad (2.62)$$

where  $\mathcal{U}(t, t')$  is the evolution operator for the full system. The current is calculated considering  $\rho_{\text{NESS}}(0)$  as the initial state.

### Calculation for current

The operator for the energy current flowing from one of the lead, say the left lead, is defined as the rate of change of the energy of the left lead Hamiltonian and is written as ( $t > 0$ )

$$\mathcal{I}_L(t) = -\frac{d\mathcal{H}_L^H(t)}{dt} = \frac{i}{\hbar} [\mathcal{H}_L^H(t), \mathcal{H}] = p_L^T(t)V^{LC}u_C(t), \quad (2.63)$$

where the operators are in the Heisenberg picture. Now taking the average with respect to the steady state density operator  $\rho_{\text{NESS}}(0)$ , the average current can be expressed in terms of the Green's function as

$$\langle \mathcal{I}_L(t) \rangle = i\hbar \frac{\partial}{\partial t'} \text{Tr} \left[ V^{LC} G_{CL}^>(t, t') \right]_{t'=t}. \quad (2.64)$$

Since  $[\dot{u}_L(t), u_C(t)] = 0$ , we can also write the above expression as

$$\langle \mathcal{I}_L(t) \rangle = i\hbar \frac{\partial}{\partial t'} \text{Tr} \left[ V^{LC} G_{CL}^<(t, t') \right]_{t'=t}. \quad (2.65)$$

We see that the energy current is directly related to the lesser and greater

Green's function. After symmetrization we obtain

$$\langle \mathcal{I}_L(t) \rangle = \frac{i\hbar}{2} \frac{\partial}{\partial t'} \text{Tr} \left[ V^{LC} G_{CL}^K(t, t') \right]_{t'=t}, \quad (2.66)$$

where  $G_{CL}^K = G_{CL}^< + G_{CL}^>$ . Now our main task is to obtain  $G_{CL}^<, >$  components. To obtain these, we work in the contour-ordered version of  $G_{CL}$  which for the general case can be written as,

$$G_{\alpha\beta}(\tau, \tau') = -\frac{i}{\hbar} \langle T_c u_\alpha(\tau) u_\beta^T(\tau') \rangle_{\rho_{\text{NESS}}(0)} \quad \alpha, \beta = L, C, R. \quad (2.67)$$

Let us now show how we can perform perturbative calculation on contour and obtain Dyson's equation by working in the interaction picture. Two key steps are

- Express the Green's function  $G_{\alpha\beta}$  in terms of the decoupled initial condition  $\rho_{\text{prod}}(t_0)$  because we know how to calculate the bare of free Green's functions for such initial condition.
- Transform to the interaction picture with respect to the decoupled Hamiltonian  $\mathcal{H}_0 = \mathcal{H}_L + \mathcal{H}_C + \mathcal{H}_R$  and work with the interaction  $\mathcal{H}_{LC} + \mathcal{H}_{RC}$ .

For simplicity, let us consider the greater component of  $G_{\alpha\beta}$

$$\begin{aligned}
 G_{\alpha\beta}^>(t, t') &= -\frac{i}{\hbar} \langle u_\alpha(t) u_\beta^T(t') \rangle_{\rho_{\text{NESS}}(0)} \\
 &= -\frac{i}{\hbar} \text{Tr} \left[ \rho_{\text{NESS}}(0) \mathcal{U}^\dagger(t, 0) u_\alpha \mathcal{U}(t, t') u_\beta^T \mathcal{U}(t', 0) \right] \\
 &= -\frac{i}{\hbar} \text{Tr} \left[ \rho_{\text{prod}}(t_0) \mathcal{U}^\dagger(t_0, t) u_\alpha \mathcal{U}(t, t') u_\beta^T \mathcal{U}(t', t_0) \right]. \quad (2.68)
 \end{aligned}$$

We now go to the interaction picture with respect to  $\mathcal{H}_0$  and consider  $t_0$  as the synchronization tim. Then we can decompose the full unitary operator as the product of free and interacting evolution part

$$\mathcal{U}(t, t_0) = \mathcal{U}_0(t, t_0) \mathcal{U}_I(t, t_0), \quad (2.69)$$

with

$$\mathcal{U}_0(t, t_0) = e^{-\frac{i}{\hbar} \mathcal{H}_0 (t-t_0)}, \quad \mathcal{U}_I(t, t_0) = T e^{-\frac{i}{\hbar} \int_{t_0}^t \hat{\mathcal{V}}(t') dt'}. \quad (2.70)$$

(The symbol caret is used to denote that the operators are in the interaction picture with respect to the free Hamiltonian  $\mathcal{H}_0$ ).  $\hat{\mathcal{V}}(t)$  is given as

$$\begin{aligned}
 \hat{\mathcal{V}}(t) &= \mathcal{U}_0^\dagger(t, t_0) [\mathcal{H}_{LC} + \mathcal{H}_{CR}] \mathcal{U}_0(t, t_0) \\
 &= \hat{u}_L^T(t) V^{LC} \hat{u}_C(t) + \hat{u}_R^T(t) V^{RC} \hat{u}_C(t). \quad (2.71)
 \end{aligned}$$

Eq. (2.68) in the interaction picture can be written as

$$G_{\alpha\beta}^>(t, t') = -\frac{i}{\hbar} \text{Tr} \left[ \rho_{\text{prod}}(t_0) \mathcal{S}^\dagger(t, t_0) \hat{u}_\alpha(t) \mathcal{S}(t, t') \hat{u}_\beta^T(t') \mathcal{S}(t', t_0) \right].$$

Now on contour we can simply write

$$G_{\alpha\beta}(\tau, \tau') = -\frac{i}{\hbar} \langle T_C \hat{u}_\alpha(\tau) \hat{u}_\beta^T(\tau') e^{-\frac{i}{\hbar} \int_C \hat{V}(\tau'') d\tau''} \rangle_{\rho_{\text{prod}}(t_0)}, \quad (2.72)$$

where the contour now runs from initial time  $t_0$  to the  $\max(t, t')$  and comes back to  $t_0$ . As mentioned before, this particular form is useful for perturbative calculation.

Let us now compute the  $G_{CL}(\tau, \tau')$  given as

$$G_{CL}(\tau, \tau') = -\frac{i}{\hbar} \langle T_C \hat{u}_C(\tau) \hat{u}_L^T(\tau') e^{-\frac{i}{\hbar} \int_C \hat{V}(\tau'') d\tau''} \rangle_{\rho_{\text{prod}}(t_0)}, \quad (2.73)$$

and can be shown to satisfy the following equation

$$G_{CL}(\tau, \tau') = \int d\tau'' G_{CC}(\tau, \tau'') V^{CL} g_L(\tau'', \tau'). \quad (2.74)$$

---

**Proof:**

To prove the above equation we use an alternate method known as the equations of motion approach for the contour-ordered Green's functions. Let us write down  $G_{CL}(\tau, \tau')$  in the Heisenberg picture

$$\begin{aligned} G_{CL}(\tau, \tau') &= -\frac{i}{\hbar} \langle T_C u_C(\tau) u_L^T(\tau') \rangle_{\rho_{\text{NESS}}(0)}, \\ &= -\frac{i}{\hbar} \left[ \theta(\tau, \tau') \langle u_C(\tau) u_L^T(\tau') \rangle + \theta(\tau', \tau) \langle u_L(\tau') u_C^T(\tau) \rangle^T \right]. \end{aligned} \quad (2.75)$$

Taking derivatives with respect to contour time  $\tau'$  and using the relations  $\partial\theta(\tau, \tau')/\partial\tau =$

$\delta(\tau, \tau')$  and  $\partial\theta(\tau', \tau)/\partial\tau = -\delta(\tau, \tau')$  we obtain

$$\frac{\partial^2 G_{CL}(\tau, \tau')}{\partial\tau'^2} = -\frac{i}{\hbar} \langle T_C u_C(\tau) \ddot{u}_L^T(\tau') \rangle_{\rho_{\text{NESS}}(0)}, \quad (2.76)$$

where we use  $[\dot{u}_L(\tau), u_C(\tau)] = 0$ . Now using the equation of motion for  $u_L$  on contour,

$$\ddot{u}_L(\tau) = -K^L u_L(\tau) - V^{LC} u_C(\tau), \quad (2.77)$$

we obtain the the equation of motion for  $G_{CL}$  as

$$\frac{\partial^2 G_{CL}(\tau, \tau')}{\partial\tau'^2} + G_{CL}(\tau, \tau') K^L = -G_{CC}(\tau, \tau') V^{CL}. \quad (2.78)$$

This equation can be solved by defining a Green's function of the left-lead, satisfy the following differential equation

$$\left[ \frac{\partial^2}{\partial\tau'^2} + K^L \right] g_L(\tau, \tau') = -I\delta(\tau, \tau'). \quad (2.79)$$

By multiplying Eq. (2.78) by  $g_L(\tau, \tau')$  on the right, and multiplying Eq. (2.79) by  $G_{CL}(\tau, \tau')$  on the left, then integrating by parts the subtraction of Eq. (2.78) and Eq. (2.79), we obtain

$$\begin{aligned} G_{CL}(\tau, \tau') &= \int d\tau'' G_{CC}(\tau, \tau'') V^{CL} g_L(\tau'', \tau') \\ &+ \frac{\partial G_{CL}(\tau, \tau'')}{\partial\tau''} g_L(\tau'', \tau') - G_{CL}(\tau, \tau'') \frac{\partial g_L(\tau'', \tau')}{\partial\tau''} \Big|_{-t_0+i\epsilon}^{-t_0-i\epsilon} \end{aligned} \quad (2.80)$$

At both ends of the contour, the center and the baths are decoupled. Therefore for  $\tau'' = -t_0 \pm i\epsilon$ ,  $G_{CL}(\tau, \tau'') = \frac{\partial G_{CL}(\tau, \tau'')}{\partial\tau''} = 0$  and we obtain Eq. (2.74). This equation can also be proved by performing perturbative expansion of Eq. (2.73). (See [15])

It is important to note that in deriving the above equation we didn't assume that the center is harmonic. Therefore this equation is also valid for the interacting center. The only crucial requirement is that the leads are non-interacting (harmonic). The Green's function  $g_\alpha$  introduced in Eq. (2.79) is known as the bare or free equilibrium Green's functions calculated at temperature  $T_\alpha$  and is defined as

$$g_{\alpha\beta}(\tau, \tau') = -\frac{i}{\hbar} \text{Tr}[\rho_\alpha T_C \hat{u}_\alpha(\tau) \hat{u}_\beta(\tau')] \delta_{\alpha\beta} \quad \alpha, \beta = L, C, R. \quad (2.81)$$

Using Langreth's rule we write the lesser and greater components of  $G_{CL}$  in real time as

$$G_{CL}^{>,<}(t, t') = \int_{t_0}^t dt'' \left[ G_{CC}^r(t, t'') V^{CL} g_L^{>,<}(t'' - t') + G_{CC}^{>,<}(t, t'') V^{CL} g_L^a(t'' - t') \right]. \quad (2.82)$$

Note that the bare Green's functions are time-translationally invariant. Then using Eq. (2.66) we get the expression for current as

$$\langle \mathcal{I}_L(t) \rangle = \frac{i\hbar}{2} \int_{t_0}^t dt'' \frac{\partial}{\partial t'} \text{Tr} \left[ G_{CC}^r(t, t'') \Sigma_L^K(t'' - t') + G_{CC}^K(t, t'') \Sigma_L^a(t'' - t') \right]_{t'=t}. \quad (2.83)$$

This expression is valid for any transient time  $t$  and also for interacting center which could be explicitly time-dependent. Here  $\Sigma_L = V^{CL} g_L V^{LC}$  is the self-energy for the left lead. Similar definition also exist for the right lead.

The main task now is to calculate the center Green's function  $G_{CC}(\tau, \tau')$ .

As before in the interaction picture we can write

$$G_{CC}(\tau, \tau') = -\frac{i}{\hbar} \langle T_C \hat{u}_C(\tau) \hat{u}_C^T(\tau') e^{-\frac{i}{\hbar} \int_C \hat{V}(\tau'') d\tau''} \rangle_{\rho_{\text{prod}}(t_0)}. \quad (2.84)$$

For the harmonic center  $G_{CC}$  can be obtained exactly which we now denote as  $G_{CC}^0$  and using Feynman diagrams it is easy to show that  $G_{CC}^0$  obeys a Dyson equation

$$G_{CC}^0(\tau, \tau') = g_C(\tau, \tau') + \int_C d\tau_1 \int_C d\tau_2 g_C(\tau, \tau_1) \Sigma(\tau_1, \tau_2) G_{CC}^0(\tau_2, \tau'). \quad (2.85)$$

where  $\Sigma = \Sigma_L + \Sigma_R$  is the total self-energy. This equation is similar to Eq. (2.43).

---

### **Proof:**

Let us expand the exponential in Eq. (2.84) and consider the terms order by order. The first term (0-th order in  $\hat{V}$ ) is given as

$$-\frac{i}{\hbar} \langle T_C \hat{u}_C(\tau) \hat{u}_C^T(\tau') \rangle_{\rho_C} = -\frac{i}{\hbar} \text{Tr} \left[ \rho_C \hat{u}_C(\tau) \hat{u}_C^T(\tau') \right] = g_C(\tau, \tau'). \quad (2.86)$$

The second term contains average of odd number of  $u_\alpha, \alpha = L, C, R$  which is zero as  $\rho_{\text{prod}}(t_0)$  is quadratic. The third term (2-nd order in  $\hat{V}$ ) can be written as

$$\frac{1}{2!} \left( \frac{-i}{\hbar} \right)^3 \int d\tau_1 \int d\tau_2 \langle T_C \hat{u}_C(\tau) \hat{u}_C^T(\tau') \hat{V}(\tau_1) \hat{V}(\tau_2) \rangle_{\rho_{\text{prod}}(t_0)}. \quad (2.87)$$

Let us consider  $ij$  component of this matrix. For the moment we consider only the left-center coupling term in  $\hat{\mathcal{V}}$  given in Eq. (2.71). The contribution due to other coupling term is additive. We can write  $ij$  component of the integrand in Eq. (2.87) as

$$\langle T_C \hat{u}_C^i(\tau) \hat{u}_C^j(\tau') \hat{u}_L^{i_1}(\tau_1) V_{i_1, j_1}^{LC} \hat{u}_C^{j_1}(\tau_1) \hat{u}_L^{i_2}(\tau_2) V_{i_2, j_2}^{LC} \hat{u}_C^{j_2}(\tau_2) \rangle_{\rho_{\text{prod}}(t_0)}, \quad (2.88)$$

where we write the coupling term  $\hat{u}_L^T(\tau) V^{LC} \hat{u}_C(\tau_1) = \hat{u}_L^{i_1}(\tau_1) V_{i_1, j_1}^{LC} \hat{u}_C^{j_1}(\tau_1)$  (summation over repeated index is implied). Now since  $\rho_{\text{prod}}(t_0)$  is decoupled we can separate the contour-ordered as

$$\langle T_C \hat{u}_C^i(\tau) \hat{u}_C^j(\tau') \hat{u}_C^{j_1}(\tau_1) \hat{u}_C^{j_2}(\tau_2) \rangle_{\rho_C} \langle T_C \hat{u}_L^{i_1}(\tau_1) \hat{u}_L^{i_2}(\tau_2) \rangle_{\rho_L} V_{i_1, j_1}^{LC} V_{i_2, j_2}^{LC} \quad (2.89)$$

We see that the first term consists of 4  $u_C$  operators. According to Wick's theorem this can be separated as products of two  $u_C$  operators, *i.e.*,

$$\begin{aligned} \langle T_C \hat{u}_C^i(\tau) \hat{u}_C^j(\tau') \hat{u}_C^{j_1}(\tau_1) \hat{u}_C^{j_2}(\tau_2) \rangle &= \langle T_C \hat{u}_C^i(\tau) \hat{u}_C^j(\tau') \rangle \langle T_C \hat{u}_C^{j_1}(\tau_1) \hat{u}_C^{j_2}(\tau_2) \rangle \\ &+ \langle T_C \hat{u}_C^i(\tau) \hat{u}_C^{j_1}(\tau_1) \rangle \langle T_C \hat{u}_C^j(\tau') \hat{u}_C^{j_2}(\tau_2) \rangle \\ &+ \langle T_C \hat{u}_C^i(\tau) \hat{u}_C^{j_2}(\tau_2) \rangle \langle T_C \hat{u}_C^{j_1}(\tau_1) \hat{u}_C^j(\tau') \rangle. \end{aligned} \quad (2.90)$$

Out of these three terms, first term will give disconnected diagram which can be shown to be zero [15] and other two terms are connected diagrams and contribute identically which cancels  $1/2!$  originating from the expansion of the exponential in Eq. (2.87). The  $(-i/\hbar)^3$  factor absorbs in three Green's functions. Therefore

this term can be written as

$$\begin{aligned} & \int d\tau_1 \int d\tau_2 g_C^{i,j_1}(\tau, \tau_1) \Sigma_L^{j_1, j_2}(\tau_1, \tau_2) g_C^{j_2, j}(\tau_2, \tau') \\ & \int d\tau_1 \int d\tau_2 \left[ g_C(\tau, \tau_1) \Sigma_L(\tau_1, \tau_2) g_C(\tau_2, \tau') \right]_{ij}, \end{aligned} \quad (2.91)$$

where  $\Sigma_L^{j_1, j_2}(\tau_1, \tau_2) = V_{CL}^{j_1, i_1} g_L^{i_1, i_2}(\tau_1, \tau_2) V_{LC}^{i_2, j_2}$ . and similar equation exist if we include the right-center coupling term. Therefore the total contribution in the 2-nd order is

$$\int d\tau_1 \int d\tau_2 \left[ g_C(\tau, \tau_1) \Sigma(\tau_1, \tau_2) g_C(\tau_2, \tau') \right]_{ij}. \quad (2.92)$$

This feature repeats for the higher-order terms and for general  $n$ -th order ( $n$  is even) it can be shown that

$$\begin{aligned} & \frac{1}{n!} \left( \frac{-i}{\hbar} \right)^{n+1} \int d\tau_1 \int d\tau_2 \cdots \int d\tau_n \langle T_C u_C^i(\tau) u_C^j(\tau') \mathcal{V}^I(\tau_1) \mathcal{V}^I(\tau_2) \cdots \mathcal{V}^I(\tau_n) \rangle_{\rho(t_0)} \\ & = \int d\tau_1 \int d\tau_2 \cdots \int d\tau_n \left[ g_C(\tau, \tau_1) \Sigma(\tau_1, \tau_2) g_C(\tau_2, \tau_3) \Sigma(\tau_3, \tau_4) \cdots g_C(\tau_n, \tau_1) \right]_{ij}, \end{aligned} \quad (2.93)$$

and therefore we can write

$$\begin{aligned} G_{CC}^0(\tau, \tau') & = g_C(\tau, \tau') + \int \int d\tau_1 d\tau_2 g_C(\tau, \tau_1) \Sigma(\tau_1, \tau_2) g_C(\tau_2, \tau') + \cdots \\ & + \int \int \cdots \int d\tau_1 d\tau_2 \cdots d\tau_n g_C(\tau, \tau_1) \Sigma(\tau_1, \tau_2) g_C(\tau_2, \tau_3) \cdots \Sigma(\tau_{n-1}, \tau_n) \\ & \quad g_C(\tau_n, \tau') \\ & = g_C(\tau, \tau') + \int_C d\tau_1 \int_C d\tau_2 g_C(\tau, \tau_1) \Sigma(\tau_1, \tau_2) G_{CC}^0(\tau_2, \tau'). \end{aligned} \quad (2.94)$$


---

### Steady state limit and Landauer formula

Steady state limit can be achieved by letting  $t_0 \rightarrow -\infty$ . Then by performing Fourier transformation of Eq. (2.83) we obtain

$$\langle \mathcal{I}_L \rangle = - \int_{-\infty}^{\infty} \frac{d\omega}{4\pi} \hbar\omega \text{Tr} \left[ G_0^r[\omega] \Sigma_L^K[\omega] + G_0^K[\omega] \Sigma_L^a[\omega] \right]. \quad (2.95)$$

(For notational simplicity we dropped the subscript  $CC$  in  $G_{CC}^0$ ). In the frequency domain different components of  $G_0$  are obtained from the Dyson equation given in Eq. (2.85) and are written as (see appendix (E))

$$\begin{aligned} G_0^r[\omega] &= g_C^r[\omega] + g_C^r[\omega] \Sigma^r[\omega] G_{CC}^r[\omega] \\ &= \left[ (\omega + i\eta)^2 - K^C - \Sigma^r[\omega] \right]^{-1}, \\ G_0^a[\omega] &= \left[ G_0^r[\omega] \right]^\dagger, \\ G_0^K[\omega] &= G_0^r[\omega] \Sigma^K[\omega] G_0^a[\omega], \end{aligned} \quad (2.96)$$

where for the isolated center  $g_C^r[\omega] = [(\omega + i\eta)^2 - K^C]^{-1}$  (see appendix (F)).

Now we symmetrize the expression for current as

$$\langle \mathcal{I}_L \rangle = \frac{\langle \mathcal{I}_L \rangle + [\langle \mathcal{I}_L \rangle]^*}{2} = \int_{-\infty}^{\infty} \frac{d\omega}{8\pi} \hbar\omega \text{Tr} \left[ (G_0^a[\omega] - G_0^r[\omega]) \Sigma_L^K[\omega] + G_0^K[\omega] (\Sigma_L^r[\omega] - \Sigma_L^a[\omega]) \right]. \quad (2.97)$$

The lesser and greater components of the self-energy are given in the form of fluctuation-dissipation relations *i.e.*,

$$\begin{aligned} \Sigma_\alpha^<[\omega] &= f_\alpha[\omega] (\Sigma_\alpha^r[\omega] - \Sigma_\alpha^a[\omega]), \\ \Sigma_\alpha^>[\omega] &= (1 + f_\alpha[\omega]) (\Sigma_\alpha^r[\omega] - \Sigma_\alpha^a[\omega]), \quad \alpha = L, R, \end{aligned} \quad (2.98)$$

where  $f_\alpha[\omega] = 1/(e^{\beta_\alpha \hbar \omega_\alpha} - 1)$  is the Bose distribution function for the leads.

We define the spectral function for the leads as

$$\Gamma_\alpha[\omega] = i(\Sigma_\alpha^r[\omega] - \Sigma_\alpha^a[\omega]) \quad \alpha = L, R. \quad (2.99)$$

Using these relations and an important identity given by (see appendix (E))

$$G_0^a[\omega] - G_0^r[\omega] = i G_0^r[\omega] (\Gamma_L[\omega] + \Gamma_R[\omega]) G_0^a[\omega], \quad (2.100)$$

we can simplify the expression for current and obtain the Landauer formula as

$$\langle \mathcal{I}_L \rangle = \int_{-\infty}^{\infty} \frac{d\omega}{4\pi} \hbar \omega \text{Tr}[\mathcal{T}(\omega)] (f_L[\omega] - f_R[\omega]), \quad (2.101)$$

where  $\text{Tr}[\mathcal{T}[\omega]]$  is known as the Transmission function and given by the Caroli formula [31]

$$\mathcal{T}[\omega] = G_0^r[\omega] \Gamma_L[\omega] G_0^a[\omega] \Gamma_R[\omega]. \quad (2.102)$$

From the expression for current, the conductance  $\sigma$  can be obtained as

$$\sigma(T) = \lim_{T_L \rightarrow T, T_R \rightarrow T} \frac{\langle \mathcal{I}_L \rangle}{T_L - T_R} = \int_{-\infty}^{\infty} \frac{d\omega}{4\pi} \hbar \omega \text{Tr}[\mathcal{T}(\omega)] \frac{\partial f[\omega]}{\partial T}, \quad (2.103)$$

where  $T$  is the equilibrium temperature.

# Bibliography

- [1] J. Schwinger, J. Math. Phys. (New York) **2**, 407 (1961).
- [2] L.P. Kadanoff, G. Baym, *Quantum Statistical Mechanics* (Benjamin/Cummings, 1962).
- [3] L.V. Keldysh, Soviet Phys. JETP **20**, 1018 (1965).
- [4] J. Rammer and H. Smith, Rev. Mod. Phys. **58**, 323 (1986).
- [5] J. Rammer *Quantum Field Theory of Nonequilibrium States* (Cambridge 2007).
- [6] A. Ozpineci, S. Ciraci, Phys. Rev. B **63**, 125415 (2001).
- [7] T. Yamamoto, K. Watanabe, Phys. Rev. Lett. **96**, 255503 (2006).
- [8] A. Dhar, Adv. Phys. **57**, 457 (2008).
- [9] J.-S. Wang, J. Wang, N. Zeng, Phys. Rev. B **74**, 033408 (2006).
- [10] J.-S. Wang, N. Zeng, J. Wang, C.K. Gan, Phys. Rev. E **75**, 061128 (2007).
- [11] N. Mingo, Phys. Rev. B **74**, 125402 (2006).

## BIBLIOGRAPHY

---

- [12] H.-P. Liu, L. Yi, *Chin. Phys. Lett.* **23**, 3194 (2006).
- [13] M. Galperin, A. Nitzan, M.A. Ratner, *Phys. Rev. B* **75**, 155312 (2007).
- [14] S. Datta, *Electronic Transport in Mesoscopic Systems* (Cambridge Univ. Press, 1995).
- [15] H. Haug and A.-P. Jauho, *Quantum Kinetics in Transport and Optics of Semiconductors*, 2nd ed. (Springer, New York, 2008).
- [16] M. D. Ventra, *Electrical Transport in Nanoscale Systems* (Cambridge University Press, Cambridge, 2008).
- [17] J.-S. Wang, J. Wang, and J. T. Lü, *Eur. Phys. J. B* **62**, 381 (2008).
- [18] R van Leeuwen and N E Dahlen, *An Introduction to Nonequilibrium Green Functions, Lecture notes* (2005).
- [19] H. Bruus, K. Flensberg, *Many-Body Quantum Theory in Condensed Matter Physics, an introduction* (Oxford Univ. Press, 2004).
- [20] G.D. Mahan, *Many-Particle Physics*, 3rd edn. (Kluwer Academic, 2000).
- [21] Kubo, R., M. Toda, and N. Hashitsume, 1998, *Statistical Physics II: Nonequilibrium Statistical Mechanics*, 2nd ed. (Springer, New York).
- [22] A.A. Abrikosov, L.P. Gorkov, I.E. Dzyaloshinski, *Methods of Quantum Field Theory in Statistical Physics* (Dover Publ., 1963).
- [23] A.L. Fetter, J.D. Walecka, *Quantum Theory of Many-Particle Systems* (McGraw-Hill, 1971).

## BIBLIOGRAPHY

---

- [24] R. Landauer, IBM J. Res. Dev. **1**, 223 (1957).
- [25] R. Landauer, Philos. Mag. **21**, 863 (1970).
- [26] Y. Meir, N.S. Wingreen, Phys. Rev. Lett. **68**, 2512 (1992).
- [27] A. P. Jauho, N.S. Wingreen, and Y. Meir, Phys. Rev. B. **68**, 5528 (1994).
- [28] D. Segal, A. Nitzan, P. Hanggi, J. Chem. Phys. **119**, 6840 (2003).
- [29] A. Dhar, D. Roy, J. Stat. Phys. **125**, 805 (2006).
- [30] J.-S. Wang, Phys. Rev. Lett. **99**, 160601 (2007).
- [31] C. Caroli, R. Combescot, P. Nozieres, D. Saint-James, J. Phys. C: Solid St. Phys. 4, **916** (1971).

## Chapter 3

# Full-counting statistics (FCS) in heat transport for ballistic lead-junction-lead setup

In the previous chapter we have introduced the lead-junction-lead setup to study heat transport with the junction part considered as harmonic. Based on this model, we study here the energy-counting statistics *i.e.*, the statistics of heat (integrated current), transferred through the center (denoted by  $C$ ) (Fig. 3.1) during a given time interval  $[0, t_M]$ . In addition, we consider the situation where the atoms in the junction part could be driven by external time-dependent force. This opens up the possibility to study energy-dissipation, heat-pumping behavior, and also Jarzynski equality in the context of fluctuation theorems. Employing NEGF-Keldysh

formalism we obtain the cumulant generating function (CGF) under this general scenario. The developed formalism can deal with both transient and steady-state on equal footing and also various initial conditions for the density operator. Such investigations gives definite answer to some of the very general *queries* in quantum dissipative transport such as

1. Under what conditions the system reaches steady state and whether it is unique or not?
2. How initial conditions and quantum measurements affect the transient?
3. What are the effects of system parameters on the steady state.

In this chapter, we try to give answers to these questions. We also show that the effect of energy measurement to obtain heat is reflected in CGF via the shifted time argument for the self-energy. In the steady state we obtain explicit expression for the CGF which is similar to the Levitov-Lesovik formula [1, 2] for electrons and satisfy Gallavotti-Cohen(GC) [3, 4] fluctuation symmetry. In the later part of this chapter we derive the CGF corresponding to the joint probability distribution  $P(Q_L, Q_R)$ , and discuss the correlation between  $Q_L$  and  $Q_R$ .

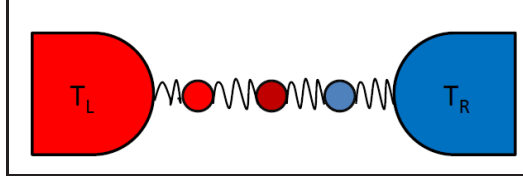


Figure 3.1: A schematic representation of lead-junction-lead setup. The left ( $L$ ) and right ( $R$ ) leads are at temperatures  $T_L$  and  $T_R$  respectively. The leads are modeled as coupled harmonic oscillators. The center ( $C$ ) here consists of 3 atoms.

### 3.1 The general lattice model

Here we introduce a very general lattice model to study heat transport. As before, the full system is divided into three parts the left, right and the center. The leads are modeled as infinite collection of coupled harmonic oscillators. Such heat baths are named after Rubin and often called as Rubin heat baths [5, 6]. The Hamiltonian for these three parts are given as

$$\mathcal{H}_\alpha = \frac{1}{2} p_\alpha^T p_\alpha + \frac{1}{2} u_\alpha^T K^\alpha u_\alpha, \quad \alpha = L, C, R, \quad (3.1)$$

where the meaning of  $p_\alpha, u_\alpha$  and  $K^\alpha$  are the same, as explained in Chapter 2 (see Sec. 2.4). The center part can also have nonlinear interactions such as phonon-phonon interactions and takes the following form

$$\mathcal{H}_n = \frac{1}{3} \sum_{ijk} T_{ijk} u_i^C u_j^C u_k^C + \frac{1}{4} \sum_{ijkl} T_{ijkl} u_i^C u_j^C u_k^C u_l^C. \quad (3.2)$$

The quartic interaction is important in stabilizing the system, as a purely cubic term makes the energy unbounded from below. The coupling between the center and the leads is quadratic in position and the coupling

matrix in our formalism could be time-dependent. Therefore the coupling Hamiltonian is given as

$$\mathcal{H}_T(t) = u_L^T V^{LC}(t) u_C + u_R^T V^{RC}(t) u_C. \quad (3.3)$$

Note that  $V^{LC}(t) = [V^{CL}(t)]^T$  and similarly for  $V^{CR}(t)$ .  $T$  here stands for the matrix transpose. Such time-dependent coupling are useful for manipulating current, developing devices such as thermal switch, heat pump [7, 8] etc. The dynamic matrix of the full linear system is

$$K = \begin{bmatrix} K^L & V^{LC}(t) & 0 \\ V^{CL}(t) & K^C & V^{CR}(t) \\ 0 & V^{RC}(t) & K^R \end{bmatrix}. \quad (3.4)$$

We assume that there is no direct interaction between the leads. For  $t > 0$ , an external time-dependent force is applied to the center atoms, which couples only with the position operators *i.e.*,

$$\mathcal{V}_C(t) = -f^T(t) u_C, \quad (3.5)$$

where  $f(t)$  is the time-dependent force vector. The force can be in the form of electromagnetic field. Choice of this particular type of coupling helps us to obtain an analytical solution for the CGF, as the entire system is still harmonic. Therefore the full Hamiltonian for  $t > 0$  (in the Schrödinger picture) is given as

$$\mathcal{H}(t) = \mathcal{H}(0^-) + \mathcal{V}_C(t) = \mathcal{H}_C + \mathcal{H}_L + \mathcal{H}_R + \mathcal{H}_T(t) + \mathcal{H}_n + \mathcal{V}_C(t). \quad (3.6)$$

In this chapter we will focus on the harmonic junction. *i.e.*,  $\mathcal{H}_n = 0$  and discuss the nonlinear effects in chapter 6.

## 3.2 Definition of current, heat and entropy-production

In this thesis, we will be looking at the statistics of two nonequilibrium quantities namely the heat and the entropy-production. Let us say that we are interested in the energy flowing out of the left lead during the time interval  $[0, t_M]$ . Then the heat operator is defined as the time integral of the left lead current operator  $\mathcal{I}_L$ .

### Heat operator for the left-lead

The left lead heat operator is given as the change of energy of left lead Hamiltonian.

$$\mathcal{Q}_L(t_M) = \int_0^{t_M} \mathcal{I}_L(t') dt' = \mathcal{H}_L(0) - \mathcal{H}_L^H(t_M), \quad (3.7)$$

where the current operator  $\mathcal{I}_L(t)$ , as defined previously, is the rate of change of energy of the left-lead *i.e.*,

$$\mathcal{I}_L(t) = -\frac{d\mathcal{H}_L^H(t)}{dt} = \frac{i}{\hbar} [\mathcal{H}_L^H(t), \mathcal{H}^H(t)] = p_L^T(t) V^{LC}(t) u_C(t), \quad (3.8)$$

Here the operators are in the Heisenberg picture. The dependence of  $t$  in

$V^{LC}(t)$  is parametric.  $\mathcal{H}_L [= \mathcal{H}_L(0)]$  is the Schrödinger operator of the free left lead and

$$\mathcal{H}_L^H(t) = \mathcal{U}(0, t) \mathcal{H}_L \mathcal{U}(t, 0). \quad (3.9)$$

$\mathcal{U}(t, t')$  is the evolution operator corresponding to the full Hamiltonian  $\mathcal{H}(t)$  and satisfies the Schrödinger equation with the formal solution

$$\mathcal{U}(t, t') = \begin{cases} T \exp \left[ -\frac{i}{\hbar} \int_{t'}^t \mathcal{H}(t_1) dt_1 \right] & \text{for } t > t' \\ \bar{T} \exp \left[ \frac{i}{\hbar} \int_t^{t'} \mathcal{H}(t_1) dt_1 \right] & \text{for } t' > t \end{cases}$$

where  $T$  ( $\bar{T}$ ) is the time order (anti-time ordered) operator which orders the operators with increasing time from right (left) to left (right).

### Entropy-production in the leads

Based on the idea of macroscopic thermodynamics, we also define the net entropy-production in the leads due to exchange of heat as [9, 10]

$$\Sigma(t_M) = - \sum_{\alpha=L,R} \beta_\alpha \mathcal{Q}_\alpha(t_M) = \sum_{\alpha=L,R} \beta_\alpha \left( \mathcal{H}_\alpha^H(t_M) - \mathcal{H}_\alpha(0) \right) \quad (3.10)$$

with  $\beta_\alpha = 1/k_B T_\alpha$  is related to the inverse temperature of the leads.

## 3.3 Characteristic function (CF)

The primary interest in FCS for charge/heat transport is to obtain the probability distribution for the transferred quantity. However calculating

these distributions directly is highly nontrivial if not impossible. The most convenient approach to get the distribution is to work with the characteristic function (CF) which is simply the Fourier transformation of the probability distribution. Once the CF is known, physical observables *i.e.*, the moments of charge/heat are then obtained by the derivatives of this CF and the inverse Fourier transformation will give the probability distribution.

### **CF for heat**

Based on the definition of heat in Eq. (3.7) and following the derivation for the CF using two-time measurement procedure, in the introduction chapter (see Eq. (1.18)), we can identify operator  $\mathcal{A}$  as  $\mathcal{H}_L$  and the transferred quantity as  $Q_L = a_0 - a_{t_M}$  where  $a_0$  and  $a_{t_M}$  are the eigenvalues associated with the measurement of  $\mathcal{H}_L$  at time 0 and  $t_M$  respectively. (Note that  $Q$  of non-calligraphic font is a classical variable). Here  $\mathcal{H}_L$  does not depend on time explicitly. Thus the CF is simply given as [11]

$$\begin{aligned}
 \mathcal{Z}(\xi_L) &= \langle e^{i\xi_L Q_L} \rangle = \langle e^{i\xi_L(a_0 - a_{t_M})} \rangle = \sum_{a_0, a_{t_M}} e^{i\xi_L(a_0 - a_{t_M})} P(a_{t_M}, a_0) \\
 &= \langle e^{i\xi_L \mathcal{H}_L} e^{-i\xi_L \mathcal{H}_L^H(t_M)} \rangle_{\rho'(0)} \\
 &= \langle e^{i\xi_L \mathcal{H}_L/2} e^{-i\xi_L \mathcal{H}_L^H(t_M)} e^{i\xi_L \mathcal{H}_L/2} \rangle_{\rho'(0)}. \tag{3.11}
 \end{aligned}$$

The average here is with respect to the *projected* density matrix *i.e.*,

$$\rho'(0) = \sum_{a_0} \Pi_{a_0} \rho(0) \Pi_{a_0}, \tag{3.12}$$

which captures the information about the initial measurement.  $\rho(0)$  is the density operator of the entire system. Note that the above expression for the CF is valid for general interacting center and therefore is also the starting point for calculations for anharmonic systems. Once this CF is known the probability distribution for  $Q_L$  is obtained as

$$P(Q_L) = \int_{-\infty}^{\infty} \frac{d\xi_L}{2\pi} e^{-i\xi_L Q_L} \mathcal{Z}(\xi_L). \quad (3.13)$$

### Generalization of the CF

Based on this two-time measurement procedure, it is easy to generalize the CF corresponding to the measurement of multiple operators. This is possible only if the operators commute with each other at the same instant of time. Then according to quantum mechanics such measurements are allowed and Nelson's theorem [12] guarantees that the probability distribution in such case is well-defined.

For example, in this model, it is possible to measure the Hamiltonians  $\mathcal{H}_\alpha, \alpha = L, C, R$  for the leads and the center simultaneously as they all commute with each other at any given time. Therefore if we perform two-time measurement for these operators once at time  $t = 0$  and then at the final time  $t = t_M$  the CF can be generalized as

$$\begin{aligned} \mathcal{Z}(\xi_L, \xi_C, \xi_R) &= \langle e^{i\xi_L Q_L + i\xi_C Q_C + i\xi_R Q_R} \rangle \\ &= \langle e^{i \sum_{\alpha=L,C,R} \xi_\alpha \mathcal{H}_\alpha} e^{-i \sum_{\alpha=L,C,R} \xi_\alpha \mathcal{H}_\alpha^H(t_M)} \rangle_{\rho'(0)}, \end{aligned} \quad (3.14)$$

where we now modify the *projected* density operator as

$$\rho'(0) = \sum_{a_0, b_0, c_0} \Pi_{a_0}^L \Pi_{b_0}^C \Pi_{c_0}^R \rho(0) \Pi_{a_0}^L \Pi_{b_0}^C \Pi_{c_0}^R. \quad (3.15)$$

Here  $a_0, b_0$  and  $c_0$  are the eigenvalues of  $\mathcal{H}_L$ ,  $\mathcal{H}_C$  and  $\mathcal{H}_R$  respectively corresponding to the measurements at time  $t = 0$ . For this CF the inverse Fourier transformation will give the joint probability distribution  $P(Q_L, Q_C, Q_R)$ ,

$$P(Q_L, Q_C, Q_R) = \int_{-\infty}^{\infty} \int_{-\infty}^{\infty} \int_{-\infty}^{\infty} \frac{d\xi_L}{2\pi} \frac{d\xi_C}{2\pi} \frac{d\xi_R}{2\pi} e^{-(i\xi_L Q_L + i\xi_C Q_C + i\xi_R Q_R)} \mathcal{Z}(\xi_L, \xi_C, \xi_R). \quad (3.16)$$

In the later part of this chapter we derive an explicit expression for a restricted version of this CF which is  $\mathcal{Z}(\xi_L, \xi_R)$  at  $\xi_C = 0$  to obtain the correlations between the left and the right lead heat and also the CF for entropy-production.

### Nazarov's definition of CF

Another definition of CF which is used mostly for the electronic transport case is given by Nazarov et al. [13, 14]. It is defined as

$$\mathcal{Z}_1(\xi_L) = \langle \bar{T} e^{i\xi_L Q_L/2} T e^{i\xi_L Q_L/2} \rangle. \quad (3.17)$$

The time (or anti-time) order operator here is meant to apply to the integrand when the exponential is expanded and  $Q_L$  is expressed as integral

over  $\mathcal{I}_L$  as in Eq. (3.7) *i.e.*,

$$T e^{i\xi_L \mathcal{Q}_L/2} = \sum_{n=0}^{\infty} \frac{1}{n!} \left( \frac{i\xi_L}{2} \right)^n \int_0^{t_M} dt_1 \int_0^{t_M} dt_2 \cdots \int_0^{t_M} dt_n T[\mathcal{I}_L(t_1)\mathcal{I}_L(t_2)\cdots\mathcal{I}_L(t_n)]. \quad (3.18)$$

In the last section of this chapter we will show how this CF can be derived starting from  $\mathcal{Z}(\xi_L)$  given in Eq. (3.11) under a particular assumption and will present the long-time limit expression for  $\mathcal{Z}_1(\xi_L)$  for this harmonic model. We will show that this CF does not respect the Gallavotti-Cohen (GC) fluctuation symmetry, however the first two cumulants of heat matches with the ones obtained from  $\mathcal{Z}(\xi_L)$  which also followed from the definitions.

### 3.4 Initial conditions for the density operator

In this chapter, we derive analytic expressions for the CF of heat  $\mathcal{Z}(\xi_L)$  for three different initial conditions of the density operator and discuss the behavior of the moments (cumulants) of heat at transient as well as at long time. We choose three different initial conditions as:

#### Product initial state:

We assume at  $t < 0$ , the three parts of the full system *i.e.*, the center ( $C$ ) and the leads ( $L$  and  $R$ ) are decoupled and equilibrated at their respective

equilibrium temperatures  $T_\alpha$  ( $\alpha = L, C, R$ ) by keeping them in weak contacts with respective heat baths. Therefore each system will be in their own equilibrium distributions. At  $t = 0$  the heat baths are removed and the connection between the system and the leads are switched on suddenly. Therefore the initial density matrix at  $t = 0$  is given by the direct product state of  $L, C$  and  $R$  *i.e.*,

$$\rho_{\text{prod}}(0) = \rho_L \otimes \rho_C \otimes \rho_R, \quad \rho_\alpha = \frac{e^{-\beta_\alpha \mathcal{H}_\alpha}}{\text{Tr}[e^{-\beta_\alpha \mathcal{H}_\alpha}]} \text{ for } \alpha = L, C, R, \quad (3.19)$$

where  $\beta_\alpha = 1/(k_B T_\alpha)$  is the inverse temperature. Note that for such initial condition the initial projection operators in Eq. (3.12) and Eq. (3.15) do not play any role as  $[\mathcal{H}_\alpha, \Pi_\beta] = 0$  ( $\alpha, \beta = L, C, R$ ) and therefore  $\rho'(0)$  coincides with  $\rho_{\text{prod}}(0)$ .

### Steady state as initial state:

Here we consider the initial density operator as the nonequilibrium steady state denoted as  $\rho_{\text{NESS}}(0)$ . As mentioned before (while deriving the Landauer formula in chapter 2), this particular nonequilibrium state can be achieved by starting with the decoupled initial state  $\rho_{\text{prod}}$  at  $t = -\infty$  and then switching on the couplings between the center and the leads adiabatically up to time  $t = 0$  when the couplings become full *i.e.*,

$$\begin{aligned} \mathcal{H}_T(t) &= (\mathcal{H}_{LC} + \mathcal{H}_{RC})e^{-\epsilon|t|}, \quad \text{for } -\infty < t < 0, \quad \epsilon \rightarrow 0^+, \\ &= \mathcal{H}_{LC}(t) + \mathcal{H}_{RC}(t) \quad \text{for } t > 0. \end{aligned} \quad (3.20)$$

We assume that at  $t = 0$  the system reaches to a unique steady state,

independent of the center temperature  $T_C$ . We can then relate  $\rho_{\text{NESS}}(0)$  with  $\rho_{\text{prod}}(0)$  by the following equation

$$\rho_{\text{NESS}}(0) = \mathcal{U}(0, -\infty)\rho_{\text{prod}}(-\infty)\mathcal{U}(-\infty, 0). \quad (3.21)$$

where  $\mathcal{U}(0, -\infty) = T \exp \left[ -\frac{i}{\hbar} \int_{-\infty}^0 \mathcal{H}_0 + (\mathcal{H}_{LC} + \mathcal{H}_{RC})e^{-\epsilon|t|} dt \right]$  and  $\mathcal{H}_0 = \mathcal{H}_L + \mathcal{H}_C + \mathcal{H}_R$ .

### **Projected initial state:**

To capture the effect of the initial measurement explicitly we consider the projected density matrix  $\rho'(0)$  by choosing  $\rho(0)$  as the NESS. Since  $[\rho_{\text{NESS}}, \Pi_\alpha] \neq 0$ ,  $\rho'(0)$  does not coincide with  $\rho_{\text{NESS}}(0)$ .

---

### **Consistent Quantum Framework**

Based on the CF  $\mathcal{Z}(\xi_L)$  the first moment or the heat is given as

$$\langle Q_L(t_M) \rangle = \left. \frac{\partial \mathcal{Z}(\xi_L)}{\partial (i\xi_L)} \right|_{\xi_L=0} = \text{Tr} \left[ \rho'(0) (\mathcal{H}_L(0) - \mathcal{H}_L^H(t_M)) \right], \quad (3.22)$$

and the heat current is just the time derivative of the heat *i.e.*,

$$\langle \mathcal{I}_L(t_M) \rangle = -\text{Tr} \left[ \rho'(0) \frac{d\mathcal{H}_L^H(t_M)}{dt_M} \right]. \quad (3.23)$$

On the contrary, it is possible to calculate the current from the natural definition, introduced in the previous chapter, and is given as

$$\langle \mathcal{I}_L(t_M) \rangle = -\text{Tr} \left[ \rho(0) \frac{d\mathcal{H}_L^H(t_M)}{dt_M} \right]. \quad (3.24)$$

Note the difference in the density operator for these two cases. These two definitions are certainly not consistent and therefore thermal current deriving from the CF will not be equal to the natural definition of it. It is only for the product initial state when these two definitions matches and assures a consistent quantum framework for the problem. For details see [15, 16].

---

In the following section we derive analytic expressions for the CF of heat starting from Eq. (3.11) considering these three initial conditions.

## 3.5 Derivation of the CF $\mathcal{Z}(\xi_L)$ for heat

### 3.5.1 $\mathcal{Z}(\xi_L)$ for product initial state $\rho_{\text{prod}}(0)$ using Feynman diagrammatic technique

In this subsection we derive the CF for heat  $\mathcal{Z}(\xi_L)$  starting with the product initial state  $\rho_{\text{prod}}(0)$  Because in this case the initial projection does not play any role the calculation for CF simplifies greatly. To obtain the CF we take the following steps:

- Express the CF as an effective evolution of the unitary operators on the Keldysh contour.

- Write the CF in the interaction picture with respect to the decoupled Hamiltonians i.e.,  $\mathcal{H}_0 = \mathcal{H}_L + \mathcal{H}_R + \mathcal{H}_C$  and treating  $\mathcal{H}_T(t) + \mathcal{V}_C(t)$  as interaction.
- Expand the CF in the interaction picture and use Wick's theorem and Feynman diagrammatic technique to obtain the final result.

Step 1: CF on Keldysh contour:

Following Eq. (3.11) we can write

$$\begin{aligned}
 \mathcal{Z}(\xi_L) &= \left\langle e^{i\xi_L \mathcal{H}_L/2} e^{-i\xi_L \mathcal{H}_L(t_M)} e^{i\xi_L \mathcal{H}_L/2} \right\rangle \\
 &= \left\langle e^{i\xi_L \mathcal{H}_L/2} \mathcal{U}(0, t_M) e^{-i\xi_L \mathcal{H}_L/2} e^{-i\xi_L \mathcal{H}_L/2} \mathcal{U}(t_M, 0) e^{i\xi_L \mathcal{H}_L/2} \right\rangle \\
 &= \left\langle \mathcal{U}_{\xi_L/2}(0, t_M) \mathcal{U}_{-\xi_L/2}(t_M, 0) \right\rangle, \tag{3.25}
 \end{aligned}$$

where we define the modified unitary operator  $\mathcal{U}_x(t, t')$  ( $x = \pm\xi_L/2$ ) as

$$\begin{aligned}
 \mathcal{U}_x(t, t') &= e^{ix\mathcal{H}_L} \mathcal{U}(t, t') e^{-ix\mathcal{H}_L} \\
 &= \sum_{n=0}^{\infty} \left( -\frac{i}{\hbar} \right)^n \int_{t'}^t dt_1 \int_{t'}^{t_1} dt_2 \cdots \int_{t'}^{t_{n-1}} dt_n \\
 &\quad \times e^{ix\mathcal{H}_L} \mathcal{H}(t_1) \mathcal{H}(t_2) \cdots \mathcal{H}(t_n) e^{-ix\mathcal{H}_L} \\
 &= T \exp \left\{ -\frac{i}{\hbar} \int_{t'}^t \mathcal{H}_x(t') dt' \right\}. \tag{3.26}
 \end{aligned}$$

which is an evolution operator associated with the modified total Hamiltonian  $\mathcal{H}_x(t)$  and obeys the following Schrödinger equation

$$i\hbar \frac{d\mathcal{U}_x(t, t')}{dt} = \mathcal{H}_x(t) \mathcal{U}_x(t, t'), \tag{3.27}$$

with  $\mathcal{H}_x$  given as

$$\begin{aligned}\mathcal{H}_x(t) &= e^{ix\mathcal{H}_L}\mathcal{H}(t)e^{-ix\mathcal{H}_L}, \\ &= \mathcal{H}(t) + (u_L(\hbar x) - u_L)^T V^{LC} u_C,\end{aligned}\quad (3.28)$$

where  $u_L(\hbar x) = e^{ix\mathcal{H}_L}u_L e^{-ix\mathcal{H}_L}$  is the free left lead Heisenberg evolution to time  $t = \hbar x$ . Since the leads are harmonic  $u_L(\hbar x)$  can be explicitly obtained.

$$u_L(\hbar x) = \cos(\sqrt{K_L}\hbar x)u_L + \frac{1}{\sqrt{K_L}}\sin(\sqrt{K_L}\hbar x)p_L. \quad (3.29)$$

The matrix  $\sqrt{K_L}$  is well-defined as the matrix  $K_L$  is positive definite.  $u_L$  and  $p_L$  are the initial values at  $t = 0$ . The final expression for  $\mathcal{H}_x(t)$  is

$$\mathcal{H}_x(t) = \mathcal{H}(t) + [u_L^T \mathcal{C}(x) + p_L^T \mathcal{S}(x)]u_C, \quad (3.30)$$

where

$$\begin{aligned}\mathcal{C}(x) &= (\cos(\hbar x\sqrt{K_L}) - I)V^{LC}, \\ \mathcal{S}(x) &= (1/\sqrt{K_L})\sin(\hbar x\sqrt{K_L})V^{LC}.\end{aligned}\quad (3.31)$$

We see that the effective Hamiltonian now has two additional terms with respect to the full  $\mathcal{H}(t)$ . The term  $u_L^T \mathcal{C}(x)u_C$  is like the harmonic coupling term which modifies the coupling matrix  $V^{LC}(t)$ .

Now we will make use of NEGF technique, introduced in the previous chapter. As explained before, if we read Eq. (3.25) from right to left, it says given a state it will evolve from initial time  $t = 0$  to a maximum time  $t_M$  under the unitary operator  $\mathcal{U}_{-\xi_L/2}(t, 0)$  and then evolves back from time  $t_M$  to 0 with unitary evolution  $\mathcal{U}_{\xi_L/2}^\dagger(t, 0)$ . Therefore, we can represent the CF on the Keldysh contour as

$$\mathcal{Z}(\xi_L) = \text{Tr} \left[ \rho_{\text{prod}}(0) T_C e^{-\frac{i}{\hbar} \int_C \mathcal{H}_x(\tau) d\tau} \right]. \quad (3.32)$$

and  $T_C$  is the same contour-ordered operator defined in chapter 2 (operator later on contour placed at the left). If we transform back to the real time, the upper (lower) branch corresponds to the evolution  $\mathcal{U}_{-\xi_L/2}(t, 0)$  ( $\mathcal{U}_{\xi_L/2}^\dagger(t, 0)$ ) (see subsection 2.3.2). Running with two different evolutions on the two branches of the contour is the main essence of FCS study. Note for  $\xi_L = 0$  the normalization condition  $\mathcal{Z}(0) = 1$  is satisfied as  $\mathcal{U}^\dagger(t, 0)\mathcal{U}(t, 0) = 1$ . We introduce the contour function  $x(\tau)$  as (see Fig 3.2)

$$x^\pm(t) = \begin{cases} \mp \frac{\xi_L}{2} & \text{for } 0 \leq t \leq t_M \\ 0 & \text{for } t > t_M \end{cases} \quad (3.33)$$

The plus and minus sign in the superscript of  $x$  corresponds to the upper and lower branch of the contour respectively.

### Step 2: Interaction picture with respect to decoupled Hamiltonian

Now we can write down Eq. (3.32) in the interaction picture with respect to the decoupled Hamiltonian  $\mathcal{H}_0 = \sum_{\alpha=L,C,R} \mathcal{H}_\alpha$ . Then the interaction

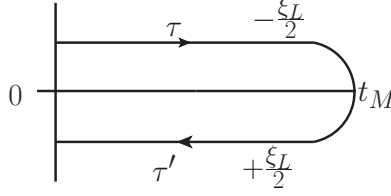


Figure 3.2: The complex time contour  $C$  for product initial state. The path of the contour begins at time 0 and goes to time  $t_M$  with unitary evolution  $\mathcal{U}_{-\xi_L/2}(t_M, 0)$ , and then returns to time  $t = 0$  with unitary evolution  $\mathcal{U}_{\xi_L/2}^\dagger(t_M, 0)$ .  $\tau$  and  $\tau'$  are complex-time variables along the contour.

part of the Hamiltonian on the contour  $C \equiv [0, t_M]$  is given as

$$\hat{\mathcal{V}}_x(\tau) = -f^T(\tau)\hat{u}_C(\tau) + \hat{u}_R^T(\tau)V^{RC}(\tau)\hat{u}_C(\tau) + \hat{u}_L^T(\tau + \hbar x(\tau))V^{LC}(\tau)\hat{u}_C(\tau). \quad (3.34)$$

(The symbol caret is used to denote that the operators are in the interaction pictures with respect to the free Hamiltonian  $\mathcal{H}_0$  *e.g.*,  $\hat{u}_C(\tau) = e^{\frac{i}{\hbar}\mathcal{H}_0\tau}u_C e^{-\frac{i}{\hbar}\mathcal{H}_0\tau}$ ) The density matrix  $\rho_{\text{prod}}(0)$  remains unaffected by this transformation as it commutes with  $\mathcal{H}_0$ . Therefore the CF in the interaction picture can be written as

$$\mathcal{Z}(\xi_L) = \text{Tr} \left[ \rho_{\text{prod}}(0) T_c e^{-\frac{i}{\hbar} \int_C \hat{\mathcal{V}}_x(\tau) d\tau} \right]. \quad (3.35)$$

### Step 3: Wick's theorem and Feynman diagrammatic technique

Expanding the exponential in Eq. (3.35), we generate various terms of product of  $u_\alpha$ . Since the density matrix is quadratic these terms can be decomposed in pairs according to Wick's theorem [17]. For a non-vanishing contribution each type of  $u$  should come in an even number of times because  $\langle u_C \rangle_{\rho_{\text{prod}}(0)} = 0$ ,  $\langle u_C u_L \rangle_{\rho_{\text{prod}}(0)} = 0$ . We define the decoupled or free Green's

functions as

$$-\frac{i}{\hbar}\langle T_C \hat{u}_\alpha(\tau) \hat{u}_{\alpha'}(\tau')^T \rangle_{\rho_{\text{prod}}(0)} = \delta_{\alpha,\alpha'} g_\alpha(\tau, \tau'), \quad \alpha, \alpha' = L, C, R. \quad (3.36)$$

We collect the diagrams of all orders to sum the series. Since  $\hat{\mathcal{V}}_x$  contains only two-point couplings, the diagrams are all ring type. The combinatorial factors can be worked out as  $1/(2n)$  for a ring containing  $n$  vertices. We now make use of linked-cluster theorem [18] which says  $\ln \mathcal{Z}$  contains only connected graphs, and the disconnected graphs cancel exactly when we take the logarithm. Therefore, the final result can be expressed as (in the discrete contour time) (see appendix (A))

$$\ln \mathcal{Z}(\xi_L) = -\frac{1}{2} \text{Tr}_{j,\tau} \ln [\mathbf{1} - \mathbf{g}_C \tilde{\Sigma}] - \frac{i}{2\hbar} \text{Tr}_{j,\tau} [\tilde{\mathbf{G}} \mathbf{f} \mathbf{f}^T]. \quad (3.37)$$

(Bold symbol refers to the matrix representation of the Green's functions in discrete contour time and functions with  $(\tilde{\phantom{x}})$  means they are counting field dependent) Here we define  $\tilde{\Sigma}(\tau, \tau')$  as

$$\tilde{\Sigma}(\tau, \tau') \equiv \Sigma_L(\tau + \hbar x(\tau), \tau' + \hbar x'(\tau')) + \Sigma_R(\tau, \tau') = \Sigma(\tau, \tau') + \Sigma_L^A(\tau, \tau'), \quad (3.38)$$

where  $\Sigma(\tau, \tau') \equiv \sum_{\alpha=L,R} \Sigma_\alpha(\tau, \tau')$  is the total self-energy coming from the leads and defined as  $\Sigma_\alpha(\tau, \tau') = V^{C\alpha} g_\alpha(\tau, \tau') V^{\alpha C}$ . The notation  $\text{Tr}_{j,\tau}$  means trace over both in space index  $j$  and discretized contour time  $\tau, i.e.,$

$$\text{Tr}_{j,\tau} [\mathbf{A} \mathbf{B} \cdots \mathbf{C}] \equiv \int_C \int_C \cdots \int_C d\tau_1 d\tau_2 \cdots d\tau_n \text{Tr}_j [A(\tau_1, \tau_2) B(\tau_2, \tau_3) \cdots C(\tau_n, \tau_1)], \quad (3.39)$$

with  $A, B, \dots, C$  are two point Green's functions. Similarly  $\text{Tr}_{j,\tau} [\tilde{\mathbf{G}} \mathbf{f} \mathbf{f}^T]$  reads as

$$\text{Tr}_{j,\tau} [\tilde{\mathbf{G}} \mathbf{f} \mathbf{f}^T] = \int_C \int_C d\tau_1 d\tau_2 \text{Tr}_j [\tilde{G}(\tau_1, \tau_2) f(\tau_2) f^T(\tau_1)], \quad (3.40)$$

with  $\tilde{G}(\tau, \tau')$  satisfy the following Dyson's equation

$$\tilde{G}(\tau, \tau') = g_C(\tau, \tau') + \int_C \int_C d\tau_1 d\tau_2 g_C(\tau, \tau_1) \tilde{\Sigma}(\tau_1, \tau_2) \tilde{G}(\tau_2, \tau'). \quad (3.41)$$

We introduce a new quantity  $\Sigma_L^A$  defined via Eq. (3.38) as the difference between the shifted self-energy and the usual one, *i.e.*,

$$\Sigma_L^A(\tau, \tau') = \Sigma_L(\tau + \hbar x(\tau), \tau' + \hbar x(\tau')) - \Sigma_L(\tau, \tau'). \quad (3.42)$$

This self-energy turns out to be the central quantity for this FCS problem.

Eq. (3.37) can also be written in a different form which will be useful later for deriving long-time limit as well as for numerical calculations. As we know that the steady state limit, for example, the Landauer formula for heat current is expressed in terms of  $G_0$ , the Green's function in presence of leads, we therefore express the bare Green's function  $g_C$  in terms of  $G_0$ . This can be achieved by introducing the Dyson's equation for  $G_0$  for the ballistic system as derived in chapter 2 (see Eq. (2.85))

$$G_0(\tau, \tau') = g_C(\tau, \tau') + \int_C \int_C d\tau_1 d\tau_2 g_C(\tau, \tau_1) \Sigma(\tau_1, \tau_2) G_0(\tau_2, \tau'), \quad (3.43)$$

In discretized contour time we can write the above equation as

$$\mathbf{G}_0 = \mathbf{g}_C + \mathbf{g}_C \boldsymbol{\Sigma} \mathbf{G}_0 \quad (3.44)$$

which implies  $\mathbf{G}_0^{-1} = \mathbf{g}_C^{-1} - \boldsymbol{\Sigma}$ . Using this we can simplify the term  $\mathbf{1} - \mathbf{g}_C \tilde{\boldsymbol{\Sigma}}$  as follows

$$\begin{aligned} \mathbf{1} - \mathbf{g}_C \tilde{\boldsymbol{\Sigma}} &= \mathbf{1} - \mathbf{g}_C (\boldsymbol{\Sigma} + \boldsymbol{\Sigma}_L^A) \\ &= \mathbf{g}_C (\mathbf{g}_C^{-1} - \boldsymbol{\Sigma} - \boldsymbol{\Sigma}_L^A) = \mathbf{g}_C (\mathbf{G}_0^{-1} - \boldsymbol{\Sigma}_L^A) \\ &= \mathbf{g}_C \mathbf{G}_0^{-1} (\mathbf{1} - \mathbf{G}_0 \boldsymbol{\Sigma}_L^A) = (\mathbf{1} - \mathbf{g}_C \boldsymbol{\Sigma}) (\mathbf{1} - \mathbf{G}_0 \boldsymbol{\Sigma}_L^A). \end{aligned} \quad (3.45)$$

The two factors above are in matrix (and contour time) multiplication. Using the relation between trace and determinant,  $\ln \det(\mathbf{M}) = \text{Tr} \ln \mathbf{M}$ , and the fact,  $\det(\mathbf{A}\mathbf{B}) = \det(\mathbf{A}) \det(\mathbf{B})$ , we find that the two terms give two factors for  $\mathcal{Z}$ . Now the factor due to  $\mathbf{1} - \mathbf{g}_C \boldsymbol{\Sigma}$  is a counting field independent term and can be shown to be equal to 1 (see appendix (B)). We then have [19, 20]

$$\ln \mathcal{Z}(\xi_L) = -\frac{1}{2} \text{Tr}_{j,\tau} \ln [\mathbf{1} - \mathbf{G}_0 \boldsymbol{\Sigma}_L^A] - \frac{i}{2\hbar} \text{Tr}_{j,\tau} [\tilde{\mathbf{G}} \mathbf{f} \mathbf{f}^T], \quad (3.46)$$

Using the same procedure as above  $\tilde{G}(\tau, \tau')$  in Eq. (3.41) can also be expressed in terms of  $G_0(\tau, \tau')$  as

$$\tilde{G}(\tau, \tau') = G_0(\tau, \tau') + \int_C \int_C d\tau_1 d\tau_2 G_0(\tau, \tau_1) \boldsymbol{\Sigma}_L^A(\tau_1, \tau_2) \tilde{G}(\tau_2, \tau'). \quad (3.47)$$

**Contour time to real time and Keldysh Rotation :**

As explained in chapter 2 that it is always convenient to perform a Keldysh rotation (Eq. (2.49)) for the contour ordered Green's functions and work with the retarded, advanced and Keldysh components. Moreover as Keldysh rotation is an orthogonal transformation, the trace appearing in the CGF *i.e.*,  $\text{Tr}_{j,\tau}(\mathbf{1} - \mathbf{G}_0 \Sigma_L^A)$  as well as  $\text{Tr}_{j,\tau}[\tilde{\mathbf{G}} \mathbf{f} \mathbf{f}^T]$  remain invariant.

---

**Proof**

As defined in Eq. (3.39),  $\text{Tr}_{j,\tau}(\mathbf{A}\mathbf{B}\cdots\mathbf{C})$  is given as,

$$\text{Tr}_{j,\tau}[\mathbf{A}\mathbf{B}\cdots\mathbf{C}] \equiv \int_C \int_C \cdots \int_C d\tau_1 d\tau_2 \dots d\tau_n \text{Tr}_j [A(\tau_1, \tau_2) B(\tau_2, \tau_3) \cdots C(\tau_n, \tau_1)] \quad (3.48)$$

Changing from contour to real-time integration *i.e.*, using  $\int d\tau = \sum_{\sigma=\pm 1} \int \sigma dt$  we have

$$\begin{aligned} \text{Tr}_{j,\tau}[\mathbf{A}\mathbf{B}\cdots\mathbf{C}] &= \sum_{\sigma_1, \sigma_2, \dots, \sigma_n} \int dt_1 \int dt_2 \cdots \int dt_n \text{Tr}_j [\sigma_1 A^{\sigma_1 \sigma_2}(t_1, t_2) \sigma_2 B^{\sigma_2 \sigma_3}(t_2, t_3) \\ &\quad \cdots \sigma_n C^{\sigma_n \sigma_{n+1}}(t_n, t_1)]. \end{aligned} \quad (3.49)$$

By absorbing the extra  $\sigma$  into the definition of branch components it can be easily seen that

$$\begin{aligned} \text{Tr}_{j,\tau}[\mathbf{A}\mathbf{B}\cdots\mathbf{C}] &= \int dt_1 \int dt_2 \cdots \int dt_n \text{Tr}_{j,\sigma} [\bar{A}(t_1, t_2) \bar{B}(t_2, t_3) \cdots \bar{C}(t_n, t_1)], \\ &\equiv \text{Tr}_{t,j,\sigma} [\bar{\mathbf{A}}\bar{\mathbf{B}}\cdots\bar{\mathbf{C}}]. \end{aligned} \quad (3.50)$$

where  $\bar{A} = \sigma_z A$  with  $\sigma_z = \text{diag}(1, -1)$ . Now since the Keldysh rotation is an orthogonal transformation transforming the matrix  $\bar{A}$  to  $\check{A}$  such that  $\check{A} = O^T \bar{A} O$  (see Eq. (2.49) in chapter 2) we can easily see that,

$$\text{Tr}_{t,j,\sigma}[\bar{\mathbf{A}}\bar{\mathbf{B}}\cdots\bar{\mathbf{C}}] = \text{Tr}_{t,j,\sigma}[\check{\mathbf{A}}\check{\mathbf{B}}\cdots\check{\mathbf{C}}]. \quad (3.51)$$

Therefore we have

$$\text{Tr}_{j,\tau}[\mathbf{A}\mathbf{B}\cdots\mathbf{C}] = \text{Tr}_{t,j,\sigma}[\bar{\mathbf{A}}\bar{\mathbf{B}}\cdots\bar{\mathbf{C}}] = \text{Tr}_{t,j,\sigma}[\check{\mathbf{A}}\check{\mathbf{B}}\cdots\check{\mathbf{C}}]. \quad (3.52)$$

For later convenience, we also perform two-frequency Fourier transformation defined as

$$\check{A}[\omega, \omega'] = \int_{-\infty}^{+\infty} dt \int_{-\infty}^{+\infty} dt' \check{A}(t, t') e^{i(\omega t + \omega' t')}. \quad (3.53)$$

Then from Eq. (3.50) we can compute the trace in frequency domain as,

$$\begin{aligned} \text{Tr}_{(j,\tau)}[\mathbf{A}\mathbf{B}\cdots\mathbf{C}] &= \int \frac{d\omega_1}{2\pi} \int \frac{d\omega_2}{2\pi} \cdots \int \frac{d\omega_n}{2\pi} \text{Tr} [ \\ &\quad \bar{A}[\omega_1, -\omega_2] \bar{B}[\omega_2, -\omega_3] \cdots \bar{C}[\omega_n, -\omega_1]] \\ &\equiv \text{Tr}_{j,\sigma,\omega}[\bar{\mathbf{A}}\bar{\mathbf{B}}\cdots\bar{\mathbf{C}}] = \text{Tr}_{j,\sigma,\omega}[\check{\mathbf{A}}\check{\mathbf{B}}\cdots\check{\mathbf{C}}]. \end{aligned} \quad (3.54)$$

The last line defines what we mean by trace in the frequency domain.

---

If the Green's functions are counting field independent *e.g.*,  $G_0(\tau, \tau')$  then in the Keldysh space,

$$\check{G}_0 = \begin{pmatrix} G_0^r & G_0^K \\ 0 & G_0^a \end{pmatrix}. \quad (3.55)$$

However this is not the case for  $\Sigma_L^A(\tau, \tau')$  as well as for  $\tilde{G}(\tau, \tau')$  as they depend on the counting field  $\xi_L$ . For example, using Eq. (3.42), in real time different components for  $\Sigma_L^A(\tau, \tau')$  are given as

$$\begin{aligned}\Sigma_A^{\sigma\sigma'}(t, t') &= \Sigma_L^{\sigma\sigma'}(t + \hbar x^\sigma(t), t' + \hbar x^{\sigma'}(t')) - \Sigma_L^{\sigma\sigma'}(t, t'), \\ &= \Sigma_L^{\sigma\sigma'}(t - t' + \hbar(x^\sigma(t) - x^{\sigma'}(t'))) - \Sigma_L^{\sigma\sigma'}(t - t')\end{aligned}\quad (3.56)$$

which is time-translationally invariant because the lead is always in thermal equilibrium. Now using the values  $x^\pm(t) = \mp \xi_L/2$  we obtain the components as

$$\begin{aligned}\Sigma_A^t(t) &= \Sigma_A^{\bar{t}}(t) = 0, \\ \Sigma_A^>(t) &= \Sigma_L^>(t + \hbar\xi_L) - \Sigma_L^>(t) \equiv a(t), \\ \Sigma_A^<(t) &= \Sigma_L^<(t - \hbar\xi_L) - \Sigma_L^<(t) \equiv b(t).\end{aligned}\quad (3.57)$$

for  $0 \leq t \leq t_M$  and is zero outside the measurement time interval *i.e.*,  $t > t_M$ . Therefore after Keldysh rotation  $\check{\Sigma}_L^A$  matrix is given as ( $0 < t < t_M$ )

$$\check{\Sigma}_L^A(t) = \begin{bmatrix} a(t) - b(t) & a(t) + b(t) \\ -a(t) - b(t) & -a(t) + b(t) \end{bmatrix}. \quad (3.58)$$

Note that the  $\bar{K}$  component is non-zero here. Finally we obtain the CF in the Keldysh space as

$$\ln \mathcal{Z}(\xi_L) = -\frac{1}{2} \text{Tr}_{j,t,\sigma} \ln \left[ \mathbf{1} - \check{\mathbf{G}}_0 \check{\Sigma}_L^A \right] - \frac{i}{2\hbar} \text{Tr}_{j,t,\sigma} \left[ \check{\mathbf{G}} \mathbf{f} \check{\mathbf{f}}^T \right], \quad (3.59)$$

The external force  $f(t)$  does not depend on the branch index  $\sigma$ . Therefore the matrix  $\check{\mathbf{f}} \check{\mathbf{f}}^T$  in the Keldysh space reads ,

$$\check{\mathbf{f}} \check{\mathbf{f}}^T = \begin{bmatrix} 0 & 2 \mathbf{f} \mathbf{f}^T \\ 0 & 0 \end{bmatrix}. \quad (3.60)$$

### Importance of the final result

Eq.(3.59) is one of the central result of this chapter which got the following importance for this particular model:

- The expressions for the CGF is valid for any arbitrary measurement time  $t_M$  which need not to be large and hence one can study both transient and steady state properties.
- The effect of measurements of  $\mathcal{H}_L$  to obtain heat, is to shift the contour time argument of the corresponding self-energy by an amount  $\hbar x$  *i.e.*,  $\Sigma_L(\tau, \tau') \rightarrow \Sigma_L(\tau + \hbar x, \tau' + \hbar x')$ .
- The expression is valid for finite size of the heat baths and it is therefore interesting to study the corresponding effects on the cumulants.
- The CGF is valid for arbitrary time-dependent coupling between the leads and the junction.

- The expression is valid in higher dimension for the system and for the heat-baths.
- The force constant matrix for the center  $K^C$  may be time-dependent. In that case the bare Green's functions for the center *i.e.*,  $g_C(t, t')$  is no more time-translationally invariant. However the Dyson equation (Eq. (3.43)) is still valid. A recent study [21] has investigated what happens to the thermal current in such case.

In the following we will derive the CGF for two other initial conditions *i.e.*,  $\rho_{\text{NESS}}(0)$  and  $\rho'(0)$  based on Feynman path-integral formalism.

### 3.5.2 Feynman path-integral formalism to derive $\mathcal{Z}(\xi_L)$ for initial conditions $\rho_{\text{NESS}}(0)$ and $\rho'(0)$

In this subsection we derive the CF starting from Eq. (3.11) for the initial conditions  $\rho_{\text{NESS}}(0)$  and  $\rho'(0)$  using path-integral approach. The major problem for formulating the path integral for these initial conditions is that they do not commute with the initial projection operator  $\Pi_a$  unlike the product initial state. However we can remove this projection operator by putting it into part of an evolution of  $\mathcal{H}_L$  by introducing another integration variable  $\lambda$ . The key observation is that, the projector can be represented by the Dirac  $\delta$  function *i.e.*,  $\Pi_a = \delta(a - \mathcal{H}_L) = \int_{-\infty}^{\infty} d\lambda / (2\pi) e^{-i\lambda(a - \mathcal{H}_L)}$ . Substituting the Fourier integral representation into the expression for  $\rho'(0)$

we obtain

$$\rho'(0) \propto \int da \Pi_a \rho_{\text{NESS}}(0) \Pi_a \quad (3.61)$$

$$= \int \frac{d\lambda}{2\pi} e^{i\lambda\mathcal{H}_L} \rho_{\text{NESS}}(0) e^{-i\lambda\mathcal{H}_L}. \quad (3.62)$$

Then using the expression for  $\mathcal{Z}(\xi_L)$  in Eq. (3.11) we write

$$\begin{aligned} \mathcal{Z}(\xi_L) &= \langle e^{i\xi_L\mathcal{H}_L/2} e^{-i\xi_L\mathcal{H}_L(t)} e^{i\xi_L\mathcal{H}_L/2} \rangle' \\ &\propto \int \frac{d\lambda}{2\pi} \text{Tr} \{ \rho(0) \mathcal{U}_{\xi_L/2-\lambda}(0, t_M) \mathcal{U}_{-\xi_L/2-\lambda}(t_M, 0) \} \\ &= \int \frac{d\lambda}{2\pi} \mathcal{Z}(\xi_L, \lambda). \end{aligned} \quad (3.63)$$

The proportionality constant will be fixed later by the condition  $\mathcal{Z}(0) = 1$ .

As before, the CF on Keldysh contour can be written as

$$\mathcal{Z}(\xi_L, \lambda) = \text{Tr} \left[ \rho_{\text{NESS}}(0) T_C e^{-\frac{i}{\hbar} \int_C \mathcal{H}_x(\tau) d\tau} \right], \quad (3.64)$$

which can be expressed in terms of the product initial state  $\rho_{\text{prod}}$  using the relation in Eq. (3.21) connecting  $\rho_{\text{prod}}$  and  $\rho_{\text{NESS}}(0)$ . Then we obtain

$$\mathcal{Z}(\xi_L, \lambda) = \text{Tr} \left[ \rho_{\text{prod}}(-\infty) T_C e^{-\frac{i}{\hbar} \int_K \mathcal{H}_x(\tau) d\tau} \right]. \quad (3.65)$$

Note that for product initial state, the contour  $C$  was running from 0 to  $t_M$  and back to 0, while in this case the contour  $K$  is running from  $-\infty$  to  $t_M$  and back to  $-\infty$  (see Fig (3.3)). We define the function  $x(\tau)$  on the

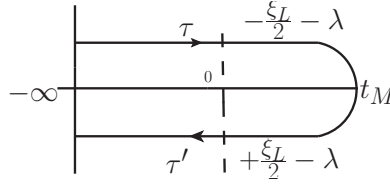


Figure 3.3: The complex time contour  $K$  for projected initial state. The path of the contour begins at time  $-\infty$ , goes to time  $t_M$ , and then goes back to time  $-\infty$ .  $\tau$  and  $\tau'$  are complex-time variables along the contour. The function  $x(\tau)$  is nonzero in the interval  $0 \leq t \leq t_M$ .

contour  $K$  as

$$x^\pm(t) = \begin{cases} \mp \frac{\xi_L}{2} - \lambda & \text{for } 0 \leq t \leq t_M \\ 0 & \text{for } t < 0 \text{ and } t > t_M. \end{cases}$$

Here we take the following steps to get the final result,

- First we write down  $\mathcal{Z}(\xi_L, \lambda)$  in the path integral representation.
- Then we obtain the Lagrangian corresponding to the modified Hamiltonian  $\mathcal{H}_x$ .
- Then integrate out the bath variables to obtain the influence functional.
- Finally we get an effective action and integrate it over the center variables to obtain the CF.

Step 1: Path integral representation of  $\mathcal{Z}(\xi_L, \lambda)$

Using Feynman path integral technique we can write Eq. (3.64) as

$$\mathcal{Z}(\xi_L, \lambda) = \int \mathcal{D}[u_C] \mathcal{D}[u_L] \mathcal{D}[u_R] \rho_{\text{prod}}(-\infty) e^{(i/\hbar) \int_K d\tau (\mathcal{L}_C + \mathcal{L}_L + \mathcal{L}_R + \mathcal{L}_{LC} + \mathcal{L}_{CR})}, \quad (3.66)$$

where  $\mathcal{D}[u_\alpha]$  are the integration volume elements and  $\rho_{\text{prod}}(-\infty)$  is shorthand notation for the matrix element  $\langle u'_L u'_C u'_R | \rho_{\text{prod}}(-\infty) | u_L, u_C, u_R \rangle$ .

Step 2: The Lagrangian corresponding to  $\mathcal{H}_x$

The Lagrangians associated with the Hamiltonian  $\mathcal{H}_x$  are:

$$\begin{aligned} \mathcal{L} &= \mathcal{L}_L + \mathcal{L}_C + \mathcal{L}_R + \mathcal{L}_{LC} + \mathcal{L}_{CR}, \\ \mathcal{L}_\alpha &= \frac{1}{2} \dot{u}_\alpha^2 - \frac{1}{2} u_\alpha^T K^\alpha u_\alpha, \quad \alpha = L, R \\ \mathcal{L}_C &= \frac{1}{2} \dot{u}_C^2 + f^T u_C - \frac{1}{2} u_C^T (K^C - \mathcal{S}^T \mathcal{S}) u_C, \\ \mathcal{L}_{LC} &= -\dot{u}_L^T \mathcal{S} u_C - u_L^T (V^{LC} + \mathcal{C}) u_C, \\ \mathcal{L}_{CR} &= -u_R^T V^{RC} u_C. \end{aligned} \quad (3.67)$$

where  $\mathcal{C}$  and  $\mathcal{S}$  are defined in Eq. (3.31) but with a different meaning for  $x(\tau)$  which is now defined on the contour  $K$ . For notational simplicity, we have dropped the argument  $\tau$  in the Lagrangians. The vector or matrices  $f$ ,  $\mathcal{C}$ , and  $\mathcal{S}$  are parametrically dependent on the contour time  $\tau$ . They are zero except on the interval  $0 < t < t_M$ .

Step 3: Influence functional on contour

Following Feynman and Vernon [22], we can eliminate the leads by performing Gaussian integrals. Since the coupling to the center is linear, the

result will be a quadratic form in the exponential, *i.e.*, another Gaussian.

Therefore the influence functional for the left lead is given by [23]

$$\begin{aligned}
 I_L[u_C(\tau)] &\equiv \int \mathcal{D}[u_L] \rho_L(-\infty) e^{\frac{i}{\hbar} \int d\tau (\mathcal{L}_L + \mathcal{L}_{LC})} \\
 &= \text{Tr} \left[ \frac{e^{-\beta_L \mathcal{H}_L}}{Z_L} T_c e^{-\frac{i}{\hbar} \int d\tau \hat{\mathcal{V}}_x(\tau)} \right] \\
 &= \exp \left[ -\frac{i}{2\hbar} \int \int d\tau d\tau' \hat{u}_C^T(\tau) \Pi_L(\tau, \tau') \hat{u}_C(\tau') \right], \quad (3.68)
 \end{aligned}$$

$$\hat{\mathcal{V}}_x(\tau) = \hat{u}_L^T(\tau + \hbar x(\tau)) V^{LC}(\tau) \hat{u}_C(\tau) + \frac{1}{2} \hat{u}_C^T(\tau) \mathcal{S}^T \mathcal{S} \hat{u}_C(\tau). \quad (3.69)$$

In the above expressions, the contour function  $\hat{u}_C(\tau)$  is not a dynamical variable but only a parametric function. Note that  $\hat{\mathcal{V}}_x$  is the interaction picture operator with respect to  $\mathcal{H}_L$ , as a result,  $e^{it\mathcal{H}_L/\hbar} \hat{u}_L(\hbar x) e^{-it\mathcal{H}_L/\hbar} = \hat{u}_L(t + \hbar x)$ .

We now define the important influence functional self-energy on the contour as

$$\Pi_L(\tau, \tau') = \Sigma_L^A(\tau, \tau') + \Sigma_L(\tau, \tau') + \mathcal{S}^T \mathcal{S} \delta(\tau, \tau'), \quad (3.70)$$

$$\begin{aligned}
 \Sigma^A(\tau, \tau') + \Sigma_L(\tau, \tau') &= V^{CL}(\tau) g_L(\tau + \hbar x(\tau), \tau' + \hbar x(\tau')) V^{LC}(\tau') \\
 &= \Sigma_L(\tau + \hbar x(\tau), \tau' + \hbar x(\tau')), \quad (3.71)
 \end{aligned}$$

$\delta(\tau, \tau')$  here is the Dirac delta function on the contour. Equation (3.71) is similar to what we got for the product initial state (Eq. 3.38) with two differences

- The Green's functions are defined on the contour which is running

from  $-\infty$  to  $t_M$  and back to  $-\infty$ .

- The meaning of the parameter  $x(\tau)$  is different as it got a  $\lambda$  dependence coming from the initial projection operator.

Similarly the influence functional for the right lead can be obtained as

$$I_R[u_C(\tau)] = \exp \left[ -\frac{i}{2\hbar} \int \int d\tau d\tau' u_C^T(\tau) \Sigma_R(\tau, \tau') u_C(\tau') \right]. \quad (3.72)$$

This is the usual influence functional as no measurement is performed using the right lead Hamiltonian  $\mathcal{H}_R$ .

#### Step 4: Effective action and the CGF

The CF can now be written as

$$\begin{aligned} \mathcal{Z}(\xi_L, \lambda) &= \int \mathcal{D}[u_C] \rho_C(-\infty) e^{(i/\hbar) \int d\tau \mathcal{L}_C} I_L[u_C] I_R[u_C] \\ &= \int \mathcal{D}[u_C] \rho_C(-\infty) e^{\frac{i}{\hbar} S_{\text{eff}}} \end{aligned} \quad (3.73)$$

where

$$S_{\text{eff}} = \frac{1}{2} \int d\tau \int d\tau' u_C^T(\tau) D(\tau, \tau') u_C(\tau') + \int f^T(\tau) u_C(\tau) d\tau \quad (3.74)$$

and we define the differential operator  $D(\tau, \tau')$  as

$$\begin{aligned} D(\tau, \tau') &= - \left[ \left( I \frac{\partial^2}{\partial \tau^2} + K^C \right) \delta(\tau, \tau') + \Sigma(\tau, \tau') \right] - \Sigma_L^A(\tau, \tau') \\ &= D_0(\tau, \tau') - \Sigma_L^A(\tau, \tau'). \end{aligned} \quad (3.75)$$

Therefore the final CF is obtained by doing another Gaussian integration and is of the following form

$$\mathcal{Z}(\xi_L) \propto \det(\mathbf{D})^{-1/2} e^{-\frac{i}{2\hbar} \mathbf{f}^T \mathbf{D}^{-1} \mathbf{f}}. \quad (3.76)$$

We can identify that Green's function  $G_0(\tau, \tau')$  in Eq. (3.43) and  $\tilde{G}(\tau, \tau')$  in Eq. (3.47) satisfying the following equations

$$\int D_0(\tau, \tau'') G_0(\tau'', \tau') d\tau'' = I \delta(\tau, \tau'). \quad (3.77)$$

$$\int D(\tau, \tau'') \tilde{G}(\tau'', \tau') d\tau'' = I \delta(\tau, \tau'). \quad (3.78)$$

We view the differential operator (integral operator)  $D$  and  $D^{-1}$  as matrices that are indexed by space  $j$  and contour time  $\tau$ . The proportionality constant in Eq. (3.76) can be fixed by noting that  $\mathcal{Z}(\xi_L = 0, \lambda = 0) = 1$ . Since, when  $\xi_L = 0$  and  $\lambda = 0$ , we have  $x = 0$  and thus  $\Sigma_L^A(\tau, \tau') = \Sigma_L(\tau + \hbar x, \tau' + \hbar x') - \Sigma_L(\tau, \tau') = 0$ , so  $D = D_0$ . The properly normalized CF is

$$\mathcal{Z}(\xi_L, \lambda) = \det(\mathbf{D}_0^{-1} \mathbf{D})^{-1/2} e^{-\frac{i}{2\hbar} \mathbf{f}^T \mathbf{D}^{-1} \mathbf{f}}. \quad (3.79)$$

Finally making use of the formulas for operators or matrices  $\det(\mathbf{M}) = e^{\text{Tr} \ln \mathbf{M}}$ , and  $\ln(\mathbf{1} - \mathbf{y}) = -\sum_{k=1}^{\infty} \frac{\mathbf{y}^k}{k}$  we can write the CGF in terms of  $\Sigma_L^A$

for the projected initial condition  $\rho'(0)$  as,

$$\begin{aligned}
 \ln \mathcal{Z}(\xi_L) &= \lim_{\lambda \rightarrow \infty} \ln \mathcal{Z}(\xi_L, \lambda) \\
 &= \lim_{\lambda \rightarrow \infty} \left\{ -\frac{1}{2} \text{Tr}_{j,\tau} \ln(\mathbf{1} - \mathbf{G}_0 \Sigma_L^A) - \frac{i}{2\hbar} \text{Tr}_{j,\tau} (\tilde{\mathbf{G}} \mathbf{f} \mathbf{f}^T) \right\} \\
 &= \lim_{\lambda \rightarrow \infty} \sum_{n=1}^{\infty} \frac{1}{2n} \text{Tr}_{(j,\tau)} \left[ (\mathbf{G}_0 \Sigma_L^A)^n \right] - \frac{i}{2\hbar} \text{Tr}_{j,\tau} \left[ \tilde{\mathbf{G}} \mathbf{f} \mathbf{f}^T \right],
 \end{aligned}$$

where to obtain  $\mathcal{Z}(\xi_L)$  from  $\mathcal{Z}(\xi_L, \lambda)$  we took the limit  $\lambda \rightarrow \infty$  because  $\mathcal{Z}(\xi_L, \lambda)$  approaches a constant as  $|\lambda| \rightarrow \infty$  and therefore the value of the integral is dominated by the value at infinity. Following the same technique as before the above CGF in the Keldysh space reads

$$\ln \mathcal{Z}(\xi_L) = \lim_{\lambda \rightarrow \infty} \left\{ -\frac{1}{2} \text{Tr}_{j,t,\sigma} \ln \left[ \mathbf{1} - (\check{\mathbf{G}}_0 \check{\Sigma}_L^A) \right] - \frac{i}{2\hbar} \text{Tr}_{j,t,\sigma} \left[ \check{\mathbf{G}} \check{\mathbf{f}} \check{\mathbf{f}}^T \right] \right\}. \quad (3.80)$$

Now for steady state initial condition  $\rho_{\text{NESS}}(0)$  the CGF can be immediately written down as

$$\ln \mathcal{Z}(\xi_L) = \lim_{\lambda \rightarrow 0} \ln \mathcal{Z}(\xi_L, \lambda). \quad (3.81)$$

### Conclusion

For all three different initial conditions the CGF for heat is written in a compact way. The CGF is a sum of infinite terms with products of  $G_0$  and  $\Sigma_L^A$  which are in convolutions. The meaning of these Green's functions depends on the initial conditions and accordingly is defined either on the

contour  $C[0, t_M]$  with parameter  $x^\pm(t) = \mp \xi_L/2$  for  $(0 < t < t_M)$  or on the contour  $K[-\infty, t_M]$  with parameter  $x^\pm(t) = \mp \xi_L/2 - \lambda$  for  $(0 < t < t_M)$  and zero otherwise.

### CF for the right lead

Similar relations also exist if we want to calculate the CGF for the right lead heat  $Q_R$ . In that case one has to measure the right lead Hamiltonian  $\mathcal{H}_R$  at two times. The final formula for the CGF remains the same except that  $\Sigma_L^A$  should be replaced by  $\Sigma_R^A$ .

## 3.6 Long-time limit ( $t_M \rightarrow \infty$ ) and steady state fluctuation theorem (SSFT)

For the long-time limit calculation we can use either Eq. (3.46) or Eq. (3.80). For convenience of taking the large time limit, *i.e.*,  $t_M$  large, we prefer to set interval to  $(-t_M/2, t_M/2)$ . In this way, when  $t_M \rightarrow \infty$ , the interval becomes the full domain and Fourier transforms to all the Green's functions and self-energy can be performed (where the translational invariance is restored). Applying the convolution theorem to the trace formula in Eq. (3.59), we find that there is one more time integral left with integrand independent of  $t$ . This last one can be set from  $-t_M/2$  to  $t_M/2$ , obtaining an overall factor of  $t_M$  and we have

$$\text{Tr}_{(j,\tau)}[\mathbf{A}\mathbf{B}\cdots\mathbf{C}] = t_M \int \frac{d\omega}{2\pi} \text{Tr}_{j,\sigma} [\check{A}(\omega)\check{B}(\omega)\cdots\check{C}(\omega)]. \quad (3.82)$$

**Proof**

In the long-time limit, the time-translational invariance of the Green's functions implies

$$\check{A}[\omega, \omega'] = 2\pi \check{A}[\omega] \delta(\omega + \omega') \quad (3.83)$$

Thus from Eq. (3.54) we write

$$\text{Tr}_{(j,\tau)}(\mathbf{A}\mathbf{B}\cdots\mathbf{C}) = \delta(0) \int d\omega \text{Tr}_{j,\sigma}[\check{A}[\omega]\check{B}[\omega]\cdots\check{C}[\omega]]. \quad (3.84)$$

We write  $\delta(0)$ , which got the dimension of inverse frequency, as  $t_M/2\pi$ .

---

In the long-time limit,  $\Sigma_L^A[\omega]$  is obtained by the Fourier transformation of Eq. (3.58) and given as

$$a[\omega] \equiv \Sigma_L^>[\omega](e^{-i\hbar\omega\xi_L} - 1) = -i(1 + f_L[\omega])\Gamma_L[\omega](e^{-i\hbar\omega\xi_L} - 1), \quad (3.85)$$

$$b[\omega] \equiv \Sigma_L^<[\omega](e^{i\hbar\omega\xi_L} - 1) = -if_L[\omega]\Gamma_L[\omega](e^{i\hbar\omega\xi_L} - 1), \quad (3.86)$$

where we use the fluctuation-dissipation relations for the self-energy.  $\Gamma_\alpha[\omega] = i(\Sigma_\alpha^r[\omega] - \Sigma_\alpha^a[\omega])$ ,  $\alpha = L, R$  is the spectral function and  $f_\alpha[\omega] = 1/(e^{\beta_\alpha\hbar\omega} - 1)$  is the Bose-Einstein distribution function for the leads. Note that  $\Sigma_L^A$  is supposed to depend on both  $\xi$  and  $\lambda$ . However in the long-time limit, the  $\lambda$  dependence drops out which makes the steady state result independent of the initial distribution. Finally, the CGF for large  $t_M$  is given as

$$\ln \mathcal{Z}(\xi_L) = -t_M \int \frac{d\omega}{4\pi} \text{Tr} \ln \left[ 1 - \check{G}_0[\omega] \check{\Sigma}_L^A[\omega] \right] - \frac{i}{\hbar} \int \frac{d\omega}{4\pi} \text{Tr} \left[ \check{G}[\omega] \check{\mathcal{F}}[\omega, -\omega] \right], \quad (3.87)$$

where  $\check{G}[\omega]$  is obtained by solving the Dyson equation given in Eq. (3.47) in frequency domain.  $\check{\mathcal{F}}[\omega, -\omega]$  is written as

$$\check{\mathcal{F}}[\omega, -\omega] = \begin{bmatrix} 0 & f[\omega] f^T[-\omega] \\ 0 & 0 \end{bmatrix}. \quad (3.88)$$

So for the linear system the full CGF is separated into two parts. The first part is independent of the driving force and depends on the temperature of the leads. The second part is the contribution coming from the driving force. Therefore we write the CGF as

$$\ln \mathcal{Z}(\xi_L) = \ln \mathcal{Z}^s(\xi_L) + \ln \mathcal{Z}^d(\xi_L). \quad (3.89)$$

In the following and subsequent sections we discuss about  $\mathcal{Z}^s(\xi_L)$  and will return to  $\mathcal{Z}^d(\xi_L)$  in the next chapter.

### Explicit expression for $\ln \mathcal{Z}^s(\xi_L)$ in long-time

In order to obtain the explicit expression for  $\ln \mathcal{Z}^s(\xi_L)$  in the long-time we need to compute the matrix product

$$\check{G}_0[\omega] \check{\Sigma}_L^A[\omega] = \frac{1}{2} \begin{bmatrix} G_0^r & G_0^K \\ 0 & G_0^a \end{bmatrix} \begin{bmatrix} a-b & a+b \\ -(a+b) & b-a \end{bmatrix}. \quad (3.90)$$

(we omit the argument  $\omega$  from  $G_0^{r,K,a}$ ,  $a$  and  $b$  for notational simplicity) We rewrite the term  $\text{Tr} \ln(1 - M)$  as a determinant *i.e.*,  $\ln \det(1 - M)$  and use the formula

$$\det \begin{bmatrix} A & B \\ C & D \end{bmatrix} = \det(A - BD^{-1}C) \det(D) = \det(AD - BC), \quad (3.91)$$

assuming  $[C, D] = 0$  and  $D$  to be an invertible matrix. This two conditions are satisfied here. By doing this the dimensions of the determinant matrix reduces by half. Finally using the steady state solutions for  $G_0^{r,K,a}$  and  $\Sigma_L^A$  we obtain the steady state solution for  $\mathcal{Z}^s(\xi_L)$  which reads

$$\begin{aligned} \ln \mathcal{Z}^s(\xi_L) &= -t_M \int \frac{d\omega}{4\pi} \ln \det \left[ I - G_0^r \Gamma_L G_0^a \Gamma_R \mathcal{K}(\omega; \xi_L) \right], \\ \mathcal{K}(\omega; \xi_L) &= (e^{i\xi_L \hbar \omega} - 1) f_L (1 + f_R) + (e^{-i\xi_L \hbar \omega} - 1) f_R (1 + f_L). \end{aligned} \quad (3.92)$$

If we consider the full system as a one-dimensional linear chain with nearest-neighbor interaction, then because of the special form of  $\Gamma_\alpha$  matrices (only one entry of the  $\Gamma$  matrices are non-zero) it can be easily shown that

$$\det[I - (G_0^r \Gamma_L G_0^a \Gamma_R) \mathcal{K}(\omega; \xi_L)] = 1 - \text{Tr}[\mathcal{T}[\omega]] \mathcal{K}(\omega; \xi_L) \quad (3.93)$$

where  $\mathcal{T}[\omega] = (G_0^r \Gamma_L G_0^a \Gamma_R)$  is the transmission matrix and  $\text{Tr}[\mathcal{T}[\omega]]$  is the transmission function and known as the Caroli formula [24, 25]. For one-dimensional linear chain, this steady state result was first derived by Saito and Dhar [26] in the phononic case.

### Gallavotti-Cohen symmetry

The CF  $\mathcal{Z}^s(\xi)$  in the steady state obeys the following symmetry

$$\mathcal{Z}^s(\xi_L) = \mathcal{Z}^s(-\xi_L + i(\beta_R - \beta_L)), \quad (3.94)$$

where  $\beta_R - \beta_L$  is known as the thermodynamic affinity. This can be shown by using the relation  $f_R(1 + f_L) = f_L(1 + f_R)e^{(\beta_L - \beta_R)\hbar\omega}$ . This particular symmetry of the CF is known as Gallavotti-Cohen (GC) symmetry [3, 4]. The immediate consequence is that the probability distribution for transferred heat  $Q_L$ , given by the Fourier transform of the CF, *i.e.*,  $P_{t_M}(Q_L) = \frac{1}{2\pi} \int_{-\infty}^{\infty} d\xi \mathcal{Z}(\xi_L) e^{-i\xi_L Q_L}$  obeys the following relation in the large  $t_M$  limit,

$$P_{t_M}(Q_L) = e^{(\beta_R - \beta_L)Q_L} P_{t_M}(-Q_L). \quad (3.95)$$

or equivalently

$$\lim_{t_M \rightarrow \infty} \ln \left[ \frac{P_{t_M}(Q_L)}{P_{t_M}(-Q_L)} \right] = (\beta_R - \beta_L)Q_L. \quad (3.96)$$

This relation is known as the steady state fluctuation theorem which quantifies the ratio of positive and negative heat flux and therefore make precise statement about the violation of second law of thermodynamics.

### First two cumulants of heat

The cumulants of heat can obtained by taking derivative of the CGF with

respect to the counting field  $\xi_L$  at  $\xi_L = 0$  *i.e.*,

$$\langle\langle Q^n \rangle\rangle = \left. \frac{\partial^n \ln \mathcal{Z}(\xi_L)}{\partial (i\xi_L)^n} \right|_{\xi_L=0} \quad (3.97)$$

The first cumulant is given as

$$\langle \mathcal{I}_L \rangle \equiv \frac{\langle\langle Q_L \rangle\rangle}{t_M} = \int_{-\infty}^{\infty} \frac{d\omega}{4\pi} \hbar \omega \text{Tr}[\mathcal{T}(\omega)] (f_L - f_R), \quad (3.98)$$

which is the Landauer-like formula in thermal transport. An alternate derivation starting from the definition of current is shown in chapter 2.

Similarly the second cumulant  $\langle\langle Q_L^2 \rangle\rangle = \langle Q_L^2 \rangle - \langle Q_L \rangle^2$ , which describes the fluctuation of the heat transferred, can be written as [26–28],

$$\frac{\langle\langle Q_L^2 \rangle\rangle}{t_M} = \int_{-\infty}^{\infty} \frac{d\omega}{4\pi} (\hbar\omega)^2 \left\{ \text{Tr}[\mathcal{T}^2(\omega)] (f_L - f_R)^2 + \text{Tr}[\mathcal{T}(\omega)] (f_L + f_R + 2f_L f_R) \right\}. \quad (3.99)$$

The higher cumulants can also be obtained systematically.

In the following section we present details about numerical calculations for obtaining the cumulants of heat in one-dimensional linear chain system connected with Rubin heat baths and also for graphene junction for these three different initial conditions.

## 3.7 Numerical Results for the cumulants of heat

The central quantity to calculate the CGF numerically is the shifted self-energy  $\Sigma_L^A$  which is given by

$$\Sigma_L^A(\tau, \tau') = \Sigma_L(\tau + \hbar x(\tau), \tau' + \hbar x(\tau')) - \Sigma_L(\tau, \tau'). \quad (3.100)$$

The main computational task for a numerical evaluation of the cumulants using Eq. (3.37,3.59) is to compute the matrix series  $-\ln(1 - M) = M + \frac{1}{2}M^2 + \dots$  where  $M \propto \check{G}_0 \check{\Sigma}_L^A$ . It can be seen due to the nature of  $\Sigma_L^A$  that for the product initial state, exact  $n$  terms up to  $M^n$  is required for the  $n$ -th cumulants, as the infinite series terminates due to  $\Sigma_L^A(\xi_L = 0) = 0$ . Numerically, we also observed for the projected initial state  $\rho'(0)$ , exactly  $3n$  terms is required (although we don't have a proof) if calculation is performed in time domain.

We need to perform convolution integrations in the time or frequency domain. For projected and steady state initial condition all components of  $G_0$  are time translationally invariant, as they are calculated at the steady state, it is advantageous to work in the frequency domain (see appendix (C)). But for the product initial state there is no such preference and one has to solve the Dyson equation given in Eq. (3.43) (see appendix (D)) numerically. The cumulants are then obtained by taking derivatives *i.e.*,  $\langle\langle Q^n \rangle\rangle = \frac{\partial^n \ln Z}{\partial (i\xi_L)^n} |_{\xi_L=0}$ .

**Results for projected  $\rho'(0)$  and product initial state  $\rho_{\text{prod}}(0)$**

In Fig. 3.4 and 3.5 we show results for the first four cumulants of heat for both left and right lead  $Q_L$  and  $Q_R$  starting with the projected  $\rho'(0)$  and product state  $\rho_{\text{prod}}(0)$  respectively. The system is a one-dimensional (1D) linear chain connected with Rubin heat baths. (One can consider other type of heat baths such as Ohmic or Lorentz-Drude bath [6]. In such cases the self-energy expressions should be modified.) By Rubin baths [5, 6] we mean a uniform linear chain with all spring constant  $k$  and a small onsite  $k_0$ . We consider only one atom at the center. The atoms of the left and right side of the center are considered baths. The expressions for  $G_0$  and the self-energy are given in appendix (E) and (F). We choose  $k = 1 \text{ eV}/(\text{u}\text{\AA}^2)$  and the onsite potential  $k_0 = 0.1 \text{ eV}/(\text{u}\text{\AA}^2)$  in all our calculations. For pure harmonic chain the onsite potential is important to achieve the steady state dynamically [29]. Few important observations for the cumulants are mentioned in the following:

- First of all we see that the cumulants greater than two are nonzero, which confirms that the distribution for heat  $P(Q_L)$  or  $P(Q_R)$  is non-Gaussian. This can also be seen from the steady state expression for CGF.
- The generic features are almost the same for both these initial conditions. However the fluctuations are larger for the product initial state  $\rho_{\text{prod}}(0)$  as the couplings between the center and the leads are switched on suddenly. On the contrary, for the initial state  $\rho'(0)$  the fluctuations are relatively small and the system reaches steady state

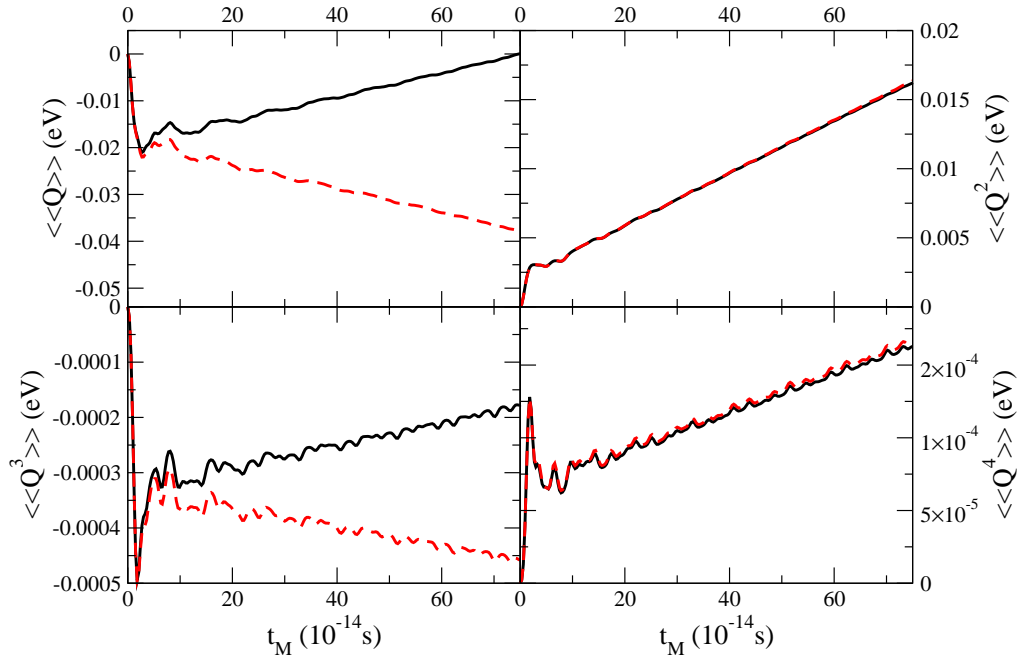


Figure 3.4: The cumulants  $\langle\langle Q_L^n \rangle\rangle$  and  $\langle\langle Q_R^n \rangle\rangle$  for  $n=1, 2, 3$ , and  $4$  for one-dimensional linear chain connected with Rubin baths, for the projected initial state  $\rho'(0)$ . The black (solid) and red (dashed) curves corresponds to  $\langle\langle Q_L^n \rangle\rangle$  and  $\langle\langle Q_R^n \rangle\rangle$  respectively. The temperatures of the left and the right lead are 310 K and 290 K, respectively. The center (C) consists of one particle.

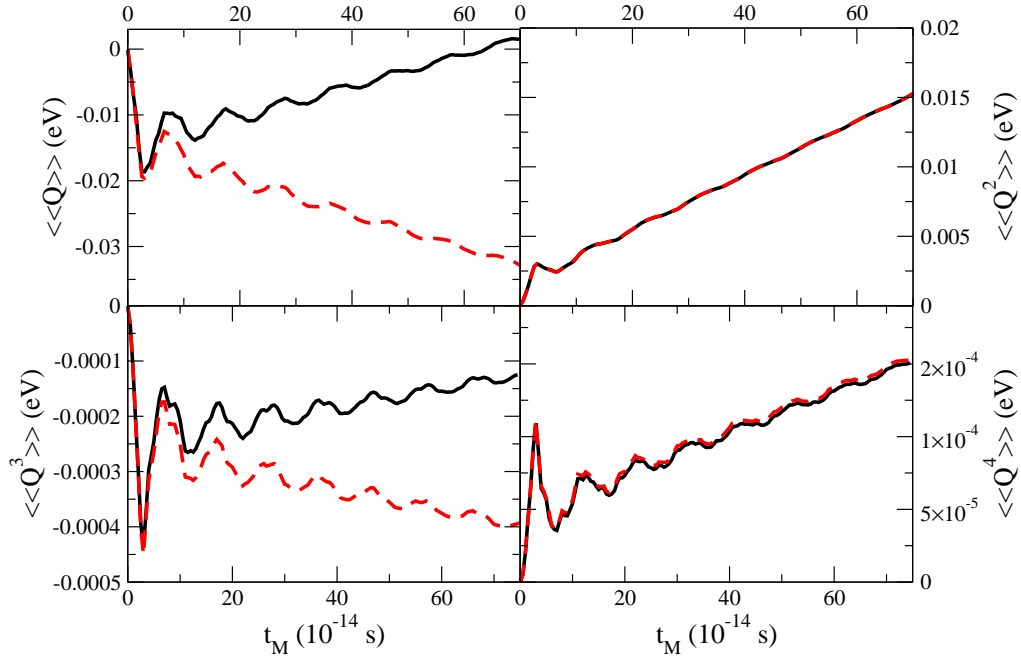


Figure 3.5: The cumulants  $\langle\langle Q_L^n \rangle\rangle$  and  $\langle\langle Q_R^n \rangle\rangle$  for  $n=1, 2, 3,$  and  $4$  for one-dimensional linear chain connected with Rubin baths for product initial state  $\rho_{\text{prod}}(0)$ . The black (solid) and red (dashed) curves corresponds to  $\langle\langle Q_L^n \rangle\rangle$  and  $\langle\langle Q_R^n \rangle\rangle$  respectively. The temperatures of the left, the center and the right lead are 310 K, 300 K and 290 K, respectively.

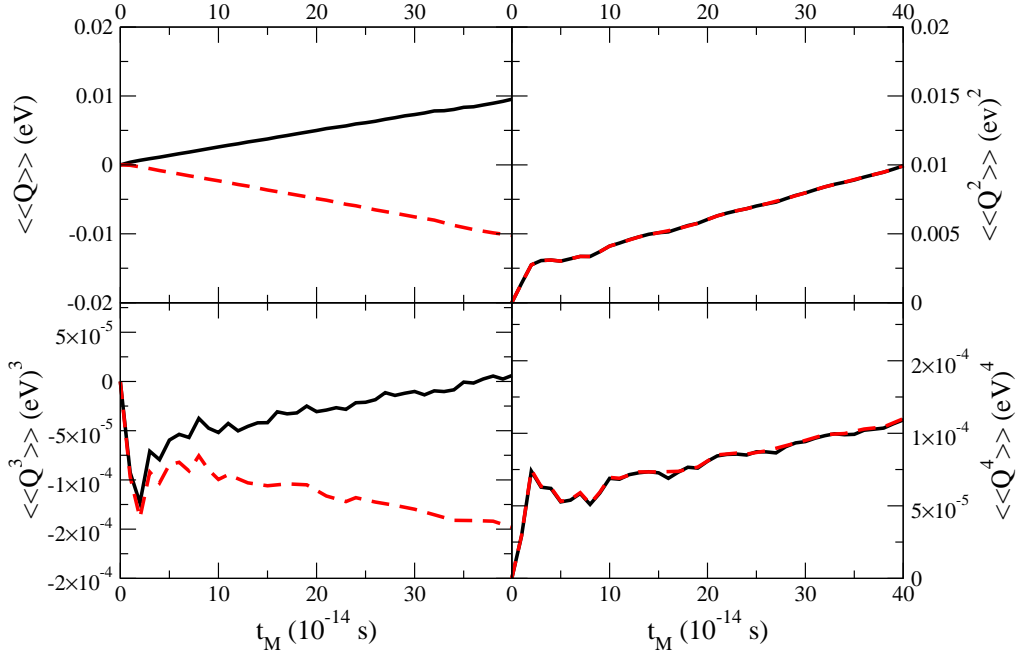


Figure 3.6: The cumulants  $\langle\langle Q_L^n \rangle\rangle$  and  $\langle\langle Q_R^n \rangle\rangle$  for  $n=1, 2, 3$ , and  $4$  for one-dimensional linear chain connected with Rubin baths for steady state initial state  $\rho_{\text{NESS}}(0)$ . The black (solid) and red (dashed) curves corresponds to  $\langle\langle Q_L^n \rangle\rangle$  and  $\langle\langle Q_R^n \rangle\rangle$  respectively. The temperatures of the left and the right lead are 310 K and 290 K, respectively.

much faster as compared with the product initial state.

- For  $\rho'(0)$  due to the effect of the measurement, at starting time heat flux or the current (derivative of  $\langle Q \rangle$  with  $t_M$ ) (see Fig. 3.4) goes into the leads, which is quite surprising. But for  $\rho_{\text{prod}}(0)$  although initial measurement do not play any role, energy still goes into the leads. This can also be shown analytically (see Appendix (G)).
- At the starting time the behavior of both  $Q_L$  and  $Q_R$  are very similar and can be intuitively understood as both the leads are identical and the effect of temperature difference is not realized in such a short time scale. At longer times the odd cumulants starts differing and

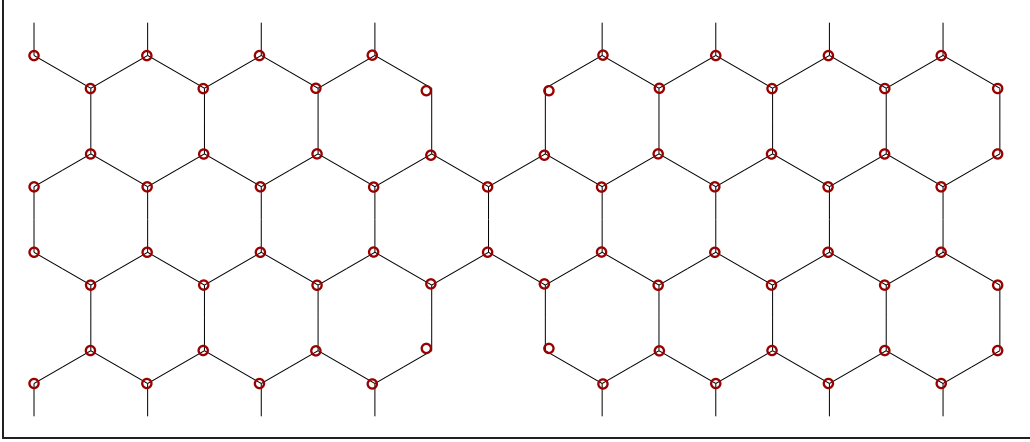


Figure 3.7: The structure of a graphene junction with 6 degrees of freedom with two carbon atoms as the center.

finally grows linearly with time  $t_M$  and agrees with the corresponding long-time predictions.

### Result for steady-state initial condition $\rho_{\text{NESS}}(0)$

In Fig. 3.6 we show the results for the steady state initial condition,  $\rho_{\text{NESS}}(0)$  by taking the limit  $\lambda \rightarrow 0$ . Since in this case the measurement effect is ignored the dynamics of the full system starts with the actual steady state. Therefore the first cumulant of heat increases linearly from the starting time at  $t = 0$  and  $\langle Q_L \rangle = t \langle I_L \rangle$  where the slope gives the correct prediction with the Landauer-like formula. However, higher order cumulants still shows transient behavior. In this case the whole system achieve steady state much faster as compared to the other two initial conditions.

### Result for graphene junction

We also present numerical results for graphene system. In Fig. (3.7) we show the structure for the graphene junction system. The center region

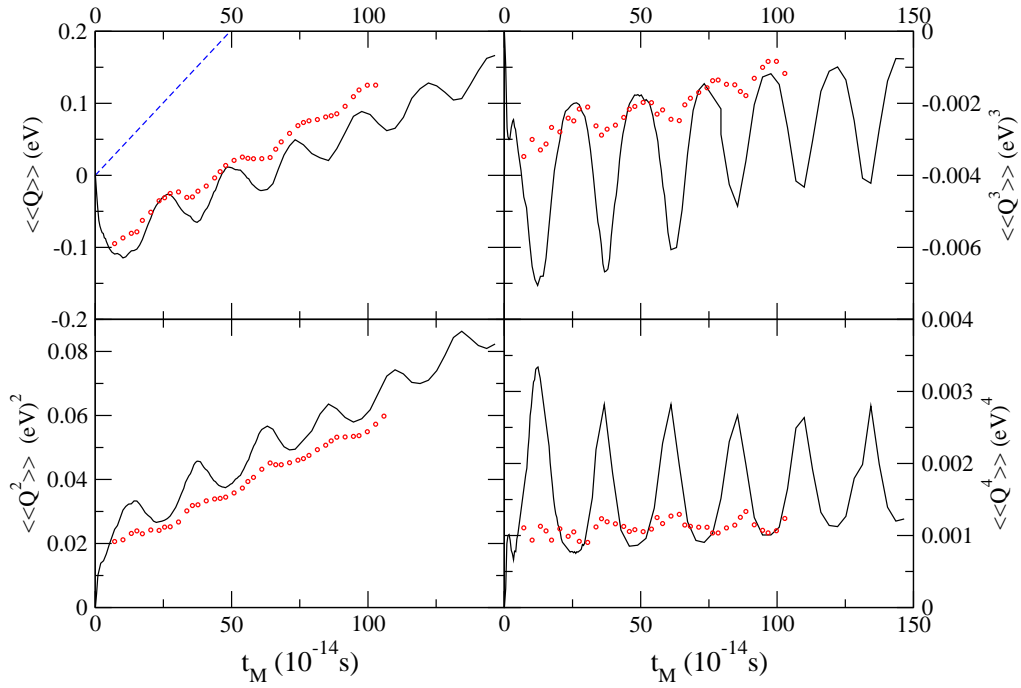


Figure 3.8: The cumulants  $\langle\langle Q^n \rangle\rangle$  as a function of  $t_M$  for graphene junction for  $n = 1, 2, 3$  and  $4$ . The curves are for the product initial state; the circles are for steady-state initial state. The dotted line is for the classical limit ( $\hbar \rightarrow 0$  keeping  $\lambda$  finite) for the steady-state initial condition. The temperature of the left lead is 330 K and that of the right lead is 270 K. For the product initial state, the center temperature is 300 K.

consists of two atoms with six degrees of freedom, while the two leads are symmetrically arranged as strips (with periodic boundary conditions in the vertical direction). We obtained the force constants using the second generation Brenner potential. The computational effort required for convergence is huge for the graphene junction.

From the Fig. (3.8) we can see that similar to the 1D case, in graphene junction also, fluctuations are much larger for  $\rho_{\text{prod}}(0)$  as compared to  $\rho_{\text{NESS}}(0)$ . As before for product initial state current goes into the leads at the beginning. If the system were classical, the measurement could not disturb the system. We should expect the current to be constant once the steady state is established. The dotted line in the figure correspond to the classical limit. The nonlinear  $t_M$  dependence observed here in  $\langle Q \rangle$  is fundamentally quantum mechanical in origin.

### 3.8 CF $\mathcal{Z}(\xi_L, \xi_R)$ corresponding to the joint probability distribution $P(Q_L, Q_R)$

In this section we derive the CF  $\mathcal{Z}(\xi_L, \xi_R)$  for  $\xi_C = 0$  introduced in Eq. (3.14). This CF corresponds to the joint probability distribution  $P(Q_L, Q_R)$ . Here we only consider the product initial state  $\rho_{\text{prod}}(0)$ . Other initial conditions can be handled as before. Following the same technique developed earlier

the generalized CGF reads

$$\ln \mathcal{Z}(\xi_L, \xi_R) = -\frac{1}{2} \text{Tr}_{(j, \tau)} \ln \left[ \mathbf{1} - [\mathbf{G}_0(\boldsymbol{\Sigma}_L^A + \boldsymbol{\Sigma}_R^A)] \right], \quad (3.101)$$

where an additional term  $\Sigma_R^A$  appears as an additive term due to the measurement of right Hamiltonian  $\mathcal{H}_R$ . Therefore we now need to shift the contour-time arguments for both left and right lead self-energies, *i.e.*,

$$\begin{aligned} \Sigma_\alpha^A(\tau, \tau') &= \Sigma_\alpha(\tau + \hbar x_\alpha(\tau), \tau' + \hbar x_\alpha(\tau')) - \Sigma_\alpha(\tau, \tau'), \quad \alpha = L, R \\ x_\alpha^\pm(\tau) &= \begin{cases} \mp \frac{\xi_\alpha}{2} & \text{for } 0 < t < t_M \\ 0 & \text{for } t > t_M \end{cases} \end{aligned}$$

The CGF for the left-lead heat can be recovered trivially by substituting  $\xi_R = 0$ .

### Long time limit of the generalized CGF

In the long-time limit due to time-translational invariance  $\mathcal{Z}(\xi_L, \xi_R)$  becomes a function of difference of the counting fields [30, 31] *i.e.*,  $\xi_L - \xi_R$ . The final expression for the CGF is the same as  $\ln \mathcal{Z}^s(\xi_L)$  except that now the counting field  $\xi_L$  should be replaced by  $\xi_L - \xi_R$ . Therefore we have

$$\begin{aligned} \ln \mathcal{Z}^s(\xi_L - \xi_R) &= -t_M \int \frac{d\omega}{4\pi} \ln \det \left[ I - \mathcal{T}[\omega] \mathcal{K}(\omega; \xi_L - \xi_R) \right] \\ \mathcal{K}(\omega; \xi_L - \xi_R) &= (e^{i(\xi_L - \xi_R)\hbar\omega} - 1) f_L (1 + f_R) + (e^{-i(\xi_L - \xi_R)\hbar\omega} - 1) f_R (1 + f_L). \end{aligned} \quad (3.102)$$

$G_0$  satisfies the same Dyson equation as before. Here we assume  $[\Gamma_L, \Gamma_R] =$

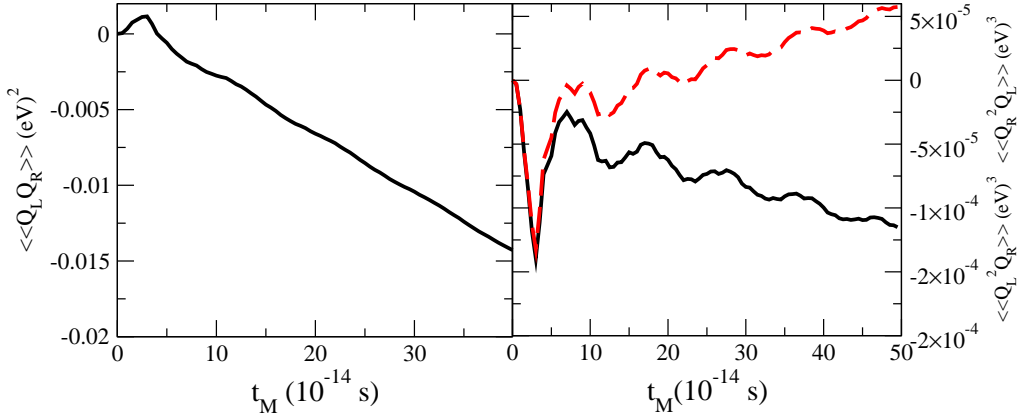


Figure 3.9: First three cumulants of the correlations between left and right lead heat flux for one dimensional linear chain connected with Rubin baths, starting with product initial state  $\rho_{\text{prod}}(0)$ . The left graph corresponds to  $\langle\langle Q_L Q_R \rangle\rangle$  and the right graph corresponds to cumulants  $\langle\langle Q_L^2 Q_R \rangle\rangle$  (black curve, solid) and  $\langle\langle Q_R^2 Q_L \rangle\rangle$  (red curve, dashed). The left, center and right lead temperatures are 310 K, 290 K and 300 K respectively. The center (C) consists of one particle.

0. By performing Fourier transformation of the CGF the joint probability distribution is given as  $P(Q_L, Q_R) = P(Q_L) \delta(Q_L + Q_R)$ . The appearance of the delta function is a consequence of the steady state which also implies that if we calculate the CGF for heat for the center part, then it will be independent of the counting field in the long-time limit.

The cumulants for the correlation between left and right lead heat flux can be obtained from by taking derivative of the CGF with respect to the counting fields  $\xi_L$  and  $\xi_R$ , i.e.,

$$\langle\langle Q_L^n Q_R^m \rangle\rangle = \frac{\partial^{n+m} \ln \mathcal{Z}^s(\xi_L - \xi_R)}{\partial (i\xi_L)^n \partial (i\xi_R)^m} \Big|_{\xi_L = \xi_R = 0}. \quad (3.103)$$

In the steady state the cumulants obey  $\langle\langle Q_L^n Q_R^m \rangle\rangle = (-1)^m \langle\langle Q_L^{m+n} \rangle\rangle =$

$(-1)^n \langle\langle Q_R^{m+n} \rangle\rangle$ . The first cumulant give us the left and right lead correlation  $\langle\langle Q_L Q_R \rangle\rangle = \langle Q_L Q_R \rangle - \langle Q_L \rangle \langle Q_R \rangle$  and in the steady state is equal to  $-\langle\langle Q_L^2 \rangle\rangle$ .

### Results for correlations of left and right lead heat flux

In Fig. (3.9) we plot first few cumulants for the correlations of heat for one dimensional linear chain connected with Rubin bath and the center consists of only one atom. Initially the cumulant  $\langle\langle Q_L Q_R \rangle\rangle$  is positively correlated as both  $Q_L$  and  $Q_R$  are negative, however in the longer time since  $Q_L = -Q_R$  the correlation becomes negative. We also give plots for  $\langle\langle Q_L^2 Q_R \rangle\rangle$  (black, solid lines) and  $\langle\langle Q_R^2 Q_L \rangle\rangle$  (red, dashed lines) which in the long-time limit are negative and positively correlated respectively and match with the long-time predictions.

### Results for Entropy production in the reservoir

From the two parameter CGF in Eq. (3.101) we can immediately write down the CGF for total entropy production in the leads given as  $\Sigma = -\beta_L Q_L - \beta_R Q_R$ . In order to calculate this CGF we just make the substitutions  $\xi_L \rightarrow -\beta_L \xi$  and  $\xi_R \rightarrow -\beta_R \xi$  in Eq. (3.101). In the long-time limit the expression for entropy-production is similar to  $\ln \mathcal{Z}(\xi_L, \xi_R)$  with  $\xi_L - \xi_R$  replaced by  $\mathcal{A}$  and therefore it becomes an explicit function of thermodynamic affinity  $\beta_R - \beta_L$  [30, 31]. The CGF now satisfy the GC symmetry as  $\mathcal{Z}(\xi) = \mathcal{Z}(-\xi + i)$ . In Fig. (3.10) we give results for the first four cumulants of the entropy production. All cumulants are positive and in the long-time limit give correct predictions.

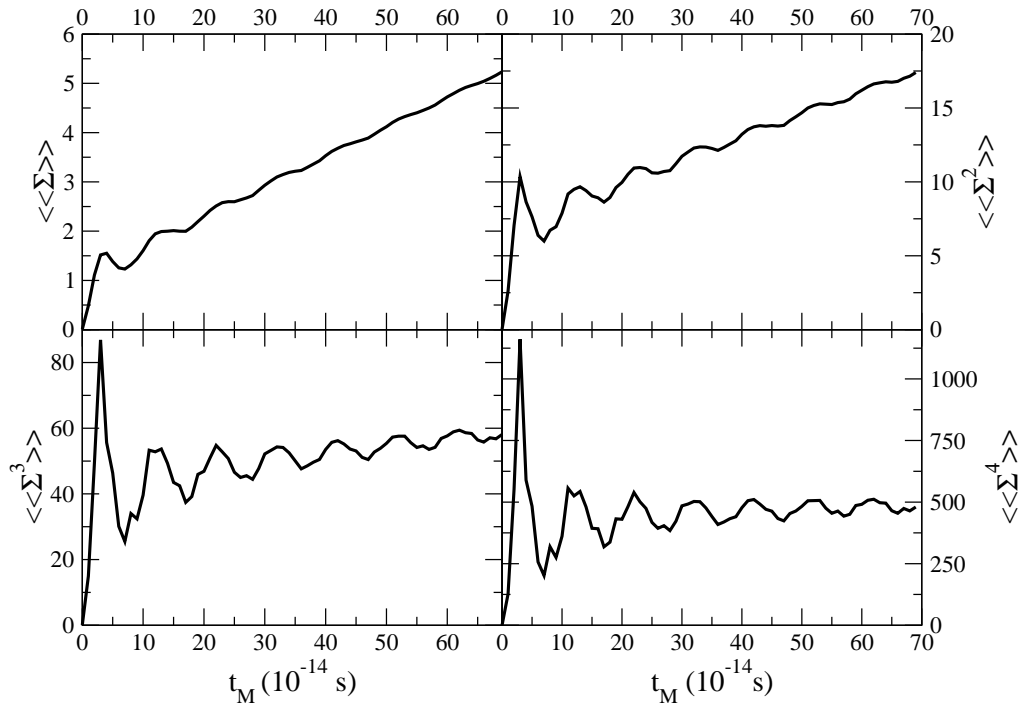


Figure 3.10: The cumulants of entropy production  $\langle\langle\Sigma^n\rangle\rangle$  for  $n=1, 2, 3, 4$  for one dimension linear chain connected with Rubin baths, for product initial state  $\rho_{\text{prod}}(0)$ . The left, center and right lead temperatures are 510 K, 400 K, and 290 K respectively. The center (C) consists of one particle.

### 3.9 Classical limit of the CF

In this section we will give the classical limit of the steady state expression for the CGF's  $\ln \mathcal{Z}^s(\xi_L)$  given in Eq. (3.92). First of all we note that retarded and advanced Green's functions, i.e.,  $G_0^r$  and  $G_0^a$  are the same for quantum and classical case which can also be seen from the definitions as commutators gets replaced by the Poisson brackets. We know that in the classical limit  $f_\alpha \rightarrow \frac{k_B T_\alpha}{\hbar\omega}$  and also  $e^{ix} = 1 + ix + \frac{(ix)^2}{2} + \dots$ , where  $x = \xi_L \hbar\omega$ . Using this we obtain the classical limit of  $\mathcal{Z}^s(\xi_L)$  as

$$\ln \mathcal{Z}_{\text{cls}}^s(\xi_L) = -t_M \int_{-\infty}^{\infty} \frac{d\omega}{4\pi} \ln \det \left[ I - \mathcal{T}[\omega] \frac{i\xi_L}{\beta_L \beta_R} (i\xi_L + (\beta_R - \beta_L)) \right]. \quad (3.104)$$

This result reproduces that of Ref. [32] which was obtained from Langevin dynamics with white noise reservoirs. However above formula is valid for arbitrary colored noise which are written in terms of the self-energy of the leads. Similar to the quantum case, here the CGF obeys the GC symmetry, i.e.,  $\mathcal{Z}_{\text{cls}}^s(\xi_L) = \mathcal{Z}_{\text{cls}}^s(-\xi_L + i(\beta_R - \beta_L))$ .

It is worth mentioning that very recently, the above study is extended for a general lead-junction-lead model including direct coupling between the leads and it is found that the long-time CGF can be written in a similar form as given in Eq. (3.92) with a different transmission function but the form of the counting-field dependent function is the same and therefore

satisfy GC symmetry. For details see Ref. [16, 33]

### 3.10 Nazarov's definition of CF and long-time limit expression

In this section we first derive Nazarov's CF [13, 14, 26] given by Eq. (3.17), starting from the CF derived using two-time measurement concept (see Eq. (3.11)) and then obtain the long-time limit expression for the harmonic lead-junction-lead model.

#### Derivation for Nazarov's CF from two-time measurement CF

Employing two-time measurement method the CF is written as

$$\begin{aligned} \mathcal{Z}(\xi_L) &= \langle e^{i\xi_L \mathcal{H}_L} e^{-i\xi_L \mathcal{H}_L^H(t)} \rangle \\ &= \langle \mathcal{U}_{\xi_L/2}(0, t) \mathcal{U}_{-\xi_L/2}(t, 0) \rangle. \end{aligned} \quad (3.105)$$

where  $\mathcal{U}_x(t, 0) = T \exp[-\frac{i}{\hbar} \int_0^t \mathcal{H}_x(t') dt']$  and the modified Hamiltonian is given as

$$\begin{aligned} \mathcal{H}_x(t) &= e^{ix\mathcal{H}_L} \mathcal{H}(t) e^{-ix\mathcal{H}_L}, \\ &= \mathcal{H}(t) + (u_L(\hbar x) - u_L)^T V^{LC} u_C, \end{aligned} \quad (3.106)$$

Now let us consider small  $x = \pm\xi_L/2$  limit. Then the modified Hamiltonian

can be approximated as

$$\mathcal{H}_x(t) \approx \mathcal{H}(t) + \hbar x \mathcal{I}_L(0) + \mathcal{O}(x^2), \quad (3.107)$$

where  $\mathcal{I}_L(0) = u_L^T V^{LC} u_C$ . The modified unitary operator then written as

$$\mathcal{U}_x(t, 0) = T \exp \left[ -\frac{i}{\hbar} \int_0^t (\mathcal{H}(\bar{t}) + \hbar x \mathcal{I}_L(0)) d\bar{t} \right]. \quad (3.108)$$

Now we can consider  $\hbar x \mathcal{I}_L(0)$  as the interaction Hamiltonian and write the full unitary operator  $\mathcal{U}_x$  as a product of two unitary operators as following

$$\begin{aligned} \mathcal{U}_x(t, 0) &= \mathcal{U}(t, 0) \mathcal{U}_x^I(t, 0), \\ \mathcal{U}(t, 0) &= T \exp \left[ -\frac{i}{\hbar} \int_0^t \mathcal{H}(t') dt' \right] \\ \mathcal{U}_x^I(t, 0) &= T \exp \left[ -\frac{i}{\hbar} \int_0^t \hbar x \mathcal{I}_L(t') dt' \right], \end{aligned} \quad (3.109)$$

with  $\mathcal{I}_L(t') = \mathcal{U}^\dagger(t', 0) \mathcal{I}_L(0) \mathcal{U}(t', 0)$  is the current operator in the Heisenberg picture. It is important to note that  $\mathcal{U}$  is the usual unitary operator which evolves with the full Hamiltonian  $\mathcal{H}(t)$  in and has no counting-field dependence. Therefore in the small  $\xi_L$  approximation and using the expressions for  $\mathcal{U}_x$  we can write the CF as

$$\mathcal{Z}_1(\xi_L) = \text{Tr} \left[ \rho_{\text{prod}}(0) \mathcal{U}_{\xi_L/2}^I(0, t) \mathcal{U}_{-\xi_L/2}^I(t, 0) \right], \quad (3.110)$$

where we use the property of unitary operator, *i.e.*,  $\mathcal{U}^\dagger(t, 0) \mathcal{U}(t, 0) = 1$ .

Finally using the definition of heat operator  $\mathcal{Q}_L$  the CF reads

$$\mathcal{Z}_1(\xi_L) = \left\langle \bar{T} e^{i\xi \mathcal{Q}_L(t)/2} T e^{i\xi \mathcal{Q}_L(t)/2} \right\rangle, \quad (3.111)$$

which is the same as in Eq. (3.17).

### Long-time limit for Nazarov's CF

In the following we will give the long-time limit expression for this CGF. In order to calculate the CGF, we go to the interaction picture with respect to the Hamiltonian  $\mathcal{H}_0 = \mathcal{H}_L + \mathcal{H}_C + \mathcal{H}_R$ , as we know how to calculate Green's functions for operators which evolves with  $\mathcal{H}_0$  and treat the rest part as the interaction  $\mathcal{V}_x = \mathcal{H}_{\text{int}} + \hbar x \mathcal{I}_L(0)$ . So the CF on contour  $C = [0, t_M]$  can be written as

$$\mathcal{Z}_1(\xi_L) = \left\langle T_c e^{-\frac{i}{\hbar} \int \hat{\mathcal{V}}_x(\tau) d\tau} \right\rangle, \quad (3.112)$$

where  $\hat{\mathcal{V}}_x(\tau)$  is now given by

$$\hat{\mathcal{V}}_x(\tau) = \hat{u}_L^T(\tau) V^{LC} \hat{u}_C(\tau) + \hat{u}_R^T(\tau) V^{RC} \hat{u}_C(\tau) + \hbar x(\tau) \hat{p}_L(\tau) V^{LC} \hat{u}_C(\tau), \quad (3.113)$$

where  $p_L = \dot{u}_L$ . The time-dependence  $\tau$  is coming from the free evolution with respect to  $\mathcal{H}_0$ .  $x(\tau)$  has the similar meaning as before, *i.e.*, on the upper branch of the contour  $x^+(t) = -\xi_L/2$  and on the lower branch  $x^-(t) = \xi_L/2$ . Now using the same idea as before, we expand the series, use Wick's theorem and finally obtain the CGF as

$$\ln \mathcal{Z}_1(\xi_L) = -\frac{1}{2} \text{Tr}_{j,\tau} \ln \left[ \mathbf{1} - \mathbf{G}_0 \boldsymbol{\Sigma}_L^A \right]. \quad (3.114)$$

Here  $G_0$  is the same as in Eq. (3.43). In this case however the shifted self-energy  $\Sigma_L^A$  is different and is written as

$$\Sigma_L^A(\tau, \tau') = \hbar x(\tau) \Sigma_{p_L u_L}(\tau, \tau') + \hbar x(\tau') \Sigma_{u_L p_L}(\tau, \tau') + \hbar^2 x(\tau) x(\tau') \Sigma_{p_L p_L}(\tau, \tau'). \quad (3.115)$$

The notation  $\Sigma_{AB}(\tau, \tau')$  means

$$\Sigma_{AB}(\tau, \tau') = -\frac{i}{\hbar} \left[ V^{CL} \langle T_c A(\tau) B^T(\tau') \rangle V^{LC} \right]. \quad (3.116)$$

The average here is with respect to equilibrium distribution of the left lead. It is possible to express the correlation functions such as  $\Sigma_{p_L u_L}(\tau, \tau')$  in terms of the  $\Sigma_{u_L, u_L}(\tau, \tau') = \Sigma_L(\tau, \tau')$  correlations.  $\Sigma_{p_L u_L}(\tau, \tau')$  and  $\Sigma_{u_L p_L}(\tau, \tau')$  is simply related to  $\Sigma_L(\tau, \tau')$  by the contour-time derivative whereas for  $\Sigma_{p_L p_L}(\tau, \tau')$  the expression is

$$\Sigma_{p_L p_L}(\tau, \tau') = \frac{\partial^2 \Sigma_{u_L u_L}(\tau, \tau')}{\partial \tau \partial \tau'} + \delta(\tau, \tau') \Sigma_L^I. \quad (3.117)$$

Where  $\Sigma_L^I = V^{CL} V^{LC}$ . Now in the frequency domain different components of  $\Sigma_L^A$  takes the following form

$$\begin{aligned} \Sigma_A^t[\omega] &= \frac{\hbar^2 \xi_L^2 \omega^2}{4} \Sigma_L^t[\omega] + \frac{\hbar^2 \xi_L^2}{4} \Sigma_L^I, \\ \Sigma_A^{\bar{t}}[\omega] &= \frac{\hbar^2 \xi_L^2 \omega^2}{4} \Sigma_L^{\bar{t}}[\omega] - \frac{\hbar^2 \xi_L^2}{4} \Sigma_L^I, \\ \Sigma_A^<[\omega] &= \left( i\hbar \xi_L \omega - \frac{\hbar^2 \xi_L^2 \omega^2}{4} \right) \Sigma_L^<[\omega], \\ \Sigma_A^>[\omega] &= \left( -i\hbar \xi_L \omega - \frac{\hbar^2 \xi_L^2 \omega^2}{4} \right) \Sigma_L^>[\omega]. \end{aligned} \quad (3.118)$$

Finally using the fluctuation-dissipation relations between the self-energy, the long-time limit of the CGF can be explicitly written down as,

$$\begin{aligned} \ln \mathcal{Z}_1(\xi_L) &= -t_M \int \frac{d\omega}{4\pi} \ln \det \left[ 1 - (i\xi_L \hbar \omega) \mathcal{T}[\omega] (f_L - f_R) \right. \\ &\quad \left. - \frac{(i\xi_L \hbar \omega)^2}{4} \left( \mathcal{T}[\omega] (1 + 2f_L)(1 + 2f_R) - G_0^a \Sigma_L^r \right. \right. \\ &\quad \left. \left. + G_0^r \Sigma_L^a - G_0^r \Gamma_L G_0^a \Gamma_L \right) + \mathcal{J}(\xi_L^2, \xi_L^4) \right], \end{aligned} \quad (3.119)$$

where  $\mathcal{J}(\xi_L^2, \xi_L^4)$  is given by

$$\begin{aligned} \mathcal{J}(\xi_L^2, \xi_L^4) &= -\frac{\hbar^2 \xi_L^2}{4} (G_0^a + G_0^r) \Sigma_L^I - \frac{1}{4} \frac{(i\xi_L \hbar \omega)^2}{2} \frac{\hbar^2 \xi_L^2}{2} \\ &\quad + (G_0^r \Sigma_L^a G_0^a \Sigma_L^I + G_0^r \Sigma_L^I G_0^a \Sigma_L^r) + \frac{1}{4} \frac{(i\xi_L \hbar \omega)^4}{4} \\ &\quad G_0^r \Sigma_L^a G_0^a \Sigma_L^r + \frac{1}{4} \frac{(\hbar^4 \xi_L^4)}{4} G_0^r \Sigma_L^I G_0^a \Sigma_L^I. \end{aligned} \quad (3.120)$$

This CGF *does not obey* the GC fluctuation symmetry. However it gives the correct first and second cumulant as the definitions turn out to be the same for both the CF's  $\mathcal{Z}(\xi_L)$  and  $\mathcal{Z}_1(\xi_L)$  and are given as

$$\begin{aligned} \langle\langle Q \rangle\rangle &= \langle Q \rangle = \frac{\partial \ln \mathcal{Z}(\xi_L)}{\partial(i\xi_L)} = \frac{\partial \ln \mathcal{Z}_1(\xi_L)}{\partial(i\xi_L)} = \int_0^t dt_1 \langle \mathcal{I}_L(t_1) \rangle, \\ \langle\langle Q^2 \rangle\rangle &= \langle Q^2 \rangle - \langle Q \rangle^2 = \frac{\partial^2 \ln \mathcal{Z}(\xi_L)}{\partial(i\xi)^2} = \frac{\partial^2 \ln \mathcal{Z}_1(\xi_L)}{\partial(i\xi_L)^2} \\ &= \int_0^t dt_1 \int_0^t dt_2 \langle \mathcal{I}_L(t_1) \mathcal{I}_L(t_2) \rangle - \left[ \int_0^t dt_1 \langle \mathcal{I}_L(t_1) \rangle \right]^2. \end{aligned} \quad (3.121)$$

Expressions for higher cumulants are different for the two CF and therefore the final expressions for the CGF's are completely different from each other.

### 3.11 Summary

In summary, we present an elegant way of deriving the CGF for heat for a harmonic system connected with two heat baths. Using two-time measurement concept we derive the CGF based on NEGF and path-integral technique. We generalize the model by including time-dependent driving force at the center and also making the coupling between the leads and the center time-dependent. The leads in our formalism could be finite. The CGF is obtained for arbitrary transient time  $t_M$ . For this harmonic junction the CGF is written as a sum of two contributions. In this chapter we discuss the temperature bias part of the CGF which is written in terms of the center Green's function and shifted self-energy of the measured lead. We found that the counting of the energy is related to the shifting in contour time for the corresponding self-energy. For the electron case also similar conclusion can be drawn (see appendix (H)). In addition to the energy measurement, for electrons, particle number measurement generates a contour-time dependent phase in the self-energy. We consider three different initial conditions for the density operator and show numerically that for 1D harmonic chain, connected with Rubin baths, transient behaviors significantly differ from each other but eventually reaches a unique steady state in the long-time limit. We also present results for graphene junction. An intriguing feature is that a measurement, even in the steady state, causes energy flow into the leads. We give explicit expressions of the CGF in the steady state invoking the time translational invariance of the center Green's functions. The CGF obeys the GC fluctuation symmetry.

We also obtain a two-parameter CGF which is useful for calculating the correlations between heat flux and also the total entropy production in the leads. The classical limit for the CGF is obtained which also satisfy the GC symmetry. We would like to point out that the effect of magnetic field can be similarly studied by including an additional term in the Hamiltonian given in the form  $u_C^T A p_C$  where  $A$  is an antisymmetric matrix and depends on the magnetic field. Such a model is used to explain a recently discovered phenomena known as Phonon Hall effect [34–36].

# Bibliography

- [1] L. S. Levitov and G. B. Lesovik, JETP Lett. **58**, 230 (1993).
- [2] L. S. Levitov, H.-W. Lee, and G. B. Lesovik, J. Math. Phys. **37**, 4845 (1996).
- [3] G. Gallavotti and E. G. D. Cohen. Phys. Rev. Lett. **74**, 2694 (1995).
- [4] G. Gallavotti and E. G. D. Cohen. J. Stat. Phys. **80**, 931 (1995).
- [5] R. J. Rubin and W. L. Greer, J. Math. Phys. **12**, 1686 (1971).
- [6] U. Weiss, *Quantum Dissipative Systems*, 2nd edn. (World Scientific, 1999).
- [7] E. C. Cuansing and J.-S. Wang, Phys. Rev. B **81**, 052302 (2010);  
erratum **83**, 019902(E) (2011).
- [8] E. C. Cuansing and J.-S. Wang, Phys. Rev. E **82**, 021116 (2010).
- [9] S. Deffner and E. Lutz, Phys. Rev. Lett, **107**, 140404 (2011).
- [10] M. Esposito, K. Lindenberg, and C. Van den Broeck, New. J. Phys. **12**, 013013 (2010).

## BIBLIOGRAPHY

---

- [11] M. Esposito, U. Harbola, and S. Mukamel, *Rev. Mod. Phys.* **81**, 1665 (2009).
- [12] H. -P. Breuer and F. Peteruccione, *The Theory of Open Quantum Systems*, Oxford University Press, Oxford, 2002.
- [13] W. Belzig and Y. V. Nazarov, *Phys. Rev. Lett.* **87**, 197006 (2001).
- [14] Y. V. Nazarov and M. Kindermann, *Eur. Phys. J. B* **35**, 413 (2003).
- [15] R. B. Griffiths, *Consistent Quantum Theory*, Cambridge Univ. Press, Cambridge (2002).
- [16] Huanan. Li, Bijay. K. Agarwalla, and J. -S. Wang *Phys. Rev. B* **86**, 165425 (2012).
- [17] J. Rammer and H. Smith, *Rev. Mod. Phys.* **58**, 323 (1986).
- [18] G.D. Mahan, *Many-Particle Physics*, 3rd edn. (Kluwer Academic, 2000).
- [19] J.-S. Wang, B. K. Agarwalla, and H. Li, *Phys. Rev. B* **84**, 153412, (2011).
- [20] B. K. Agarwalla, B. Li, and J.-S. Wang, *Phys. Rev. E* **85**, 051142 (2012).
- [21] L. Arrachea and B. Rizzo, arXiv: 1212.3181.
- [22] R. P. Feynman and F. L. Vernon, *Ann. Phys.* **24**, 118 (1963).
- [23] J. T. Stockburger and H. Grabert, *Phys. Rev. Lett.* **88**, 170407 (2002).

## BIBLIOGRAPHY

---

- [24] C. Caroli, R. Combescot, P. Nozieres, D. Saint-James, J. Phys. C: Solid St. Phys. **4**, 916 (1971).
- [25] J.-S. Wang, J. Wang, and J. T. Lü, Eur. Phys. J. B **62**, 381 (2008).
- [26] K. Saito and A. Dhar, Phys. Rev. Lett. **99**, 180601 (2007).
- [27] H. Haug and A.-P. Jauho, *Quantum Kinetics in Transport and Optics of Semiconductors*, 2nd ed. (Springer, New York, 2008).
- [28] Ya. M. Blanter and M. Büttiker, Physics Reports, **336**, 2, (2000).
- [29] E. C. Cuansing, H. Li, and J.-S. Wang, Phys. Rev. E **86**, 031132 (2012).
- [30] D. Andrieux, P. Gaspard, T. Monnai, and S. Tasaki, New. J. Phys. **11**, 043014 (2009).
- [31] K. Saito and Y. Utsumi, Phys. Rev. B **78**, 115429 (2008).
- [32] A. Kundu, S. Sabhapandit, and A. Dhar, J. Stat. Mech (2011) P03007.
- [33] Huanan. Li, Bijay. K. Agarwalla, and J.-S. Wang Phys. Rev. E **86**, 011141 (2012).
- [34] B. K. Agarwalla, L. Zhang, J.-S. Wang, and B. Li , Eur. Phys. J. B **81**, 197 (2011).
- [35] C. Strohm, G.L.J.A. Rikken, P. Wyder, Phys. Rev. Lett. **95**, 155901 (2005).
- [36] L. Zhang, J. Ren, J.-S. Wang, B. Li, Phys. Rev. Lett. **105**, 225901 (2010).

## Chapter 4

# Full-counting statistics (FCS) and energy-current in the presence of driven force

Understanding the general features of energy current in a force-driven system is of significant interest. One of the major goal here is to control the current by applying periodic driving force and to convert the system to act like a heat pump [1–4]. *i.e.*, to direct heat against thermal bias by using external force. As an example, Ai et al [5] showed the heat pumping behavior in Frenkel- Kontorova (FK) chain by adjusting the frequency of the ac driving force. On the contrary, Marathe et al [6] showed that under periodic driving two coupled harmonic oscillators connected with thermal reservoirs fails to act as a heat pump.

On the other hand, a recent study on driven quantum Langevin model for any arbitrary time-dependent potential shows that the energy dissipation flow to thermal environment is related to the violation of the fluctuation-dissipation relation [7, 8]. Moreover, for systems driven arbitrarily far from equilibrium it is possible to relate the work done during the nonequilibrium process with the free energy difference between two equilibrium states through Jarzynski's equality (JE) [9–11]. Finding explicit forms of nonequilibrium distribution functions for work and henceforth averages for different systems is another major interest in this field [12–15].

In the previous chapter, for a forced-driven harmonic lead-junction-lead model we found that the full CGF can be separated into two terms (see Eq. (3.89)). The force independent term in the long-time limit reduces to the Levitov-Lesovik like formula for phonons. In this chapter we investigate the other term of the CGF coming due to the driving force. We first obtain the long-time limit expression for the CGF and then generalize it by introducing another counting field for the right lead heat to study driven force induced entropy production in the leads. This also satisfy fluctuation symmetry. For periodic driving we derive an explicit expression for the CGF when the system is connected with Rubin heat baths and then explore the effects on steady state energy current due to system size and applied frequency. In addition we compare the effects of Rubin [16] and Ohmic [17] heat baths on energy current. We also present an alternate derivation for transient energy current starting from the basic definition of the current operator.

## 4.1 Long-time result for the driven part of the CGF $\ln \mathcal{Z}^d(\xi_L)$

In this section we derive an explicit expression for the forced-driven CGF  $\ln \mathcal{Z}^d(\xi_L)$  in the long-time limit (for periodic driven force) which is given by (Eq. (3.87))

$$\ln \mathcal{Z}^d(\xi_L) = -\frac{i}{\hbar} \int \frac{d\omega}{4\pi} \text{Tr}_{j,\sigma} \left[ \check{G}[\omega] \check{\mathcal{F}}[\omega, -\omega] \right], \quad (4.1)$$

where  $\check{G}$  is the counting field dependent Green's function and satisfy the Dyson equation on the contour  $C[0, t_M]$

$$\check{G}(\tau, \tau') = G_0(\tau, \tau') + \int_C \int_C d\tau_1 d\tau_2 G_0(\tau, \tau_1) \Sigma_L^A(\tau_1, \tau_2) \check{G}(\tau_2, \tau'). \quad (4.2)$$

and the force matrix  $\check{\mathcal{F}}[\omega, -\omega]$  is given as

$$\check{\mathcal{F}}[\omega, -\omega] = \begin{bmatrix} 0 & f[\omega] f^T[-\omega] \\ 0 & 0 \end{bmatrix}. \quad (4.3)$$

Using Keldysh rotation and invoking time-translation invariance in the long-time limit ( $\check{G}$  does not depend on time-depdnt force and therefore it will have a proper long-time limit) *i.e.*,  $\check{G}(t, t') = \check{G}(t - t')$ , we obtain the solution for  $\check{G}[\omega]$  in terms of  $G_0$  and  $\Sigma_L^A$  as

$$\check{G}[\omega] = \left[ I - \check{G}_0[\omega] \check{\Sigma}_L^A[\omega] \right]^{-1} \check{G}_0[\omega], \quad (4.4)$$

with

$$\check{G}_0[\omega] = \begin{bmatrix} G_0^r[\omega] & G_0^K[\omega] \\ 0 & G_0^a[\omega] \end{bmatrix} \quad \text{and} \quad \check{\Sigma}_L^A[\omega] = \frac{1}{2} \begin{bmatrix} a-b & a+b \\ -(a+b) & -(a-b) \end{bmatrix}, \quad (4.5)$$

$$\begin{aligned} a &\equiv \Sigma_L^>[\omega](e^{-i\hbar\omega\xi_L} - 1), \\ b &\equiv \Sigma_L^<[\omega](e^{i\hbar\omega\xi_L} - 1). \end{aligned} \quad (4.6)$$

Equation (4.4) can be solved by calculating the inverse of a  $2 \times 2$  matrix. Let us now make an assumption that the product of  $f(t)$  and  $f(t')$  is a time translationally invariant function, *i.e.*,  $f(t)f^T(t') = F(t-t')$  in order to get rid of  $t+t'$  dependent term. In the Fourier domain this means  $f[\omega]f^T[\omega'] = 2\pi F[\omega]\delta(\omega+\omega')$ . Therefore we have  $\check{\mathcal{F}}_{12}[\omega, -\omega] \propto \delta(0)F[\omega]$  with  $\delta(0) = t_M/2\pi$ . Using these results the CGF can be expressed as

$$\ln \mathcal{Z}^d(\xi_L) = it_M \int \frac{d\omega}{4\pi\hbar} \frac{1}{\mathcal{N}(\xi_L)} \text{Tr} \left[ G_0^r[\omega](a+b)G_0^a[\omega]F[\omega] \right], \quad (4.7)$$

Using the fluctuation-dissipation relations for the self-energy *i.e.*,  $\Sigma_L^<[\omega] = f_L(\Sigma_L^r[\omega] - \Sigma_L^a[\omega]) = -if_L\Gamma_L$  and  $\Sigma_L^>[\omega] = e^{\beta_L\hbar\omega}\Sigma_L^<[\omega]$ ,  $\Gamma_L[\omega] = i(\Sigma_L^r[\omega] - \Sigma_L^a[\omega])$  the CGF reduces to

$$\ln \mathcal{Z}^d(\xi_L) = t_M \int \frac{d\omega}{4\pi\hbar} \frac{\mathcal{M}_L(\omega; \xi_L)}{\mathcal{N}(\omega; \xi_L)} \text{Tr} [\mathcal{S}_L[\omega]], \quad (4.8)$$

with

$$\begin{aligned}
 \mathcal{S}_L[\omega] &= G_0^r[\omega]\Gamma_L[\omega]G_0^a[\omega]F[\omega], \\
 \mathcal{M}_L(\omega; \xi_L) &= (e^{i\xi_L\hbar\omega}-1)f_L + (e^{-i\xi_L\hbar\omega}-1)(1+f_L), \\
 \mathcal{N}(\omega; \xi_L) &= \det\left[I - \mathcal{T}[\omega]\mathcal{K}(\omega; \xi_L)\right], \\
 \mathcal{K}(\omega; \xi_L) &= (e^{i\xi_L\hbar\omega}-1)f_L(1+f_R) + (e^{-i\xi_L\hbar\omega}-1)f_R(1+f_L). \quad (4.9)
 \end{aligned}$$

We call  $\mathcal{S}_L[\omega]$  as the force-driven transmission matrix which is independent of  $\hbar$  and the temperature of the heat baths. Also note that  $\mathcal{M}_L(\omega; \xi_L)$  depends only on left lead temperature and follow the symmetry relation  $\mathcal{M}_L(\omega; \xi_L) = \mathcal{M}_L(\omega; -\xi_L - i\beta_L)$ . Therefore we immediately obtain  $\mathcal{Z}^d(-i\beta_L) = 1$  which is completely independent of the right lead information. If we consider the two leads at the same temperature ( $\beta_L = \beta_R = \beta$ ), this particular form of symmetry is then closely related to the Jarzynski equality (JE) [9–11]. However since  $\mathcal{N}(\omega; \xi_L)$  is not invariant under this transformation  $\xi_L = -\xi_L - i\beta_L$  (it remains invariant when  $\xi_L \rightarrow -\xi_L + i(\beta_R - \beta_L)$ ) in general  $\mathcal{Z}^d(\xi_L) \neq \mathcal{Z}^d(-\xi_L - i\beta_L)$ . This however does not violate JE as the CF  $\mathcal{Z}^d(\xi_L)$  is defined for the quantity heat, not for the work done by the external force as defined by Jarzynski.

It is also possible to generalize the CGF by introducing another counting field  $\xi_R$  corresponding to  $Q_R^d$  ( $d$  here refers to the contribution due to the driven force), as done in chapter 2. Then the force induced entropy production in the leads can be computed easily. It can be shown that the effect of measuring other lead is additive to the final CGF because the

Dyson equation in Eq. (4.2) gets an additional term  $\tilde{\Sigma}_R^A(\tau, \tau')$ , *i.e.*,

$$\tilde{G}(\tau, \tau') = G_0(\tau, \tau') + \int_C \int_C d\tau_1 d\tau_2 G_0(\tau, \tau_1) (\Sigma_L^A + \Sigma_R^A)(\tau_1, \tau_2) \tilde{G}(\tau_2, \tau'). \quad (4.10)$$

and we obtain in the long-time limit

$$\ln \mathcal{Z}^d(\xi_L, \xi_R) = t_M \int \frac{d\omega}{4\pi\hbar} \frac{1}{\mathcal{N}(\omega; \xi_L - \xi_R)} \sum_{\alpha=L,R} \mathcal{M}_\alpha(\omega; \xi_\alpha) \text{Tr}[\mathcal{S}_\alpha[\omega]]. \quad (4.11)$$

Note that the forced-driven CGF is not a function of the difference of the counting fields. The functional form for  $\mathcal{M}_\alpha$  is the same as before *i.e.*,

$$\mathcal{M}_\alpha(\omega; \xi_\alpha) = (e^{i\xi_\alpha\hbar\omega} - 1)f_\alpha + (e^{-i\xi_\alpha\hbar\omega} - 1)(1 + f_\alpha) \quad \alpha = L, R \quad (4.12)$$

We now see that this CGF is invariant under the transformation  $\xi_\alpha = -\xi_\alpha - i\beta_\alpha$   $\alpha = L, R$  *i.e.*,  $\mathcal{M}_\alpha(\xi_\alpha) = \mathcal{M}_\alpha(-\xi_\alpha - i\beta_\alpha)$  and  $\mathcal{N}(\xi_L - \xi_R) = \mathcal{N}(-(\xi_L - \xi_R) + i(\beta_R - \beta_L))$ . (we omitted the  $\omega$  argument for simplicity) Therefore in the long time limit the work-induced entropy production satisfies  $\mathcal{Z}^d(-i\beta_L, -i\beta_R) = 1$  or equivalently  $\langle e^{\beta_L Q_L^d + \beta_R Q_R^d} \rangle = 1$ .

### First two cumulants

Let us now give explicit expressions for the first and second cumulant of forced-driven heat flowing out of the left lead by taking derivatives of  $\ln \mathcal{Z}^d(\xi_L)$  with respect to the counting field  $\xi_L$  and evaluating at  $\xi_L = 0$ .

The first cumulant, same as the first moment, is given as [18]

$$\langle \mathcal{I}_L^d \rangle \equiv \frac{\langle \langle Q_L^d \rangle \rangle}{t_M} \equiv \frac{1}{t_M} \left. \frac{\partial \ln \mathcal{Z}^d(\xi_L)}{\partial (i\xi_L)} \right|_{\xi_L=0} = - \int \frac{d\omega}{4\pi} \omega \text{Tr}[\mathcal{S}_L[\omega]]. \quad (4.13)$$

Note that since  $\omega \mathcal{S}_L[\omega]$  is positive the energy current always goes into the lead. Therefore the average rate of work done is positive which is consistent with the second law of thermodynamics. Also the current is independent of temperature and the expression is same in classical and quantum case.

The second and similarly the higher order cumulants however depend on temperature of the baths. For example, the second cumulant reads

$$\frac{\langle \langle (Q_L^d)^2 \rangle \rangle}{t_M} = \int \frac{d\omega}{4\pi\hbar} (\hbar\omega)^2 \text{Tr}[\mathcal{S}_L[\omega]] \left[ (1 + 2f_L) - 2 \text{Tr}[\mathcal{T}(\omega)](f_L - f_R) \right]. \quad (4.14)$$

Similarly all higher order cumulants can be obtained from the CGF. Therefore we can conclude that the distribution  $P(Q_d)$  is non-Gaussian.

## 4.2 Classical limit of $\ln \mathcal{Z}^d(\xi_L, \xi_R)$

Let us now get the classical limit ( $\hbar \rightarrow 0$ ) for the generalized CGF  $\ln \mathcal{Z}^d(\xi_L, \xi_R)$  using Eq. (4.11). Following above relations the function  $\mathcal{M}_\alpha(\xi_\alpha)$  in the limit  $\hbar \rightarrow 0$  reduces to

$$\mathcal{M}_\alpha^{\text{cls}}(\omega, \xi_\alpha) = -\hbar\omega \left( i\xi_\alpha + \frac{\xi_\alpha^2}{\beta_\alpha} \right). \quad (4.15)$$

The transmission matrices  $\mathcal{S}_L[\omega]$  and  $\mathcal{S}_R[\omega]$  remain the same as they are independent of  $\hbar$ . So in the classical limit  $\ln \mathcal{Z}^d(\xi_L, \xi_R)$  reduces to

$$\ln \mathcal{Z}_{\text{cls}}^d(\xi_L, \xi_R) = -t_M \int \frac{d\omega}{4\pi} \frac{\omega}{\mathcal{N}_{\text{cls}}(\xi_L - \xi_R)} \sum_{\alpha=L,R} \left( i\xi_\alpha + \frac{\xi_\alpha^2}{\beta_\alpha} \right) \text{Tr}[\mathcal{S}_\alpha[\omega]], \quad (4.16)$$

where  $\mathcal{N}_{\text{cls}}(\omega; \xi_L) = \det \left[ I - \mathcal{T}[\omega] \frac{i\xi_L}{\beta_L \beta_R} (i\xi_L + (\beta_R - \beta_L)) \right]$ . This classical limit is also invariant with respect to  $\xi_\alpha = -\xi_\alpha - i\beta_\alpha$ ,  $\alpha = L, R$  and therefore satisfy the fluctuation theorem.

From now on we will consider a specific form of the force given as  $f(t) = f_0 e^{-i\omega_0 t} + c.c$  where  $f_0$  is a column vector with complex amplitude and  $\omega_0$  is the driven frequency. Here *c.c* means the complex conjugate. Then we have

$$F[\omega] = 2\pi [\delta(\omega - \omega_0) + \delta(\omega + \omega_0)] f_0 f_0^\dagger. \quad (4.17)$$

Because of the presence of delta function, the integrand in (4.11) picked the value at the driving frequency  $\omega_0$ . Therefore the CGF reads

$$\ln \mathcal{Z}^d(\xi_L, \xi_R) = \frac{t_M}{\hbar \mathcal{N}(\omega_0; \xi_L - \xi_R)} \sum_{\alpha=L,R} \mathcal{M}_\alpha(\omega_0, \xi_\alpha) \text{Tr}[\mathcal{S}_\alpha[\omega_0]], \quad (4.18)$$

where we use the property that  $\mathcal{M}_\alpha(\omega, \xi_\alpha)$  ( $\mathcal{K}_\alpha(\omega, \xi_\alpha)$ ) is an odd (even) function of  $\omega$ . In the later part we will use this CGF and derive an explicit expression for an one-dimensional harmonic junction connected with Rubin and Ohmic heat baths.

---

### 4.3 The expression for transient current under driven force

In this section, starting from the basic definition of the current operator, we derive an alternative expression for the transient current flowing out of the left lead in the presence of driving force. The current is simply expressed in terms of the average displacement of the center atoms and the self-energy of the left lead. The main quantity to calculate here is the one and two point correlation functions involving  $u_C$  operators. By knowing these correlations it is possible to obtain the moments or the cumulants for Jarzynski's work as well as for mechanical work [13].

Let us once again write down the expression for the transient current for arbitrary junction part (see Eq. (2.83))

$$\langle \mathcal{I}_L(t) \rangle = \frac{i\hbar}{2} \int_{t_0}^t dt'' \frac{\partial}{\partial t'} \text{Tr} \left[ G_{CC}^r(t, t'') \Sigma_L^K(t'' - t') + G_{CC}^K(t, t'') \Sigma_L^a(t'' - t') \right]_{t'=t}. \quad (4.19)$$

The important point to note is that here  $G_{CC}(t, t')$  does not have time-translational invariance because of the presence of time-dependent force whereas the self-energy  $\Sigma_L$  obeys this property as it is calculated at equilibrium. Our main task now is to calculate the center Green's function.

#### One-point Green's function for the center

Let us first consider the one-point contour-ordered Green's function for the center which is defined as

$$G_j^C(\tau) = -\frac{i}{\hbar} \langle T_C u_j^C(\tau) \rangle, \quad (4.20)$$

where  $T_C$  is the contour-ordering operator. For one-point Green's function this

operator does not play any role.  $u_i^C(\tau)$  is the operator in the Heisenberg picture evolving with the full  $\mathcal{H}(t)$  given in Eq. (3.6) with  $\mathcal{H}_n = 0$  ( $V^{LC}$  and  $V^{RC}$  are considered to be time independent here). Note that the starting time  $t_0$  is chosen arbitrary. Transforming to the interaction picture with respect to the Hamiltonian  $\mathcal{H}'_0 = \mathcal{H}_L + \mathcal{H}_R + \mathcal{H}_C + \mathcal{H}_{LC} + \mathcal{H}_{RC}$  and taking the interaction Hamiltonian as  $\mathcal{V}(t) = -\theta(t - t_0)f^T(t)u^C$  we can write the contour ordered Green's function as

$$G_j^C(\tau) = -\frac{i}{\hbar} \left\langle T_C \hat{u}_j^C(\tau) e^{\sum_k \frac{i}{\hbar} \int d\tau' f_k(\tau') \hat{u}_k(\tau')} \right\rangle_{G_0}, \quad (4.21)$$

(The symbol caret is used to denote that the operators are in the interaction picture with respect to the Hamiltonian  $\mathcal{H}'_0$ ) Here  $G_0$  is the Green's function calculated with the Hamiltonian  $\mathcal{H}'_0$  *i.e.*, in the presence of the leads. Now if we expand the exponential function, the terms with odd numbers of  $u^C$  will be zero since the average is with respect to a quadratic Hamiltonian. So the expression will contain terms with even number of  $u^C(\tau)$  and odd number of  $f(\tau)$  and finally can be written in the matrix form as

$$G^C(\tau) = \frac{i}{\hbar} \int d\tau' G_0(\tau, \tau') f(\tau') + \text{higher order terms}, \quad (4.22)$$

(For notational simplicity we have omitted the superscript  $CC$  on the two-point Green's function of center). In Fig. (4.1) we draw Feynman diagrams for  $G_i^C(\tau)$  up to third order of force. The contribution from the first diagram is nonzero. But the next and all the higher order terms contain the same type of vacuum diagrams which are zero. Vacuum diagram is defined as a diagram where all variables are integrated and the result is independent of space or time. The

$$\bigcirc_{i, \tau}^{\underline{\quad}} = \frac{F_j(\tau')}{i, \tau \quad j, \tau'} + \frac{F_j(\tau') \quad F_l(\tau'') \quad F_m(\tau''')}{i, \tau \quad j, \tau' \quad l, \tau'' \quad m, \tau'''} + \text{higher order terms}$$

Figure 4.1: The Feynman diagram for one-point Green's function of the center in the presence of time-dependent force.

expression for such a diagram in terms of contour variable can be written as

$$\begin{aligned} & \int \int d\tau d\tau' f^T(\tau) G_0^{CC}(\tau, \tau') f(\tau') \\ &= \sum_{\sigma, \sigma'} \int \int \sigma dt \sigma' dt' f^\sigma(t)^T G_0^{\sigma, \sigma'}(t, t') f^{\sigma'}(t'). \end{aligned} \quad (4.23)$$

The last line is obtained by going to the real time using Langreth's rule. Since the driven force  $f$  does not depend on the branch index  $f^+(t) = f^-(t) = f(t)$ , we can take the summation inside and obtain [19]

$$\sum_{\sigma, \sigma'} \sigma \sigma' G_0^{\sigma, \sigma'} = G_0^t + G_0^{\bar{t}} - G_0^< - G_0^> = 0. \quad (4.24)$$

It can be easily shown that all higher order terms in this series contain such vacuum diagrams and hence do not contribute to the one-point Green's function. So the exact expression for  $\langle u_C(\tau) \rangle$  is now given by

$$\langle u_C(\tau) \rangle = - \int d\tau' G_0(\tau, \tau') f(\tau'). \quad (4.25)$$

From this expression it is also clear that  $\langle u_C(\tau) \rangle$  does not depend on the branch index *i.e.*,  $\langle u_C^+(t) \rangle = \langle u_C^-(t) \rangle$ . So in real time we obtain

$$\langle u_C(t) \rangle = - \int_{t_0}^t dt' G_0^r(t - t') f(t'). \quad (4.26)$$

where  $G_0^r$  is the retarded Green's function and also known as the response function in the linear response theory. In fact, the same result, Eq. (4.26), can also be derived from the standard linear response theory.

### Two-point Green's functions for the center

Similarly the two-point Green's function in the interaction picture is also calculated and is given as

$$G_{jk}(\tau, \tau') = -\frac{i}{\hbar} \langle T_C \hat{u}_j^C(\tau) \hat{u}_k^C(\tau') e^{\sum_m \frac{i}{\hbar} \int d\tau'' f_m(\tau'') \hat{u}_m(\tau'')} \rangle_{G_0}. \quad (4.27)$$

As discussed above we can expand the exponential and the terms greater than  $\mathcal{O}(f^2)$  vanishes as they contain vacuum diagrams. The exact expression can be written as

$$G_{jk}(\tau, \tau') = G_{0,jk}(\tau, \tau') - \frac{i}{\hbar} \sum_{ms} \int d\tau_1 d\tau_2 G_{0,jm}(\tau, \tau_1) G_{0,ks}(\tau', \tau_2) f_m(\tau_1) f_s(\tau_2). \quad (4.28)$$

In terms of  $\langle u_C(\tau) \rangle$ , the center Green's function now become

$$G(\tau, \tau') = G_0(\tau, \tau') - \frac{i}{\hbar} \langle u_C(\tau) \rangle \langle u_C(\tau') \rangle^T. \quad (4.29)$$

From the above equation we can write  $G = G_0 + \delta G$  with  $\delta G = -\frac{i}{\hbar} \langle u_C(\tau) \rangle \langle u_C(\tau') \rangle^T$ .

Now using the property of  $\langle u_C(\tau) \rangle$  we can write

$$\delta G^{++} = \delta G^{+-} = \delta G^{-+} = \delta G^{--} \quad (4.30)$$

which implies that  $\delta G^r = \delta G^a = 0$  and  $\delta G^< = \delta G^> = \delta \bar{G} = -\frac{i}{\hbar} \langle u_C(t) \rangle \langle u_C(t') \rangle^T$ .

So using Eq. (4.19) the expression for the current reduces to

$$\begin{aligned}
 \langle \mathcal{I}_L(t) \rangle &= i\hbar \frac{\partial}{\partial t'} \int_{t_0}^t dt'' \text{Tr} \left[ \bar{\Sigma}_L(t' - t'') G_0^a(t'', t) + \Sigma_L^r(t' - t'') \bar{G}_0(t'', t) \right]_{t'=t} \\
 &+ \int_{t_0}^t dt'' \text{Tr} \left[ \langle u_C(t) \rangle \langle u_C(t'') \rangle^T \frac{\partial}{\partial t'} \Sigma_L^a(t'' - t') \right]_{t'=t} \\
 &= \langle \mathcal{I}_L^s(t) \rangle + \langle \mathcal{I}_L^d(t) \rangle.
 \end{aligned} \tag{4.31}$$

By writing  $\langle \mathcal{I}_L(t) \rangle$  in this form it is clear that the contribution to the energy current is separated into two parts.  $\langle \mathcal{I}_L^d(t) \rangle$  is the current due to driven force and  $\langle \mathcal{I}_L^s(t) \rangle$  is due to the temperature difference between the heat baths. This separation is possible because the system is linear and the driving force is not correlated with the heat baths. In the long time limit i.e,  $t \rightarrow \infty$ ,  $\langle \mathcal{I}_L^s(t) \rangle$  is the steady-state heat flux and is given by the Landauer like formula [19]

$$\langle \mathcal{I}_L^s \rangle = \frac{1}{4\pi} \int_{-\infty}^{\infty} d\omega \hbar \omega \text{Tr} [\mathcal{T}[\omega]] (f_L - f_R). \tag{4.32}$$

If we consider the two heat baths at the same temperature, *i.e.*,  $\Delta T = T_L - T_R = 0$ , then  $\langle \mathcal{I}_L^s \rangle$  is zero. So in the linear case the final expression for current with  $\Delta T = 0$  is

$$\langle \mathcal{I}_L^d(t) \rangle = \int_{t_0}^t dt'' \text{Tr} \left[ \langle u_C(t) \rangle \langle u_C(t'') \rangle^T \frac{\partial}{\partial t'} \Sigma_L^a(t'', t') \right]_{t'=t}, \tag{4.33}$$

where  $\Sigma_L^a(t'' - t') = 0$  if  $t'' - t' \geq 0$ . This equation can be used to calculate the current both in transient as well as in the steady state with arbitrary form of force. This expression is valid for systems connected with finite heat baths and in higher dimensions.

### Current due to periodic driven force

We consider the form of force given by  $f(t) = f_0 e^{-i\omega_0 t} + c.c$  where  $f_0$  is a column vector with complex amplitude and  $\omega_0$  is the driven frequency. Then from Eq. (4.26)  $\langle u_C(t) \rangle$  can be written as

$$\langle u_C(t) \rangle = G_0^r[\omega_0] f_0 e^{-i\omega_0 t} + c.c. \quad (4.34)$$

where  $G_0^r[\omega_0]$  is given by

$$G_0^r[\omega_0] = \left[ (\omega_0 + i\eta)^2 I - K_C - \Sigma_L^r[\omega_0] - \Sigma_R^r[\omega_0] \right]^{-1}, \quad (4.35)$$

with  $\eta \rightarrow 0^+$  and  $I$  is the identity matrix. We set  $t_0 \rightarrow -\infty$  for steady state oscillation and finally average over a time period  $\bar{\mathcal{I}}_L^d = \frac{1}{\tau} \int_0^\tau \langle \mathcal{I}_L^d(t) \rangle dt$  where  $\tau = 2\pi/\omega_0$  is the time period of the driving field, we finally get from Eq. (4.33),

$$\bar{\mathcal{I}}_L^d = -\omega_0 \mathcal{S}_L[\omega_0], \quad (4.36)$$

$$\mathcal{S}_L[\omega_0] = G_0^r[\omega_0] \Gamma_L[\omega_0] G_0^a[\omega_0] f_0 f_0^\dagger, \quad (4.37)$$

where  $\Gamma_L[\omega_0] = i[\Sigma_L^r[\omega_0] - \Sigma_L^a[\omega_0]]$  is the spectral function for the left lead. For this particular case the same result can also be obtained using linear response theory. This result matches with the one obtained using CGF in Eq. (4.18). We can write the expression for current in another form by using the following relation between  $G_0^r$  and  $G_0^a$ , obtained from Eq. (4.35),

$$G_0^r[\omega_0] - G_0^a[\omega_0] = -i G_0^r[\omega_0] (\Gamma_L[\omega_0] + \Gamma_R[\omega_0]) G_0^a[\omega_0], \quad (4.38)$$

then we can write

$$\bar{\mathcal{I}}_L^d = -\bar{\mathcal{I}}_C^d - \bar{\mathcal{I}}_R^d, \quad (4.39)$$

which is a consequence of energy conservation. Here  $\bar{\mathcal{I}}_C^d = i\omega_0 \text{Tr}[(G_0^r[\omega_0] - G_0^a[\omega_0])f_0 f_0^\dagger]$  which is simply related with the density of states of the center.

We also like to point out that using the solutions for one and two point Green's functions the moments (cumulants) for Jarzynski's work  $W_J = -\int_{t_0}^t \dot{f}^T(t')u_C(t')dt'$  and also for the mechanical work  $W = \int_{t_0}^t f^T(t')u_C(t')dt'$  can be obtained. In the classical case since  $P(W)$  is Gaussian, the JE can be easily checked by verifying the relation  $\langle\langle W_J^2 \rangle\rangle = \frac{2}{\beta}[\langle W_J \rangle - \Delta F]$  where  $\beta$  is the inverse of the equilibrium temperature and  $\Delta F$  is the free energy change.

---

### 4.3.1 Application to 1D chain

In this subsection we study energy transport properties for 1D chain connected with different type of heat baths such as Rubin or Ohmic.

#### Rubin bath

Here we consider a 1D chain with inter-particle spring constant  $k$ . We divide the full infinite system into three parts, the center, the left and the right lead. We want to study the energy current contribution only due to the driven force and hence kept the leads at the same temperature with the center. Then we drive the center with the force  $f(t)$  and evaluate the forced-driven transmission function  $\mathcal{S}_\alpha[\omega]$ .

The classical equation of motion for the center atoms is given by

$$\ddot{u}_j = k(u_{j-1} - 2u_j + u_{j+1}) + f_j(t), \quad 1 \leq j \leq N_C, \quad (4.40)$$

where  $N_C$  is the number of particles in the center. The leads obey similar equations with  $f_j(t) = 0$ . Here we will consider the force  $f_j(t) = f_0^j e^{-i\omega_0 t} + c.c.$  where  $f_0^j = (-1)^j f_0$  which mimic the structure of a crystal having alternate charges at the sites.

### Solution for $G_0^r[\omega_0]$ for pure harmonic chain

To obtain an explicit expression for the transmission function we need to solve the equilibrium Green's function  $G_0^r[\omega_0]$  given in Eq. (4.35). Since the full system is homogeneous the retarded Green's function can be obtained by solving [20]  $[(\omega_0 + i\eta)^2 - K]G_0^r[\omega] = I$ , where  $K$  is the force constant matrix for the full linear system and is infinite in both directions with  $2k$  along the diagonals and  $-k$  on the first off-diagonals. The solution for the Green's function is translationally invariant in space index and is given as (see appendix (E))

$$G_{0,jk}^r[\omega_0] = \frac{\lambda^{|j-k|}}{k(\lambda - \frac{1}{\lambda})}, \quad (4.41)$$

with

$$\lambda = -\frac{\Omega}{2k} \pm \frac{1}{2k} \sqrt{\Omega^2 - 4k^2} \equiv e^{\pm iq}, \quad (4.42)$$

$$\Omega = (\omega_0 + i\eta)^2 - 2k = -2k \cos q. \quad (4.43)$$

The last equation is the phonon dispersion relation for one-dimensional harmonic chain with nearest-neighbor interaction. Here  $q$  is the phonon wave

vector. The choice between plus and minus sign is made by the condition  $|\lambda| \leq 1$ . Because of the nearest-neighbor interaction the surface Green's function for Rubin bath in frequency space is given by (see appendix (E))

$$\begin{aligned} (\Sigma_L^r)_{jk}[\omega_0] &= -k\lambda\delta_{jk}\delta_{j1}, \\ (\Sigma_R^r)_{jk}[\omega_0] &= -k\lambda\delta_{jk}\delta_{jN_C}. \end{aligned} \quad (4.44)$$

It is clear from the expression of  $\lambda$  that it is complex within the phonon bandwidth *i.e.*,  $0 \leq \omega_0 \leq 2\sqrt{k}$  and is real outside this range. Therefore the spectral function  $\Gamma_L$  is zero outside the phonon band.

### Calculation for $\text{Tr}[\mathcal{S}_L[\omega]]$

Knowing all the Green's functions we can now calculate the transmission function for the driven part  $\text{Tr}[\mathcal{S}_L[\omega]]$  considering the force  $f_j(t) = (-1)^j f_0 e^{-i\omega_0 t} + c.c.$ . We can write

$$\begin{aligned} \text{Tr}[\mathcal{S}_L[\omega_0]] &= \text{Tr}[G_0^r[\omega_0]\Gamma_L[\omega_0]G_0^a[\omega_0]f_0f_0^\dagger] \\ &= \sum_{ijkl} (-1)^{i+j} G_{0,i1}^r(\Gamma_L)_{11} G_{0,1j}^a |f_0|^2 \\ &= \begin{cases} 2|f_0|^2 k \text{Im}\lambda \left( \sum_i (-1)^i G_{0,i1}^r \right) \left( \sum_j (-1)^j G_{0,1j}^a \right), & 0 \leq \omega_0 \leq 2\sqrt{k} \\ 0 & \text{for } \omega_0 \geq 2\sqrt{k} \end{cases} \end{aligned}$$

Using the solution for  $G_0^r[\omega_0]$  in Eq. (4.41) and  $G_0^a[\omega] = (G_0^r[\omega])^\dagger$  we obtain

$$\text{Tr}[\mathcal{S}_L[\omega_0]] = \begin{cases} \frac{|f_0|^2}{2k \sin q} \left[ \frac{1 - (-1)^{N_C} \cos(N_C q)}{1 + \cos q} \right] & \text{for } 0 \leq \omega_0 \leq 2\sqrt{k} \\ 0 & \text{for } \omega_0 \geq 2\sqrt{k} \end{cases}$$

Similarly  $\mathcal{S}_R[\omega]$  can also be calculated and in this case it is same as  $\mathcal{S}_L[\omega]$  because of the translational invariance of the full system. Therefore one parameter CGF is written as

$$\ln \mathcal{Z}^d(\xi_L) = \begin{cases} \frac{t_M \mathcal{M}_L(\omega_0; \xi_L)}{\hbar \mathcal{N}(\omega_0; \xi_L)} \frac{|f_0|^2}{2k \sin q} \left[ \frac{1 - (-1)^{N_C} \cos(N_C q)}{1 + \cos q} \right] & \text{for } 0 \leq \omega_0 \leq 2\sqrt{k} \\ 0 & \text{for } \omega_0 \geq 2\sqrt{k}, \end{cases}$$

with  $\mathcal{N}(\omega; \xi_L) = \det[1 - \mathcal{K}(\omega; \xi_L)]$  as  $\text{Tr}[\mathcal{T}[\omega]] = \text{Tr}[G_0^r[\omega] \Gamma_L[\omega] G_0^a[\omega] \Gamma_R[\omega]] = 1$  (within the phonon band otherwise it is zero) for homogeneous system.

## 4.4 Behavior of energy-current

### Rubin bath:

The expression for current can be easily obtained from the CGF and is given as

$$\bar{\mathcal{I}}_L^d = \begin{cases} -\frac{\omega_0 |f_0|^2}{2k} \frac{(1 - (-1)^{N_C} \cos(N_C q))}{\sin q (1 + \cos q)}, & \text{for } 0 \leq \omega_0 \leq 2\sqrt{k}, \\ 0, & \text{for } \omega_0 \geq 2\sqrt{k}. \end{cases} \quad (4.45)$$

Here  $\bar{\mathcal{I}}_L^d$  is of order 1 and  $q$  is given by the dispersion relation  $\omega_0^2 = 2k(1 - \cos q)$ .

In Fig. 4.2 and 4.3, we plot energy current as a function of applied frequency for different system size. The value of force constant is chosen as  $k = 1$  eV/(uÅ<sup>2</sup>) and  $f_0 = 1$  nN in all our calculation. In Fig. 4.3, the current

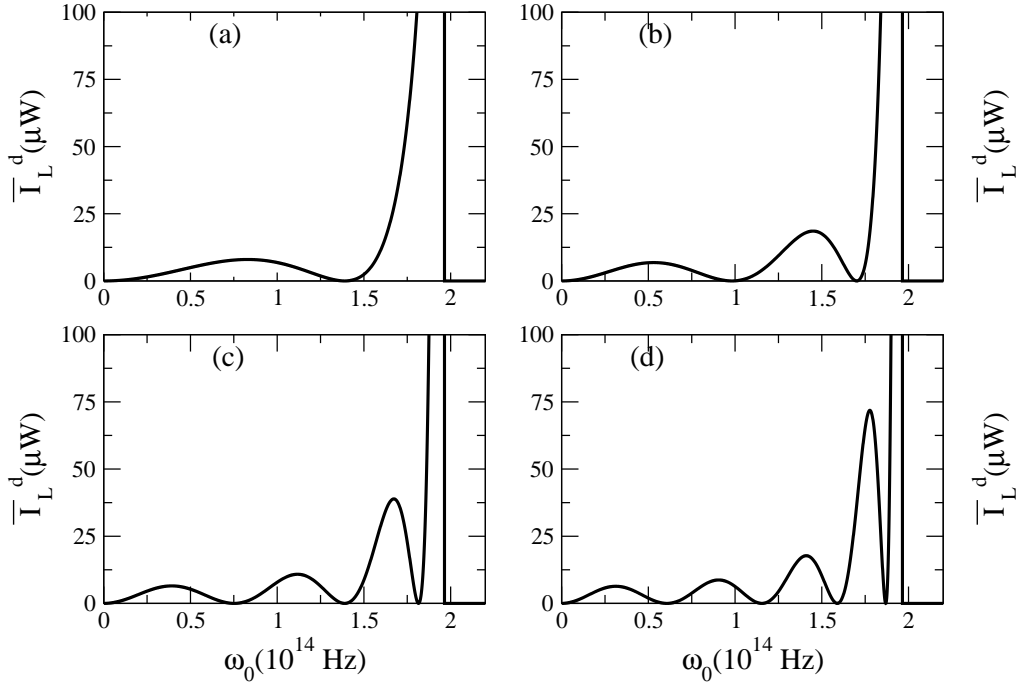


Figure 4.2: Energy current  $\bar{I}_L^d$  as a function applied frequency for different system size of one-dimensional chain with force  $f_j(t) = (-1)^j f_0 e^{-i\omega_0 t} + c.c.$  (a)  $N_C=4$ , (b)  $N_C=6$ , (c)  $N_C=8$ , (d)  $N_C=10$ .  $k=1$  eV/( $\text{\AA}^2$ ).

is nonzero at zero frequency because the system as a whole is not charge neutral. For  $N_C = 1$  the current  $\bar{I}_L^d$  is proportional to the density of states (DOS).

More importantly the current is exactly zero when the applied frequency matches with the normal mode frequency of the system and the corresponding wave number is given by for even  $N_C$ ,  $q = 2\pi n/N_C$  and for odd  $N_C$ ,  $q = (2n + 1)\pi/N_C$  with  $n = 0, 1, \dots, N_C - 1$ . Therefore the number of resonance peaks and number of zero's depends on the eigenfrequencies and hence on the size of the center system. The average current diverges

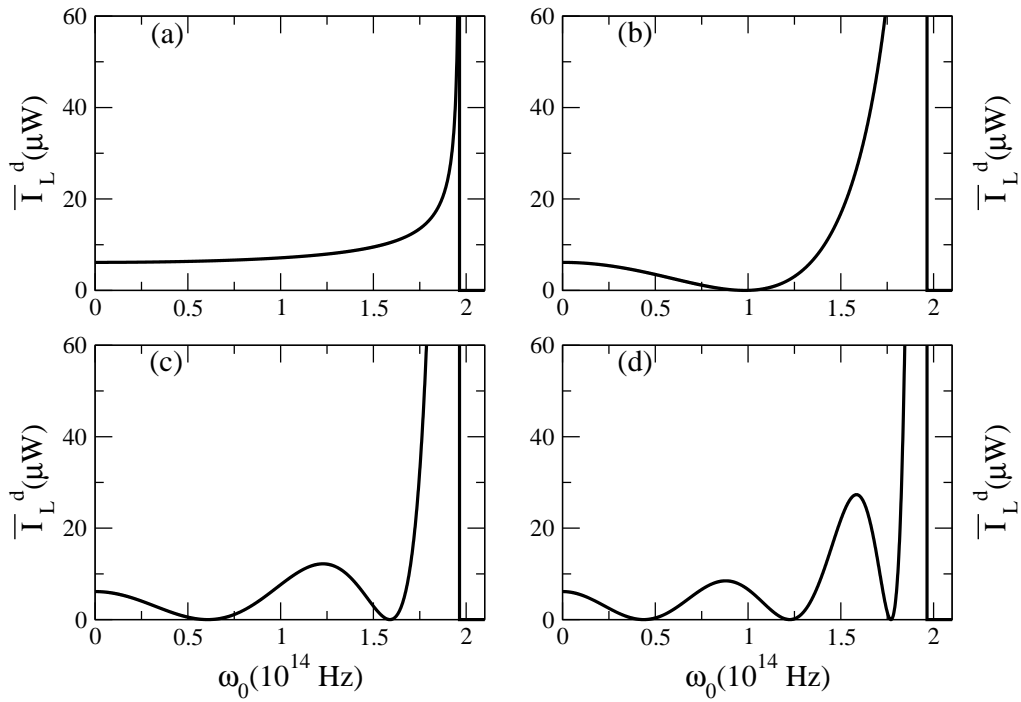


Figure 4.3: Energy current  $|\bar{I}_L^d|$  as a function applied frequency for different system sizes of one-dimensional linear chain with force  $f_j(t) = (-1)^j f_o e^{-i\omega_0 t} + c.c.$  (a)  $N_C=1$ , (b)  $N_C=3$ , (c)  $N_C=5$ , (d)  $N_C=7$ .  $k=1$  eV/(uÅ<sup>2</sup>).

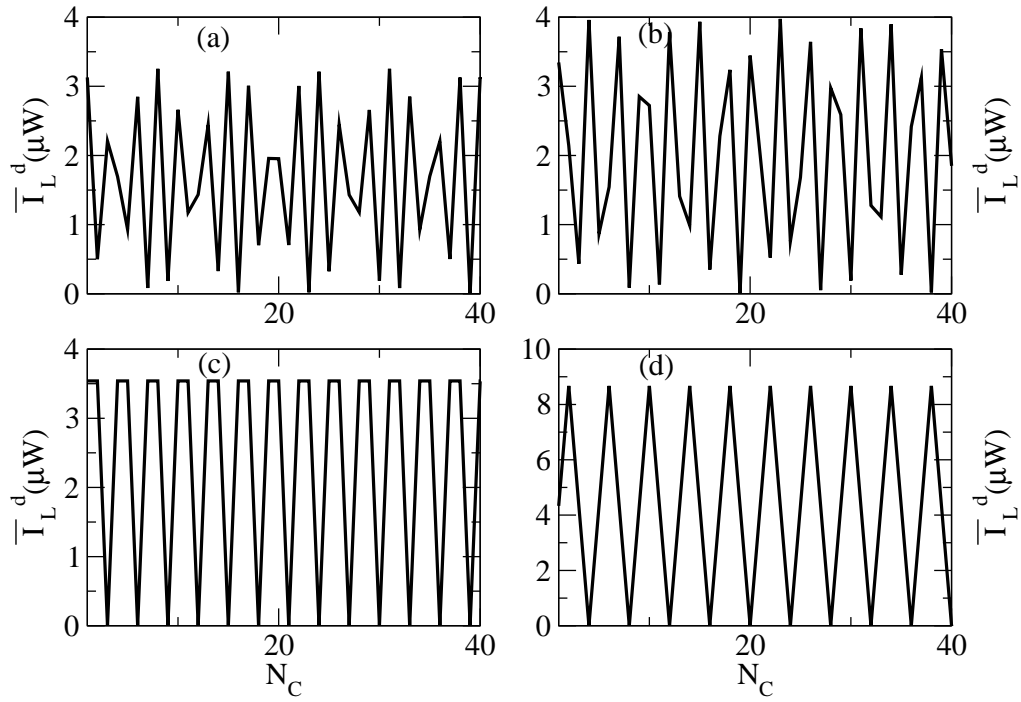


Figure 4.4: Energy current  $|\bar{\mathcal{I}}_L^d|$  versus length of the center for different applied frequencies for one-dimensional linear chain. Here (a)  $\omega_0=0.39$ , (b)  $\omega_0=0.78$ , (c)  $\omega_0=0.98$ , (d)  $\omega_0=1.40$ . The frequencies are given in  $10^{14}$ (Hz) unit. The other parameters same as in Fig. 4.3.

at  $\omega_0 = 2\sqrt{k}$  as the DOS of the full system diverges at the maximum frequency of the whole system. For  $\omega_0 \geq 2\sqrt{k}$  the system does not allow energy to pass through. Similarly one can calculate the right lead current  $\bar{\mathcal{I}}_R^d$  and the expression is the same with Eq. (4.45). Since we apply force on all the atoms of the center by symmetry argument we can say that the total input current  $\bar{\mathcal{I}}_C^d$  divides into two equal parts and goes into the leads *i.e.*,  $|\bar{\mathcal{I}}_L^d| = |\bar{\mathcal{I}}_R^d| = |\bar{\mathcal{I}}_C^d|/2$ .

In Fig. 4.4, we give results for energy current as a function of total number of particles in the center for different values of external frequency. For finite systems the current oscillates with system size and depending on the values of  $\omega_0$  it shows periodicity with respect to  $N_C$ . The maximum amplitude of the average current is fixed and is proportional to  $\omega_0 f_0^2 / 2K$ .

### Ohmic bath

Here we consider that the center part is connected with two Ohmic baths. The difference between Rubin and Ohmic bath is that, the self energy in this case is approximated as  $\Sigma^r[\omega_0] = -i\gamma\omega_0$  where  $\gamma$  is the friction coefficient. More precisely the  $\Sigma_L^r$  and  $\Sigma_R^r$  matrices are given by

$$\begin{aligned} (\Sigma_L^r)_{jk}[\omega_0] &= -i\gamma\omega_0 \delta_{jk} \delta_{j1}, \\ (\Sigma_R^r)_{jk}[\omega_0] &= -i\gamma\omega_0 \delta_{jk} \delta_{jN_C}. \end{aligned} \quad (4.46)$$

Using this form of self-energy the forced-driven transmission function is

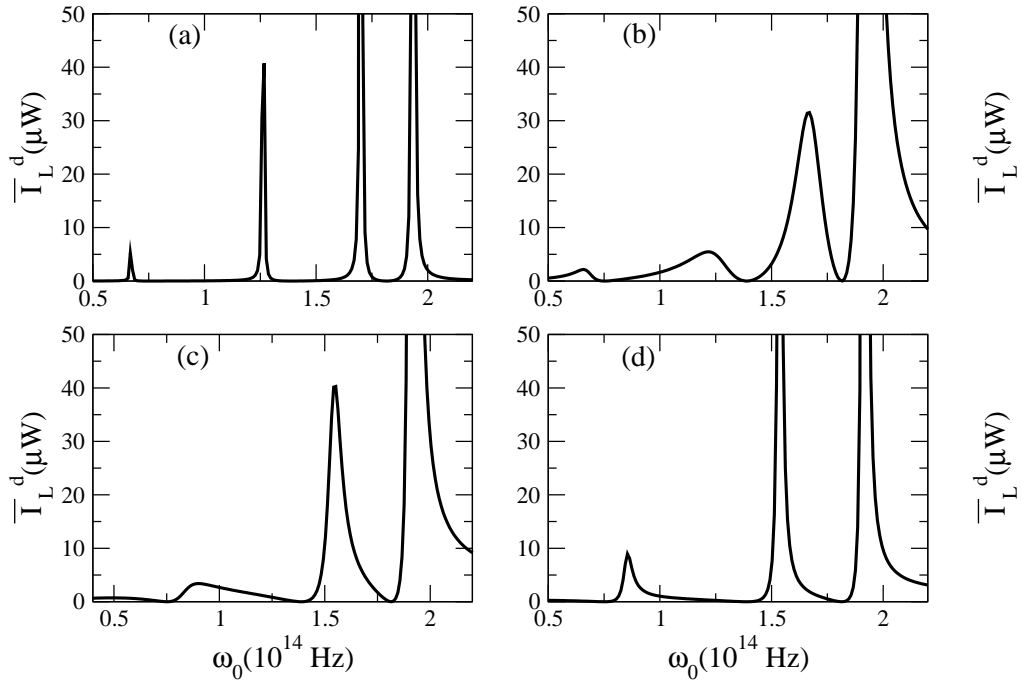


Figure 4.5: Energy current  $|\bar{I}_L^d|$  as a function applied frequency for different values of friction coefficient  $\gamma$  of one-dimensional linear chain with force  $f_j(t) = (-1)^j f_o e^{-i\omega_0 t} + c.c.$  (a)  $\gamma=0.01$ , (b)  $\gamma=0.5$ , (c)  $\gamma=3.0$ , (d)  $\gamma=5.0$ .  $k=1$  eV/(uÅ<sup>2</sup>) and  $N_C=8$ .

given as

$$\begin{aligned}\mathrm{Tr}[\mathcal{S}_L[\omega_0]] &= 2\gamma\omega_0|f_0|^2|g[\omega_0]|^2 \\ g[\omega_0] &= \sum_{j=1}^{N_C}(-1)^j G_{1j}^r[\omega_0]\end{aligned}\quad (4.47)$$

Therefore the CGF for this case is written as

$$\ln \mathcal{Z}^d(\xi_L) = \frac{t_M \mathcal{M}_L(\omega_0; \xi_L)}{\hbar \mathcal{N}(\omega_0; \xi_L)} 2\gamma\omega_0|f_0|^2|g[\omega_0]|^2 \quad (4.48)$$

As before we will focus on the first cumulant or the energy current which is given as

$$\bar{\mathcal{I}}_L^d = -2\gamma\omega_0^2 f_0^2 |g[\omega_0]|^2 \quad (4.49)$$

From the above expression it is clear that energy current depends on the denominator  $A[\omega_0] = |\det[D[\omega_0]]|^2$  where  $D[\omega_0] = (\omega_0^2 I - K^C + i\omega_0 \gamma_L + i\omega_0 \gamma_R)$  is  $N_C \times N_C$  matrix. The matrix elements are given by  $D_{ij} = \delta_{i,j}(\omega_0^2 - 2k - i\omega_0 \gamma(\delta_{i,1} + \delta_{i,N})) - k \delta_{i,j+1} - k \delta_{i,j-1}$ . If we denote  $P_{N_C}[\omega_0] = \det(\omega_0^2 - K^C)$  to be the characteristic polynomial of the matrix  $K^C$  with  $N_C$  particles then it can be shown that [1]

$$A[\omega_0] = [P_{N_C}[\omega_0] - \gamma^2 \omega_0^2 P_{N_C-2}[\omega_0]]^2 + 4\gamma^2 \omega_0^2 P_{N_C-1}^2[\omega_0], \quad (4.50)$$

where  $P_{N_C-1}[\omega_0]$  is the polynomial of the  $(N_C - 1) \times (N_C - 1)$  force constant matrix  $K^C$  with first row and column or last row and column taken out from  $K^C$  and similarly  $P_{N_C-2}[\omega_0]$  is the polynomial of the  $(N_C - 2) \times (N_C - 2)$  matrix by taking out the first and last rows and columns from

$K^C$ . The resonance and the zero's of current corresponds to the minimum and maximum value of  $A[\omega_0]$  respectively. It is difficult to obtain explicit solution in this case. However the equation become simple for small and large value of  $\gamma$ , the friction coefficient. For small friction it is clear from Eq. (4.50) that  $A[\omega_0] = P_{N_C}^2[\omega_0]$ . So the resonant frequencies depends on  $N_C$  eigenfrequencies of the force constant matrix  $K^C$ . In the opposite limit i.e, for large  $\gamma$  we obtain  $A[\omega_0] = P_{N_C-2}^2[\omega_0]$ . So depending on the value of  $\gamma$  the resonance peaks shift from  $N_C$  to  $N_C - 2$ .

In Fig. 4.5, we plot the current with applied frequency for different values of damping coefficient  $\gamma$ . The value of  $\gamma$  is chosen in proper units. The zero values of the current is same as in Rubin's case. However there is a gradual shift in the resonance peak depending on the parameter  $\gamma$ . The current doesn't diverge at  $\omega_0 = 2\sqrt{k}$  and the width of the peaks depends of  $\gamma$ . We check numerically the behavior of  $\bar{\mathcal{I}}_L^d$  with system length and we found that the behavior is similar with Rubin baths. In this case also we have  $|\bar{\mathcal{I}}_L^d| = |\bar{\mathcal{I}}_R^d| = |\bar{\mathcal{I}}_C^d|/2$ .

As mentioned before similar Ohmic model was also investigated by Marathe et. al [6] for  $N_C = 2$  where they conclude that this model cannot work either as a heat pump or as a heat engine. Our calculation agrees with their results. It is also possible to calculate current in the overdamped regime by dropping the term  $(\omega_0 + i\eta)^2$  in  $G^r[\omega_0]$  given in Eq (4.35). In this regime for  $N = 1$  our result agrees with the result obtained by Jayannavar et. al [14] for magnetic field  $B = 0$ .

**Comparison between Rubin and Ohmic bath for driving force on single site**

As we have seen that if we apply force on all the atoms of the center because of the symmetry of the problem if we interchange the left and right lead (which we assume to be the same) the value of the current should not change and hence we have the only possible solution  $|\bar{\mathcal{I}}_L^d| = |\bar{\mathcal{I}}_R^d| = |\bar{\mathcal{I}}_C^d|/2$ . But this is not the case, at least for Ohmic bath if we apply force on a single or multi-particles but not on all. If we consider the force on the  $\alpha$ th particle as  $f_i(t) = \delta_{i\alpha}(f_0^i e^{-i\omega_0 t} + c.c)$  then for the Rubin bath case using Eq. (4.36) and Eq. (4.37) we get

$$\begin{aligned}\bar{\mathcal{I}}_L^d &= -2\omega_0 k \text{Im}(\lambda) f_0^\alpha (f_0^\alpha)^* |G_{0,\alpha 1}|^2 \\ \bar{\mathcal{I}}_R^d &= -2\omega_0 k \text{Im}(\lambda) f_0^\alpha (f_0^\alpha)^* |G_{0,N\alpha}|^2\end{aligned}\quad (4.51)$$

Using the solution for  $G_0^r[\omega_0]$  given in Eq. (4.41) we obtain

$$\bar{\mathcal{I}}_L^d = \bar{\mathcal{I}}_R^d = \begin{cases} -\frac{\omega_0}{2k \sin q} f_0^\alpha (f_0^\alpha)^*, & \text{for } 0 \leq \omega_0 \leq 2\sqrt{k}, \\ 0, & \text{for } \omega_0 \geq 2\sqrt{k}. \end{cases}\quad (4.52)$$

which says that, because the full system is translationally invariant in space, the magnitude of current does not depend on which site the force is applied and hence  $|\bar{\mathcal{I}}_L^d| = |\bar{\mathcal{I}}_R^d| = |\bar{\mathcal{I}}_C^d|/2$  is the only possible solution. The result is similar with  $N_C = 1$  in Eq. (4.45).

However, this scenario is not valid for Ohmic bath. In this case the full translational symmetry is broken and hence applying force on different

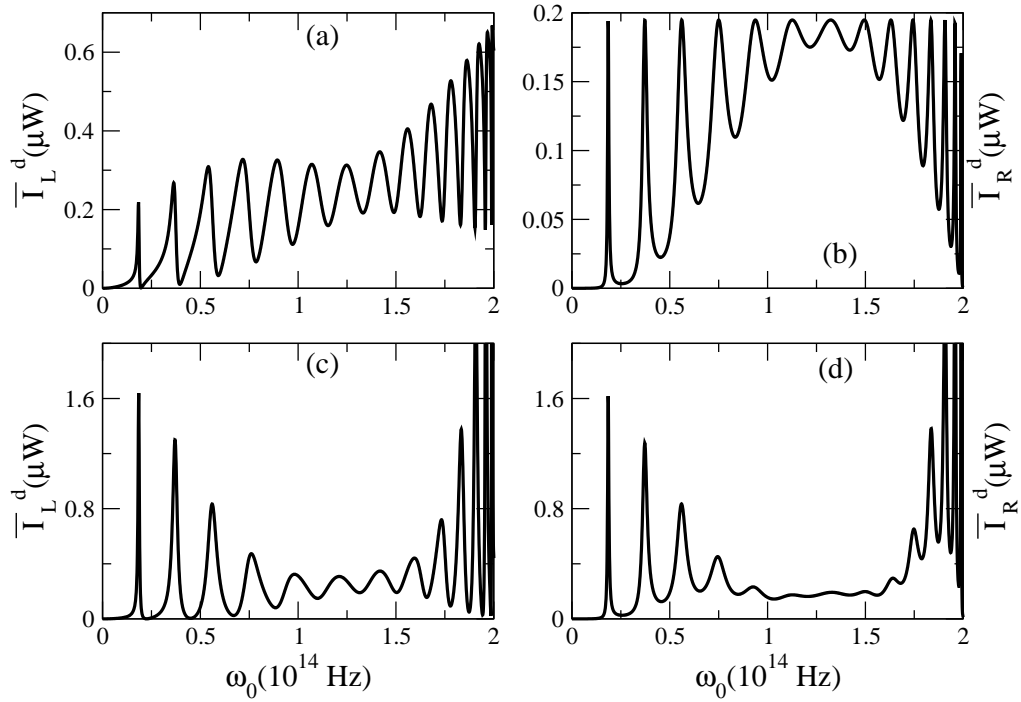


Figure 4.6: Energy current  $|\bar{\mathcal{I}}_L^d|$  and  $|\bar{\mathcal{I}}_R^d|$  as a function of applied frequency for driven force at different site of one-dimensional chain connected to Ohmic bath. (a) and (b) are for  $\alpha=1$  and (c) and (d) are for  $\alpha = 3$ ,  $N_C=16$ .  $k = 1 \text{ eV}/(\text{u}\text{\AA}^2)$ .

sites generate different magnitudes of current on left and right lead. In Fig. 4.6, we plot the heat current  $\bar{\mathcal{I}}_L^d$  and  $\bar{\mathcal{I}}_R^d$  for one-dimensional chain as a function applied driving frequency at different sites. Clearly  $\bar{\mathcal{I}}_L^d$  and  $\bar{\mathcal{I}}_R^d$  are different in magnitudes. Hence by applying force on different sites it is possible to control current in both the leads for Ohmic case.

### Heat pump

Heat pump by definition transfers heat from cooler region to hotter region. One-dimensional linear system with force applying on any number of sites fails to work as a heat pump. To understand the reasoning we look at the total current coming out of the left lead  $\bar{\mathcal{I}}_L$  which is a sum of two terms. If we assume  $T_L > T_R$  then the temperature dependent term in Eq. (4.32) gives the steady state heat is positive *i.e.*, current goes from left to right lead and the driving term which does not depend on temperature, always contribute a negative value to both  $\bar{\mathcal{I}}_L$  and  $\bar{\mathcal{I}}_R$ . Hence  $\bar{\mathcal{I}}_R$  is always negative independent of whether we apply force on one site or on all the sites. So it is not possible to transfer heat from right lead to left lead in this case.

## 4.5 Summary

In summary, for a forced-driven harmonic junction connected with two thermal baths we present an analytic expression for the driven part of the CGF in the long time limit. It is expressed in terms of force dependent transmission function. By introducing two parameter CGF we show that

the driven force induced entropy production in the leads satisfy fluctuation symmetry. Exploring the translational symmetry for one dimensional linear chain connected with Rubin heat baths we obtain an explicit expression for the CGF under periodic driven force. The effect on energy current due to two different types of heat baths is analyzed in detail. For ballistic model we found that the driven current is temperature independent and is the same in classical and quantum regime but the fluctuations are not. An alternative expression for the transient current is also derived using the basic definition for the current operator.

# Bibliography

- [1] S. Zhang, J. Ren, and B. Li, Phys. Rev. E **84**, 031122 (2011).
- [2] J. Ren and B. Li, Phys. Rev. E **81**, 021111 (2010).
- [3] N. Li, P. Hänggi, and B. Li, Europhys. Lett. **84**, 40009 (2008).
- [4] N. Li, F. Zhan, P. Hänggi, and B. Li, Phys. Rev. E **80**, 011125 (2009).
- [5] B. Q. Ai, D. He, and B. Hu, Phys. Rev. E **81**, 031124 (2010).
- [6] R. Marathe, A. M. Jayannavar, and A. Dhar, Phys. Rev. E **75**, 030103(R) (2007).
- [7] K. Saito, EPL, **83**, 50006 (2008).
- [8] T. Harada, and S. I. Sasa, Phys. Rev. E **73**, 026131 (2006).
- [9] C. Jarzynski, Phys. Rev. Lett. **78**, 2690 (1997).
- [10] C. Jarzynski, Phys. Rev. E **56**, 5018 (1997).
- [11] P. Talkner, P. S. Burada, and P. Hänggi, Phys. Rev. E **78**, 011115 (2008).

## BIBLIOGRAPHY

---

- [12] A. Dhar, Phys. Rev. E **71**, 036126 (2005).
- [13] T. Mai and A. Dhar, Phys. Rev. E **75**, 061101 (2007).
- [14] A. M. Jayannavar and M. Sahoo, Phys. Rev. E **75**, 032102 (2007).
- [15] T. Monnai, Phys. Rev. E **81**, 011129 (2010).
- [16] R. J. Rubin and W. L. Greer, J. Math. Phys. **12**, 1686 (1971).
- [17] U. Weiss, *Quantum Dissipative Systems*, 2nd edn. (World Scientific, 1999).
- [18] B. K. Agarwalla, J.-S. Wang, and B. Li, Phys. Rev. E **84**, 041115 (2011).
- [19] J.-S. Wang, J. Wang, and J. T. Lü, Eur. Phys. J. B, **62**, 381 (2008).
- [20] J.-S. Wang, N. Zeng, J. Wang, and C. K. Gan, Phys. Rev. E **75**, 061128 (2007).

## Chapter 5

# Heat exchange between multi-terminal harmonic systems and exchange fluctuation theorem (XFT)

In this chapter, we generalize the FCS study for transferred heat and entropy-production for multi-terminal systems without the presence of a finite junction (see Fig. (5.1)). Such a setup is important from the point of view of verifying exchange fluctuation theorem (XFT), mentioned in the introduction chapter. Also for two-terminal case without junction this reduces to an interface problem which is relevant for many experimental

studies [1–4]. For this general setup we obtain the expression for the generalized cumulant generating function (CGF), on the contour, involving counting fields for heat, flowing out from all the terminals. We discuss both transient and steady-state fluctuation theorems for heat and entropy production. For two-terminal case, we obtain a new transmission function which is similar to the Caroli formula involving the junction part. We also address the effect of coupling strength on the XFT. Finally we discuss the effect of finite heat baths on the cumulants of heat.

Using principle of micro-reversibility of the underlying Hamiltonian dynamics, Jarzynski and Wójcik [5] first showed the identity  $\langle e^{-\Delta\beta Q_L} \rangle_{t_M} = 1$  for two weakly connected systems  $L$  and  $R$ . Here  $\Delta\beta = \beta_R - \beta_L$ ,  $\beta_\alpha = 1/(k_B T_\alpha)$  and  $Q_L$  is the amount of heat transferred from the left system over the time interval  $[0, t_M]$ . A more generalized version of this XFT for multi-terminal system was later derived by Saito and Utsumi [6] and Andrieux et al [7–9] which states that  $\langle e^{-\Sigma} \rangle_{t_M} = 1$ , where  $\Sigma = -\sum_{\alpha=1}^r \beta_\alpha Q_\alpha$  is the total entropy-production and  $r$  is the number of reservoirs. This relation is valid for arbitrary time-dependent coupling between the systems (see the proof in section 1.3) and reduces to Jarzynski and Wójcik relation for  $r = 2$  in the limit of weak coupling. Recently an experimental verification of the XFT's is reported for electrons [10]. For phonons nanoresonator seems to be a potential candidate for performing such FCS experiments.

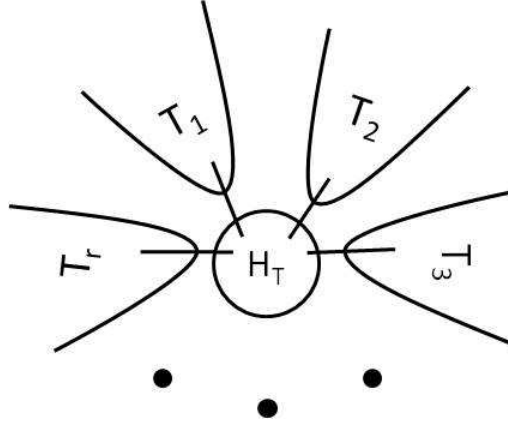


Figure 5.1: A schematic representation for exchange fluctuation theorem setup consists of multi-terminals without a junction. The terminals are at their respective equilibrium temperatures  $T_\alpha = (k_B\beta_\alpha)^{-1}$ . The reservoirs are interacting via the Hamiltonian  $\mathcal{H}_T(t)$  which is switched on at  $t = 0$ .

## 5.1 Model Hamiltonian

We consider  $r$  phonon reservoirs each consists of finite number of coupled harmonic oscillators and is given by the Hamiltonian

$$\mathcal{H}_\alpha = \sum_{i=1}^{N_\alpha} \frac{(p_i^\alpha)^2}{2} + \sum_{i,j=1}^{N_\alpha} \frac{1}{2} K_{ij}^\alpha u_i^\alpha u_j^\alpha \quad \alpha = 1, 2, \dots, r, \quad (5.1)$$

where as before  $p_i^\alpha$  is the momentum of the  $i$ -th particle in the  $\alpha$ -th reservoir,  $u_i^\alpha$  is the mass normalized position operators. They obey the Heisenberg commutation relations  $[u_j^\alpha(t), p_k^\beta(t)] = i\hbar \delta_{jk} \delta^{\alpha\beta}$ ,  $\alpha, \beta = 1, 2, \dots, r$ .  $N_\alpha$  is the number of oscillators in each system.  $K^\alpha$  is the force constant matrix. In the limit  $N_\alpha \rightarrow \infty$  each system behaves like a heat bath. The interaction Hamiltonian  $\mathcal{H}_T(t)$  between the systems is taken in the following

form

$$\mathcal{H}_T(t) = \frac{1}{2} \sum_{\alpha \neq \beta} u_\alpha^T V^{\alpha\beta}(t) u_\beta. \quad (5.2)$$

The interaction is switched on at  $t > 0$ . Therefore the total Hamiltonian after the connection is

$$\mathcal{H}(t) = \sum_{\alpha=1}^r \mathcal{H}_\alpha + \mathcal{H}_T(t), \quad t > 0. \quad (5.3)$$

In this chapter, we present numerical results for the cumulants of exchanged heat between two-terminals (denoted as  $L$  and  $R$ ) for two specific types of the coupling  $V^{LR}(t) = V^{LR} \theta(t)$ , where  $\theta(t)$  is the Heaviside step function. Such form of coupling corresponds to the sudden connection between the two systems. Another form of the coupling we choose as  $V^{LR}(t) = V^{LR} \tanh(\omega_d t)$ , where  $\omega_d$  is the driving frequency. This particular form of the coupling is useful to study when the coupling between the device is switched on gradually. Note that one can recover Heaviside step function from this coupling in the limit  $\omega_d \rightarrow \infty$ . Other forms of coupling can also be handled easily in this formalism.

## 5.2 Generalized characteristic function $\mathcal{Z}(\{\xi_\alpha\})$

In order to work with generalized CF, defined below, we perform two-time measurements for all system Hamiltonians  $\mathcal{H}_\alpha$ ,  $\alpha = 1, 2, \dots, r$ , at  $t = 0$  and at  $t = t_M$ . Following the same recipe as before we construct the generalized

CF as [6]

$$\mathcal{Z}(\{\xi_\alpha\}) = \langle W^\dagger \mathcal{U}^\dagger(t_M, 0) W^2 \mathcal{U}(t_M, 0) W^\dagger \rangle, \quad (5.4)$$

where  $\{\xi_\alpha\} = (\xi_1, \xi_2, \dots, \xi_r)$  is the set of counting fields corresponding to  $\{Q_\alpha\}$  and  $W = \prod_{\alpha=1}^r W_\alpha = \prod_{\alpha=1}^r \exp(-i\xi_\alpha \mathcal{H}_\alpha/2)$  contains the counting field for energy measurement. For simplicity we choose the the initial density matrix as product initial state

$$\rho_{\text{prod}}(0) = \prod_{\alpha=1}^r \frac{e^{-\beta_\alpha \mathcal{H}_\alpha}}{\text{Tr}(e^{-\beta_\alpha \mathcal{H}_\alpha})}, \quad (5.5)$$

As before we write the CF on the Keldysh contour as

$$\mathcal{Z}(\{\xi_\alpha\}) = \langle \mathcal{U}_{-\xi/2}(0, t_M) \mathcal{U}_{\xi/2}(t_M, 0) \rangle, \quad (5.6)$$

where  $\mathcal{U}_{\vec{x}}(t, 0) = T \exp \left[ -\frac{i}{\hbar} \int_0^t dt \mathcal{H}_{\vec{x}}(t) \right]$  and

$$\begin{aligned} \mathcal{H}_{\vec{x}}(t) &= e^{i\vec{x} \cdot \vec{\mathcal{H}}_0} \mathcal{H}(t) e^{-i\vec{x} \cdot \vec{\mathcal{H}}_0} \\ &= \sum_{\alpha=1}^r \mathcal{H}_\alpha + \frac{1}{2} \sum_{\alpha, \beta} u_\alpha^T(\hbar x_\alpha) V^{\alpha\beta}(t) u_\beta(\hbar x_\beta), \end{aligned} \quad (5.7)$$

where  $\vec{\mathcal{H}}_0 = (\{\mathcal{H}_\alpha\})$  and  $\vec{x} = (\{x_\alpha\})$ .

Transforming to the interaction picture with respect to  $\mathcal{H}_0 = \sum_{\alpha=1}^r \mathcal{H}_\alpha$  and making use of linked-cluster theorem the cumulant generating function

(CGF)  $\ln \mathcal{Z}(\{\xi_\alpha\})$  reads as

$$\begin{aligned}\ln \mathcal{Z}(\{\xi_\alpha\}) &= -\frac{1}{2} \ln \det \left( \mathbb{I} - \mathbb{V}g^x \right) \\ &= -\frac{1}{2} \text{Tr}_{j,\tau} \ln \left( \mathbb{I} - \mathbb{V}g^x \right),\end{aligned}\quad (5.8)$$

where  $\mathbb{V}$  is a  $r \times r$  off-diagonal matrix with matrix elements  $V_{\alpha\beta}(t)$  with  $\alpha, \beta = 1, 2, \dots, r$  given as

$$\mathbb{V}_{\alpha\beta}(\tau, \tau') = \delta(\tau, \tau') V_{\alpha\beta}(\tau), \quad (5.9)$$

and  $g^x$  is a  $r \times r$  diagonal matrix with matrix elements  $\tilde{g}_\alpha$  where

$$\tilde{g}_\alpha(\tau, \tau') = -\frac{i}{\hbar} \langle T_c u_\alpha(\tau + \hbar x_\alpha(\tau)) u_\alpha^T(\tau' + \hbar x_\alpha(\tau')) \rangle, \quad (5.10)$$

with  $x_\alpha^\pm(t) = \mp \xi_\alpha/2$  for  $0 \leq t \leq t_M$  and zero otherwise. The meaning of trace is same as before. Note that in the above expression only  $\tilde{g}$  depends on counting fields  $\{\xi_\alpha\}$ . The CGF can be further simplified to explicitly satisfy the normalization condition and can be re-written as

$$\ln \mathcal{Z}(\{\xi_\alpha\}) = -\frac{1}{2} \ln \det \left( \mathbb{I} - (\mathbb{I} + \mathbb{V}\mathbb{G})\mathbb{V}g^A \right). \quad (5.11)$$

This expression is valid for both transient and stationary state and for arbitrary time-dependent couplings between the leads. The matrix  $\mathbb{G}$  consists of elements  $G_{\alpha\beta}(\tau, \tau')$  and satisfies the Dyson equation in the matrix form

$$\mathbb{G}(\tau, \tau') = g(\tau, \tau') + \int_c d\tau_1 \int d\tau_2 g(\tau, \tau_1) \mathbb{V}(\tau_1, \tau_2) \mathbb{G}(\tau_2, \tau'), \quad (5.12)$$

and we define  $g^A(\tau, \tau') = \tilde{g}(\tau, \tau') - g(\tau, \tau')$  which is also a diagonal matrix. It is now easy to see that for  $\xi_\alpha = 0$ ,  $g^A = 0$  and therefore  $\mathcal{Z}(\{0\})$  satisfy the normalization condition. Note that due to the presence of the coupling matrix  $\mathbb{V}$  only surface-Green's functions are required to compute the cumulants and thus reduces the complexity of the problem. The explicit form of these matrices for two-terminal case is discussed in the later part. From this generalized CGF, the cumulants of heat can be obtained as

$$\begin{aligned}\langle\langle Q_\alpha \rangle\rangle &= \frac{\partial \ln \mathcal{Z}(\{0\})}{\partial(i\xi_\alpha)}, \\ \langle\langle Q_\alpha Q_\beta \rangle\rangle &= \frac{\partial^2 \ln \mathcal{Z}(\{0\})}{\partial(i\xi_\alpha) \partial(i\xi_\beta)}.\end{aligned}\tag{5.13}$$

Note that the CGF for heat  $Q_\alpha$  can be obtained trivially from  $\mathcal{Z}(\{\xi_\alpha\})$  by substituting all counting parameters to zero except  $\xi_\alpha$ .

### 5.3 Long-time result for the CGF for heat

In this section, we derive the long-time limit expression for the CGF of heat. In order to achieve the stationary state with infinite recurrence time the we need the following criterions to be satisfied,

- The size of all the systems should be infinite, *i.e.*,  $N_\alpha \rightarrow \infty$ ,  $\alpha = 1, 2, \dots, r$  which are then called dissipative leads, so that the waves can't scatter back from the boundaries. The effect of finite boundaries are discussed at the end of this chapter.

- The final measurement time  $t_M$  should approach to infinity.
- The coupling  $V^{\alpha\beta}(t)$  between the systems should be time-independent or reach a constant value in short time scale.

Let us calculate the heat flowing out from the  $\alpha$ -th lead. Using the matrix form for  $\mathbb{V}$  and  $\mathbb{G}$ , Eq. (5.11) in the frequency domain is written as

$$\ln \mathcal{Z}(\xi_\alpha) = -t_M \int_{-\infty}^{\infty} \frac{d\omega}{4\pi} \ln \det \left[ \mathbb{I} - (\check{g}_\alpha^{-1} \check{G}_{\alpha\alpha} - \mathbb{I}) \check{g}_\alpha^{-1} \check{g}_\alpha^A \right], \quad (5.14)$$

where,

$$\check{g}_\alpha = \begin{bmatrix} g_\alpha^r & g_\alpha^K \\ 0 & g_\alpha^a \end{bmatrix}, \quad \check{G}_{\alpha\alpha} = \begin{bmatrix} G_{\alpha\alpha}^r & G_{\alpha\alpha}^K \\ 0 & G_{\alpha\alpha}^a \end{bmatrix}, \quad (5.15)$$

$$\check{g}_\alpha^A = \frac{1}{2} \begin{bmatrix} a - b & a + b \\ -a - b & -a + b \end{bmatrix}, \quad (5.16)$$

$$a = g_\alpha^> (e^{-i\xi\hbar\omega} - 1), \quad b = g_\alpha^< (e^{i\xi\hbar\omega} - 1)$$

An important quantity to define in this case is  $\tilde{\Gamma}_\alpha$

$$\tilde{\Gamma}_\alpha[\omega] = i \left[ (g_\alpha^a)^{-1}[\omega] - (g_\alpha^r)^{-1}[\omega] \right]. \quad (5.17)$$

For any finite size system using the solution for  $g_\alpha^{r,a}[\omega] = [(\omega \pm i\eta)^2 - K^\alpha]^{-1}$  (see appendix (F)) it can be easily shown that  $\tilde{\Gamma}_\alpha[\omega] = 4\omega\eta$  is zero in the limit  $\eta \rightarrow 0^+$ . However for infinite system size this is not valid.

Now in order to get final expression for the steady-state CGF we need to know the different components of the matrix  $\check{G}_{\alpha\alpha}$ . Two important relations that are required to derive the CGF are

$$\begin{aligned} G_{\alpha\alpha}^<[\omega] &= -i \sum_{\gamma=1}^r f_j G_{\alpha\gamma}^r[\omega] \tilde{\Gamma}_\gamma[\omega] G_{\gamma\alpha}^a[\omega] \\ G_{\alpha\alpha}^r[\omega] - G_{\alpha\alpha}^a[\omega] &= -i \sum_{\gamma=1}^r G_{\alpha\gamma}^r[\omega] \tilde{\Gamma}_\gamma[\omega] G_{\gamma\alpha}^a[\omega], \end{aligned} \quad (5.18)$$

which are obtained by simplifying the Dyson equation given in Eq. (5.12) in the frequency domain. When all the systems are in thermal equilibrium the above equations are related by fluctuation-dissipation theorem.

Substituting the expressions for different components of  $G_{\alpha\alpha}^{<,r,a}$  and after a lengthy calculation the long-time limit expression for the CGF for heat is given as

$$\ln \mathcal{Z}(\xi_\alpha) = -t_M \int_{-\infty}^{\infty} \frac{d\omega}{4\pi} \ln \det \left[ 1 - \sum_{\gamma \neq \alpha=1}^r \mathcal{T}_{\alpha\gamma}[\omega] \mathcal{K}_{\gamma\alpha}(\omega; \xi_\alpha) \right], \quad (5.19)$$

where the function  $\mathcal{K}_{\gamma\alpha}(\omega; \xi_\alpha)$  is the same as before and written as

$$\mathcal{K}_{\gamma\alpha}(\omega; \xi_\alpha) = f_\alpha(1 + f_\gamma)(e^{i\xi_\alpha \hbar \omega} - 1) + f_\gamma(1 + f_\alpha)(e^{-i\xi_\alpha \hbar \omega} - 1). \quad (5.20)$$

This function satisfies the Gallavotti-Cohen type symmetry  $\mathcal{K}_{\gamma\alpha}(\omega; \xi_\alpha) = \mathcal{K}_{\gamma\alpha}(\omega; -\xi_\alpha + i(\beta_\gamma - \beta_\alpha))$  and  $\mathcal{T}_{\alpha\gamma}[\omega]$  is the new transmission matrix between

the system  $\alpha$  and  $\gamma$  and is of the following form

$$\mathcal{T}_{\alpha\gamma}[\omega] = G_{\alpha\gamma}^r \tilde{\Gamma}_\gamma G_{\gamma\alpha}^a \tilde{\Gamma}_\alpha. \quad (5.21)$$

This new transmission matrix reduces to the transmission function for one-dimensional case and is useful for the interface study in two-terminal situation. Note that the CGF for heat does not have Gallavotti-Cohen fluctuation symmetry for more than two-terminal situation.

## 5.4 Special Case: Two-terminal situation

In this section we present numerical results for heat  $Q$  for two-terminal case  $r = 2$  denoted as the left ( $L$ ) and the right ( $R$ ) lead. We first derive the CGF for heat, valid for arbitrary time  $t_M$ , using Eq. (5.11) and then give the numerical details. The matrix  $\mathbb{V}$  and  $\mathbb{G}$  introduced in Eq. (5.11) for  $r = 2$ , are given as

$$\mathbb{V}(\tau, \tau') = \delta(\tau, \tau') \begin{bmatrix} 0 & V^{LR}(\tau) \\ V^{RL}(\tau) & 0 \end{bmatrix}, \mathbb{G}(\tau, \tau') = \begin{bmatrix} G_{LL}(\tau, \tau') & G_{LR}(\tau, \tau') \\ G_{RL}(\tau, \tau') & G_{RR}(\tau, \tau') \end{bmatrix}, \quad (5.22)$$

and since we are interested in the CGF for heat, only the left-lead Hamiltonian is measured twice. Therefore

$$g^A(\tau, \tau') = \begin{bmatrix} g_L^A(\tau, \tau') & 0 \\ 0 & 0 \end{bmatrix}. \quad (5.23)$$

For the calculation of entropy-production the second diagonal element of  $g^A$  will be non-zero. Multiplying the matrices explicitly the CGF for heat is given as

$$\ln \mathcal{Z}(\xi_L) = -\frac{1}{2} \text{Tr}_{j,\tau} \ln \left[ 1 - G_{RR} \Sigma_L^A \right], \quad (5.24)$$

where  $\Sigma_L^A = V^{RL} g_L^A V^{LR}$  and  $G_{RR}$  obeys the Dyson equation

$$G_{RR}(\tau, \tau') = g_R(\tau, \tau') + \int d\tau_1 \int d\tau_2 g_R(\tau, \tau_1) \Sigma_L(\tau_1, \tau_2) G_{RR}(\tau_2, \tau'). \quad (5.25)$$

Similarly the expression for the entropy-production can also be obtained. Note that the above expression is similar to the one obtained in the third chapter. However the meaning of  $G^{RR}$  and  $\Sigma_L^A$  are different. The long-time limit result can be obtained following the same steps as previous and it is given as

$$\ln \mathcal{Z}(\xi_L) = -t_M \int \frac{d\omega}{4\pi} \ln \det \left[ \mathbb{I} - [G_{RR}^r \tilde{\Gamma}_R G_{RR}^a \Gamma_L] \mathcal{K}(\omega; \xi_L) \right]. \quad (5.26)$$

The new transmission matrix for the interface is of the following form

$$\mathcal{T}_{RL}[\omega] = G_{RR}^r \tilde{\Gamma}_R G_{RR}^a \Gamma_L, \quad (5.27)$$

where  $\Gamma_L = i(\Sigma_L^r - \Sigma_L^a)$  is the spectral function. Note the difference of  $\Gamma$  matrices for left and right lead. We call this transmission matrix as the Caroli formula for ballistic interface.

---

**Explicit formula for interface transmission function  $\mathcal{T}[\omega]$  for**

**One-dimensional linear chain:**

Here we derive an explicit expression for the transmission function for one-dimensional harmonic chain with single interface *i.e.*, the left and right leads are directly connected and the center part is removed. The transmission function reads

$$\mathcal{T}_I[\omega] = \text{Tr}[G_{RR}^r \tilde{\Gamma}_R G_{RR}^a \Gamma_L] \quad (5.28)$$

Let us consider that the force constant for left and the right leads are  $k_1$  and  $k_2$  respectively and the interface coupling strength is  $k_{12}$  with additional on-site potential  $k_0$  on all the atoms. This is a quite general scenario for a one-dimensional harmonic chain. Therefore the form of the semi-infinite force constant matrix say  $K^L$  consisting of  $k_{12} + k_1 + k_0$  as the first diagonal and  $2k_1 + k_0$  along rest of the diagonals and  $-k_1$  along the first off-diagonals. Similarly for  $K^R$  with  $k_1$  replaced by  $k_2$ . In order to obtain the explicit form for  $\mathcal{T}_I[\omega]$  we need to compute the retarded component of the surface Green's function  $g_\alpha^r$  for both the leads. Knowing  $g_\alpha^r$ ,  $G^{RR}$  can be obtained from Eq. (5.25).

Let us calculate the surface Green's function for the left lead. Then for the right lead it can be obtained just by replacing  $k_1$  with  $k_2$ . Retarded green's function for the left lead satisfies the following equation

$$[(\omega + i0^+)^2 - K^L] g_L^r[\omega] = I \quad (5.29)$$

Now we write  $K^L = K_0^L + \Delta K$  where  $\Delta K$  is the semi-infinite matrix with only first element nonzero  $\Delta K_{11} = k_{12} - k_1$ .  $K_0^L$  is now a familiar matrix which also appears in the Rubin bath case with all force constants same. Using  $\Delta K$  as a

perturbation we can write

$$g_L^r[\omega] = g_{L,0}^r[\omega] + g_{L,0}^r[\omega] \Delta K g_L^r[\omega] \quad (5.30)$$

Since in this case only first atom of the left lead is connected with the first atom of the right lead we only need  $(1, 1)^{\text{th}}$  element of  $g_L^r$ . Now

$$[g_L^{r,0}]_{1,1}[\omega] = -\frac{\lambda_1}{k_1}, \quad |\lambda_1| \leq 1, \quad (5.31)$$

with  $\lambda_1 = -\frac{\Omega}{2k_1} \pm \frac{1}{2k_1} \sqrt{\omega^2 - 4k_1^2}$  and  $\Omega = (\omega + i\eta)^2 - 2k_1 - k_0$ . Therefore we obtain

$$[g_L^r]_{1,1}[\omega] = \frac{1}{k_1 - k_{12} - k_1/\lambda_1}, \quad |\lambda_1| \leq 1, \quad (5.32)$$

and similarly the self-energy for the lead is given as

$$[\Sigma_L^r]_{1,1}[\omega] = \frac{k_{12}^2}{k_1 - k_{12} - k_1/\lambda_1}, \quad |\lambda_1| \leq 1 \quad (5.33)$$

Knowing this Green's function we can easily obtain  $\mathcal{T}_I[\omega]$  which reads

$$\mathcal{T}_I[\omega] = -\frac{k_1 k_2 k_{12}^2 (\lambda_1 - \lambda_1^*) (\lambda_2 - \lambda_2^*)}{|(k_1 - k_{12} - k/\lambda_1)(k_2 - k_{12} - k/\lambda_2) - k_{12}^2|^2} \quad (5.34)$$

where  $\lambda_2$  is similarly defined as  $\lambda_1$  with  $k_1$  replaced by  $k_2$ . We note that it matches exactly with the result in Ref [4], where this expression is obtained from a wave-scattering method. As a special case for pure chain *i.e.*, if  $k_1 = k_2 = k_{12} = k$  then we have perfect transmission meaning  $\mathcal{T}_I[\omega] = 1$  for  $\omega$  within the phonon band width  $k_0 \leq \omega^2 \leq 4k + k_0$  and 0 outside this region.

---

### 5.4.1 Numerical Results and discussion

In this section we present numerical results for the first four cumulants of heat, obtained from Eq. (5.24) by taking derivative of the CGF with respect to the counting field  $\xi_L$  i.e,  $\langle\langle Q_L^n \rangle\rangle = \frac{d \ln \mathcal{Z}(\xi_L)}{d(i\xi_L)^n} |_{\xi_L=0}$ , as a function of measurement time  $t_M$ . We choose two identical semi-infinite ( $N_\alpha = \infty$ ) one-dimensional linear harmonic chain with only nearest-neighbor interactions and connected via time-dependent coupling, for performing numerical simulations. In order to obtain the cumulants we need to solve the Dyson equation for  $G_{RR}$  obtained from Eq. (5.12) and the shifted self-energy  $\Sigma_L^A$  in the time-domain which can be obtained from the surface Green's functions. Since the baths are at their respective equilibrium knowing one Green's function is sufficient to obtain the rest. In this particular case, the analytical form of the retarded component of surface Green's function is known in the frequency domain and is given as

$$g_{ij}^{\alpha,r}[\omega] = -\frac{\lambda}{k} \lambda^{|i-j|}, \quad 1 \leq i, j \leq N_\alpha, \quad \alpha = L, R, \quad (5.35)$$

where

$$\lambda = -\frac{\Omega}{2k} \pm \frac{1}{2k} \sqrt{\Omega^2 - 4k^2} \equiv e^{iq}, \quad (5.36)$$

where  $q$  is the wave vector and  $\Omega = (\omega + i\eta)^2 - 2k - k_0 = -2k \cos q$ . The choice between plus and minus sign is made on satisfying  $|\lambda| < 1$ . For nearest-neighbor coupling we need only  $g_{11}$  component. Note that the inverse Fourier transformation for lesser and greater components are easy to perform as the range of integration in  $\omega$  space is confined within the phonon

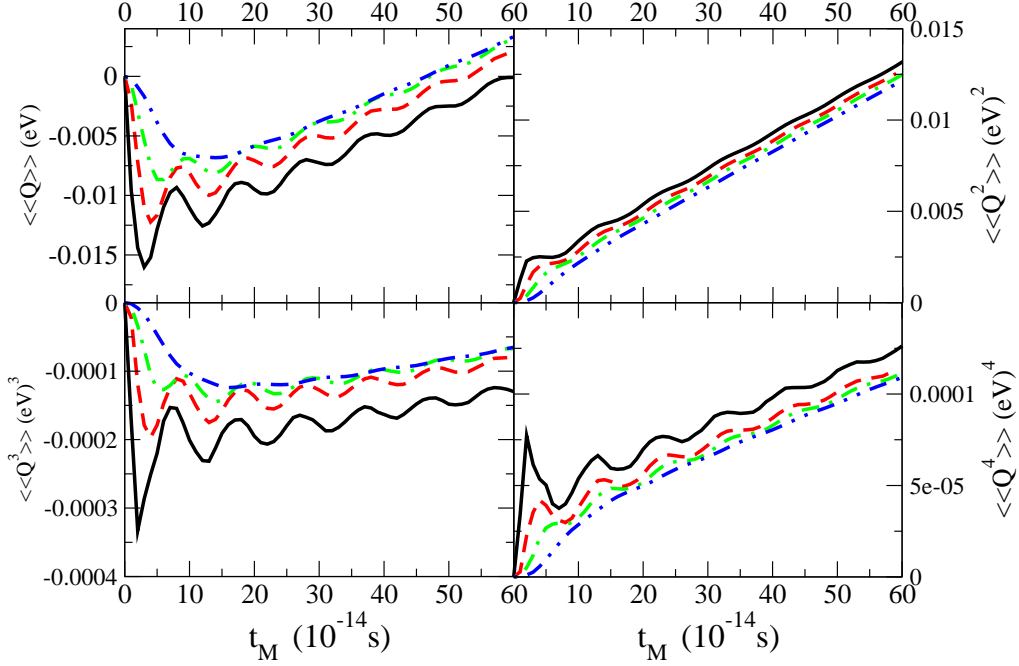


Figure 5.2: The cumulants of heat  $\langle\langle Q_L^n \rangle\rangle$  for  $n=1, 2, 3$ , and  $4$  for one-dimensional linear chain for two types of coupling as a function of measurement time. The solid line corresponds to  $V^{LR}(t) = k_{12}\theta(t)$ . The dash, dash-dotted and dash-dotted-dotted lines corresponds to  $V^{LR}(t) = k_{12}\tanh(\omega_d t)$  with  $\omega_d = 1.0[1/t], 0.5[1/t], 0.25[1/t]$  respectively. The temperatures of the left and the right lead are 310 K and 290 K, respectively.  $k = k_{12} = 1 \text{ eV}/(\text{u}\text{\AA}^2)$  and  $k_0 = 0.1 \text{ eV}/(\text{u}\text{\AA}^2)$ .

band  $k_0 < \omega^2 < 4k + k_0$ . Then using the relation  $g^r - g^a = g^> - g^<$  we get both the retarded and advanced Green's functions in the time-domain. Obtaining  $g_\alpha^{r,a}(t)$  directly from  $g_\alpha^r[\omega]$  by inverse Fourier transform is numerically difficult as there is no such cut-off in the frequency space. Therefore the non-equilibrium Green's functions i.e.,  $G_{RR}^{<, >, r, a}$  can be calculated from the integrals of this equilibrium Green's functions.

### Time-dependent behavior of the cumulants

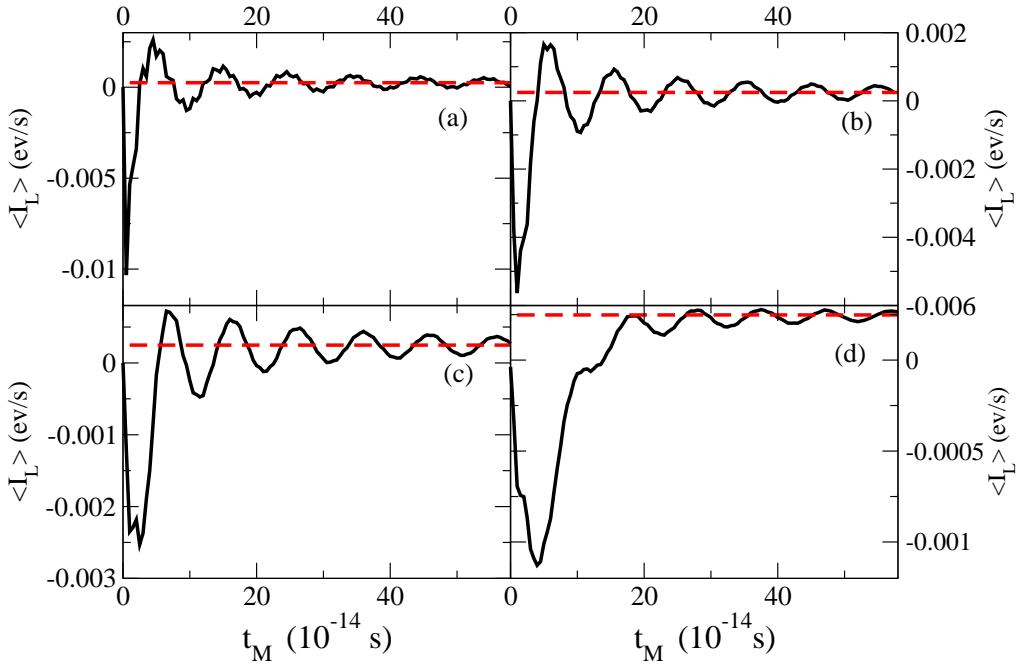


Figure 5.3: Plot of current as a function of measurement time  $t_M$  for different couplings  $V^{LR}(t)$ . Fig (a) corresponds to  $V^{LR}(t) = k_{12}\theta(t)$ . Fig (b),(c) and (d) corresponds to  $V^{LR}(t) = k_{12}\tanh(\omega_d t)$  with  $\omega_d = 1.0 [1/t], 0.5 [1/t], 0.25 [1/t]$  respectively. The temperatures of the left and the right lead are 310 K and 290 K, respectively.  $k = k_{12} = 1 \text{ eV}/(\text{u}\text{\AA}^2)$  and  $k_0 = 0.1 \text{ eV}/(\text{u}\text{\AA}^2)$ . Dashed lines are the steady state values obtained using Landauer formula with unit transmission.

In Fig. (5.2) we show the time-dependent behavior of the first four cumulants of heat  $\langle\langle Q_L^n \rangle\rangle$  for two different forms of the coupling  $V^{LR}(t) = k_{12}\theta(t)$  and  $V^{LR}(t) = k_{12}\tanh(\omega_d t)$  where  $k_{12}$  is the interface force constant. The form of this couplings decides how the device is switched on. We set the inter-particle and interface coupling  $k = k_{12} = 1 \text{ eV}/(\text{u}\text{\AA}^2)$  and the on-site potential  $k_0 = 0.1 \text{ eV}/(\text{u}\text{\AA}^2)$ . These choices of units fix the time scale of our problem which we also use as the unit of time  $[t] = 10^{-14} \text{ s}$ . We observe that the fluctuations are larger for the sudden switch on case as compared to the slow switch on of the couplings using hyperbolic tangent form. By gradually reducing the driving frequency  $\omega_d$  the system evolves to the unique steady state with less and less oscillations.

In Fig. (5.3) we plot the current  $\langle\mathcal{I}_L\rangle$  by taking derivative of the first cumulant with respect to the measurement time  $t_M$ . We also obtain the steady-state values of the current using Landauer formula with unit transmission within the phonon band which are also shown with dashed lines. In all cases, at the initial time current is negative, *i.e.*, heat flows into the left lead as before. The current that goes into the leads is in the form of mechanical energy which is coming from the work that is required to couple both the systems at  $t = 0$ . We also see that at earlier times the amplitude of the current depends on the values of  $\omega_d$ . Higher driving frequency produce larger transient currents. However at later times the coupling reaches to a constant value  $k_{12}$  and the current settles down to the value predicted by Landauer formula.

### 5.4.2 Exchange Fluctuation Theorem (XFT)

In this section we examine the validity of XFT for different coupling strength  $k_{12}$  for the sudden switch on case. This particular fluctuation theorem was first discussed by Jarzynski and Wójcik which states that  $\langle e^{-\Delta\beta Q_L} \rangle_{t_M} = 1$  for two weakly connected systems. The relation is true for any transient time  $t_M$ . We use Eq. (5.24) and calculate the CGF for  $\xi_L = i\Delta\beta$ . In Fig. (5.4) we plot  $\langle e^{-\Delta\beta Q_L} \rangle$  as a function of  $t_M$  for different values of interface coupling strength  $k_{12}$  and absolute temperatures  $T_L$  and  $T_R$  of the baths. For weak coupling ( $k_{12} = 0.001k$ ) the fluctuation symmetry is satisfied [11] and for higher values of the coupling strength the quantity  $\langle e^{-\Delta\beta Q_L} \rangle - 1$  increases. It is important to note that the meaning of weak coupling, in order to satisfy XFT, also depends on the absolute temperatures of the heat baths. This is simply due to the presence of the factor  $\Delta\beta Q_L$  in the exponent. Since the cumulants of heat depends on the interface coupling strength (In the long-time limit  $\langle\langle Q_L^n \rangle\rangle \propto k_{12}^2$  in weak coupling ( $k_{12}$ ) limit and in the presence of on-site potential  $k_0$ ), keeping the value of  $k_{12}$  constant, if we lower the value of  $\Delta\beta$  maintaining the same temperature difference it is possible to reduce the value of  $\langle e^{-\Delta\beta Q_L} \rangle - 1$ , as shown by the dashed lines for two values of  $k_{12} = 1.0 \text{ eV}/(\text{u}\text{\AA}^2)$  and  $0.1 \text{ eV}/(\text{u}\text{\AA}^2)$ . So both the weak-coupling as well as the absolute temperature of the baths are important to check the validity of XFT. Also note that in the long-time limit ( $t_M \rightarrow \infty$ ) according to SSFT [12]  $\langle e^{-\Delta\beta Q_L} \rangle = 1$  which is true for arbitrary coupling strength and can be proved trivially from the relation  $\langle e^{-\Sigma} \rangle = 1$  as in the steady state  $Q_L = -Q_R$ . In Fig. (5.4), in the

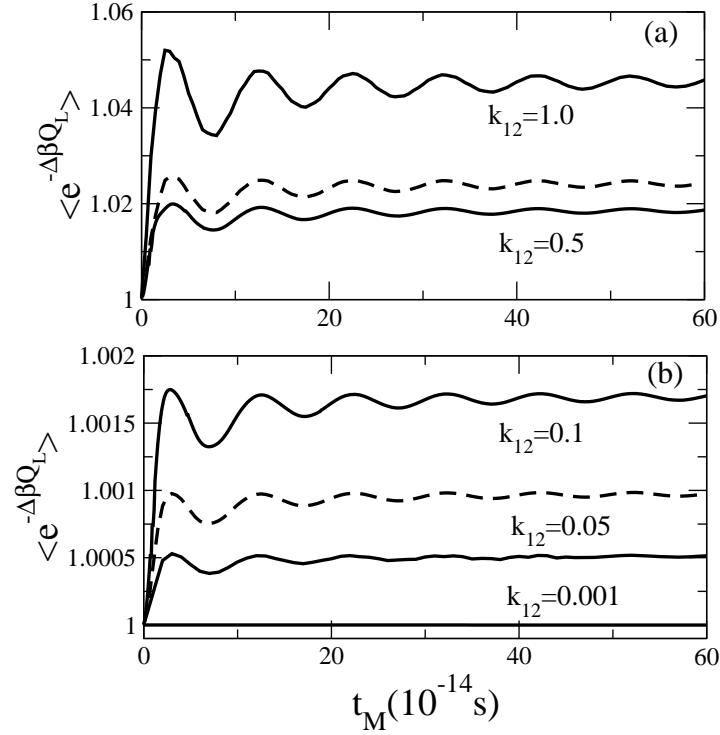


Figure 5.4: Plot of  $\langle e^{-\Delta\beta Q_L} \rangle$  as a function measurement time  $t_M$  for different values of interface coupling strength  $k_{12}$  and absolute temperatures of the heat baths for sudden switch on case. The solid lines corresponds to temperatures of the left and the right lead 310 K and 290 K respectively and for dashed lines the temperatures are 510 K and 490 K respectively. The unit of force constants is in  $\text{eV}/(\text{u}\text{\AA}^2)$

long time limit  $\langle e^{-\Delta\beta Q_L} \rangle \neq 1$ . However this is not a violation to SSFT as the theorem is valid only to the leading order of  $t_M$ . In general, the next order correction to the CGF is a constant in  $t_M$  and can be written as follows [6]

$$\mathcal{Z}(\xi_L) = b(\xi_L) e^{-t_M a(\xi_L)} + \text{lower orders in } t_M. \quad (5.37)$$

where  $a(\xi_L)$  is given in Eq. (5.26) and  $b(\xi)$  is the correction to the leading order. Since  $\langle e^{-\Delta\beta Q_L} \rangle$  is calculated taking into account the contributions due to all order of  $t_M$ , it is not equal to one in the long-time limit. Note that the correction term  $b(\xi_L)$  is often important to know for obtaining the large deviation function corresponding to the probability distribution  $P(Q_L)$ . For classical harmonic chain model this correction term is obtained analytically by Kundu et al [13–15]. For the quantum case obtaining  $b(\xi_L)$  requires further investigations.

## 5.5 Effect of finite size of the system on the cumulants of heat

In this section we examine the impact of finite size of the systems on the cumulants of heat [16]. We only focus on the coupling of the form  $V^{LR}(t) = k_{12} \theta(t)$ . In the case for finite number of one-dimensional coupled harmonic oscillators with nearest-neighbor coupling the (1, 1) component

for the surface Green's function can be written as

$$(g_\alpha^r[\omega])_{11} = -\frac{\lambda}{k} \frac{1 - \lambda^{2N_\alpha}}{1 - \lambda^{2N_\alpha+2}}, \quad \alpha = L, R, \quad (5.38)$$

where the meaning of  $\lambda$  is same as before. In the limit  $N_\alpha \rightarrow \infty$  one can recover the surface Green's function for the lead. Unlike for the leads  $g_\alpha^r[\omega]$  for finite system is not a smooth function of  $\omega$  but rather consists of delta peaks determined by the normal-mode frequencies. Fourier transformations for such functions are difficult to obtain numerically. So we evaluate these Green's functions directly in the time-domain by solving the Heisenberg equations of motion with fixed boundary conditions. As before knowing one Green's function is enough to determine the rest. We write down the expression for greater component given as

$$\begin{aligned} g_{ij}^{\alpha,>}(t) &= -\frac{i}{\hbar} \langle u_i^\alpha(t) u_j^\alpha(0) \rangle, \quad \alpha = L, R, \\ &= -\frac{i}{\hbar} \sum_{k=1}^{N_\alpha} S_{ik}^\alpha \left[ \frac{\hbar}{2\omega_k^\alpha} (1 + 2f_k^\alpha) \cos(\omega_k^\alpha t) - \frac{i\hbar \sin \omega_k^\alpha t}{2 \omega_k^\alpha} \right] S_{jk}^\alpha, \end{aligned} \quad (5.39)$$

where  $(\omega_k^\alpha)^2 = 2k[1 - \cos(\frac{n\pi}{N+1})] + k_0$ ,  $n = 1, 2, \dots, N_\alpha$  are the normal mode frequencies and the eigenfunctions are given by  $\epsilon_j^n = \sqrt{\frac{2}{N+1}} \sin(\frac{n\pi j}{N+1})$ . The symmetric matrix  $S$  consists of this eigenfunctions which diagonalizes the force constant matrix  $K^\alpha$  which is a  $N_\alpha \times N_\alpha$  tridiagonal matrix with  $2k + k_0$  along the diagonals and  $-k$  along the two off-diagonals.

In Fig. (5.5) we show the results for the cumulants of heat for two finite harmonic chain connected suddenly at  $t = 0$ . We see that all the cumulants

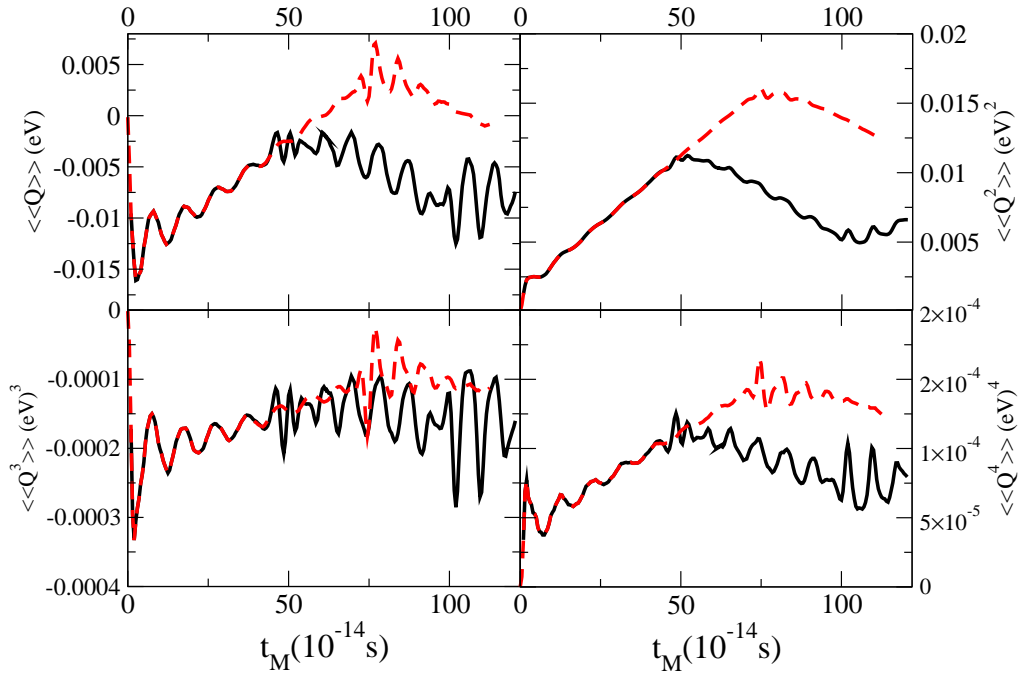


Figure 5.5: Plot of the cumulants of heat  $\langle\langle Q_L^n \rangle\rangle$  for  $n=1, 2, 3,$  and  $4$  for two finite harmonic chain connected suddenly at  $t = 0$ . The black (solid) and red (dashed) line corresponds to  $N_L = N_R = 20$  and  $N_L = N_R = 30$  respectively. The temperatures of the left and the right lead are 310 K and 290 K, respectively.

reaches to a quasi-steady state [17] with a finite recurrence time  $t_r$  which is the product of the total length of the system and the velocity of sound waves. After time  $t_r$  the phonon modes travelling from  $L$  to  $R$  gets reflected from the boundary and then interfere with the incoming waves from  $L$  resulting in the cumulants to oscillate rapidly. In the limit when the leads are semi infinite  $N_\alpha \rightarrow \infty$  we observe complete irreversible behavior of the cumulants. The FT in this case is valid only in the range  $0 < t < t_r$ .

## 5.6 Proof of transient fluctuation theorem

In this section we proof the transient fluctuation theorem given as  $\langle e^{-\Sigma} \rangle_{t_M} = 1$  where  $\Sigma = -\sum_\alpha \beta_\alpha Q_\alpha$ . The important relation that goes into the proof is the generalized version of the Kubo-Martin-Schwinger (KMS) condition [18] for the correlation functions, given as

$$g_\alpha^<(t - \hbar\xi_\alpha) = g_\alpha^<(-t + \hbar\xi_\alpha + i\beta_\alpha\hbar) = g_\alpha^>(t - \hbar\xi_\alpha - i\beta_\alpha\hbar), \quad \alpha = 1, 2, \dots, r. \quad (5.40)$$

For  $\xi_\alpha = 0$  correlations functions satisfy the standard KMS condition *i.e.*,  $g_\alpha^<(t + i\beta_\alpha\hbar) = g_\alpha^>(t)$  and in the frequency space it reads as the detailed balanced condition *i.e.*,  $g_\alpha^>(\omega) = e^{\beta_\alpha\hbar\omega} g_\alpha^<(\omega)$ .

To prove the fluctuation theorem we proceed from Eq. (5.8) and consider the  $2n$ -th term of the log series which can be written in the contour time

$\tau$  as

$$A_{2n} = \int d\tau_1 \int d\tau_2 \cdots \int d\tau_{2n} \text{Tr}_j \left[ \mathbb{V}(\tau_1, \tau_2) g^x(\tau_2, \tau_3) \cdots \mathbb{V}(\tau_{2n-1}, \tau_{2n}) g^x(\tau_{2n}, \tau_1) \right]. \quad (5.41)$$

Now using  $\mathbb{V}(\tau, \tau') = \delta(\tau, \tau') \mathbb{V}(\tau)$  we have

$$A_{2n} = \int d\tau_1 \int d\tau_2 \cdots \int d\tau_n \text{Tr}_j \left[ \mathbb{V}(\tau_1) g^x(\tau_1, \tau_2) \cdots \mathbb{V}(\tau_n) g^x(\tau_n, \tau_1) \right]. \quad (5.42)$$

Let us define a new matrix  $\mathcal{G}_x(\tau, \tau') = \mathbb{V}(\tau) g^x(\tau, \tau')$ , then in the real time we can write

$$A_{2n} = \int dt_1 \int dt_2 \cdots \int dt_n \sum_{\sigma_1 \sigma_2 \cdots \sigma_n} \text{Tr}_j \left[ \sigma_1 \mathcal{G}_x^{\sigma_1 \sigma_2}(\tau_1, \tau_2) \cdots \sigma_n \mathcal{G}_x^{\sigma_n \sigma_1}(\tau_n, \tau_1) \right], \quad (5.43)$$

which in a compact notation can also be written as

$$A_{2n} = \int dt_1 \int dt_2 \cdots \int dt_n \text{Tr}_{j, \sigma} \left[ \bar{\mathcal{G}}_x(t_1, t_2) \cdots \bar{\mathcal{G}}_x(t_n, t_1) \right], \quad (5.44)$$

where we define  $\bar{\mathcal{G}}_x = \sigma_z \mathcal{G}_x$  and  $\sigma_z$  is the third-Pauli matrix. The explicit form of  $\bar{\mathcal{G}}_x$  is

$$\bar{\mathcal{G}}_x(t, t') = \begin{bmatrix} \mathbb{V}(t) g^t(t - t') & \mathbb{V}(t) g^<(t - t' - \hbar(x^+ - x^-)) \\ -\mathbb{V}(t) g^>(t - t' - \hbar(x^- - x^+)) & -\mathbb{V}(t) g^{\bar{t}}(t - t') \end{bmatrix}. \quad (5.45)$$

Now substituting  $\xi_\alpha = -i\beta_\alpha$ ,  $\forall \alpha = 1, 2 \cdots r$  and using KMS boundary condition we immediately see that the lesser and greater Green's functions gets interchanged whereas time-ordered and anti-time ordered Green's functions stay the same, as they are independent of the counting fields. Therefore

after the substitution we have

$$\bar{\mathcal{G}}_{x_\alpha=i\beta_\alpha}(t, t') = \begin{bmatrix} \mathbb{V}(t)g^t(t-t') & \mathbb{V}(t)g^>(t-t') \\ -\mathbb{V}(t)g^<(t-t') & -\mathbb{V}(t)g^{\bar{t}}(t-t') \end{bmatrix}. \quad (5.46)$$

Now performing Keldysh rotation to this matrix we obtain

$$\begin{aligned} \check{\mathcal{G}}_{x_\alpha=i\beta_\alpha}(t, t') &= O^T \bar{\mathcal{G}}_{x_\alpha=i\beta_\alpha}(t, t') O \\ &= \begin{bmatrix} \mathbb{V}(t)g^a(t-t') & \mathbb{V}(t)g^k(t-t') \\ 0 & \mathbb{V}(t)g^r(t-t') \end{bmatrix}, \end{aligned} \quad (5.47)$$

which is a tridiagonal matrix. And because the Keldysh rotation is an orthogonal transformation the trace in Eq. (5.44) remain invariant. Therefore we write

$$A_{2n} = \int dt_1 \int dt_2 \cdots \int dt_n \text{Tr}_{j,\sigma} [\check{\mathcal{G}}_{i\beta_\alpha}(t_1, t_2) \cdots \check{\mathcal{G}}_{i\beta_\alpha}(t_n, t_1)], \quad (5.48)$$

Now as the product of the tridiagonal matrices are tridiagonal, then finally the trace over the branch index will give

$$\begin{aligned} A_{2n} &= \int dt_1 \int dt_2 \cdots \int dt_n \text{Tr}_j \left[ \mathbb{V}(t_1)g^a(t_1-t_2) \mathbb{V}(t_2)g^a(t_2-t_3) \cdots \mathbb{V}(t_n)g^a(t_n-t_1) \right. \\ &\quad \left. + \mathbb{V}(t_1)g^r(t_1-t_2) \mathbb{V}(t_2)g^r(t_2-t_3) \cdots \mathbb{V}(t_n)g^r(t_n-t_1) \right]. \end{aligned} \quad (5.49)$$

This expression is zero because  $t_1 > t_2 \cdots t_n > t_1$  or  $t_1 < t_2 \cdots t_n < t_1$  is never satisfied. Therefore  $\ln \mathcal{Z}(\{\xi_\alpha = -i\beta_\alpha\}) = 0$  which implies  $\langle e^{-\Sigma} \rangle_{t_M} = 1$  for arbitrary  $t_M$  and time-dependent coupling.

We also like to point out that similar analysis can be carried out in the presence of a finite junction connected with multiple terminals. In this case the the long-time CGF for the heat flowing out from  $\alpha$ -th terminal is given as [19]

$$\ln \mathcal{Z}(\xi_\alpha) = -t_M \int \frac{d\omega}{4\pi} \ln \det \left[ 1 - \sum_{\gamma \neq \alpha=1}^r (G_0^r \Gamma_\alpha G_0^a \Gamma_\gamma) \mathcal{K}_{\gamma\alpha}(\omega; \xi_\alpha) \right]. \quad (5.50)$$

## 5.7 Summary

In summary, we have extended the study of FCS for heat transport from a lead-junction-lead setup to a multi-terminal system without the junction part. We found a concise expression for the generalized CGF on contour. In the stationary state the expression for CGF for heat is obtained. The transient and steady-state fluctuation theorems are explicitly verified. For two-terminal case the effect on the cumulants and current for two specific form of the coupling are shown. It is interesting to study the heat-current for other forms of time-dependent coupling as studied in Ref. [1] to manipulate the heat flow through the leads and model it to act as a heat-pump. In the long-time limit, invoking time translational invariance we show that the CGF can be expressed in terms of a new transmission function which is useful for the study of interface effects. We also discuss the effect of interface coupling and absolute temperature of the heat baths on XFT which are important for the validity of the theorem. The consequences on the cumulants of heat due to finite size of the systems is also studied.

# Bibliography

- [1] E. C. Cuansing, and J.-S. Wang, Phys. Rev. E **82**, 021116, (2010).
- [2] E. C. Cuansing, and J.-S. Wang, Phys. Rev. B **81**, 052302, (2010).
- [3] E. C. Cuansing, G. Liang, J. Appl. Phys **110**, 083704 (2011).
- [4] L. Zhang, P. Keblinski, J.-S. Wang, and B. Li, Phys. Rev. B **83**, 064303 (2011).
- [5] C. Jarzynski, D. K. Wójcik, Phys. Rev. Lett. **92** 230602 (2004).
- [6] K. Saito and Y. Utsumi, Phys. Rev. B **78**, 115429 (2008).
- [7] D. Andrieux, P. Gaspard, T. Monnai, and S. Tasaki, New. J. Phys. **11**, 043014 (2009).
- [8] M. Campisi, P. Hänggi, and P. Talkner, Rev. Mod. Phys. **83**, 771 (2011).
- [9] M. Esposito, U. Harbola, and S. Mukamel, Rev. Mod. Phys. **81**, 1665 (2009).

## BIBLIOGRAPHY

---

- [10] Y. Utsumi, D. S. Golubev, M. Marthaler, K. Saito, T. Fujisawa, and Gerd Schön, Phys. Rev. B **81**,125331 (2010).
- [11] S Akagawa and N Hatano, Prog. Theor. Phys. **6**, 121 (2009).
- [12] G. Gallavotti and E. G. D. Cohen, Phys. Rev. Lett. **74**,2694 (1995).
- [13] A. Kundu, S. Sabhapandit, and A. Dhar, J. Stat. Mech (2011) P03007.
- [14] Sanjib Sabhapandit EPL **96**, 20005 (2011).
- [15] P. Visco, J. Stat. Mech.P06006 (2006).
- [16] E. C. Cuansing, H. Li, and J.-S. Wang, Phys. Rev. E **86**, 031132 (2012).
- [17] M. Di ventra, *Electrical Transport in Nanoscale Systems*, (Cambridge University Press, Cambridge, 2008).
- [18] Kubo, R., M. Toda, and N. Hashitsume, 1998, *Statistical Physics II: Nonequilibrium Statistical Mechanics*, 2nd ed. (Springer, New York).
- [19] B. K. Agarwalla, B. Li, and J.-S. Wang, Phys. Rev. E **85**, 051142 (2012).

## Chapter 6

# Full-counting statistics in nonlinear junctions

Up to now our main focus was on the FCS for transferred heat in ballistic systems. The task is now to develop a formalism to study FCS theory for general anharmonic junctions. It is a well known fact that nonlinearity plays an important role in thermal transport. For example it is crucial for umklapp scattering which gives rise to finite thermal conductivity for bulk systems as pointed out by Peierls [1]. The nonlinearity, such as the phonon-phonon interaction, has been found of special importance in the construction of many phononic devices such as thermal rectifier, heat pump [2–4]. In addition, recently it has been noted that the nonlinearity of interaction is crucial to the manifestation of geometric heat flux. [5, 6] Therefore, it is desirable to establish a systematic and practical formalism to properly

deal with cumulants of heat transfer in the presence of nonlinearity.

Some works have already been devoted to the analysis of fluctuation considering the effect of nonlinearity in the electronic transport such as the FCS in molecular junctions with electron-phonon interaction [7–9], Anderson impurity model, quantum dot in Aharonov-Bohm interferometer [10] and in the classical limit through Langevin dynamics [11, 12]. Also, many of these developed approaches dealing with nonlinear FCS problems mainly focus on single-particle systems, such as in Ref. [13].

In this chapter we study the FCS for heat transfer flowing across a quantum junction in the presence of general phonon-phonon interactions. Based on the nonequilibrium version of Feynman-Hellmann theorem we construct a concise and rigorous cumulant generating function (CGF) expression for the heat transfer in this general situation which is valid for arbitrary transient time. As an illustration of this general formalism we consider a single site junction with a quartic nonlinear on-site pinning potential and obtain the CGF exact up to first order of the nonlinear interaction strength. We also employ a self-consistent scheme to numerically illustrate the nonlinear effects on first three cumulants of heat transfer. We explicitly verify the Gallavotti-Cohen fluctuation symmetry in the first order.

## 6.1 Hamiltonian Model

As before, we consider the lead-junction-lead model initially prepared in a product state  $\rho(t_0) = \prod_{\alpha=L,C,R} \frac{e^{-\beta_\alpha \mathcal{H}_\alpha}}{\text{Tr}(e^{-\beta_\alpha \mathcal{H}_\alpha})}$ . It can be imagined that left lead ( $L$ ), center junction ( $C$ ), and right lead ( $R$ ) in this model were in contact with three different heat baths at the inverse temperatures  $\beta_L = (k_B T_L)^{-1}$ ,  $\beta_C = (k_B T_C)^{-1}$  and  $\beta_R = (k_B T_R)^{-1}$ , respectively, for time  $t < t_0$ . At time  $t = t_0$ , all the heat baths are removed, and couplings of the center junction with the leads  $\mathcal{H}_{LC} = u_L^T V^{LC} u_C$  and  $\mathcal{H}_{CR} = u_C^T V^{CR} u_R$  and the nonlinear term  $\mathcal{H}_n$  appearing in the center junction are switched on abruptly. Now the total Hamiltonian is given by

$$\mathcal{H} = \mathcal{H}_L + \mathcal{H}_C + \mathcal{H}_R + \mathcal{H}_{LC} + \mathcal{H}_{CR} + \mathcal{H}_n, \quad (6.1)$$

where  $\mathcal{H}_\alpha = \frac{1}{2} p_\alpha^T p_\alpha + \frac{1}{2} u_\alpha^T K^\alpha u_\alpha$ ,  $\alpha = L, C, R$ , represents coupled harmonic oscillators. The formalism developed here does not require to specify the explicit form of  $\mathcal{H}_n$ .

### Nonequilibrium version of Feynman-Hellman theorem

Based on the two-time observation protocol the characteristic function (CF) for heat transfer during the time  $t_M - t_0$  is written as before [14–17],

$$\mathcal{Z}(\xi) = \langle \mathcal{U}_{\xi/2}(t_0, t_M) \mathcal{U}_{-\xi/2}(t_M, t_0) \rangle_{\rho(t_0)}, \quad (6.2)$$

The key step to derive the nonequilibrium Feynman-Hellman theorem is to generalize the CF by introducing two different parameters  $\lambda_1$  and  $\lambda_2$  on

the upper and lower branches respectively and construct a general CF as

$$\mathcal{Z}(\lambda_2, \lambda_1) \equiv \langle \mathcal{U}_{\lambda_2}(t_0, t_M) \mathcal{U}_{\lambda_1}(t_M, t_0) \rangle_{\rho(t_0)} = \left\langle T_C e^{-\frac{i}{\hbar} \int_C d\tau \mathcal{T}_\lambda(\tau)} \right\rangle_{\rho(t_0)}, \quad (6.3)$$

with  $\mathcal{T}_\lambda(\tau)$  is in the interaction picture, given as

$$\mathcal{T}_\lambda(\tau) = \hat{u}_L^{x,T}(\tau) V^{LC} \hat{u}_C(\tau) + \hat{u}_C^T(\tau) V^{CR} \hat{u}_R(\tau) + \hat{\mathcal{H}}_n(\tau). \quad (6.4)$$

(a caret is put above operators to denote their  $\tau$  dependence with respect to the free Hamiltonian  $\mathcal{H}_0 = \mathcal{H}_L + \mathcal{H}_C + \mathcal{H}_R$  such as  $\hat{u}_C(\tau) = e^{\frac{i}{\hbar} \mathcal{H}_C \tau} u_C e^{-\frac{i}{\hbar} \mathcal{H}_C \tau}$ , and  $\hat{u}_L^x(\tau) = \hat{u}_L(\tau + \hbar x(\tau))$  with  $x(\tau) = \lambda_1$  ( $\lambda_2$ ) for  $\tau = t^+$  ( $t^-$ ) on the upper (lower) branch of the contour  $C$ .

Now we define an adiabatic potential  $\mathcal{U}(t, \lambda_2, \lambda_1)$  satisfying [13]

$$\mathcal{Z}(\lambda_2, \lambda_1) = \exp \left[ -\frac{i}{\hbar} \int_{t_0}^{t_M} dt \mathcal{U}(t, \lambda_2, \lambda_1) \right], \quad (6.5)$$

so that we could apply the nonequilibrium version of the Feynman-Hellmann theorem [18] to get

$$\begin{aligned} \frac{\partial}{\partial \lambda_1} \mathcal{U}(t, \lambda_2, \lambda_1) &= \frac{1}{\mathcal{Z}(\lambda_2, \lambda_1)} \left\langle T_C \frac{\partial \mathcal{T}_\lambda(t^+)}{\partial \lambda_1} e^{-\frac{i}{\hbar} \int_C d\tau \mathcal{T}_\lambda(\tau)} \right\rangle \\ &\equiv \left\langle T_C \frac{\partial \mathcal{T}_\lambda(t^+)}{\partial \lambda_1} \right\rangle_\lambda. \end{aligned} \quad (6.6)$$

Note that in Eq. (6.6) we define the  $\lambda$  dependent average as

$$\langle \mathcal{A}(t^+) \rangle_\lambda = \langle T_C \mathcal{A}(t^+) e^{-\frac{i}{\hbar} \int d\tau \mathcal{T}_\lambda(\tau)} \rangle \quad (6.7)$$

and similarly for the multipoint averages. Also note that  $\langle \mathcal{A}(t^+) \rangle_\lambda \neq \langle \mathcal{A}(t^-) \rangle_\lambda$ . Therefore in this formulation, to obtain the adiabatic potential one needs to calculate these  $\lambda$  dependent Green's functions.

### Generalized Meir-Weingreen formula

Computing the derivative  $\partial \mathcal{T}_\lambda / \partial \lambda_1$  we obtain

$$\frac{\partial T_\lambda(t^+)}{\partial \lambda_1} = \hbar \frac{\partial \hat{u}_L^T(t^+)}{\partial t^+} V^{LC} u_C(t^+). \quad (6.8)$$

After the treatment of symmetrization on Eq. (6.6), we can write

$$\frac{\partial \ln \mathcal{Z}(\lambda_2, \lambda_1)}{\partial \lambda_1} = \frac{\hbar}{2} \int_{t_0}^{t_M} dt \frac{\partial}{\partial t'} \text{Tr} \left[ \tilde{G}_{CL}^t(t, t') V^{LC} + \tilde{G}_{LC}^t(t', t) V^{CL} \right]_{t'=t}. \quad (6.9)$$

The contour-ordered version for  $\tilde{G}_{LC}(\tau, \tau')$  is given as

$$\begin{aligned} \tilde{G}_{LC}(\tau_1, \tau_2) &= -\frac{i}{\hbar} \langle T_\tau \hat{u}_L(\tau_1) \hat{u}_C^T(\tau_2) \rangle_\lambda \\ &= \int_C d\tau \tilde{g}_L(\tau_1, \tau) V^{LC} \tilde{G}_{CC}(\tau, \tau_2), \end{aligned} \quad (6.10)$$

where the shifted bare Green's function for the left-lead is given by

$$\tilde{g}_L(\tau_1, \tau_2)_{jk} = -\frac{i}{\hbar} \langle T_\tau \hat{u}_{L,j}^x(\tau_1) \hat{u}_{L,k}^x(\tau_2) \rangle_{\rho_L(t_0)}, \quad (6.11)$$

and  $V^{CL} = (V^{LC})^T$ . Similar expression is also valid for  $\tilde{G}_{CL}(\tau_1, \tau_2)$ . Here

$\tilde{G}_{CC}$  is defined as

$$\begin{aligned} \left[ \tilde{G}_{CC}(\tau_1, \tau_2) \right]_{jk} &\equiv -\frac{i}{\hbar} \langle T_C \hat{u}_{C,j}(\tau_1) \hat{u}_{C,k}(\tau_2) \rangle_\lambda \\ &= \begin{bmatrix} \tilde{G}_{CC}^t(t_1, t_2) & \tilde{G}_{CC}^<(t_1, t_2) \\ \tilde{G}_{CC}^>(t_1, t_2) & \tilde{G}_{CC}^{\bar{t}}(t_1, t_2) \end{bmatrix}, \end{aligned} \quad (6.12)$$

Using these in Eq. (6.9) we obtain a generalized Meir-Wingreen formula [19] as

$$\frac{\partial \ln \mathcal{Z}(\lambda_2, \lambda_1)}{\partial \lambda_1} = -\frac{\hbar}{2} \int_{t_0}^{t_M} dt dt' \text{Tr} \left[ \tilde{G}_{CC}^>(t, t') \frac{\partial \tilde{\Sigma}_L^<(t', t)}{\partial t'} + \tilde{G}_{CC}^<(t, t') \frac{\partial \tilde{\Sigma}_L^>(t', t)}{\partial t} \right], \quad (6.13)$$

where the lesser and greater version of  $\tilde{\Sigma}_L$  is defined as  $\tilde{\Sigma}_L^{<,>} = V^{CL} \tilde{g}_L^{<,>} V^{LC}$ . Here we employ the procedure of symmetrization to get rid of the time-ordered version of  $\tilde{G}_{CC}(\tau_1, \tau_2)$ , which will appear in Eq. (6.13) without symmetrization. The components for the shifted self energy are written in terms of the ordinary self energy as

$$\begin{aligned} \tilde{\Sigma}_L^<(t', t) &= \Sigma_L^<(t' - t + \hbar\lambda_1 - \hbar\lambda_2) \\ \tilde{\Sigma}_L^>(t', t) &= \Sigma_L^>(t' - t + \hbar\lambda_2 - \hbar\lambda_1). \end{aligned} \quad (6.14)$$

Furthermore, later after realizing that  $\mathcal{Z}(\lambda_2, \lambda_1) = \mathcal{Z}(\lambda_2 - \lambda_1)$ , and setting  $\lambda_1 = -\xi/2$  and  $\lambda_2 = \xi/2$ , Eq. (6.13) can be lumped into a compact form

$$\frac{\partial \ln \mathcal{Z}}{\partial (i\xi)} = \frac{1}{2} \int_C d\tau \int_C d\tau' \text{Tr} \left[ \tilde{G}_{CC}(\tau, \tau') \frac{\partial \tilde{\Sigma}_L(\tau', \tau)}{\partial (i\xi)} \right], \quad (6.15)$$

which shows that the derivative of the connected vacuum diagrams are closely related to the contour-ordered Green's functions, and could be also obtained based on the field theoretical/diagrammatic method [20, 21]. The tilde on the Green's functions emphasizes the fact that they are counting field  $\xi$ -dependent. And if needed, the proper normalization for the CGF, *i.e.*,  $\ln \mathcal{Z}(\xi)$ , can be determined by the constraint  $\ln \mathcal{Z}(0) = 0$ .

---

### Ballistic case $\mathcal{H}_n = 0$

For harmonic junction we previously obtain an analytic expression for  $\ln \mathcal{Z}(\xi)$ . Here we show that the derivative of the CGF for the ballistic system can also be written in the above form. The CGF as shown previously reads as (see Eq. (3.46))

$$\ln \mathcal{Z}(\xi) = -\frac{1}{2} \text{Tr}_{j,\tau} \ln \left[ \mathbf{1} - \mathbf{G}_0 \Sigma_L^A \right], \quad (6.16)$$

Let us now consider the  $n$ -th order term of the log series and take the derivative with respect to the counting field  $\xi$ . Note that here the counting field dependence is only through  $\Sigma_L^A$ .

The  $n$ -th order term in the continuous contour time is written as

$$\int d\tau_1 \int d\tau_2 \cdots \int d\tau_n \frac{1}{2^n} \text{Tr}_j \left[ G_0(\tau_1, \tau_2) \Sigma_L^A(\tau_2, \tau_3) \cdots G_0(\tau_{n-1}, \tau_n) \Sigma_L^A(\tau_n, \tau_1) \right]. \quad (6.17)$$

The derivative of the above expression with respect to  $i\xi$  will generate  $n$  terms, which are all equal due to the dummy integration variables and therefore cancel the factor  $n$  sitting in the denominator. We may then write

$$\int d\tau_1 \int d\tau_2 \cdots \int d\tau_n \frac{1}{2} \text{Tr}_j \left[ G_0(\tau_1, \tau_2) \Sigma_L^A(\tau_2, \tau_3) \cdots G_0(\tau_{n-1}, \tau_n) \frac{\partial \tilde{\Sigma}_L(\tau_n, \tau_1)}{\partial(i\xi)} \right], \quad (6.18)$$

Where  $\Sigma_L^A = \tilde{\Sigma}_L - \Sigma$  and  $\partial \Sigma_L^A / \partial(i\xi) = \partial \tilde{\Sigma}_L / \partial(i\xi)$ . So the derivative of the CGF can be written as

$$\frac{\partial \ln \mathcal{Z}}{\partial(i\xi)} = -\frac{1}{2} \text{Tr}_{j,\tau} \left[ (\mathbf{G}_0 + \mathbf{G}_0 \Sigma_L^A \mathbf{G}_0 + \cdots) \frac{\partial \tilde{\Sigma}_L}{\partial(i\xi)} \right]. \quad (6.19)$$

Now defining a new Green's function  $\tilde{\mathbf{G}}_0 = \mathbf{G}_0 + \mathbf{G}_0 \Sigma_L^A \mathbf{G}_0 + \cdots$ , we write the above equation as

$$\frac{\partial \ln \mathcal{Z}}{\partial(i\xi)} = -\frac{1}{2} \text{Tr}_{j,\tau} \left[ \tilde{\mathbf{G}}_0 \frac{\partial \tilde{\Sigma}_L}{\partial(i\xi)} \right], \quad (6.20)$$

or more explicitly (in the continuous contour time notation) it reads

$$\frac{\partial \ln \mathcal{Z}}{\partial(i\xi)} = -\frac{1}{2} \int d\tau \int d\tau' \text{Tr} \left[ \tilde{G}_0(\tau, \tau') \frac{\partial \tilde{\Sigma}_L(\tau', \tau)}{\partial(i\xi)} \right]. \quad (6.21)$$

Note that in the absence of  $\mathcal{H}_n$   $\tilde{G}_{CC}$  defined in Eq. (6.12) is equal to  $\tilde{G}_0$ .

### Interaction-interaction picture

In order to evaluate  $\ln \mathcal{Z}$ , a closed equation for  $\tilde{G}_{CC}(\tau_1, \tau_2)$  is needed, which could be deduced by a transformation from  $\hat{\mathcal{O}}(\tau)$  to  $\mathcal{O}^I(\tau)$  taking  $t_0^+$  as a fixed reference time such as  $u_C^I(\tau) = \mathcal{V}(t_0^+, \tau) \hat{u}_C(\tau) \mathcal{V}(\tau, t_0^+)$ , with

$$\mathcal{V}(\tau, t_0^+) = T_C e^{-\frac{i}{\hbar} \int_C [\tau, t_0^+] d\tau' [\hat{u}_L^{x,T} V^{LC} \hat{u}_C + \hat{u}_C^T V^{CR} \hat{u}_R]}, \quad (6.22)$$

and  $\mathcal{V}(t_0^+, \tau) = \mathcal{V}(\tau, t_0^+)^{-1}$ , where the subscript  $C[\tau, t_0^+]$  denotes the path along the contour  $C$  from  $t_0^+$  to  $\tau$ . Instructively, alternative forms for  $\mathcal{V}(\tau, t_0^+)$  can be given as

$$\mathcal{V}(t^-, t_0^+) = e^{\frac{i}{\hbar} ht} \mathcal{U}_{\lambda_2}^0(t, t_M) \mathcal{U}_{\lambda_1}^0(t_M, t_0) e^{-\frac{i}{\hbar} ht_0} \quad (6.23)$$

$$\mathcal{V}(t^+, t_0^+) = e^{\frac{i}{\hbar} ht} \mathcal{U}_{\lambda_1}^0(t, t_0) e^{-\frac{i}{\hbar} ht_0}, \quad (6.24)$$

Where, the superscript 0 in  $\mathcal{U}_{\lambda_1}^0(t_M, t_0)$  denotes that the nonlinear term  $\mathcal{H}_n = 0$  in the corresponding  $\mathcal{U}_{\lambda_1}(t_M, t_0)$ . Based on this form, we easily notice that the group property  $\mathcal{V}(\tau_3, \tau_1) = \mathcal{V}(\tau_3, \tau_2) \mathcal{V}(\tau_2, \tau_1)$  hold on the contour. The present transformation defined on the contour  $C$  is necessary, since the coupling Hamiltonian with counting field is different on the upper and lower branch respectively.

Then according to Eq. (6.12),  $\tilde{G}_{CC}(\tau_1, \tau_2)$  can be rewritten as

$$\left[ \tilde{G}_{CC}(\tau_1, \tau_2) \right]_{jk} = -\frac{i}{\hbar} \text{Tr} \left[ \rho^I(t_0) T_C u_{C,j}^I(\tau_1) u_{C,k}^I(\tau_2) e^{-\frac{i}{\hbar} \int_C d\tau \mathcal{H}_n^I(\tau)} \right] \frac{1}{\mathcal{Z}_n}, \quad (6.25)$$

in terms of  $\rho^I(t_0) = \rho(t_0)A/\mathcal{Z}_0$  ( $\text{Tr}(\rho^I(t_0)) = 1$ ) and  $\mathcal{Z}_n = \mathcal{Z}/\mathcal{Z}_0$ , where

$$\mathcal{Z}_0 = \left\langle T_C e^{-\frac{i}{\hbar} \int_C d\tau (\hat{u}_L^x T V^{LC} \hat{u}_C + \hat{u}_C^T V^{CR} \hat{u}_R)} \right\rangle, \quad (6.26)$$

is the CF when  $\mathcal{H}_n = 0$  and  $A \equiv \mathcal{V}(t_0^-, t_M) \mathcal{V}(t_M, t_0^+)$ . Now the benefit of the transformation to the second interaction picture defined on the contour is remarkable, that is, the extra term  $A$  always appearing at the left-most position after contour-ordering can be taken out of  $T_C$  to combine with  $\rho(t_0)/\mathcal{Z}_0$  to yield  $\rho^I(t_0)$ .

Still in this transformed picture  $I$  the Wick theorem is valid, which is directly inherited from the validity of Wick's theorem in the interaction picture with respect to  $\hbar$ , and thus the Dyson equation for  $\tilde{G}_{CC}$  is obtained from Eq. (6.25) as

$$\tilde{G}_{CC}(\tau_1, \tau_2) = \tilde{G}_{CC}^0(\tau_1, \tau_2) + \int_C \int_C d\tau d\tau' \tilde{G}_{CC}^0(\tau_1, \tau) \tilde{\Sigma}_n(\tau, \tau') \tilde{G}_{CC}(\tau', \tau_2), \quad (6.27)$$

which in the matrix (in discretized contour time) representation is written as  $\tilde{\mathbf{G}}_{CC} = \tilde{\mathbf{G}}_{CC}^0 + \tilde{\mathbf{G}}_{CC}^0 \tilde{\Sigma}_n \tilde{\mathbf{G}}_{CC}$  and  $\tilde{G}_{CC}^0 = -\frac{i}{\hbar} \text{Tr} \left[ \rho^I(t_0) T_\tau u_C^I(\tau_1) u_C^{I,T}(\tau_2) \right]$  is given as

$$\tilde{\mathbf{G}}_{CC}^0 = \mathbf{g}_C + \mathbf{g}_C \left( \tilde{\Sigma}_L + \Sigma_R \right) \tilde{\mathbf{G}}_{CC}^0, \quad (6.28)$$

Note that the nonlinear self energy  $\tilde{\Sigma}_n$  constructed by  $\tilde{G}_{CC}^0$  is solely due to

the nonlinear Hamiltonian  $\mathcal{H}_n$ .

After introducing the Dyson equation for the ballistic system

$$\mathbf{G}_{CC}^0 = \mathbf{g}_C + \mathbf{g}_C (\boldsymbol{\Sigma}_L + \boldsymbol{\Sigma}_R) \mathbf{G}_{CC}^0, \quad (6.29)$$

and combining it with Eqs. (6.27) and (6.28), the closed Dyson equation for  $\tilde{G}_{CC}(\tau_1, \tau_2)$  could be obtained as

$$\tilde{\mathbf{G}}_{CC} = \mathbf{G}_{CC}^0 + \mathbf{G}_{CC}^0 \left( \boldsymbol{\Sigma}_L^A + \tilde{\boldsymbol{\Sigma}}_n \right) \tilde{\mathbf{G}}_{CC}, \quad (6.30)$$

where the shifted self energy  $\Sigma_L^A \equiv \tilde{\Sigma}_L - \Sigma_L$ , which first appear in Ref. [14], accounts for the FCS in ballistic systems. Now it is clear that  $\mathcal{Z}(\lambda_2, \lambda_1) = \mathcal{Z}(\lambda_2 - \lambda_1)$ , since the elementary block  $\tilde{G}_{CC}^0$  constructing the nonlinear self energy  $\tilde{\Sigma}_n$  satisfy Eq. (6.28) and  $\tilde{\Sigma}_L$  depends only on  $\lambda_2 - \lambda_1$ .

From now on, for notational simplicity, all the subscripts  $CC$  of the Green's functions will be suppressed and the superscript 0 in both  $\tilde{G}_{CC}^0$  and  $G_{CC}^0$  will be re-expressed as a subscript.

## 6.2 Steady state limit

Proceeding to study cumulants of steady-state heat transfer explicitly, one simply set  $t_0 \rightarrow -\infty$  and  $t_M \rightarrow +\infty$  simultaneously, and technically assume that real-time versions of  $\tilde{G}(\tau_1, \tau_2)$  are time-translationally invariant. Then

going to the Fourier space, Eq. (6.15) for  $\frac{\partial \ln \mathcal{Z}}{\partial(i\xi)}$  in steady state could be rewritten as

$$\frac{1}{t_M - t_0} \frac{\partial \ln \mathcal{Z}(\xi)}{\partial(i\xi)} = \int_{-\infty}^{\infty} d\omega \frac{\hbar\omega}{4\pi} \text{Tr} \left[ \tilde{G}^<[\omega] \Sigma_L^>[\omega] e^{-i\hbar\omega\xi} - \tilde{G}[\omega]^> \Sigma_L^<[\omega] e^{i\hbar\omega\xi} \right], \quad (6.31)$$

which after taking into account  $\tilde{G}^>[-\omega] = \tilde{G}^<[\omega]^T$  and  $\Sigma_L^<[-\omega] = \Sigma_L^>[\omega]^T$  can also be written as

$$\frac{1}{t_M - t_0} \frac{\partial \ln \mathcal{Z}(\xi)}{\partial(i\xi)} = \int_{-\infty}^{\infty} d\omega \frac{\hbar\omega}{2\pi} \text{Tr} \left[ \tilde{G}^< \Sigma_L^> e^{-i\hbar\omega\xi} \right]. \quad (6.32)$$

In the Fourier space, due to Eq. (6.30) exact result for  $\tilde{G}[\omega]$  could be yielded as

$$\tilde{G}[\omega] = \left( G_0[\omega]^{-1} - \Sigma_A[\omega] - \tilde{\Sigma}_n[\omega] \right)^{-1}, \quad (6.33)$$

when keeping in mind the convention that the contour-order Green's function such as  $\tilde{G}(\tau_1, \tau_2)$  in frequency space is written as

$$\tilde{G}[\omega] = \begin{bmatrix} \tilde{G}^t[\omega] & \tilde{G}^<[\omega] \\ -\tilde{G}^>[\omega] & -\tilde{G}^{\bar{t}}[\omega] \end{bmatrix} \quad (6.34)$$

(Note that here  $\tilde{G}[\omega]$  is already multiplied with the Pauli  $\sigma_z$  matrix)

One step forward, solving Eq. (6.33) for the less component of  $\tilde{G}[\omega]$ , the

CGF in Eq. (6.32) can be explicitly written as

$$\begin{aligned} \ln \mathcal{Z}(\xi) = & i(t_M - t_0) \int d\xi \int_{-\infty}^{\infty} d\omega \frac{\hbar\omega}{2\pi} e^{-i\hbar\omega\xi} \text{Tr} \left\{ \Sigma_\eta^{>-1} \Sigma_L^> \right. \\ & \left. \times \left[ I + \Sigma_\eta^{>-1} \left( g_C^{a-1} + \Sigma_\eta^{\bar{t}} \right) \Sigma_\eta^{<-1} \left( g_C^{r-1} - \Sigma_\eta^t \right) \right]^{-1} \right\}, \end{aligned} \quad (6.35)$$

with

$$\Sigma_\eta^> [-\omega]^T = \Sigma_\eta^< [\omega] = \Sigma_R^< [\omega] + \Sigma_L^< [\omega] e^{i\hbar\omega\xi} + \tilde{\Sigma}_n^< [\omega] \quad (6.36)$$

$$\Sigma_\eta^t [\omega] = \Sigma_R^t [\omega] + \Sigma_L^t [\omega] + \tilde{\Sigma}_n^t [\omega] \quad (6.37)$$

$$\Sigma_\eta^{\bar{t}} [\omega] = \Sigma_R^{\bar{t}} [\omega] + \Sigma_L^{\bar{t}} [\omega] + \tilde{\Sigma}_n^{\bar{t}} [\omega]. \quad (6.38)$$

### 6.3 Application and verification

#### Monoatomic molecule with a quartic on-site pinning potential

Now we apply the general formalism developed above to study a Monoatomic molecule with a quartic nonlinear on-site pinning potential, that is,

$$\mathcal{H}_n = \frac{1}{4} \lambda u_{C,0}^4, \quad (6.39)$$

in Eq. (6.1). In this case, nonlinear contour-order self energy exact up to first order in nonlinear strength

$$\tilde{\Sigma}_n(\tau, \tau') = 3i\hbar\lambda \tilde{G}_0(\tau, \tau') \delta(\tau, \tau'), \quad (6.40)$$

where the generalized  $\delta$ -function  $\delta(\tau, \tau')$  is the counterpart of the ordinary Dirac delta function on the contour  $C$ . Thus the corresponding frequency-space nonlinear self energy is

$$\tilde{\Sigma}_n[\omega] = 3i\hbar\lambda \begin{bmatrix} \tilde{G}_0^t(0) & 0 \\ 0 & \tilde{G}_0^{\bar{t}}(0) \end{bmatrix}. \quad (6.41)$$

Consequently, exact up to first order in nonlinear strength the CGF for the molecular junction could be given as

$$\begin{aligned} \frac{1}{(t_M - t_0)} \frac{\partial \ln \mathcal{Z}(\xi)}{\partial (i\xi)} &= - \int_{-\infty}^{\infty} \frac{d\omega}{4\pi} \left\{ \frac{\partial \ln D[\omega]}{\partial (i\xi)} - 3i\hbar\lambda \right. \\ &\times \left. \left[ \tilde{G}_0^t(0) G_0^t[\omega] - \tilde{G}_0^{\bar{t}}(0) G_0^{\bar{t}}[\omega] \right] \frac{\partial}{\partial (i\xi)} \frac{1}{D[\omega]} \right\}, \end{aligned} \quad (6.42)$$

with

$$\begin{aligned} D[\omega] &\equiv \det \left[ I - G_0[\omega] \Sigma_L^A[\omega] \right] = \det \left[ I - \check{G}_0[\omega] \check{\Sigma}_L^A[\omega] \right] \\ &= 1 - \text{Tr}[\mathcal{T}[\omega]] \left[ (e^{i\xi\hbar\omega} - 1) f_L(1 + f_R) + (e^{-i\xi\hbar\omega} - 1) f_R(1 + f_L) \right], \end{aligned} \quad (6.43)$$

and  $\tilde{G}_0^{t,\bar{t}}(0) = \int_{-\infty}^{\infty} \frac{d\omega}{2\pi} G_0^{t,\bar{t}}[\omega] / D[\omega]$ , where  $\text{Tr}[\mathcal{T}[\omega]] = \text{Tr}(G_0^r \Gamma_R G_0^a \Gamma_L)$  is the transmission coefficient in the ballistic system, and  $f_\alpha = [\exp(\beta_\alpha \hbar\omega) - 1]^{-1}$  is the Bose-Einstein distribution function for the phonons in the leads.  $\check{G}_0$  is in the Keldysh space. Here  $G_0^r = G_0^t - G_0^<$  and  $G_0^a = G_0^< - G_0^{\bar{t}}$  are retarded and advanced Green's functions, respectively. Also  $\Gamma_\alpha = i[\Sigma_\alpha^r - \Sigma_\alpha^a]$ , related to the spectral density of the baths, are expressed by retarded and advanced self energies similarly defined as Green's functions.

### Gallavotti-Cohen symmetry

Eq. (6.42) satisfies Gallavotti-Cohen symmetry [23] for the derivatives, since  $D[\omega]$  remains invariant under the transformation  $\xi \rightarrow -\xi + i(\beta_R - \beta_L)$ , as shown before, while the derivative  $\partial D[\omega] / \partial(i\xi)$  changes the sign.

### Recovering ballistic result

For  $\lambda = 0$  in Eq. (6.42) the integration over  $\xi$  can be performed explicitly and the CGF can be written down as

$$\ln \mathcal{Z}(\xi) = -(t_M - t_0) \int \frac{d\omega}{4\pi} \ln \det \left[ 1 - \check{G}_0[\omega] \check{\Sigma}_L^A[\omega] \right], \quad (6.44)$$

which is the ballistic result [11, 15, 16] derived in Chapter 3.

### First two cumulants

One could easily use this CGF in Eq. (6.42) to evaluate cumulants. The steady current out of the left lead is closely related to the first cumulant so that

$$\begin{aligned} \mathcal{I}_L &\equiv \frac{d}{dt_M} \left( \left. \frac{\partial \ln \mathcal{Z}(\xi)}{\partial(i\xi)} \right|_{\xi=0} \right) \\ &= \int_{-\infty}^{\infty} \frac{d\omega}{4\pi} \hbar \omega (1 + \Lambda[\omega]) \text{Tr}[\mathcal{T}[\omega]] (f_L - f_R), \end{aligned} \quad (6.45)$$

$$\Lambda[\omega] \equiv 3i\hbar\lambda G_0^t(0) (G_0^a[\omega] + G_0^r[\omega]), \quad (6.46)$$

is the first-order nonlinear correction to the transmission coefficient.

The fluctuation for steady-state heat transfer in the molecular junction is obtained by taking the second derivative with respect to  $i\xi$ , and then

setting  $\xi = 0$ :

$$\begin{aligned}
 \frac{\langle\langle Q^2 \rangle\rangle}{(t_M - t_0)} &= \int_{-\infty}^{\infty} \frac{d\omega}{4\pi} \left\{ (\hbar\omega)^2 \text{Tr}[\mathcal{T}^2[\omega]] (1 + 2\Lambda[\omega]) (f_L - f_R)^2 \right. \\
 &+ 3\hbar^2 \lambda \omega \left[ G_0^{\bar{t}}[\omega] \delta \tilde{G}_0^{\bar{t}} - G_0^t[\omega] \delta \tilde{G}_0^t \right] \text{Tr}[\mathcal{T}[\omega]] (f_L - f_R) \\
 &\left. + (\hbar\omega)^2 \text{Tr}[\mathcal{T}[\omega]] (1 + \Lambda[\omega]) (f_L + f_R + 2f_L f_R) \right\}, \quad (6.47)
 \end{aligned}$$

where,

$$\delta \tilde{G}_0^{t,\bar{t}} \equiv \left. \frac{\partial \tilde{G}_0^{\bar{t},t}(0)}{\partial \xi} \right|_{\xi=0} = -i \int_{-\infty}^{\infty} \frac{d\omega}{2\pi} \hbar\omega \text{Tr}[\mathcal{T}[\omega]] (f_L - f_R) G_0^{\bar{t},t}[\omega]. \quad (6.48)$$

Higher-order cumulants can be also systematically given by corresponding higher-order derivatives.

### **Special case: Pure harmonic chain**

It is worth mentioning that for a special case of a homogeneous spring chain plus one-site quartic nonlinear on-site potential,  $G_0^r[\omega]$  is imaginary (see appendix (E)) meaning  $\Lambda[\omega] = 0$ . In this situation, therefore, the first-order correction in nonlinear strength to the steady current Eq. (6.45) does not exist, while for the fluctuation the correction to the ballistic result is given only by the second term in Eq. (6.47).

### **6.3.1 Numerical results**

In the following, we will give a numerical illustration to the first few cumulants for heat transfer in this molecular junction using a self-consistent

procedure [8], which means that the nonlinear contour-order self energy is taken as

$$\tilde{\Sigma}_n(\tau, \tau') = 3i\hbar\lambda\tilde{G}(\tau, \tau')\delta(\tau, \tau'). \quad (6.49)$$

Very recently, it is shown that such self-consistent calculation gives extremely accurate results for the current in the case of a single site model as compared with master equation approach, [25] thus we believe that it should leads to excellent predictions for the FCS.

Specifically we self-consistently calculate  $\tilde{G}[\omega]$ ,  $\frac{\partial\tilde{G}[\omega]}{\partial(i\xi)}$  and higher derivatives based on Eq. (6.33), then the first few cumulants are obtained by the corresponding derivative of  $\ln \mathcal{Z}(\xi)$  in Eq. (6.32) with respect to  $i\xi$  at the point  $\xi = 0$ . In order to obtain  $m$ -th order cumulant one needs to solve  $(m - 1)$ -th derivative of  $\tilde{G}$  iteratively. For example, the iterative equation for computing the first derivative of  $\tilde{G}$  is given as

$$\frac{\partial\tilde{G}[\omega]}{\partial(i\xi)}\Big|_{\xi=0} = G[\omega]\left(\frac{\partial\tilde{\Sigma}_L[\omega]}{\partial(i\xi)}\Big|_{\xi=0} + \frac{\partial\tilde{\Sigma}_n[\omega]}{\partial(i\xi)}\Big|_{\xi=0}\right)G[\omega], \quad (6.50)$$

where  $G[\omega] = \tilde{G}[\omega]\Big|_{\xi=0}$ . The equation transforms to a linear equation for  $\partial\tilde{G}[\omega]/\partial(i\xi)$  by using the modified  $\tilde{\Sigma}_n[\omega]$ , which is then solved numerically by iteration. Equations for the higher derivatives can be similarly obtained.

In this numerical illustration, the Rubin baths are used, that is,  $K_\alpha$ ,  $\alpha = L, R$  in Eq. (6.1) are both the semi-infinite tridiagonal spring constant matrix consisting of  $2k + k_0$  along the diagonal and  $-k$  along the two off-diagonals. And only the nearest interaction  $V_{-1,0}^{LC}$  and  $V_{0,1}^{CR}$  between the molecular and the two bathes are considered and  $\mathcal{H}_C = \frac{1}{2}p_{C,0}^2 + \frac{1}{2}K_C u_{C,0}^2$ .

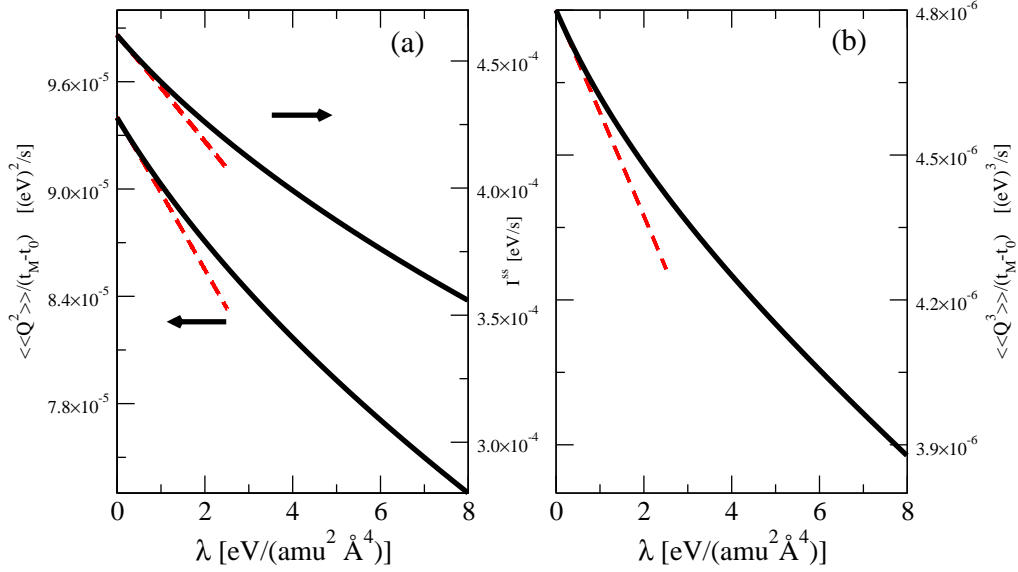


Figure 6.1: The first three steady-state cumulants with nonlinear coupling strength  $\lambda$  for  $k = 1 \text{ eV}/(\text{u}\text{\AA}^2)$ ,  $k_0 = 0.1k$ ,  $K_C = 1.1k$ , and  $V_{-1,0}^{LC} = V_{0,1}^{CR} = -0.25k$ . The solid (dashed) line shows the self-consistent (first-order in  $\lambda$ ) results for the cumulants. The temperatures of the left and right lead are 660 K and 410 K, respectively.

Figure 6.1 shows the plot for the first three cumulants with nonlinear strength  $\lambda$ . The effect of nonlinearity is to reduce the current as well as higher order fluctuations, and the fact that third and higher order cumulants are small but nonzero implies that the distribution for transferred energy is not Gaussian. For certain parameters (not shown) the third cumulant can change sign from positive to negative. Similar effect was also observed for a classical system [11].

Figure 6.2 shows the behavior of thermal conductance, defined as,

$$\sigma(T) = \lim_{T_L \rightarrow T, T_R \rightarrow T} \frac{I}{T_L - T_R}, \quad (6.51)$$

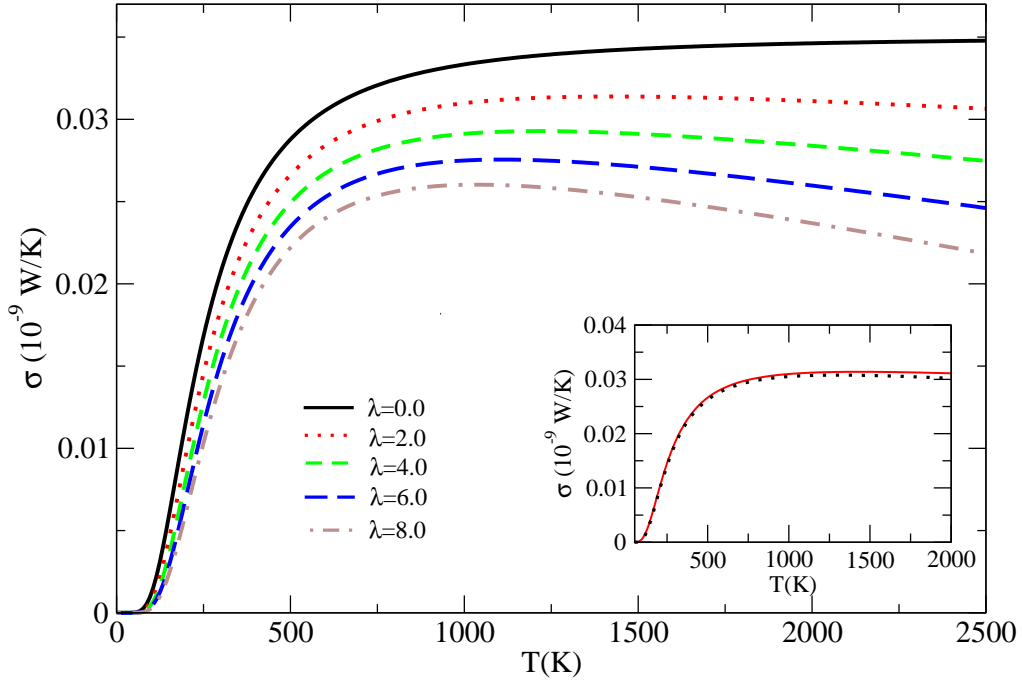


Figure 6.2: Thermal conductance with temperature for different coupling strength  $\lambda$  in unit of  $\text{eV}/(\text{amu}^2\text{\AA}^4)$  using self-consistent method for  $k = 1 \text{ eV}/(\text{amu}\text{\AA}^2)$ ,  $k_0 = 0.1k$ ,  $K_C = 1.1k$ , and  $V_{-1,0}^{LC} = V_{0,1}^{CR} = -0.25k$ . Inset shows the thermal conductance calculated using self-consistent procedure (solid line) and using Eq. (6.45) (dotted line) for  $\lambda = 2 \text{ eV}/(\text{amu}^2\text{\AA}^4)$ .

with equilibrium temperature  $T$  for different nonlinear strength  $\lambda$ . The similar self-consistent method is employed in Eq. (6.32) for  $\xi = 0$  to obtain the conductance for the above mentioned model. Reduction in conductance with nonlinearity is observed even at low-temperature regime in the chosen model.

In both the figures (see inset in Fig (6.2)) it is noted that for weak nonlinearity the first-order perturbation results coming from the established formalism, presented as dotted lines, are comparative with the corresponding self-consistent ones.

## 6.4 Summary

We develop a formally rigorous formalism dealing with cumulants of heat transfer in nonlinear quantum thermal transport. Based on NEGF techniques and most importantly nonequilibrium version of Feynman Hellman theorem we study the CGF for the heat transfer in both transient and steady-state regimes. For arbitrary nonlinear system, the derivative of the CGF with respect to the counting field is written in a closed form. A new feature of this formalism is that counting-field dependent full Green's function can be expressed solely through the nonlinear term  $\mathcal{H}_n^I(\tau)$  with an interaction picture transformation defined on a contour. Although we focus on the FCS of heat transfer in pure nonlinear phononic systems, there is no doubt that this general formalism can be readily employed to handle any other nonlinear system, such as electron-phonon interaction and Joule heating problems. Up to the first order in the nonlinear strength for the single-site quartic model, we obtain the CGF for steady-state heat transfer and also present explicit results for the steady current and fluctuation of steady-state heat transfer. We also employ a self-consistent procedure, which works well for strong nonlinearity, to check our general formalism.

# Bibliography

- [1] R. E. Peierls, *Quantum Theory of Solids* (Oxford University Press, London, 1955).
- [2] L.-A. Wu and D. Segal, Phys. Rev. Lett. **102**, 095503 (2009).
- [3] C. W. Chang, D. Okawa, A. Majumdar, and A. Zettl, Science **314**, 1121 (2006).
- [4] N. Li, J. Ren, L. Wang, G. Zhang, P. Hänggi, and B. Li, Rev. Mod. Phys. **84**, 1045 (2012).
- [5] J. Ren, P. Hänggi, and B. Li, Phys. Rev. Lett. **104**, 170601 (2010).
- [6] J. Ren, S. Liu, and B. Li, Phys. Rev. Lett. **108**, 210603 (2012).
- [7] R. Avriller and A. Levy Yeyati, Phys. Rev. B **80**, 041309 (2009).
- [8] T.-H. Park and M. Galperin, Phys. Rev. B **84**, 205450 (2011).
- [9] D. F. Urban, R. Avriller and A. Levy Yeyati, Phys. Rev. B **82**, 121414(R) (2010).
- [10] Y. Utsumi and K. Saito, Phys. Rev. B **79**, 235311 (2009).

## BIBLIOGRAPHY

---

- [11] K. Saito and A. Dhar, Phys. Rev. Lett. **99**, 180601 (2007).
- [12] S. Liu, B. K. Agarwalla, B. Li, and J.-S. Wang, arXiv:1211.5876.
- [13] A. O. Gogolin and A. Komnik, Phys. Rev. B **73**, 195301 (2006).
- [14] J.-S. Wang, B. K. Agarwalla, and H. Li, Phys. Rev. B **84**, 153412, (2011).
- [15] B. K. Agarwalla, B. Li, and J.-S. Wang, Phys. Rev. E **85**, 051142 (2012).
- [16] H. Li, B. K. Agarwalla, and J.-S. Wang, Phys. Rev. B **86**, 165425 (2012).
- [17] M. Esposito, U. Harbola, and S. Mukamel, Rev. Mod. Phys. **81**, 1665 (2009).
- [18] R. P. Feynman, Phys. Rev. **56**, 340 (1939).
- [19] H. Haug and A.-P. Jauho, *Quantum Kinetics in Transport and Optics of Semiconductors*, 2nd ed. (Springer, New York, 2008).
- [20] H. Kleinert, A. Pelster, B. Kastening, and M. Bachmann, Phys. Rev. E **62**, 1537 (2000).
- [21] A. Pelster and K. Glaum, Phys. A **335**, 455 (2004).
- [22] J.-S. Wang, J. Wang, and J. T. Lü, Eur. Phys. J. B **62**, 381 (2008).  
pen
- [23] G. Gallavotti and E. G. D. Cohen. Phys. Rev. Lett. **74**, 2694 (1995).

## BIBLIOGRAPHY

---

- [24] See Eq. (72) in J.-S. Wang, N. Zeng, J. Wang, and C. K. Gan, Phys. Rev. E **75**, 061128 (2007).
  
- [25] J. Thingna, J. L. García-palacios, and J.-S. Wang, Phys. Rev. B **85**, 195452 (2012).

# Chapter 7

## Summary and future outlook

This dissertation presents theoretical studies of energy-counting statistics and fluctuation theorems in the context of heat transport. Employing two-time projective measurement method and nonequilibrium Green's function technique we develop a formalism to study the statistics for heat and entropy production in general lattice systems.

To examine the behavior of heat, we first consider a harmonic lead-junction-lead model from a very general perspective, such as, arbitrary time-dependence of the coupling matrix between the leads and the junction, arbitrary dimensionality of the junction, finite size of the leads etc. We derive the generating function for integrated energy-current for three different initial conditions taking into consideration the initial measurement effect on the density operator. The cumulant generating function for arbitrary measurement time is expressed in terms of the Green's functions for the junction

and an argument shifted self-energy. However the meaning of this Green's functions depends on the initial conditions. In general, we show that the effect of energy measurement to obtain statistics for heat is reflected in the corresponding self-energy as the shift in the time-argument which turns out to be key quantity for the FCS problem. We perform numerical simulations for one dimensional harmonic chain and for a graphene junction and showed that the at short time the behavior of heat differs significantly from each other but finally approaches to a unique steady state, independent of the initial conditions.

For nonequilibrium steady state, we carefully examine the effect of quantum measurement. We found that the effect of measurement is always to feed energy into the measured (left) lead, even if the temperature of the left lead is lower than that of the right lead. In the long-time limit the CGF is written down simply in terms of the transmission function and a counting field dependent function satisfying the Gallavotti-Cohen (GC) fluctuation symmetry. Moreover, we introduce a generalized CGF to understand the correlations between the left and right lead heat and showed that in the steady state the CGF is a function of counting-field difference. The two-time measurement turns out to be the key concept to obtain the correct CGF in the sense that, it satisfies the GC symmetry. As an example, we explicitly show that Nazarov's CF does not respect the GC symmetry, at least for the harmonic model.

Next we investigate the CGF for heat generation for a forced-driven harmonic system connected with two thermal baths. Working with the generalized CGF we show that in the asymptotic limit forced-driven entropy production in the leads satisfy fluctuation symmetry. The CGF in long time is expressed in terms of force dependent transmission function. For Rubin heat bath we obtain explicit expression for the generalized CGF by exploiting the translational symmetry of the homogeneous system. For periodic driven force we investigate the effects on energy current for Rubin and Ohmic heat baths with system size and applied frequency. We also analyze the heat pumping behavior for this model.

Then we move to investigate the energy transport properties for a  $N$ -terminal setup without the junction part. The generalized CGF is expressed in terms of the surface Green's functions. For two-terminal case we obtain the transmission function which is useful for interface study. The transient version of the fluctuation theorem is verified where KMS boundary condition plays a crucial role. We also address the effect of coupling strength on the exchange fluctuation theorem for two terminal setup.

Finally, we generalize the counting statistics formalism for arbitrary nonlinear junction. Based on the nonequilibrium version of Feynman-Hellman theorem we show that the derivative of the cumulant generating function, with respect to the counting field, can be summed up exactly for general anharmonic potential. We derive the generalized version of the celebrated Meir-Weingreen formula using which all higher order cumulants can be systematically obtained. By introducing a new interaction picture on the

contour the center Green's function is expressed in terms of the counting field dependent nonlinear self-energy. As an illustration, we consider a molecular junction consist of a monoatomic molecule with quartic onsite potential. In the first order of the nonlinear strength we obtain analytical expression for the long-time CGF which satisfy GC symmetry. Employing self-consistent procedure for the nonlinear self-energy we investigate the behavior of the conductance and the cumulants of heat.

Overall, one key contribution of our study for the ballistic heat transport is that it generalizes numerous investigations that have only looked at what happens to the current in the stationary state. In addition of studying both transient and steady state on equal platform we consider different initial conditions where it is possible to show how system approaches to a unique steady state dynamically. Moreover the developed formalisms for the energy counting statistics is readily extendable for the charge counting as shown by an example in the appendix where we derive the famous Levitov-Lesovik formula for electrons using tight-binding Hamiltonian. For all this non-interacting problems we found that the long-time limit can be expressed by a transmission function, captures the properties of the junction and the leads, and an universal function which depends on the counting field and satisfy GC symmetry. Also thanks to the nonequilibrium version of Feynman Hellmann theorem using which the nonlinear counting statistics problem turns out to be similar in structure to the usual NEGF approach. The formally exact theory now requires the counting field dependent nonlinear self-energy as an input which can be calculated order by order of the

nonlinear strength following Feynman diagrammatic technique.

Full-counting statistics study for nonlinear systems are challenging. Feynman-Hellmann theorem seems to give an alternative way to study such systems. Therefore future studies should attempt to extend this approach for other nonlinear systems such as for phonon-phonon or electron-phonon interacting systems. Moreover, Feynman-Hellmann approach can be equally applied for an interface setup where one of the system could be anharmonic. Such a nonlinear setup is useful to study thermalization which seems to be another direction for future study. For ballistic FCS problems finding out next order quantum corrections to the long-time limit results are worthy of future exploration.

# Appendix A

## Derivation of cumulant generating function for product initial state

In this appendix we derive the cumulant generating function (CGF) given in Eq. (3.37) for product initial state. We start by writing down the characteristic function (CF) given in Eq. (3.35) i.e.,

$$\mathcal{Z}(\xi_L) = \text{Tr} \left[ \rho_{\text{prod}}(0) T_c e^{-\frac{i}{\hbar} \int_C \hat{\mathcal{V}}_x(\tau) d\tau} \right], \quad (\text{A.1})$$

with

$$\hat{\mathcal{V}}_x(\tau) = -f^T(\tau) \hat{u}_C(\tau) + \hat{u}_R^T(\tau) V^{RC}(\tau) \hat{u}_C(\tau) + \hat{u}_L^T(\tau + \hbar x(\tau)) V^{LC}(\tau) \hat{u}_C(\tau). \quad (\text{A.2})$$

Appendix A: Derivation of cumulant generating function for product initial state

---

Let us for the moment consider only the left lead ( $V^{RC} = 0$ ). The effect of the another lead is additive in terms of the self-energy according to Feynman and Vernon. Therefore the characteristic function can be written as

$$\mathcal{Z}(\xi_L) = \langle T_C e^{\frac{i}{\hbar} \int_C f^T(\tau) u_C(\tau) d\tau} e^{-\frac{i}{\hbar} \int_C \tilde{u}_L^T(\tau) V^{LC} u_C(\tau)} \rangle, \quad (\text{A.3})$$

where we use the short hand notation  $\tilde{u}_L(\tau) = u_L(\tau + \hbar x(\tau))$ . Then using Linked-cluster theorem we can write

$$\begin{aligned} \ln \mathcal{Z}(\xi_L) &= \sum_{m,n} \frac{1}{m!n!} \left(\frac{-i}{\hbar}\right)^n \left(\frac{i}{\hbar}\right)^m \int d\tau_1 d\tau_2 \cdots d\tau_m d\tilde{\tau}_1 d\tilde{\tau}_2 \cdots d\tilde{\tau}_n \\ &\quad \langle T_C u_C^{i_1}(\tau_1) u_C^{i_2}(\tau_2) \cdots u_C^{i_m}(\tau_m) u_C^{k_1}(\tilde{\tau}_1) u_C^{k_2}(\tilde{\tau}_2) \cdots u_C^{k_n}(\tilde{\tau}_n) \rangle_{\text{connected}} \\ &\quad \langle T_C \tilde{u}_L^{j_1}(\tilde{\tau}_1) \tilde{u}_L^{j_2}(\tilde{\tau}_2) \cdots \tilde{u}_L^{j_n}(\tilde{\tau}_n) \rangle_{\text{connected}} V_{j_1, k_1}^{LC} V_{j_2, k_2}^{LC} \cdots V_{j_n, k_n}^{LC} \\ &\quad f_{i_1}(\tau_1) f_{i_2}(\tau_2) \cdots f_{i_m}(\tau_m), \end{aligned} \quad (\text{A.4})$$

where we imply Einstein's summation convention. Note that both  $m$  and  $n$  can take only even integer values.

In the following we will show that in the above series for the summation index  $m$  we need to consider only  $m = 0$  and  $m = 2$ . For  $m = 0$  i.e., without the driving force, the above infinite series can be easily summed (discussed in Chap. 3 before Eq. (3.37)) and is written as

$$\begin{aligned} \ln \mathcal{Z}(\xi_L)|_{m=0} &= \sum_{n=2}^{\infty} \frac{1}{n} \int d\tilde{\tau}_1 d\tilde{\tau}_2 \cdots d\tilde{\tau}_n g_C^{k_1, k_2}(\tilde{\tau}_1, \tilde{\tau}_2) \tilde{\Sigma}_L^{k_2, k_3}(\tilde{\tau}_2, \tilde{\tau}_3) \cdots \\ &\quad g_C^{k_{n-1}, k_n}(\tilde{\tau}_{n-1}, \tilde{\tau}_n) \tilde{\Sigma}_L^{k_n, k_1}(\tilde{\tau}_n, \tilde{\tau}_1) \\ &= -\frac{1}{2} \text{Tr}_{j, \tau} \ln \left[ 1 - g_C \tilde{\Sigma}_L \right]. \end{aligned} \quad (\text{A.5})$$

Appendix A: Derivation of cumulant generating function for product initial state

---

Using Wick's theorem it is easy to see that the number of connected diagrams in this case is  $(n - 1)!$ .

For  $m = 2$  we have

$$\begin{aligned}
 \ln \mathcal{Z}(\xi_L)|_{m=2} &= \sum_{n=0}^{\infty} \frac{1}{2! n!} \left(\frac{i}{\hbar}\right)^2 \left(\frac{-i}{\hbar}\right)^n \int d\tau_1 d\tau_2 d\tilde{\tau}_1 d\tilde{\tau}_2 \cdots d\tilde{\tau}_n \langle T_C u_C^{i_1}(\tau_1) u_C^{i_2}(\tau_2) \\
 &\quad u_C^{k_1}(\tilde{\tau}_1) u_C^{k_2}(\tilde{\tau}_2) \cdots u_C^{k_n}(\tilde{\tau}_n) \rangle_{\text{connected}} \langle T_C \tilde{u}_L^{j_1}(\tilde{\tau}_1) \tilde{u}_L^{j_2}(\tilde{\tau}_2) \cdots \tilde{u}_L^{j_n}(\tilde{\tau}_n) \rangle_{\text{connected}} \\
 &\quad V_{j_1, k_1}^{LC} V_{j_2, k_2}^{LC} \cdots V_{j_n, k_n}^{LC} f_{i_1}(\tau_1) f_{i_2}(\tau_2),
 \end{aligned} \tag{A.6}$$

In this case the combinatorial factor turns out to be  $n!$  which cancels the term in the denominator. Therefore finally we have

$$\begin{aligned}
 \ln \mathcal{Z}(\xi_L)|_{m=2} &= -\frac{i}{2\hbar} \sum_n \int d\tau_1 d\tau_2 d\tilde{\tau}_1 d\tilde{\tau}_2 \cdots d\tilde{\tau}_n \left[ f^T(\tau_1) g_C(\tau_1, \tilde{\tau}_1) \tilde{\Sigma}_L(\tilde{\tau}_1, \tilde{\tau}_2) \cdots \right. \\
 &\quad \left. g_C(\tilde{\tau}_n, \tau_2) f(\tau_2) \right] \\
 &= -\frac{i}{2\hbar} \int d\tau_1 d\tau_2 f^T(\tau_1) G(\tau_1, \tau_2) f(\tau_2)
 \end{aligned} \tag{A.7}$$

where we define the Green's function  $G(\tau, \tau')$  as

$$G(\tau, \tau') = g_C(\tau, \tau') + \int \int d\tau_1 d\tau_2 g_C(\tau, \tau_1) \Sigma^{\text{tot}}(\tau_1, \tau_2) G(\tau_2, \tau') \tag{A.8}$$

All other higher order terms ( $m > 2$ ) contains vacuum diagrams given as

$$\begin{aligned}
 &\int \int d\tau d\tau' f^T(\tau) g_C(\tau, \tau') f(\tau') \\
 &= \int \int dt dt' f(t) \left[ \sum_{\sigma, \sigma'} \sigma \sigma' g_C^{\sigma, \sigma'}(t, t') \right] f(t').
 \end{aligned} \tag{A.9}$$

Appendix A: Derivation of cumulant generating function for product  
initial state

---

The last expression is zero because of the standard relations among the Green's functions i.e.,  $g_C^t + g_C^{\bar{t}} - g_C^< - g_C^> = 0$ . Finally we obtain Eq. (3.37).

# Appendix B

## Vacuum diagrams

In this appendix we will show that vacuum diagrams are zero. This fact is used in chapter 3 while deriving the characteristic function for heat. We assume that the value of  $\text{Tr} \ln(\mathbf{1} - \mathbf{g}_c \Sigma)$  is 0 (see the discussion before Eq. (3.46)). Expanding the log series we get convolutions of  $g_C$  and  $\Sigma$  in contour time, which are all vacuum diagrams. We define vacuum diagrams where all the contour time variables of the Green's functions are integrated out. Note that the Green's functions in this case are counting field independent. In general scenario such vacuum diagrams can be written as

$$V = \int_C \int_C \cdots \int_C d\tau_1 d\tau_2 \dots d\tau_n [A(\tau_1, \tau_2) B(\tau_2, \tau_3) \cdots C(\tau_n, \tau_1)]. \quad (\text{B.1})$$

Transforming the integrations from contour time to the real-time within the interval  $[t_0, t_M]$ , *i.e.*, using  $\int d\tau = \sum_{\sigma} \int \sigma dt$  ( $\sigma = \pm 1$ ) we write

$$V = \sum_{\sigma_1, \sigma_2, \dots, \sigma_n} \int dt_1 \int dt_2 \cdots \int dt_n [\sigma_1 A^{\sigma_1 \sigma_2}(t_1, t_2) \sigma_2 B^{\sigma_2 \sigma_3}(t_2, t_3) \cdots \sigma_n D^{\sigma_n \sigma_{n+1}}(t_n, t_1)]. \quad (\text{B.2})$$

By absorbing the extra  $\sigma$  factors into the definition for branch components it can be easily seen that

$$V = \int dt_1 \int dt_2 \cdots \int dt_n \text{Tr}_{\sigma} [\bar{A}(t_1, t_2) \bar{B}(t_2, t_3) \cdots \bar{C}(t_n, t_1)], \quad (\text{B.3})$$

with  $\bar{A} = \sigma_z A$  with  $\sigma_z = \text{diag}(1, -1)$ . Now let us do the Keldysh rotation which transforms the matrix  $\bar{A}$  to  $\check{A}$  related via an orthogonal transformation  $O$  such that  $\check{A} = O^T \bar{A} O$ . Then we obtain

$$V = \int dt_1 \int dt_2 \cdots \int dt_n \text{Tr}_{\sigma} [\check{A}(t_1, t_2) \check{B}(t_2, t_3) \cdots \check{C}(t_n, t_1)]. \quad (\text{B.4})$$

Now if the Green's functions are counting field independent, then in the Keldysh space each matrix is of the following form

$$\check{A} = \begin{bmatrix} A^r & A^K \\ 0 & A^a \end{bmatrix} \quad (\text{B.5})$$

The important fact used in the proof is the tridiagonal structure of these matrices. As the product of triadigonal matrices is a triadigonal matrix,

after performing trace over the branch index *i.e.*,  $\text{Tr}_\sigma$  we obtain

$$\begin{aligned}
 V = & \int dt_1 \int dt_2 \cdots \int dt_n \left[ A^r(t_1, t_2) B^r(t_2, t_3) \cdots C^r(t_n, t_1) \right. \\
 & \left. + A^a(t_1, t_2) B^a(t_2, t_3) \cdots C^a(t_n, t_1) \right] \quad (\text{B.6})
 \end{aligned}$$

Such a term is always zero because the condition

$$t_1 > t_2 > t_3 > \cdots > t_{n-1} > t_n > t_1 \quad (\text{B.7})$$

or

$$t_1 < t_2 < t_3 < \cdots < t_{n-1} < t_n < t_1 \quad (\text{B.8})$$

is never satisfied. Therefore both the retarded and the advanced components are zero which implies  $V = 0$ . Finally we have all the terms in the log series equal to zero *i.e.*,  $\text{Tr} \ln(\mathbf{1} - \mathbf{g}_c \boldsymbol{\Sigma}) = 0$ .

# Appendix C

## Details for the numerical calculation of cumulants of heat for projected and steady state initial state

In this appendix we give details about how to numerically calculate the cumulants of heat for projected ( $\rho'(0)$ ) and steady state initial state ( $\rho_{\text{NESS}}(0)$ ) in the frequency domain. Starting from Eq. (3.80) which is valid for projected ( $\lambda \rightarrow \infty$ ) as well as for nonequilibrium steady state ( $\lambda \rightarrow 0$ ) we can write in the  $\omega$ -domain

$$\ln \mathcal{Z}(\xi) = -\frac{1}{2} \text{Tr}_{j,\sigma,\omega} \ln \left[ 1 - \check{G}_0[\omega] \check{\Sigma}_L^A[\omega, \omega'] \right] \quad (\text{C.1})$$

Appendix C: Details for the numerical calculations of cumulants of heat for projected and steady state initial state

---

where the meaning of trace in  $\omega$ -domain is explained in Eq. (3.54).

Here we discuss the calculation for  $\check{\Sigma}_L^A(\omega, \omega')$  for  $\rho'(0)$  which is the starting point for doing numerical calculation. To calculate different components of  $\check{\Sigma}_L^A(\omega, \omega')$  for projected initial state  $\rho'(0)$  we define two types of theta functions  $\theta_1(t, t')$  and  $\theta_2(t, t')$ .  $\theta_1(t, t')$  is non-zero and has the value 1 when

$$0 \leq t \leq t_M, \text{ and } t' \leq 0 \text{ or } t' \geq t_M, \quad (\text{C.2})$$

or

$$0 \leq t' \leq t_M, \text{ and } t \leq 0 \text{ or } t \geq t_M, \quad (\text{C.3})$$

and  $\theta_2(t, t')$  is non-zero only in the regime where  $0 \leq t, t' \leq t_M$ . For the regions where  $\theta_1(t, t')$  is non-zero the expression for  $\Sigma_L^A$  after taking the limit  $\lambda \rightarrow \infty$  is, (assuming all correlation functions decays to zero as  $t \rightarrow \pm\infty$ )

$$\Sigma_A^{t, \bar{t}, <, >}(t, t') = -\Sigma_L^{t, \bar{t}, <, >}(t - t'). \quad (\text{C.4})$$

So using theta functions we may write  $\Sigma_L^A(t, t')$  in the full  $t, t'$  domain as

$$\begin{aligned} \Sigma_A^{t, \bar{t}}(t, t') &= -\theta_1(t, t')\Sigma_L^{t, \bar{t}}(t - t') \\ \Sigma_A^{<}(t, t') &= -\theta_1(t, t')\Sigma_L^{<}(t - t') + \theta_2(t, t') \times \\ &\quad [\Sigma_L^{<}(t - t' - \hbar\xi) - \Sigma_L^{<}(t - t')] \\ \Sigma_A^{>}(t, t') &= -\theta_1(t, t')\Sigma_L^{>}(t - t') + \theta_2(t, t') \times \\ &\quad [\Sigma_L^{>}(t - t' + \hbar\xi) - \Sigma_L^{>}(t - t')] \end{aligned} \quad (\text{C.5})$$

Appendix C: Details for the numerical calculations of cumulants of heat for projected and steady state initial state

---

By doing Fourier transform it can be easily shown that

$$\Sigma_A^{t,\bar{t}}[\omega, \omega'] = - \int_{-\infty}^{\infty} \frac{d\omega_c}{2\pi} \theta_1[\omega - \omega_c, \omega' + \omega_c] \Sigma_L^{t,\bar{t}}(\omega_c) \quad (\text{C.6})$$

and

$$\begin{aligned} \Sigma_A^{>,<}[\omega, \omega'] &= - \int_{-\infty}^{\infty} \frac{d\omega_c}{2\pi} \theta_1[\omega - \omega_c, \omega' + \omega_c] \Sigma_L^{>,<}(\omega_c) \\ &+ \int_{-\infty}^{\infty} \frac{d\omega_c}{2\pi} \theta_2[\omega - \omega_c, \omega' + \omega_c] \Sigma_L^{>,<}(\omega_c) (e^{i\omega_c \eta \xi} - 1), \end{aligned} \quad (\text{C.7})$$

where  $\eta = \pm 1$ . The positive sign is for  $\Sigma_A^{<}$  and negative sign for  $\Sigma_A^{>}$ . The theta functions are now given by

$$\begin{aligned} \theta_1(\omega_a, \omega_b) &= f(\omega_a) \cdot g(\omega_b) + f(\omega_b) \cdot g(\omega_a), \\ \theta_2(\omega_a, \omega_b) &= f(\omega_a) \cdot f(\omega_b), \end{aligned} \quad (\text{C.8})$$

where

$$\begin{aligned} f(\omega) &= \frac{e^{i\omega t_M} - 1}{i\omega}, \\ g(\omega) &= \frac{1}{i\omega + \epsilon} - \frac{e^{i\omega t_M - \eta t_M}}{i\omega - \epsilon}, \end{aligned} \quad (\text{C.9})$$

with  $\epsilon \rightarrow 0^+$ . The theta functions are of immense importance which carries all information about the measurement time  $t_M$ .

Appendix C: Details for the numerical calculations of cumulants of heat for projected and steady state initial state

---

In the limit  $t_M \rightarrow \infty$ , the region  $0 \leq t, t' \leq t_M$  dominates and corresponding theta function, i.e.,  $\theta_2(\omega, \omega')$  reduces to

$$\theta_2(\omega - \omega_c, \omega' + \omega_c) \approx \delta(\omega - \omega_c)\delta(\omega' + \omega_c), \quad (\text{C.10})$$

and is responsible for obtaining the steady state result.

To calculate all the cumulants we only need to take derivative of  $\Sigma_A(\omega, \omega')$  with respect to  $i\xi$  since  $G_0$  does not have any  $\xi$  dependence. Also  $\Sigma^A$  has  $\xi$  dependence only for  $0 \leq t, t' \leq t_M$  and hence the derivatives are given by

$$\frac{\partial^n \Sigma_A^{>, <}}{\partial (i\xi)^n}[\omega, \omega'] = \int_{-\infty}^{\infty} \frac{d\omega_c}{2\pi} (\eta\hbar\omega_c)^n \theta_2[\omega - \omega_c, \omega' + \omega_c] \Sigma_L^{>, <}(\omega_c) e^{i\omega_c \eta \xi}. \quad (\text{C.11})$$

Here  $n$  refers to the order of the derivative.

# Appendix D

## Solving Dyson equation numerically for product initial state

Here we discuss about solving the Dyson equation for  $G_0$  given in Eq. (3.43) numerically for product initial state  $\rho_{\text{prod}}(0)$ . In order to compute the matrix  $\check{G}_0(t, t')$  we have to calculate two components  $G_0^r$  and  $G_0^K$  which are written in the integral form as (applying Langreth's rule)

$$G_0^r(t, t') = g_C^r(t-t') + \int_0^{t_M} dt_1 \int_0^{t_M} dt_2 g_C^r(t-t_1) \Sigma^r(t_1-t_2) G_0^r(t_2, t'), \quad (\text{D.1})$$

and

$$\begin{aligned}
 G_0^K(t, t') = g_C^K(t-t') &+ \int_0^{t_M} dt_1 \int_0^{t_M} dt_2 g_C^r(t-t_1) \Sigma^r(t_1-t_2) G_0^K(t_2, t') \\
 &+ \int_0^{t_M} dt_1 \int_0^{t_M} dt_2 g_C^r(t-t_1) \Sigma^K(t_1-t_2) G_0^a(t_2, t') \\
 &+ \int_0^{t_M} dt_1 \int_0^{t_M} dt_2 g_C^K(t-t_1) \Sigma^a(t_1-t_2) G_0^a(t_2, t').
 \end{aligned}$$

Note that the argument for center Green's function  $g_C$  and lead self-energy  $\Sigma$  are written as time difference  $t-t'$  because these are calculated in equilibrium. The analytical expressions for  $\Sigma$  and  $g_C$  are known in frequency domain. To determine their time-dependence we numerically calculate their inverse Fourier transforms using trapezoidal rule. Then in order to solve above equations for any  $t_M$  we discretize the time variable into  $N$  total intervals of incremental length  $\Delta t = t_M/N$  and thus converting the integral into a sum. After discretization, the above equations can be written in the matrix form which are indexed by space  $j$  and discrete time  $t$ , as

$$\begin{aligned}
 \mathbf{G}_0^r &= \mathbf{g}_C^r + \mathbf{g}_C^r \mathbf{\Sigma}^r \mathbf{G}_0^r, \\
 \mathbf{G}_0^K &= \mathbf{G}_0^r \mathbf{\Sigma}^K \mathbf{G}_0^a + (\mathbf{I} + \mathbf{G}_0^r \mathbf{\Sigma}^r) \mathbf{g}_C^K (\mathbf{I} + \mathbf{\Sigma}^a \mathbf{G}_0^a). \quad (\text{D.2})
 \end{aligned}$$

So  $\mathbf{G}_0^r$  can be obtained by doing an inverse of the matrix  $(\mathbf{I} - \mathbf{g}_C^r \mathbf{\Sigma}^r)$  and then multiplying by  $\mathbf{g}_C^r$ .  $\mathbf{G}_0^a$  can be obtained by taking matrix transpose of  $\mathbf{G}_0^r$ . Once  $\mathbf{G}_0^r$  and  $\mathbf{G}_0^a$  are known we use the second equation to calculate  $\mathbf{G}_0^K$  which is simply obtained by multiplying matrices.

# Appendix E

## Green's function $G_0[\omega]$ for a harmonic center connected with heat baths

In this appendix we give expressions for nonequilibrium Green's functions  $G_0$  for harmonic junction connected with two heat baths. These expressions are used to derive the Landauer formula in chapter 2 as well as the long-time limit for the CGF in chapter 3. We write the full Hamiltonian as

$$\mathcal{H} = \mathcal{H}_C + \mathcal{H}_L + \mathcal{H}_R + \mathcal{H}_{LC} + \mathcal{H}_{RC}. \quad (\text{E.1})$$

where  $\mathcal{H}_\alpha, \alpha = L, C, R$  is the Hamiltonian for the decoupled regions. The coupling  $\mathcal{H}_{\alpha C}$  is given as  $\mathcal{H}_{\alpha C} = u_\alpha^T V^{\alpha C} u_C, \alpha = L, R$  and  $V^{\alpha C} = [V^{C\alpha}]^T$ . For simplicity we assume the coupling matrices  $V^{\alpha C}$  are time-independent.

Since the full-system is harmonic the retarded Green's function for the entire system, satisfy the following equation in the frequency domain

$$[(\omega + i\eta)^2 I - K] G_{0,F}^r[\omega] = I, \quad (\text{E.2})$$

( $F$  is used to denote the Green's function for the full system) where  $K$  is the force constant matrix for the full linear system. Both  $K$  and  $G_{0,F}$  are (infinite) matrices indexed by the labels of atomic degrees of freedom. Note that  $\eta$  here is an infinitesimal positive number ( $\eta \rightarrow 0^+$ ) required to satisfy the causality condition for the retarded component, *i.e.*,  $G_{0,F}^r(t) = 0$  for  $t < 0$ . We partition  $K$  and  $G_{0,F}$  matrices according to the left, center, and right parts. For example the full  $K$  matrix is given as

$$K = \begin{pmatrix} K^L & V^{LC} & 0 \\ V^{CL} & K^C & V^{CR} \\ 0 & V^{RC} & K^R \end{pmatrix}. \quad (\text{E.3})$$

and similarly for  $G_{0,F}^r[\omega]$ . So for the retarded component of the full system we have [1, 2]

$$\begin{pmatrix} (\omega + i\eta)^2 I - K^L & -V^{LC} & 0 \\ -V^{CL} & (\omega + i\eta)^2 I - K^C & -V^{CR} \\ 0 & -V^{RC} & (\omega + i\eta)^2 I - K^R \end{pmatrix} \times \begin{pmatrix} G_0^{LL,r} & G_0^{LC,r} & G_0^{LR,r} \\ G_0^{CL,r} & G_0^{CC,r} & G_0^{CR,r} \\ G_0^{RL,r} & G_0^{RC,r} & G_0^{RR,r} \end{pmatrix} = \begin{pmatrix} I & 0 & 0 \\ 0 & I & 0 \\ 0 & 0 & I \end{pmatrix}. \quad (\text{E.4})$$

Appendix E: Green's function  $G_0[\omega]$  for a harmonic center connected with heat baths

---

Considering only the three equations formed by each row of the first matrix multiplying the middle column of  $G_{0,F}^r[\omega]$  matrix, we have

$$[(\omega + i\eta)^2 I - K^L] G_0^{LC,r} - V^{LC} G_0^{CC,r} = 0, \quad (\text{E.5})$$

$$-V^{CL} G_0^{LC,r} + [(\omega + i\eta)^2 I - K^C] G_0^{CC,r} - V^{CR} G_0^{RC,r} = I, \quad (\text{E.6})$$

$$-V^{RC} G_0^{CC,r} + [(\omega + i\eta)^2 I - K^R] G_0^{RC,r} = 0. \quad (\text{E.7})$$

### Surface Green's functions, self-energy for the leads

Let us now introduce the retarded surface Green's functions for the leads as

$$g_\alpha^r[\omega] = [(\omega + i\eta)^2 I - K^\alpha]^{-1}, \quad \alpha = L, R, \quad (\text{E.8})$$

which is an infinite dimensional matrix. We also define the retarded self-energy of the leads from the surface Green's function (E.8) by multiplying the coupling matrices from both sides *i.e.*,

$$\Sigma_\alpha^r[\omega] = V^{C\alpha} g_\alpha^r[\omega] V^{\alpha C}, \quad \alpha = L, R, \quad (\text{E.9})$$

Typically the coupling matrix  $V^{\alpha C}$  has few non-zero entries and often one is only interested in nearest neighbor coupling between the oscillators in which case only one element of  $V^{\alpha C}$  is non-zero and therefore  $\Sigma_\alpha^r$  will also have one non-zero entry. This surface Green's functions are important input for the transport problems as they characterize the properties of the heat baths and are responsible for transfer current from the lead to the junction.

Appendix E: Green's function  $G_0[\omega]$  for a harmonic center connected with heat baths

---

Knowing  $\Sigma_\alpha^r[\omega]$  is enough to determine the other components of the self-energy. In fact since the leads are at equilibrium, the lesser and greater components of the self-energy will follow fluctuation-dissipation relations given as

$$\begin{aligned}\Sigma_\alpha^<[\omega] &= f_\alpha[\omega](\Sigma_\alpha^r[\omega] - \Sigma_\alpha^a[\omega]), \\ \Sigma_\alpha^>[\omega] &= (1 + f_\alpha[\omega])(\Sigma_\alpha^r[\omega] - \Sigma_\alpha^a[\omega]),\end{aligned}\quad (\text{E.10})$$

where  $f_\alpha[\omega] = 1/(e^{\beta_\alpha \hbar \omega_\alpha} - 1)$  is the Bose distribution function for the phonons in the heat bath.

The spectral function  $\Gamma_\alpha[\omega]$  for the leads is defined as

$$\Gamma_\alpha[\omega] = i(\Sigma_\alpha^r[\omega] - \Sigma_\alpha^a[\omega]) = -2 V^{C\alpha} \text{Im} \left[ g_\alpha^r[\omega] \right] V^{\alpha C} \quad \alpha = L, R, \quad (\text{E.11})$$

$$\Gamma_\alpha[\omega] = V^{C\alpha} (S^\alpha)^\dagger \frac{\pi}{\Omega_0} \left[ \delta(\omega - \Omega_0) - \delta(\omega + \Omega_0) \right] S^\alpha V^{\alpha C}. \quad (\text{E.12})$$

### Green's functions for the harmonic junction

Using these definition for the self-energy and Eqs. (E.5) and (E.7) we express the retarded component for the central part of the Green's function as

$$G_0^r[\omega] = \left[ (\omega + i\eta)^2 I - K^C - \Sigma_L^r[\omega] - \Sigma_R^r[\omega] \right]^{-1}, \quad (\text{E.13})$$

Form now on we omit the  $CC$  index from  $G_0^{CC,r}$ . The advanced Green's

Appendix E: Green's function  $G_0[\omega]$  for a harmonic center connected with heat baths

---

function is given by the Hermitian conjugate of the retarded one *i.e.*,

$$G_0^a[\omega] = [G_0^r[\omega]]^\dagger = \left[ (\omega - i\eta)^2 I - K^C - \Sigma_L^a[\omega] - \Sigma_R^a[\omega] \right]^{-1}. \quad (\text{E.14})$$

From these expressions for  $G_0^r[\omega]$  and  $G_0^a[\omega]$  another important identity that can be derived is

$$G_0^r[\omega] - G_0^a[\omega] = -i G_0^r[\omega] (\Gamma_L[\omega] + \Gamma_R[\omega]) G_0^a[\omega] = -i G_0^a[\omega] (\Gamma_L[\omega] + \Gamma_R[\omega]) G_0^r[\omega]. \quad (\text{E.15})$$

This identity is used to derive the Landauer like formula in chapter 2.

---

**Proof:**

Let us take the inverse of  $G_0^r[\omega]$  and  $G_0^a[\omega]$  and subtract them *i.e.*,

$$(G_0^a[\omega])^{-1} - (G_0^r[\omega])^{-1} = -4\omega i\eta + (\Sigma_L^r[\omega] - \Sigma_L^a[\omega]) + (\Sigma_R^r[\omega] - \Sigma_R^a[\omega]). \quad (\text{E.16})$$

Multiplying  $G_0^r[\omega]$  ( $G_0^a[\omega]$ ) from left and  $G_0^a[\omega]$  ( $G_0^r[\omega]$ ) from the right side and using the definition of  $\Gamma_\alpha[\omega]$  we obtain the above equation after taking the limit  $\eta \rightarrow 0^+$ .

---

In the nonequilibrium steady state in addition to  $G_0^r[\omega]$  we need lesser or greater component of  $G_0$  which can be obtained from the Dyson equation

Appendix E: Green's function  $G_0[\omega]$  for a harmonic center connected with heat baths

---

for  $G_0$  given as (see (2.85))

$$G_0(\tau, \tau') = g_C(\tau, \tau') + \int_C d\tau_1 \int_C d\tau_2 g_C(\tau, \tau_1) \Sigma(\tau_1, \tau_2) G_0(\tau_2, \tau'). \quad (\text{E.17})$$

Transforming to the real time we obtain different components as

$$\begin{aligned} G_0^r[\omega] &= g_C^r[\omega] + g_C^r[\omega] \Sigma^r[\omega] G_0^r[\omega], \\ G_0^a[\omega] &= g_C^a[\omega] + g_C^a[\omega] \Sigma^a[\omega] G_0^a[\omega], \\ G_0^K[\omega] &= g_C^K[\omega] + g_C^r[\omega] \Sigma^r[\omega] G_0^K[\omega] + g_C^r[\omega] \Sigma^K[\omega] G_0^a[\omega] + g_C^K[\omega] \Sigma^a[\omega] G_0^a[\omega], \end{aligned} \quad (\text{E.18})$$

with  $\Sigma = \Sigma_L + \Sigma_R$ . We can easily recover the retarded and advanced components from the first two equations. The Keldysh component can be simplified further and shown to be equal to

$$G_0^K[\omega] = G_0^r[\omega] \Sigma^K[\omega] G_0^a[\omega]. \quad (\text{E.19})$$

---

### **Proof**

For simplicity here we omit the  $\omega$  argument from the Green's functions. We write the Keldysh component (E.18) as

$$\begin{aligned} G_0^K &= g^K + g^r \Sigma^r G_0^K + g^r \Sigma^K G_0^a + g^K \Sigma^a G_0^a, \\ &= g^K (1 + \Sigma^a G_0^a) + g^r \Sigma^K G_0^a + g^r \Sigma^r G_0^K, \\ \implies (1 - g^r \Sigma^r) G_0^K &= g^K (1 + \Sigma^a G_0^a) + g^r \Sigma^K G_0^a. \end{aligned} \quad (\text{E.20})$$

Appendix E: Green's function  $G_0[\omega]$  for a harmonic center connected with heat baths

---

Now, from the retarded and advanced component of  $G_0$  we obtain

$$\begin{aligned} (1 + \Sigma^a G_0^a) &= (g^a)^{-1} G_0^a, \\ (1 - g^r \Sigma^r) &= g^r (G_0^r)^{-1}. \end{aligned} \quad (\text{E.21})$$

Using these expressions, we can write

$$\begin{aligned} G_0^K &= G_0^r (g^r)^{-1} g^K (g^a)^{-1} G_0^a + G_0^r \Sigma^K G_0^a, \\ &= (1 + 2f_C) G_0^r [(g^a)^{-1} - (g^r)^{-1}] G_0^a + G_0^r \Sigma^K G_0^a. \end{aligned} \quad (\text{E.22})$$

Now for finite size junction  $(g^a)^{-1} - (g^r)^{-1} \propto \eta$  and therefore is zero in the limit  $\eta \rightarrow 0^+$  and we finally obtain Eq. (E.19).

---

**Explicit Expressions for  $G_0[\omega]$  for one-dimensional pure harmonic chain**

We consider an infinite one-dimensional (1D) chain with inter-particle spring constant  $k$  and onsite spring constant  $k_0$ . We divide the full system into three parts: the center, the left and the right part. Left and right parts are semi-infinite and are known as Rubin heat baths. The classical equation of motion for the full system is

$$\ddot{u}_j = k u_{j-1} + (-2k - k_0) u_j + k u_{j+1}, \quad (\text{E.23})$$

where  $j \leq 0$  is the left-lead region,  $j = 1, \dots, N$  is the number of atoms in the center region and  $j > N$  is the right-lead region. In this case the full

Appendix E: Green's function  $G_0[\omega]$  for a harmonic center connected with heat baths

---

$K$  matrix (infinite in both directions) consists of  $2k + k_0$  on the diagonal and  $-k$  on the first off-diagonals.

### Retarded Green's function $G_0^r[\omega]$ for the center

As the full system is homogeneous, the retarded component for the center Green's function can be calculated using Eq. (E.2). Multiplying the matrices we write down the following linear equations

$$\begin{aligned} kG_{0,j-1,l}^r + \Omega G_{0,j,l}^r + kG_{0,j+1,l}^r &= 1, \\ kG_{0,j,l}^r + \Omega G_{0,j+1,l}^r + kG_{0,j+2,l}^r &= 0, \end{aligned} \quad (\text{E.24})$$

where  $1 \leq j, l \leq N$  and  $\Omega = (\omega + i\eta)^2 - 2k - k_0$ . The translational invariance of the full system ensures that the solution for  $G_{0,jl}^r[\omega]$  will be of the form  $G_{0,jl}^r[\omega] = c\lambda^{|j-l|}$ . Substituting the trial solution in the second equation gives the following quadratic equation for  $\lambda$

$$k\lambda^{-1} + \Omega + k\lambda = 0, \quad (\text{E.25})$$

and the roots are simply given as

$$\lambda = -\frac{\Omega}{2k} \pm \frac{1}{2k} \sqrt{\Omega^2 - 4k^2} \equiv e^{iq}. \quad (\text{E.26})$$

Here  $q$  is the wave number and satisfy the phonon dispersion relation for one-dimensional harmonic chain with nearest-neighbor interaction, *i.e.*,  $(\omega + i\eta)^2 = 2k(1 - \cos q) + k_0$ . We choose only one solution for  $\lambda$  satisfying the condition  $|\lambda| \leq 1$ . The constant  $c$  is fixed by the first equation

and given as  $c = \lambda - 1/\lambda$ . Finally the explicit solution is written as

$$G_{0jl}^r[\omega] = \frac{\lambda^{|j-l|}}{k(\lambda - \frac{1}{\lambda})}. \quad (\text{E.27})$$

### Surface Green's function

The surface Green's function  $g^r[\omega]$  satisfies a similar equation (E.2) as  $G_0^r[\omega]$  except that it is semi-infinite in extent. We consider the left lead ( $j \leq 0$ ). The result for the right lead is identical. Since the matrix  $V^{LC}$  is nonzero only for one corner element, we need the  $g_0^r[\omega] = g_{00}^r[\omega]$  component of the matrix  $g^r[\omega]$ . Consider only the  $j = 0$  column, the equations for  $g^r[\omega]$  in component form are

$$\Omega g_0^r[\omega] + k g_{-1}^r[\omega] = 1, \quad (\text{E.28})$$

$$k g_{j-1}^r[\omega] + \Omega g_j^r[\omega] + k g_{j+1}^r[\omega] = 0, \quad j = -1, -2, \dots \quad (\text{E.29})$$

Substituting the trial solution  $g_j^r[\omega] = c\lambda^{-j}$ , we find that

$$g_0^r[\omega] = -\frac{\lambda}{k}. \quad (\text{E.30})$$

The matrix elements of  $\Sigma^r$  are all zero except that  $\Sigma_{11}^r[\omega] = k^2 g_0^r$  and  $\Sigma_{NN}^r[\omega] = k^2 g_N^r[\omega]$ .

Therefore the spectral function  $\Gamma[\omega]$ , say for the left lead is given as

$$\Gamma_{11}[\omega] = \begin{cases} 2k \sin q = \sqrt{(\omega_D^2 - \omega^2)(\omega^2 - k_0)} & \text{for } k_0 \leq \omega^2 \leq \omega_D^2 \\ 0 & \text{for } \omega^2 > \omega_D^2, \omega^2 < k_0, \end{cases}$$

Appendix E: Green's function  $G_0[\omega]$  for a harmonic center connected with heat baths

---

where  $\omega_D^2 = 4k + k_0$ .

### Transmission function $\mathcal{T}[\omega]$ for the pure harmonic chain

The transmission function for the harmonic junction is given by the Caroli formula as

$$\mathcal{T}[\omega] = \text{Tr}[G_0^r[\omega]\Gamma_L[\omega]G_0^a[\omega]\Gamma_R[\omega]]. \quad (\text{E.31})$$

For pure harmonic chain with nearest neighbor coupling we have

$$\mathcal{T}[\omega] = (\Gamma_L)_{11}(\Gamma_R)_{NN}|(G_0^r)_{N1}|^2 = \begin{cases} \frac{4k^2 \sin^2 q}{k^2(\lambda - 1/\lambda)(\lambda^* - 1/\lambda^*)} = 1 & \text{for } k_0 \leq \omega^2 \leq \omega_D^2 \\ = 0 & \text{for } \omega^2 > \omega_D^2, \omega^2 < k_0, \end{cases}$$

where we use the fact that  $\lambda - 1/\lambda = 2i \sin q$ .

# Bibliography

- [1] A. Dhar, D. Roy, *J. Stat. Phys.* **125**, 805 (2006).
- [2] J.-S. Wang, J. Wang, and J. T. Lü, *Eur. Phys. J. B* **62**, 381 (2008).

# Appendix F

## Example: Green's functions for isolated harmonic oscillator

In this appendix we illustrate various definitions and relations between the Green's functions by calculating these functions for an isolated one-dimensional harmonic oscillator system consists of  $N$  coupled oscillators. This expressions are used for numerical calculations for the cumulants of heat.

The Hamiltonian for the isolated system is written as

$$\mathcal{H} = \frac{1}{2}p^T p + \frac{1}{2}u^T K u \quad (\text{F.1})$$

where  $p$  and  $u$  are the column vectors for the momentum and the position respectively. Note that  $u$  here is normalized by mass *i.e.*,  $u \rightarrow \sqrt{m}x$ .  $K$  is

## Appendix F: Example: Green's functions for isolated harmonic oscillator

---

the  $N \times N$  force constant matrix.

Here we are interested in calculating various Green's functions. The contour ordered Green's functions reads  $g(\tau, \tau') = -\frac{i}{\hbar} \langle T_C u(\tau) u^T(\tau') \rangle$ . The average here is with respect to the equilibrium canonical distribution *i.e.*,  $\rho = e^{-\beta\mathcal{H}} / \text{Tr}[e^{-\beta\mathcal{H}}]$ .

One particular approach to solve contour-ordered Green's function is by writing down its equations of motion. For harmonic system it is simply given as

$$\frac{\partial^2 g(\tau, \tau')}{\partial \tau^2} + K g(\tau, \tau') = -I \delta(\tau, \tau'). \quad (\text{F.2})$$

This differential equation gives following set of equations in real time,

$$\frac{\partial^2 g^{\bar{t}}(t, t')}{\partial t^2} + K g^{\bar{t}}(t, t') = I \delta(t - t'), \quad (\text{F.3})$$

$$\frac{\partial^2 g^{<, >}(t, t')}{\partial t^2} + K g^{<, >}(t, t') = 0, \quad (\text{F.4})$$

$$\frac{\partial^2 g^{r, a, t}(t, t')}{\partial t^2} + K g^{r, a, t}(t, t') = -I \delta(t - t'). \quad (\text{F.5})$$

We see that although  $g^r$ ,  $g^a$ , and  $g^t$  satisfy the same differential equation their solutions are different as they satisfy different boundary conditions. For example the causality condition for the retarded and advanced Green's function *i.e.*,  $g^r(t) = 0$  for  $t < 0$  and  $g^a(t) = 0$  for  $t > 0$ .

Solutions to these differential equations can be obtained by Fourier transformation. For example, eq. (F.5) in Fourier domain reads

$$(\omega^2 - K) g^{r, a, t}[\omega] = I. \quad (\text{F.6})$$

## Appendix F: Example: Green's functions for isolated harmonic oscillator

Now to satisfy the causality condition for  $g^{r,a}$  the correct choice for the retarded Green's function is

$$g^r[\omega] = [(\omega + i\eta)^2 - K]^{-1}, \quad (\text{F.7})$$

where  $\eta$  is an infinitesimal positive quantity to single out the correct path around the poles when performing an inverse Fourier transform. This implies that  $g^r[\omega]$  is analytic on the upper half of the complex  $\omega$  plane and all poles lie on the lower plane.

Other Green's functions can be obtained through various other relations among the Green's functions, such as fluctuation-dissipation relation reads as  $g^<[\omega] = f(\omega)(g^r[\omega] - g^a[\omega])$ . Below we give explicit expressions for different Green's functions

$$\begin{aligned} g^r(t) &= -S^\dagger \theta(t) \frac{\sin \Omega_0 t}{\Omega_0} S, \\ g^<(t) &= S^\dagger \left[ \frac{-i}{2\Omega_0} [(1 + f(\Omega_0))e^{i\Omega_0 t} + f(\Omega_0)e^{-i\Omega_0 t}] \right] S, \\ g^>(t) &= g^<(-t), \\ g^a(-t) &= g^r(t) \text{ for } t > 0, \end{aligned} \quad (\text{F.8})$$

where the matrix  $S$  is unitary which diagonalize the force constant matrix  $K$  *i.e.*,  $SKS^\dagger = \Omega_0^2 I$  and  $S^\dagger S = SS^\dagger = I$ ,  $I$  is the identity matrix and  $f(\omega) = \frac{1}{e^{\beta\hbar\omega} - 1}$  is the Bose-Einstein distribution function for phonons.  $\theta(t)$  is the Heaviside theta function.

Appendix F: Example: Green's functions for isolated harmonic oscillator

---

In the frequency domain these Green's functions reads

$$\begin{aligned}
 g^r[\omega] &= S^\dagger \frac{1}{(\omega + i\eta)^2 I - \Omega_0^2} S, \\
 g^a[\omega] &= [g^r[\omega]]^\dagger = g^r[-\omega], \\
 g^<[\omega] &= S^\dagger \left[ \frac{-i\pi}{\Omega_0} [\delta(\omega + \Omega_0)(1 + f(\Omega_0)) + \delta(\omega - \Omega_0)f(\Omega_0)] \right] S, \\
 g^>[\omega] &= g^<[-\omega].
 \end{aligned} \tag{F.9}$$

From this expressions one can easily check that  $g^r - g^a = g^> - g^<$ . In addition to this, the spectral function  $A[\omega] = i(g^r[\omega] - g^a[\omega])$  is given as

$$A[\omega] = S^\dagger \frac{\pi}{\Omega_0} [\delta(\omega - \Omega_0) - \delta(\omega + \Omega_0)] S. \tag{F.10}$$

# Appendix G

## Current at short time for product initial state $\rho_{\text{prod}}(0)$

In this appendix we show that for lead-junction-lead setup at short time current flows into the leads. According to the definition of current operator given in Eq. (3.8) the energy current flowing out of the left lead is (we assume that the driving force  $f(t) = 0$ )

$$\langle \mathcal{I}_L(t) \rangle = - \left\langle \frac{d\mathcal{H}_L^H(t)}{dt} \right\rangle = \frac{i}{\hbar} \langle [\mathcal{H}_L^H(t), \mathcal{H}] \rangle, \quad (\text{G.1})$$

where the average is with respect to  $\rho_{\text{prod}}(0)$ . If  $t$  is small we can expand  $\mathcal{H}_L^H(t)$  in a Taylor series and is given as  $\mathcal{H}_L^H(t) = \mathcal{H}_L(0) + t\dot{\mathcal{H}}_L(0) + \dots$ . Now since  $[\rho_{\text{prod}}(0), \mathcal{H}_L(0)] = 0$ , by using the cyclic property of trace it immediately follows that  $\langle [\mathcal{H}_L(0), \mathcal{H}] \rangle = 0$ . So in the linear order of  $t$  the

current is given as

$$\langle \mathcal{I}_L(t) \rangle = t \frac{i}{\hbar} \langle [\dot{\mathcal{H}}_L(0), \mathcal{H}] \rangle = -t \frac{i}{\hbar} \langle [p_L^T V^{LC} u_C, \mathcal{H}] \rangle. \quad (\text{G.2})$$

The only term in the full Hamiltonian that will contribute to the commutator is the coupling Hamiltonian  $\mathcal{H}_{LC} = u_L^T V^{LC} u_C$ . Now using Heisenberg's commutation relation  $[p_L, u_L] = -i\hbar$ , for one-dimensional linear chain with nearest-neighbor interaction we can write

$$\langle \mathcal{I}_L(t) \rangle = -t k^2 \langle (u_1^C)^2 \rangle, \quad (\text{G.3})$$

where  $u_1^C$  is the first particle in the center which is connected with the first particle of the left lead with force constant  $k$ . Since  $\langle (u_1^C)^2 \rangle$  is always positive the sign for the current is negative which implies that the energy current flows into the lead and is independent of the temperature of the leads. Note that here we didn't assume that the center is harmonic and therefore this statement is valid even if the center is anharmonic. For harmonic center,  $\langle (u_1^C)^2 \rangle$  can be easily computed and for a single particle center it is given as

$$\langle (u_1^C)^2 \rangle = \frac{\hbar}{\omega_0} \left( f_C(\omega_0) + \frac{1}{2} \right), \quad (\text{G.4})$$

where  $f_C(\omega_0)$  is the Bose distribution function for the particle with characteristic frequency  $\omega_0$  and temperature  $T_C$  coming from the initial distribution. Therefore for harmonic junction in the short time limit the current

flowing into the left lead is

$$\langle \mathcal{I}_L(t) \rangle = -t k^2 \frac{\hbar}{\omega_0} \left( f_C(\omega_0) + \frac{1}{2} \right). \quad (\text{G.5})$$

Similar conclusion can be easily drawn for the right lead. Moreover, for two-terminal without junction setup the result is valid if we identify  $u_1^C$  as  $u_1^R$ , the position operator of the right lead and thus explain the result obtained in chapter 5 (see Fig (5.3)).

# Appendix H

## A quick derivation of the Levitov-Lesovik formula for electrons using NEGF

In this appendix we derive the Levitov-Lesovik formula for the noninteracting electrons using tight-binding Hamiltonian. The CF for the noninteracting electrons was first derived by Levitov and Lesovik [1, 2] using Landauer type of wave scattering approach. Klich [3] and Schönhammer [4] re-derived the formula using a trace and determinant relation to reduce the problem from many-body to a single particle Hilbert space problem. Esposito et al. gave an approach using the superoperator nonequilibrium Green's function [5]. A more rigorous treatment is given in Ref. [6]. Here we derive the CGF for the joint probability distribution for particle and

Appendix H: A quick derivation of the Levitov-Lesovik formula for electrons using NEGF

---

energy.

Using tight-binding model the Hamiltonian of the whole system can be written as

$$\mathcal{H}^e = \sum_{\alpha=L,C,R} c_{\alpha}^{\dagger} h^{\alpha} c_{\alpha} + \sum_{\alpha=L,R} (c_{\alpha}^{\dagger} V_e^{\alpha C} c_C + \text{h.c.}) \quad (\text{H.1})$$

where  $c_{\alpha}$  is a column vector consisting of all the annihilation operator of region  $\alpha$ .  $c_{\alpha}^{\dagger}$  is a row vector of the corresponding creating operators.  $h^{\alpha}$  is the single particle Hamiltonian matrix.  $V_e^{\alpha C}$  has similar meaning as  $V^{\alpha C}$  in the phonon Hamiltonian and  $V_e^{\alpha C} = (V_e^{C\alpha})^{\dagger}$ .

We are interested in calculating the CF corresponding to the particle operator  $\mathcal{N}_L$  and energy operator  $\mathcal{H}_L$  of the left-lead where  $\mathcal{H}_L = c_L^{\dagger} h^L c_L$  and  $\mathcal{N}_L = c_L^{\dagger} c_L$ . One can easily generalize the formula for right lead also as we did in the phonon case. For electrons  $\mathcal{N}_L$  and  $\mathcal{H}_L$  can be measured simultaneously because they commute, *i.e.*,  $[\mathcal{H}_L, \mathcal{N}_L] = 0$ . In order to calculate the CGF we introduce two counting fields  $\xi_p$  and  $\xi_e$  for particle and energy respectively. Here we will consider the product initial state (with fixed temperatures and chemical potentials for the leads) and derive the long-time result.

Similar to the phonon case we can write the CF as

$$\mathcal{Z}(\xi_e, \xi_p) = \left\langle e^{i(\xi_e \mathcal{H}_L + \xi_p \mathcal{N}_L)} e^{-i(\xi_e \mathcal{H}_L^H(t) + \xi_p \mathcal{N}_L^H(t))} \right\rangle, \quad (\text{H.2})$$

where superscript  $H$  means the operators are in the Heisenberg picture at

Appendix H: A quick derivation of the Levitov-Lesovik formula for electrons using NEGF

---

time  $t$ . In terms of modified Hamiltonian the CF can be expressed as

$$\mathcal{Z}(\xi_e, \xi_p) = \left\langle \mathcal{U}_{(\frac{\xi_e}{2}, \frac{\xi_p}{2})}(0, t) \mathcal{U}_{(-\frac{\xi_e}{2}, -\frac{\xi_p}{2})}(t, 0) \right\rangle, \quad (\text{H.3})$$

where

$$\begin{aligned} \mathcal{U}_{x,y}(t, 0) &= e^{ix\mathcal{H}_L + iy\mathcal{N}_L} \mathcal{U}(t, 0) e^{-ix\mathcal{H}_L - iy\mathcal{N}_L} \\ &= \exp \left[ -\frac{i}{\hbar} \mathcal{H}_{x,y} t \right] \end{aligned} \quad (\text{H.4})$$

with  $x = \xi_e/2$  and  $y = \xi_p/2$  and  $\mathcal{U}(t, 0) = e^{-i\mathcal{H}t}$ .  $\mathcal{H}_{x,y}$  is the modified Hamiltonian which evolves with both  $\mathcal{H}_L$  and  $\mathcal{N}_L$  and is given by

$$\begin{aligned} \mathcal{H}_{x,y} &= e^{ix\mathcal{H}_L + iy\mathcal{N}_L} \mathcal{H} e^{-ix\mathcal{H}_L - iy\mathcal{N}_L} \\ &= \mathcal{H}_L + \mathcal{H}_C + \mathcal{H}_R + (e^{iy} c_L^\dagger(\hbar x) V_e^{LC} c_C + \text{h.c.}) + (c_R^\dagger V_e^{RC} c_C + \text{h.c.}) \end{aligned} \quad (\text{H.5})$$

where we have used the fact that

$$\begin{aligned} e^{ix\mathcal{H}_L} c_L(0) e^{-ix\mathcal{H}_L} &= c_L(\hbar x), \\ e^{iy\mathcal{N}_L} c_L(0) e^{-iy\mathcal{N}_L} &= e^{-iy} c_L. \end{aligned} \quad (\text{H.6})$$

So the evolution with  $\mathcal{H}_L$  and  $\mathcal{N}_L$  is to shift the time-argument and produce a phase for  $c_L, c_L^\dagger$  respectively. Next we go to the interaction picture of the modified Hamiltonian  $\mathcal{H}_{x,y}$  with respect to  $\mathcal{H}_0 = \sum_{\alpha=L,C,R} \mathcal{H}_\alpha$ . On the Keldysh contour  $C[0, t_M]$  the CGF then reads as,

$$\mathcal{Z}(\xi_e, \xi_p) = \text{Tr} \left[ \rho_{\text{prod}}(0) T_c e^{-\frac{i}{\hbar} \int d\tau \hat{V}_{x,y}(\tau)} \right], \quad (\text{H.7})$$

Appendix H: A quick derivation of the Levitov-Lesovik formula for electrons using NEGF

---

where  $\hat{\mathcal{V}}_{x,y}(\tau)$  is written in contour time as

$$\hat{\mathcal{V}}_{x,y}(\tau) = (e^{iy}\hat{c}_L^\dagger(\tau+\hbar x)V_e^{LC}\hat{c}_C(\tau)+\text{h.c.}) + (\hat{c}_R(\tau)^\dagger V_e^{RC}\hat{c}_C(\tau)+\text{h.c.}). \quad (\text{H.8})$$

Now we expand the exponential and use Feynman diagrams to sum the series. Finally the CGF can be shown to be

$$\ln \mathcal{Z}(\xi_e, \xi_p) = \text{Tr}_{j,\tau} \ln \left[ \mathbf{1} - \mathbf{G}_0^e \Sigma_{L,e}^A \right], \quad (\text{H.9})$$

The meaning of  $\text{Tr}_{j,\tau}$  is the same as explained for phonons. Here we define the shifted self-energy for the electrons as

$$\Sigma_{L,e}^A(\tau, \tau') = e^{i(y(\tau')-y(\tau))} \Sigma_{L,e}(\tau + \hbar x, \tau' + \hbar x') - \Sigma_{L,e}(\tau, \tau'). \quad (\text{H.10})$$

The counting of the electron number is associated with factor of a phase, while the counting of the energy is related to translation in time. Note that the CGF does not have the characteristic 1/2 pre-factor as compared to the phonon case because  $c$  and  $c^\dagger$  are independent variables. In the long-time limit following the same steps as we did for phonons, the CGF can be written down as (after doing Keldysh rotation)

$$\ln \mathcal{Z}(\xi_e, \xi_p) = t_M \int \frac{dE}{2\pi\hbar} \text{Tr} \ln (I - \check{G}_0^e(E) \check{\Sigma}_{L,e}^A(E)). \quad (\text{H.11})$$

Appendix H: A quick derivation of the Levitov-Lesovik formula for electrons using NEGF

---

In the energy  $E$  domain different components of the shifted self-energy are

$$\begin{aligned}
\Sigma_A^t(E) &= \Sigma_A^{\bar{t}}(E) = 0, \\
\Sigma_A^<(E) &= (e^{i(\xi_p + \xi_e E)} - 1)\Sigma_L^<(E), \\
\Sigma_A^>(E) &= (e^{-i(\xi_p + \xi_e E)} - 1)\Sigma_L^>(E).
\end{aligned} \tag{H.12}$$

Finally the CGF can be simplified as

$$\begin{aligned}
\ln \mathcal{Z} &= t_M \int \frac{dE}{2\pi\hbar} \ln \det \left\{ I + G_0^r \Gamma_L G_0^a \Gamma_R \left[ (e^{i\alpha} - 1) f_L \right. \right. \\
&\quad \left. \left. + (e^{-i\alpha} - 1) f_R - (e^{i\alpha} + e^{-i\alpha} - 2) f_L f_R \right] \right\}. \tag{H.13}
\end{aligned}$$

where  $\alpha = \xi_p + \xi_e E$  and  $f_L, f_R$  are Fermi distribution functions for left and right lead respectively. Note the difference of the signs in the CGF as compared to the phonons. If we replace  $\alpha$  by  $(E - \mu_L)\xi$ , the resulting formula is for the counting of the heat  $\mathcal{Q}_L = \mathcal{H}_L - \mu_L \mathcal{N}_L$  transferred, where  $\mu_L$  is the chemical potential of the left lead. Finally the CGF obeys the following fluctuation symmetry

$$\mathcal{Z}(\xi_e, \xi_p) = \mathcal{Z}(-\xi_e + i(\beta_R - \beta_L), -\xi_p - i(\beta_R \mu_R - \beta_L \mu_L)). \tag{H.14}$$

# Bibliography

- [1] L. S. Levitov and G. B. Lesovik, JETP Lett. **58**, 230 (1993).
- [2] L. S. Levitov, H.-W. Lee, and G. B. Lesovik, J. Math. Phys. **37**, 4845 (1996).
- [3] I. Klich, in *Quantum Noise in Mesoscopic Physics*, NATO Science Series II, Vol. 97, edited by Yu. V. Nazarov (Kluwer, Dordrecht, 2003).
- [4] K. Schönhammer, Phys. Rev. B **75**, 205329 (2007); J. Phys.:Condens. Matter **21**, 495306 (2009).
- [5] M. Esposito, U. Harbola, and S. Mukamel, Rev. Mod. Phys. **81**, 1665 (2009).
- [6] D. Bernard and B. Doyon arxiv: 1105.1695.

# List of Publications

1. B. K. Agarwalla, L. Zhang, J.-S. Wang, and B. Li, “Phonon Hall effect in ionic crystals in the presence of static magnetic field” , Eur. Phys. J. B **81**, 197 (2011).
2. B. K. Agarwalla, J.-S. Wang, and B. Li, “Heat generation and transport due to time-dependent forces”, Phys. Rev. B, **84**, 041115, (2011).
3. J.-S. Wang, B. K. Agarwalla, and H. Li, “Transient behavior of full counting statistics in thermal transport”, Phys. Rev. B, **84**, 153412, (2011).
4. B. K. Agarwalla, B. Li, and J.-S. Wang, “Counting statistics of heat transport in harmonic junctions – transient and steady states”, Phys. Rev. E **85**, 051142 (2012).
5. H. Li, B. K. Agarwalla, and J.-S. Wang, “Nonequilibrium Greens function method for steady current in the case of lead-lead interaction”, Phys. Rev. E **86**, 011141 (2012).

6. H. Li, B. K. Agarwalla, and J. -S. Wang, “Cumulant generating function formula of heat transfer in ballistic system with lead-lead coupling”, *Phys. Rev. B* **86**, 165425 (2012).
7. L. Sha, B. K. Agarwalla, B. Li, and J. -S. Wang, “Classical Heat Transport in Anharmonic Molecular Junctions: Exact Solutions”, *Phys. Rev. E* **87**, 022122 (2013).
8. Huanan. Li, B. K. Agarwalla, B. Li, and J. -S. Wang, “Cumulant of heat in nonlinear quantum thermal transport”, arXiv: 1210.2798.
9. B. K. Agarwalla, H. Li, B. Li, and J.-S. Wang, “Heat transport between  $N$  terminals and exchange fluctuation theorem ”, (submitting).
10. J.-S. Wang, B. K. Agarwalla, Huanan Li, and J. Thingna, “Nonequilibrium Green’s function method for quantum thermal transport”, (Submitting).